INVESTIGATION ON THE EFFECT OF SELECTED NANO STRUCTURES ON ACCUMULATION OF BIOMASS AND SECONDARY METABOLITES IN *IN VITRO* CULTURES OF *RUBIA CORDIFOLIA* L.

Thesis submitted to the

University of Calicut

For the award of the Degree of

DOCTOR OF PHILOSOPHY IN

BOTANY

Under the Faculty of Science

By

APARNA PRASAD

Under the Guidance of

Dr. SATHEESH GEORGE (Guide)

Dr. RENJIS T TOM (Joint-Guide)

CENTRE FOR POST GRADUATE STUDIES AND RESEARCH IN BOTANY

ST. JOSEPH'S COLLEGE (AUTONOMOUS) DEVAGIRI

CALICUT- 673008, KERALA, INDIA

January 2025

ST. JOSEPH'S COLLEGE (AUTONOMOUS),
DEVAGIRI, CALICUT, KERALA-08, INDIA
Re-accredited by NAAC with A++
Affiliated to the University of Calicut
Phone: +91 9447331351

Dr. Satheesh George M.Sc., Ph.D.
Associate Professor of Botany
e-mail: george.satheesh@gmail.com

CERTIFICATE

This is to certify that the Ph.D. thesis entitled **"INVESTIGATION ON THE EFFECT OF SELECTED NANO STRUCTURES ON ACCUMULATION OF BIOMASS AND SECONDARY METABOLITES IN *IN VITRO* CULTURES OF *RUBIA CORDIFOLIA* L."** is an authentic record of the original research work accomplished by **Ms. Aparna Prasad** under my supervision and guidance at the Centre for Post Graduate Studies and Research in Botany, St. Joseph's College (Autonomous) Devagiri, Calicut, Kerala and that no part of this thesis has been published earlier for the award of any other degree or diploma. Also certified that the contents in the thesis have subjected to **Plagiarism Check** using the software **iThenticate** and that no text or data is reproduced from other's work.

I also certify that the corrections recommended by the adjudicators is included in the present form.

Dr. Satheesh George

(Guide)

ST. JOSEPH'S COLLEGE (AUTONOMOUS), DEVAGIRI, CALICUT, KERALA-08, INDIA

Re-accredited by NAAC with A++
Affiliated to the University of Calicut
Phone: +91 9447331351

Dr. Renjis T Tom M.Sc., Ph.D.
Assistant Professor of Chemistry
e-mail:renjistom@gmail.com

CERTIFICATE

This is to certify that the Ph.D. thesis entitled **"INVESTIGATION ON THE EFFECT OF SELECTED NANO STRUCTURES ON ACCUMULATION OF BIOMASS AND SECONDARY METABOLITES IN *IN VITRO* CULTURES OF *RUBIA CORDIFOLIA* L."** is an authentic record of the original research work accomplished by **Ms. Aparna Prasad** under my supervision and guidance at the Centre for Post Graduate Studies and Research in Botany, St. Joseph's College (Autonomous) Devagiri, Calicut, Kerala and that no part of this thesis has been published earlier for the award of any other degree or diploma.

Dr. Renjis T Tom
(Joint-Guide)

DECLARATION

I hereby declare that the work presented in the thesis entitled **"INVESTIGATION ON THE EFFECT OF SELECTED NANO STRUCTURES ON ACCUMULATION OF BIOMASS AND SECONDARY METABOLITES IN *IN VITRO* CULTURES OF *RUBIA CORDIFOLIA* L."** is based on the original work done by me under the guidance of **Dr. Satheesh George,** Assistant Professor, Department of Botany, St. Joseph's College (Autonomous) Devagiri, Calicut, Kerala and with the joint-guidance of **Dr. Renjis T. Tom**, Assistant Professor, Department of Chemistry, St. Joseph's College (Autonomous), Devagiri, Calicut. This Work is entirely original in its contents and has not been included in any other thesis submitted previously for the award of any degree. The contents of the thesis have undergone plagiarism check using iThenticate software at C.H.M.K. Library, University of Calicut, and the similarity index found within the permissible limit. I also declare that the thesis is free from AI generated contents.

Place:

Date: **Aparna Prasad**

ACKNOWLEDGEMENTS

*First and foremost, I thank **God**, the Almighty, for showering blessings on the successful completion of my Ph.D. I am grateful to many people, who have supported me from the beginning till the end of this work. I would not have been able to complete this thesis without their timely help and encouragement.*

*I would like to express my sincere gratitude to my research guide **Dr. Satheesh George** for the continuous support and guidance, for his patience, motivation and extensive knowledge. Wholehearted gratitude is extended towards him for the inspiring advices and criticisms which played a key role in polishing the research output. His dedication and incredible patience led to the successful completion of the research work. I am deeply thankful for the continuous motivation, which has kept me focused and inspired. It has been an honour to learn from someone so dedicated to their field, and I am truly fortunate to have had the privilege of working under their mentorship.*

*I convey my immense sense of gratitude to my joint-guide **Dr. Renjis T Tom**, Head, Department of Chemistry, St. Joseph's College (Autonomous), Devagiri for providing facilities to undertake my research. His expertise, immense knowledge and insightful involvement were invaluable in formulating the research problem and his guidance was equally important throughout my research work.*

*I express my profound gratitude to the **University Grants Commission**, forbestowing upon me financial support in the form of a fellowship. The generousgrant provided a crucial impetus in achieving the successful culmination of myresearch work. It would not be an overstatement to acknowledge that thefellowship played an instrumental role in facilitating my research endeavour.*

*I convey my immense sense of gratitude to **Dr. Delse P. Sebastian,** Head, Department of Botany, St. Joseph's College (Autonomous), Devagiri for providing facilities to undertake my research.*

*I am extremely grateful to Principal **Dr. Boby Jose** for providingwholehearted assistance in completing this work. I would also like to express mygratitude to former principals **Dr. Sabu K. Thomas** and **Dr. Jose John Mallikasseri**, for their support and help during my research.*

*I am deeply thankful to **Dr. Arunaksharan Narayanankutty,** Assistant Professor Department of Zoology, St. Joseph's College (Autonomous), Devagiri for their invaluable support throughout the different stages of this project.*

I would like to express my utmost gratitude to ***Dr. Sulaiman C.T.,*** *Senior Scientist, Center for medicinal plant research (CMPR), Kottakkaland* ***Mr. Deepak M.*** *for their invaluable guidance in comprehending different methodologies and interpreting results. Also, express my gratitude to* ***Dr. Geetha S. Pillai,*** *Senior Scientist, CMPR,* ***Dr. Sadheeshna Kumari S,*** *Scientist, CMPR****, Dr. Blassan P George,*** *Associate Professor, Department of Health Science Laser Research Centre, University of Johannesburg, South Africaduring the study.*

Lastly, I extend my sincerest appreciation to ***Mr. Shintu Varghese*** *for the Raman spectroscopic studies and* ***Mr. Tomson A.J.****, Librarian, St. Joseph's College (Autonomous), Devagiri for his timely help during the research period.*

I would like to convey my heartfelt gratitude to ***Dr. Jojo Joseph, Dr. Abis V. Cherussery*** *and* ***Dr. George P.S.*** *former faculty members of the Dept. of Botany, St. Joseph'sCollege (Autonomous), Devagiri for their guidance and the immense knowledgeshared, which helped me to build a strong foundation in my journey. I also expressmy gratitude to* ***Dr. Manudev K.M., Dr. Ron Sunny, Mr. Peter A. A., Mr. Jithin J.*** and ***Mr. Joyal K George*** *Dept. of Botany, St. Joseph's College (Autonomous), Devagiri for their timely help during the research period.*

*I am deeply indebted to my fellow labmates****, Jameema Sidhic, Sruthi Mohan, Akshaya Prakash C., Navya C.P., Anagha Aneesh, Rekha C., Prasanth M.K., Athira C.K., Renjisha Das, Karthika Surendran, Naseeha C.P., Suvarnika V.*** *and* ***Jaseela M.P.*** *and to my formar labmates,* ***Dr. Neena A., Dr. Aparna Balakrishnan, Dr. Aswindas T.P., Dr. Abin Kurian, Dr. Mahesh Mohanan, Dr. Dilsha M.V., Dr. Bhavana R.*** *And* ***Dr. Sindhu E.S.,*** *of St. Joseph's College (Autonomous), Devagiri for their valuable help, support and encouragement during the research period.*

I extend my sincere gratitude to all my former teachers who supported meto build my academic career: ***Dr. Deena Meria Jose, Late Dr. Jija Mathew, Dr. Chandraleka C.T. and Dr. Vargeese M.C.***

I would like to express a special heartfelt gratitude to ***Dr. Binu Thomas*** *and* ***Dr. Minoo Divakaran****, my teachers, for igniting the spark of curiosity and passion for research in me. Your encouragement and support have been instrumental in shaping my academic journey. I am truly thankful for the knowledge and insights you have shared, which have played a significant role in my growth as a researcher.*

*Finally, I dedicate this work to my Achan (****Prasad T.C.****), Amma (****Usha*** *and* ***Komalavally****),my brother (****Arjun Prasad****), my beloved husbund (****Vijeesh****), my precious daughters (****Mithra and Rudhra****), my sisters (****Vijitha, Vinisha and Arathy****) and to my brothers (****Praveen Raj and Dr. Sreesanth****) for the concern, care and encouragement*

that gave me the strength and patience to complete my work successfully. I realize the depth of their sacrifices and am forever indebted to them.

Finally, I thank each and every one who crossed my life during this journey, for all the inspirations, criticism and support that pave the way to my dream
Thank You!

Aparna Prasad

UNIVERSITY OF CALICUT
CERTIFICATE ON PLAGIARISM CHECK

1.	Name of the Research Scholar	APARNA PRASAD	
2.	Title of thesis / dissertation	Investigation on the effect of selected nano structures on accumulation of biomass and secondary metabolites in *in vitro* cultures of *Rubia cordifolia* L.	
3.	Name of the Supervisor	Dr. Satheesh George	
4.	Department/Institution	Centre for post graduation studies and research in botany, St. Joseph's college (autonomous), Devagiri, Calicut- 673008	
5.	Similar content (%) identified	**Non-core**	**Core**
		Introduction/Theoretical overview/Review of literature/ Materials & Methods/ Methodology	**Analysis/Result/Discussion/ Summary/Conclusion/ Recommendations**
		8	3
	Acceptable maximum limit (%)	10	10
6.	Software used	iThenticate	
7.	Date of verification	1-1-2025	

**Report on plagiarism check, specifying included/excluded items with % of similarity to be attached.*

Checked by (with name, designation & signature)

Dr. Nasirudheen. T
Assistant Librarian
University of Calicut, Kerala.

MOHAMMED KOYA LIBRARY P.O. CALICUT UNIVERSITY UNIVERSITY OF CALICUT

Name and signature of the Researcher

Name and signature of the Supervisor.

The Doctoral Committee* has verified the report on plagiarism check with the contents of the thesis, as summarized above and appropriate measures have been taken to ensure originality of the Research accomplished herein.

Name & Signature of the HoD/HoI (Chairperson of the Doctoral Committee)

**In case of languages like Malayalam, Tamil etc. on which no software is available for plagiarism check, a manual check shall be made by the Doctoral Committee, for which an additional certificate has to be attached.*

CHAPTER-1

INTRODUCTION

Human civilizations have always had a close interaction with the environment and have depended largely on plant resources for a variety of needs, including food, shelter, and medicine. Over time, man evolved the ability to meet his needs from his surroundings after learning via trial and error and that plants may be used as food and medicine (Jamshidi-Kia *et al.*, 2017).

Green plants have a far larger historical legacy worldwide, and their outstanding application in a variety of sectors is noteworthy. Because there are less adverse effects, the usage of medicinal plants is growing daily, especially when it comes to big industries like medicine and pharmaceuticals. The use of medicinal plants is contingent on the content within them, which are isolated and extracted from various plant parts for medication. More than 50,000 plant species, or over 10% of all plant species, are used in cosmetic and pharmaceutical products. On the other hand, medicinal plants are usually collected from the population of wildlife and are not dispersed uniformly around the planet. Throughout the past few decades, demand for plant products has increased by 8% to 15% yearly in North America, Asia, and Europe (Hamilton, 2004; Huang, 2011; Rafieia-Kopaei, 2011; Verma & Singh, 2008).

For centuries, India's economy has been centred around plants. A wide range of goods, including natural pigments, food additives, cosmetics, tastes, fragrances, and odours and scents, are produced worldwide by extracting plant-based materials. The World Health Organization estimates that by 2050, the demand for medical plants which currently stands at $14 billion annually will certainly surpass US $5 trillion. As the demand for medicinal herbs continues to rise, overexploitation may lead to the eventual extinction of many valuable plants. This makes conservation necessary and demands the use of effective biotechnological techniques such *in vitro* multiplication of bioactive chemicals of interest through cell and tissue culture (Gusain *et al.*, 2021).

1.1 HISTORY AND SUSTAINABLE USE OF MEDICINAL PLANTS

The oldest collection of human knowledge, the Rigveda (4500–1600 B.C.), mentions 67 therapeutic plants, which is where the history of medicinal plants in India begins. Approximately 290 plants are mentioned in the Atharvaveda (2500–1500 B.C.) as disease-curing remedies. Ayurveda was founded by Lord Dhanvantri (2500–900 B.C.), who also laid the actual groundwork for the first medical science, which includes a detailed description of the qualities of various medications. Two Samhitas, Sushruta

(800 B.C.) and Charak (1000 B.C.), deal only with medicine and surgery, respectively, out of the eight divisions of Ayurveda. By the end of the third period, Ayurvedic medicine became widely known worldwide (Pal & Jain, 1998).

In contemporary medicine, pharmaceuticals derived from higher plants still hold a significant position. Many of the substances utilized in modern medicine have intricate structures, making it difficult to chemically synthesize at a reasonable cost. Deforestation causes a rapid loss of medicinal wealth, putting many precious plants in danger of going extinct. The majority of the materials used by pharmaceutical businesses come from naturally occurring sources, which are fast running out. One promising biotechnological approach to address the over exploitation of therapeutic plant is plant *in vitro* regeneration or plant tissue culture (Afolayan & Adebola, 2004; Dev, 1997; George & Sherrington, 1984; Shimomura *et al.*, 1997).

For the sake of protecting endangered plant species, a trustworthy *in vitro* protocol must be developed. Biotechnological tools play a vital role in the genetic improvement and propagation of medicinal plants through techniques like *in vitro* regeneration and genetic transformation. It can also be used to produce secondary metabolites in plants by employing them as bioreactors. There is a lot of promise for producing superior plant-based medications through *in vitro* plant culture. A variety of techniques can be used to accomplish this (Bramwell, 1990; Fay, 1992; Murch *et al.*, 2000; Tripathi & Tripathi, 2003). Compared to traditional vegetative propagation techniques, micropropagation offers numerous advantages. The rate of multiplication is substantially accelerated through micropropagation. It also makes it possible to produce material free of pathogens. Plants produced through meristem propagation are genetically identical to the donor plants (Cardoso *et al.*, 2018; Loberant & Altman, 2010; Suman, 2017). Positive outcomes have been observed in the regeneration of plants from shoot and stem meristems in many medicinal plants (Azad *et al.*, 2009; Bhagya *et al.*, 2013; He *et al.*, 2007; Mahendran *et al.*, 2016; Türker *et al.*, 2010).

1.2 HISTORICAL PERSPECTIVE AND BASIC PRINCIPLES OF PLANT TISSUE CULTURE

Plant tissue culture, also known as cell, *in vitro*, axenic, or sterile culture, is a valuable tool in both basic and applied studies, as well as in commercial applications. It involves the aseptic culture of cells, tissues, organs, and their components under

defined physical and chemical conditions *in vitro*. The concept originated from the ideas of the German scientist Gottlieb Haberlandt (1902) at the beginning of the 20th century. The first true callus/tissue cultures, root cultures, and embryo cultures were developed as a result of early research. New techniques were developed and existing ones were improved between the 1940s to 1960s. The development of tissue culture techniques in the mid-1960s led to their application in five main areas: cell behaviour (including cytology, nutrition, metabolism, morphogenesis, embryogenesis, and pathology), plant modification and improvement, production of pathogen-free plants and germplasm storage, clonal propagation, and the formation of products, mainly secondary metabolites (Razdan, 2002; Thorpe, 2012).

In the last 50 years, there has been a growing focus on studying plant secondary metabolites. These compounds are crucial in how plants adapt to their environment and serve as a valuable source of active pharmaceuticals. In the late 1960s, plant cell culture technologies were presented as a viable approach to the production and research of these secondary metabolites. Despite efforts over the last few decades, there have been commercial successes in using plant biotechnologies to produce valuable secondary compounds. Various strategies utilizing *in vitro* systems have been extensively researched to enhance the production of secondary plant compounds. While undifferentiated cell cultures have been the primary focus, there is also significant interest in hairy roots and other organ cultures. Specific processes have been developed to address the needs of plant cell and organ cultures in bioreactors. The emergence of recombinant DNA technology has created new possibilities for directly modifying the expression of genes related to biosynthesis, allowing for manipulating pathways leading to secondary plant compounds (Bourgaud *et al.*, 2001; Thorpe, 2012).

Plant tissue culture is a well-established method used today to investigate the organs, tissues, cells, protoplasts, and organelles of plants. Large-scale plant tissue culture is a promising strategy that ensures a steady supply of biochemical, irrespective of plant availability. Micropropagation, in particular, is the only method that enables the rapid production of uniform, superior-quality, and disease-free planting stock. This technique is capable of producing plants throughout the year, regardless of the climatic conditions or season (Shahzad *et al.*, 2017; Suman, 2017; Thorpe, 2012; Tiwari & Rana, 2015).

1.3 SECONDARY METABOLITES

Secondary metabolites are substances that contribute to an organism's or cell's interaction with its surroundings but are not requisite for the organism to survive. These substances frequently play a role in plants' defence against biotic and abiotic stressors. Secondary metabolites belong to distinct groups of metabolites and can be strongly induced in response to various stressors. When moving from an active growth phase to a stationary phase, secondary metabolites are often produced at their maximum levels. Secondary metabolites have certain economic significant as special chemicals in products including perfumes, flavourings, pharmaceuticals, insecticides, and dyes (Bizzo *et al.*, 2012; Pagare *et al.*, 2015).

It was Kossel (1891) who first made the initial distinction between secondary metabolites from primary ones. Secondary metabolites are limited to specific species, genera, or families of plants, in contrast to primary metabolites, which are present across the plant kingdom. Chemically plant secondary metabolites are of three types, terpenes (such as plant volatiles, cardiac glycosides, carotenoids and sterols), phenolic (such as phenolic acids, coumarins, lignans, stilbenes, flavonoids, tannins and lignin) and nitrogen containing compounds (Bhatla & Lal, 2023; Costa *et al.*, 2012). Various secondary metabolites are produced in different pathways like the Shikimic acid pathway, Malonic acid pathway, Mevalonic acid pathway, and Methyl Erythritol Phosphate (MEP) pathway (Taiz *et al.*, 2015).

Secondary metabolites can be classified on the basis of chemical structure, composition, their solubility in various solvents, or the pathway by which they are synthesized. Three large molecule families are generally considered: (a) phenolics; (b) terpenoids; and (c) nitrogen-containing compounds.

Phenolics

A minimum of one aromatic ring with one or more hydroxyl groups attached is what defines phenolic compounds. Phenolics can range in size from huge and complex tannins and derived polyphenols to simple, low molecular weight molecules with a single aromatic ring (Crozier *et al.*, 2006a). The flavonoids containing two aromatic rings are the most well-known class of phenolics. Resveratrol is the most abundant compound in the stilbenes, a significant subclass of phenolics that are structurally related to flavonoids. Phenolic-based polymers, like tannins, suberin, and lignin, play a

significant role in protecting plant tissues from mechanical stress and environmental abrasions like dehydration and injury. Phenolic typically concentrate in the epidermal tissue, where they carry out their biological activity (Cai *et al.*, 2004).

Flavonoids have a variety of functions in plants, including disease resistance, pigmentation, UV protection, and nitrogen-fixing nodule stimulation (Crozier *et al.*, 2006b). The flavonoids include various groups of plant metabolites such as flavanones, flavonols, isoflavonoids, flavones, chalcones, aurones, catechins, anthocyanins and leucoanthocyanidins (W. Liu *et al.*, 2021).

Terpenes

In the industrial sector, terpenoids are widely utilized as flavours, scents, spices, and in perfumery and cosmetics. They make up the largest class of natural products (Roba, 2020). Terpenes are a distinct class of naturally occurring hydrocarbon-based compounds with structures derived from isoprene units. In general, they are concentrated in large amounts in the leaf and reproductive systems of plants during and right after flowering (Theis & Lerdau, 2003). Terpenes are also a major component of plant resins. Terpenes are thought to serve both physiological and ecological roles in plants: Phytohormone (abscisic acid, gibberlellin), insecticidal, pollinating insects, and allelophathy (Roba, 2020). Conversely, elevated terpene concentrations have the potential to be poisonous, making them a valuable tool in the battle against infections and herbivores. Numerous terpenoids have been demonstrated to have antibacterial, antiviral, antifungal, anti-inflammatory, antihyperglycemic and antiparasitic properties and to be useful in chemoprevention and chemotherapy (Paduch *et al.*, 2007).

Alkaloids

Alkaloids were described as pharmacologically active, nitrogen-containing, low-molecular-weight, basic compounds of plant origin (Matsuura & Fett-Neto, 2015). Many distinct pharmacological properties are displayed by alkaloids, including analgesic, central nervous system stimulant and depressant, anti-malarial, cardiovascular, and similar properties. Most known example of alkaloids are morphine is a popular analgesic (Adejoke *et al.*, 2019).

Secondary metabolites from plants are a special source of fine chemicals, food additives, and pharmaceuticals. Certain high-value chemicals are not always convenient or commercially viable to produce through chemical synthesis and plant cultivation.

One potential avenue to meet the market need for these substances is to induce the biosynthetic pathways in intact plants. Consequently, this field of study is more focused on developing a unique, economically viable process for producing high-value phytochemicals. Since different plants react differently to external stimuli, more and more studies are required to predict the strategies for accomplishing the aim (Hussain *et al.*, 2012; Zhong, 2001).

Biotechnology plays a crucial role in the industrial production of secondary metabolites from pharmaceutical plants and in reducing the over-exploitation of natural sources. It uses various *in vitro* approaches like plant cell, tissue, and organ culture techniques to produce high-value pharmaceuticals like alkaloids, flavonoids, terpenes, and steroids. Researchers are now optimizing culture conditions through cell line selection, elicitation, precursor feeding, two-phase co-culture, and other approaches to meet industry demand, scale up production, and conserve natural sources (Isah *et al.*, 2018; Ozyigit *et al.*, 2023).

Through experimental demonstration, Zenk *et al.,* (1975) produced 2.5 g of anthraquinones per litre of medium from a dedifferentiated cell culture of *Morinda citrifolia*. This discovery led researchers to thoroughly investigate the potential applications of plant cultures for the production of secondary compounds of industrial interest. The significant roles of plant secondary metabolites are to protect and survive plants from pathogen attacks and stresses. Based on this principle, scientists have developed some strategies for culture production of the metabolites, which include treatment with various elicitors, signal compounds, and biotic stresses (Tiwari & Rana, 2015).

Plant explants, such as leaves, stems, roots, meristems, etc., can create sterile plant cell and tissue cultures for multiplication and secondary metabolite extraction. Shoot, root, callus, cell suspension, and hairy root cultures synthesize metabolites of interest. Unorganized callus or suspension cultures can be used to produce metabolites localized in multiple tissues. However, a differentiated microplant or organ culture is preferred when the target metabolite is limited to specific sections or glands in the host plant. For example, saponins in *Ginseng* are primarily produced in its roots, hence an *in vitro* root culture is preferred for synthesis. Antidepressant hypericin and hyperforin localized in foliar glands of *Hypericum perforatum* cannot be synthesized from

undifferentiated cells. The production of secondary metabolites in cell cultures can be increased by using elicitors such as methyl jasmonate, fungal carbohydrates, and yeast extract (Thirumurugan *et al.*, 2018).

Anthraquinone accumulation in *Rubia* species is minimal (1.5–2%) and varies with plant age, genotype, and phenology. As a result, researchers have developed *in vitro* culture techniques for these species (Murthy *et al.*, 2022). Similar studies by Shin (1989) in callus cultures of *R. cordifolia* and *R. akane*, as well as by Gnanaraj *et al.*, (2024) in adventitious root cultures of *R. cordifolia*, found that α-ketoglutaric acid enhanced the accumulation of alizarin and purpurin. In another study, Mischenko *et al.*, (1999) created callus cultures of *R. cordifolia* using MS medium with 0.5 mg/L Benzyl adenine (BA) and 2 mg/L Naphthalene acetic acid (NAA) from various explants. They discovered that stem and leaf petiole-derived clones had the highest levels of purpurin and munjistin.

1.4 NANOSTRUCTURES

Minerals, clays, and bacterial compounds are examples of naturally occurring nanostructures (NSs), which are not new to the environment. Because of hydrothermal activity and volcanic eruptions, it naturally occurs in the biosphere. It has been used since ancient times as a colorant for metals, but the systematic design and engineering of NSs for various uses has started only in the last few decades (Maurer-Jones *et al.*, 2013; Rahman, 2021).

According to ASTM (American Society for Testing and Materials) standards, NSs are defined as natural or manufactured materials typically ranging from 1 to 100 nm in at least one dimension and having a large relative surface area to volume ratio. (Sanzari *et al.*, 2019). Nanostructures gained interest due to their unique properties, such as morphology, chemical reactivity, optical activity, competitive binding sites, and small size-per-volume ratio in contrast to their bulk states. Their properties depend on their preparation method, temperature, and surfactants used for capping. Nanostructures vary widely according to their composition, morphology, dimensions, uniformity states and agglomeration. Nanostructures include metal-based, carbon-based, composite-based and organic-based NSs (Sengul & Asmatulu, 2020).

Metallic nanostructures (M NSs) have a metal core composed of inorganic metal (e.g., Gold, Iron, Platinum, Silver, Zinc, etc.) or their compounds (e.g., oxide, sulphides,

chlorides, hydroxides, etc.) that is typically covered with a shell made up of metal oxide or organic or inorganic material. A metal salt solution (precursor) is added to a plant extract (reducing agent) to prepare M NSs. A colour change will be the first indication for the formation of M NSs (Mélinon *et al.*, 2014; Mohamad *et al.*, 2014).

Zinc oxide (ZnO) is an inorganic semiconductor with a wide band gap, known for its large surface area and high catalytic activity. Its environmentally friendly NSs are commonly used in biological applications. Copper (II) oxide (CuO) is a narrow-band-gap, p-type semiconductor having diverse applications and industrial uses (Javed *et al.*, 2018).

Recently, MO NSs have become significant in many fields such as energy, health care, environment, agriculture etc. Among these, nano-medicine has colossal anticipation for the advancement in diagnosis and treatment of human diseases. Nanotechnologies have great potential, converting poorly soluble, poorly absorbed, and labile biologically active substances into promising deliverable substances. Nanotechnology has the potential to transfigure a wide array of tools in biotechnology so that they are more personalized, cheaper, portable, safer, and easier to administer (Alfei, 2020; Hasan, 2015).

1.5 PLANT TISSUE CULTURE VS NANOTECHNOLOGY

Tissue culture is the controlled cultivation of cells, tissues, or entire plants to create clones that are genetically identical to the original. Regardless of the season or weather, a single explant can be reproduced into thousands of plants in a very short time and space (Sengul & Asmatulu, 2020). Apart from their use as a research tool, plant tissue culture techniques have recently grown to be of major industrial importance in the fields of forestry, horticulture, agriculture, plant propagation, plant improvement, disease eradication, and the production of secondary metabolites. The widespread use of plant tissue culture technology enables large-scale plant multiplication. Plant tissue culture techniques are the most commonly utilized biotechnological tools for both fundamental and applied purposes. These include research on plant developmental processes, functional gene studies, commercial plant micropropagation, creation of transgenic plants with particular industrial and agronomical traits, plant breeding and crop improvement, virus removal from infected materials to render high-quality healthy

plant material, preservation and conservation of genetic resources, and more (Loyola-Vargas & Ochoa-Alejo, 2018; Oseni *et al.*, 2018).

In vitro and *in vivo* Studies have shown that triggering secondary metabolites with nanoparticles is complex and involves multiple signalling pathways. When nanoparticles enter plant cells and are recognized by plasma membrane receptors, Ca^{2+} ions influx occurs. This activates NADPH oxidase, generating Reactive Oxygen Species (ROS) that activate the Mitogen-Activated Protein Kinase (MAPK) pathway, upregulating transcription factors that regulate secondary metabolite production. Additionally, compounds like salicylic acid, jasmonic acid, and methyl jasmonic acid play roles in signaling pathways that enhance the formation of biologically active compounds under abiotic stress. Size, shape, surface, composition, solubility, aggregation, and particle absorption all influence ROS generation triggered by NSs (Javed *et al.*, 2022; Sengul & Asmatulu, 2020).

1.6 *RUBIA CORDIFOLIA* L. (RUBIACEAE)

Systematic position of the plant

Class : Dicotyledoneae

Subclass : Sympetalae

Order : Rubiales

Family : Rubiaceae Juss.

Genus : *Rubia*

Species : *R. cordifolia* L.

Rubia cordifolia L., a tiny perennial climber found in damp tropical forests, is a member of the Rubiaceae family. It has a long, cylindrical, flexuous root and thin red bark. *R. cordifolia* is known as Manjishta in Sanskrit. The stems of the plant typically have a long, rough, grooved, woody base. It is known that plants in this family, particularly those with roots, contain significant concentrations of Anthraquinones. Flowers appear in terminal panicles or cymes and are tiny, white or greenish. Fruits are round, dark purple, or dark black. It can be found up to 3500 meters above sea level in the lower hills of the Indian Himalayas in the north and the Western Ghats in the South, as well as in tropical Africa, Java, Indonesia, Japan, Indonesia, Ceylon, Malay Peninsula, and the Malay Peninsula in the South (Deshkar *et al.*, 2008; Patil *et al.*, 2009).

R. cordifolia is one of several botanical species that can be used for dye extraction. It was the source of an ancient anthraquinone-based dye that was widely utilized in historical dyeing techniques across the Indian subcontinent, China and Southeast Asia. The dye is extracted from the roots of *R. cordifolia*, which contain anthraquinone-based components, resulting in a colour palette of red shades. Additionally, this root extract has antimicrobial, antioxidant, and anti-inflammatory properties due to the presence of these anthraquinone constituents (Eom *et al.*, 2020; Meena *et al.*, 2010; Yusuf *et al.*, 2017). *R. cordifolia* extract has been used for dyeing silk, cotton, and wool to achieve strong colours with excellent fastness (Boominathan *et al.*, 2022; Schmidt-Przewoźna & Kicińska-Jakubowska, 2023; Vankar *et al.*, 2017; Yusuf *et al.*, 2016).

Research has revealed that *R. cordifolia* contains many different chemicals, the majority of which are anthraquinones, anthraquinone glycosides, naphthoquinones, naphthoquinone glycosides, triterpenoids, bicyclic hexapeptides, and polysaccharides. (Gao *et al.*, 2016; Itokawa *et al.*, 1993; Natarajan *et al.*, 2019; Rao *et al.*, 2006; Son *et al.*, 2008; Wen *et al.*, 2022).

Quinones: The plant contains quinines, mainly anthraquinone glycosides and include 1-hydroxy 2-methoxy anthraquinone, 1, 4- dihydroxy-2- methyl-5-methoxy anthraquinone, 1,3- dimethoxy 2- carboxy anthraquinone and rubiadin (Deshkar *et al.*, 2008).

Bicyclic hexapeptides: Lots of rubiaakane series peptide compounds with anti-tumor bicyclic hexapeptides were isolated from *R. cordifolia*, such as RA-XVIII, RA-XII (Patil *et al.*, 2009; Wen *et al.*, 2022).

Iridoids: 6-methoxygeniposidic acid is found along with manjistin, garancin and alizarin (Wu *et al.*, 1991).

Oleananes triterpenoid: Rubiprasin A, B, and C along with arborane triterpinoids, like rubiarbonol A, B, C, D, E and F have been isolated (Deshkar *et al.*, 2008; Itokawa *et al.*, 1990).

Anthraquinones: The Rubiaceae family of plants is known to contain significant levels of anthraquinones, particularly in the roots (Deshkar *et al.*, 2008). Within the world of natural chemicals, anthraquinones are a widely distributed group of compounds. They are categorized as quinones, and the majority of naturally occurring quinones are their

derivatives. This group also includes benzoquinones and naphthoquinones. The majority of these substances are generated from the fundamental structure 9,10-anthracenedione, an aromatic tricyclic chemical compound (Diaz-Munoz *et al.*, 2018). About 30% of textiles are dyed with anthraquinones, which makes them quite popular for this purpose. The type of auxochromic groups and their positions on the anthraquinone structure are critical factors in determining the dye's colour. Additionally, anthraquinones play a significant role as chromophores in cancer chemotherapy (Rushdan *et al.*, 2023).

Alizarin, munjistin, rubiadin, purpurin, techoquinone, and xanthopurpurin are among the typical chemicals, or anthraquinones, found in *R. cordifolia* (Wen *et al.*, 2022). Dosseh *et al.,* (1981) were isolated four anthraquinones from *R. cordifolia* root, 1-hydroxy 2-methoxy anthraquinone, 1,4-dihydroxy 2-methyl 5-methoxy anthraquinone or 1,4-dihydroxy 2-methyl 8-methoxy anthraquinone, 1,3-dimethoxy 2-carboxy anthraquinone, and rubiadin. *R. cordifolia* root was extracted using ethanol by Wang *et al.,* (1992) who then isolated seven anthraquinone compounds (2-methyl-1,3,6-trihydroxy-9,10-anthraquinone, 1-hydroxy-9,10-anthraquinone, 1,2,4-trihydroxy-9,10-anthrequinone, 2-methyl-1,3,6-trihydroxy-9,10-anthraquinone-3-O-β-D-glucoside, 1,2-dihydroxy-9,10-anthraquinone-2-O-β-Dxylosyl (1→6)-β-D-glucoside, 1,3-dihydroxy-2-hydroxymethyl1-9,10-anthraquinone-3-O-β-D-xylosyl (1→6)-β-Dglucoside), 2-methyl-1,3,6-trihydroxy-9,10-anthraquinone-3-O-β-Dxylosyl(1→2)-β-D-(6′-O-acetyl) glucoside (Wang *et al.*, 1992).

Other anthraquinones namely 1-hydroxy-2,7-dimethyl anthraquinone, 1-hydroxy 2-methyl anthraquinone, 2-hydroxy -6-methyl anthraquinone, 2,6-dihydroxy anthraquinone, 1,4-dihydroxy 6-methyl-anthraquinone, 1,4-dihydroxy 2-methyl anthraquinone, nordamnacanthal, physcion, 1,5-dihydroxy 2-methyl anthraquinone, cordifoliol and cordifodiol, have been isolated from the roots of *R. cordifolia*. Three new anthracene derivatives, rubiasins A–C, were isolated from the combined roots and stems of *R. cordifolia* (Chang *et al.*, 2000; Tessier *et al.*, 1981).

The colouring material found in *R. cordifolia* roots is a combination of manjistin (xanthopurpurin-2-carboxylic acid) and purpurin (trihydroxy anthraquinone) (Balachandran *et al.*, 2021). The roots contain small amounts of Pseudopurpurin (purpurin-3-carboxylic acid) and xanthopurpurin or purpuroxanthin. The plant also

contains several important compounds, including dihydromollugin, mollugin, and rubilactone. Purpurin, a member of the lipocalin family of proteins, is a fast dye used for cotton printing and can form complexes with various metal ions. It acts as both a glycosaminoglycan-binding protein and a retinol-binding protein. Alizarin, also known as 1,2-dihydroxyanthraquinone or mordant red, is a red dye originally derived from the roots of the madder plant. In 1869, it became the first natural pigment to be duplicated synthetically (Patil *et al.*, 2009; Sharma *et al.*, 2021).

Plant secondary metabolites are valuable for humanity in various aspects, but their complex biosynthesis makes chemical synthesis impractical. Plant *in vitro* cultures offer a cost-effective production method. Due to limited availability, specific metabolites command high market prices. This study aims to enhance the production of economically important Alizarin and Purpurins from *R. cordifolia*, optimizing a practical and efficient method for their increased yield.

1.7 OBJECTIVES OF THE STUDY

- Standardization of protocol for the synthesis of nanostructures.
- Characterization of synthesized nanostructures.
- Standardization of protocol for shoot multiplication in *Rubia cordifolia*.
- Investigation on the Impact of selected nanostructures on *in vitro* production of Secondary Metabolites in *Rubia cordifolia*.
- Investigation on the Impact of selected nanostructures on Biomass accumulation in *Rubia cordifolia*.
- Comparative Quantification of Secondary Metabolites in Elicited Shoot cultures of *Rubia cordifolia* using chromatographic techniques.

CHAPTER - 2

REVIEW OF LITERATURE

2.1 *RUBIA CORDIFOLIA* L.

Rubia cordifolia L. (Manjishtha), also known as 'Indian Madder,' is traditionally used for its anti-inflammatory, astringent, and blood-purifying properties. It is a key ingredient in many Ayurvedic preparations and contains various beneficial chemical constituents like anthraquinones, iridoid glycoside, naphthoic acid esters, bicyclic hexapeptides, and triterpenes (Do *et al.*, 2023; Schmidt-Przewoźna & Kicińska-Jakubowska, 2023).

R. cordifolia, one of the earliest plant resources, has significant commercial and therapeutic benefits. Traditionally, these species were used as natural dyes in commerce to enhance the flow of goods. However, the usage of these species as medicines dates back more than 2000 years to the Divine Farmer's Materia Medica, the world-renowned pharmacy book of China (Verma *et al.*, 2016). It has been shown in several studies to possess a wide range of pharmacological activities, such as anti-inflammatory, anti-tumor, anti-cancer, antioxidation, antibacterial, anti-platelet aggregation, anti-nephrotoxicity, anti-urolithiasis, hepatoprotective, and neuroprotective properties. The root of this plant is prescribed internally for the treatment of abnormal uterine bleeding, internal and external hemorrhage, bronchitis, kidney and gall bladder stones, diuretics, dysentery, and other inflammatory diseases, primarily odema, rheumatism, and acites. utilized to reduce blood pressure as well (Deshkar *et al.*, 2008; Patil *et al.*, 2009; Rao *et al.*, 2006; Verma *et al.*, 2016; Wen *et al.*, 2022).

It is an essential component of many Ayurvedic remedies, including the aqueous decoction Manjishthadi Kwath, the powder Manjishthadi Churna, and the ointment Manjishthadi Malahar (Bhatt & Deshpande, 2015). An important Ayurvedic medicine comes primarily from the roots of *R. cordifolia*. Plant drugs are known by several colloquial names, including Indian Madder in English, Mandar, Majathi in Assam, Manjith, Manjistha in Bengali, Aruna, Bhandi, Bhandiralatik in Sanskrit, Manjithi in Malayalum, Manjestha in Marathi, and Majit, Manjit in Hindi (Siril, 2013; Verma *et al.*, 2016).

The liver regulates metabolism, secretion, storage, and detoxification. Liver damage is linked to the disruption of these functions. Agents that protect the liver from hepatotoxins or counteract alterations in antioxidant defence mechanisms are called hepatoprotective (Delgado-Montemayor *et al.*, 2015). Methanolic extract of *R.*

cordifolia showed hepatoprotective properties in rats with liver damage. It reduced high serum Glutamic Oxaloacetic Transaminase (GOT) and serum Glutamate Pyruvate Transaminase (GPT) levels. "Rubiadin," a key component of *R. cordifolia*, also has strong hepatoprotective properties against liver damage caused by carbon tetrachloride in rats. (Rao *et al.*, 2006; Siddique *et al.*, 2022).

R. cordifolia is a traditional analgesic and astringent for treating inflammations, ulcers, and skin conditions. Studies have indicated that it alleviates burning, itching, and skin exudation (Devi Priya & Siril, 2014; Nyeem & Mannan, 2018). Studies on rats with carrageenan-induced paw edema have shown that the water extract of *R. codifolia* has a phenyl butazone-like anti-inflammatory effect (Deshkar *et al.*, 2008).

Significant anticancer efficacy of *R. cordifolia* extract has been observed against a variety of proliferative cells. The root's chloroform fraction contained three components with antiviral properties: mollugin, furomollugin, and dehydro-a-lapchone. Mollugin prevented mast cell degranulation in rats with lymphoid leukemia and had a mitodepressive effect on bone marrow cells in male Swiss mice. When a cyclic hexapeptide compound (RC-18), a pure isolate of *R. cordifolia*, was used to treat experimental mouse cancers, it significantly extended their lifespan (Abderrahman, 2004; Adwankar & Chitnis, 1982; Gupta *et al.*, 1999). The antiproliferative properties were tested on HeLa, ME-180, and HepG2 cells. The root extracts of *R. cordifolia* contained higher levels of antioxidants than the stem and leaf extracts. When prepared in methanol, the root extracts showed the greatest cytotoxicity in HepG2 cells (Humbare *et al.*, 2022).

Research has shown that *R. cordifolia* has antioxidant properties, particularly in preventing glutathione depletion and lipid peroxidation. These properties were found to be dose-dependent and were attributed to components like "Rubiadin" and hydroxy anthraquinones. *R. cordifolia* also exhibited strong free radical scavenging properties and the ability to elevate glutathione (GSH) (Deshkar *et al.*, 2008; Humbare *et al.*, 2022; Rawal *et al.*, 2004; Tripathi & Sharma, 1998).

Significant radio protective ability against radiation-induced lipid peroxidation, hemopoietic damage, and genotoxicity was demonstrated by the alcoholic root extract of *R. cordifolia*. At 72 hours after radiation, its LD50 value was 1200 mg/Kg body weight. Additionally, the extract prevented the production of micronuclei and lipid

peroxidation brought on by radiation. Its anti-inflammatory, metal-chelating, and antioxidant qualities are the mode of action (Tripathi & Singh, 2007; Xavier *et al.*, 2022).

Plant-based dyes offer a wide range of colours and have lasting functional properties such as UV protection, deodorizing, antibacterial, and antioxidant effects (Adeel *et al.*, 2022; Pargai *et al.*, 2020). Natural dyes are easily accessible and environmentally friendly. *R. cordifolia* is the source of an ancient dye based on anthraquinone, which has been widely used in dyeing traditions in Southeast Asia, the Indian subcontinent, and China, along with other botanical species. The roots of *R. cordifolia* can be used to create a dye extract that produces various shades of red. The dye extract contains anthraquinone-based components like rubiadin, alizarin, purpurin, pseudopurpurin, munjistin, nordamncanthal, and xanthopurpurin. Importantly, due to the presence of these anthraquinone components, the root extract has been found to have antibacterial, antioxidant, and anti-inflammatory properties (Do *et al.*, 2023; Schmidt-Przewoźna & Kicińska-Jakubowska, 2023; Yusuf *et al.*, 2013).

Textile dyeing with *R. cordifolia* extract has been documented in a number of investigations. *R. cordifolia* extract with an enzymatic mordant was used to dye silk, resulting in silk with excellent colour strength and fastness (Vankar *et al.*, 2017). The antibacterial activity of the *R. cordifolia* extract against *Staphylococcus aureus* and *Escherichia coli* was also utilized in cotton dyeing to produce the red hues (Boominathan *et al.*, 2022; Rani *et al.*, 2010). A similar range of red and brown hues with a good degree of fastness were obtained when dyeing wool with this anthraquinone-based dye. (Do *et al.*, 2023; Yusuf *et al.*, 2017).

2.2 NANOSTRUCTURES AS ELICITORS

Elicitation is a practical approach for enhancing and producing secondary metabolites. An "elicitor" is a substance that stimulates the production of specific metabolites at optimal concentrations. These compounds promote plant defence by activating secondary metabolism to protect plant cells from stress. This results in a series of reactions, including activating NADPH oxidase, producing reactive oxygen and nitrogen species, expressing defensive genes, and making secondary metabolites. These may include abiotic elicitors such as metal ions and inorganic compounds, as

well as biotic elicitors from sources such as fungi, bacteria, viruses, herbivores, plant cell wall components, or chemicals (Kazmi *et al.*, 2019; Zhao *et al.*, 2005).

In plant cell and tissue culture, NSs can be employed as an abiotic elicitor to induce the production of bioactive chemicals. Nanostructure as an elicitor for triggering the expression of genes involved in manufacturing secondary metabolites have been extensively researched in recent years. Some authors have suggested that NSs generate ROS and secondary signalling messengers, resulting in transcriptional regulation in plant secondary metabolism. Numerous investigations revealed that the application of NS caused ROS to build up in plant cells, resulting in oxidative stress that impacts the primary and secondary metabolism both *in vitro* and *ex vitro* (Rivero-Montejo *et al.*, 2021).

Nowadays, it is crucial to use nanosystems in conjunction with plant tissue culture for things like mass reproduction, conservation, genetic engineering, crop enhancement, and the generation of bioactive compounds. Particularly, nanostructured metal oxide plays a vital role in *in vitro* plant culture. The use of metal oxide nanostructures (MO NSs) has successfully removed microbial contaminants from explants and had a favourable impact on organogenesis, callus induction, metabolic changes, and production of secondary metabolites, somaclonal variation, cryopreservation and genetic transformation. Although all NSs have been used in biotechnology, M NSs are considered the safest because of their stability and other salient features (Álvarez *et al.*, 2019; Das *et al.*, 2023; Kim *et al.*, 2017).

2.2.1 Metal Oxide Nanostructures as Surface Disinfectant and Sterilizer

Micropropagation is a highly successful method for producing a large number of plants quickly. It is also useful for plant breeding. However, one of the biggest challenges it faces is microbial contamination, which can lead to the loss of valuable stocks and the lower plant quality. Therefore, the sterilization of culture material is a crucial step in plant micropropagation. Regulators of plant development and the nutritional elements of the culture medium can, regrettably, lose some of their efficacy when exposed to sterilized media. If NS is used as a culture medium ingredient, it can reduce the cost of micropropagation and improve the quality of plants and in addition it acts as a sterilizer (Prasad *et al.*, 2024; Tung *et al.*, 2021).

Titanium oxide (TiO_2) NS are excellent bactericides with an aseptic effect, with no detrimental impact on callus quality (Mandeh *et al.*, 2012). Cu NS enhanced the surface disinfection of somatic embryos in tuberous begonias (*Begonia* x *tuberhybrida* Voss) in an *in vitro* study conducted by Bao *et al.,* (2022).

Incorporation of Zn NS and ZnO NS on growth media at various concentrations can successfully eradicate microbial contaminants in *in vitro* cultures of Banana with no detrimental effects on regeneration (Helaly *et al.*, 2014). ZnO NS have been shown to reduce contamination and improve the recovery of *Coffea arabica* leaf explants cultivated *in vitro* (Devasia *et al.*, 2020). In Murashige and Skoog (MS) media containing 25 mg/L of ZnO NS, the highest explant recovery was seen (Prasad *et al.*, 2024).

The most harmful endophytic plant-pathogenic fungus, *Colletotrichum gloeosporioides* is responsible for the anthracnose disease that affects many economically significant plants. Through i*n vitro* direct and indirect model systems, bioactive bile salt sodium deoxycholate (NaDC) encapsulated Silver (Ag) NS successfully decreased the endophytic fungus with no damage to treated plants (Shanmugam *et al.*, 2015). Another best result was the effects of Ag NSs antibacterial activity on the *in vitro* establishment of the G N15 (almond-peach hybrid) rootstock in comparison to the control group. Ag NS considerably decreased external and internal contaminations whether incorporated into the culture medium directly or via immersion; however, immersion had less of an impact on bacterial and fungal contamination (Arab *et al.*, 2014). After surface sterilization, treatment with 100 mg/L Ag NS solution resulted in the highest percentage of disinfected explants (89%). The characters measured were unaffected by the Ag NS solution (Prasad *et al.*, 2024).

Ag NS was found to have a high potential for eliminating bacterial contamination from plant tissue culture processes. The change of cell membrane structure and function is just one of the any biological processes that Ag is known to disrupt microorganisms. Although the precise antibacterial action of Ag is poorly known, it also affects the expression of proteins linked to ATP generation (Prasad *et al.*, 2024). Transmembrane ATP synthesis and ion transport across cell membranes are mediated by the proteins. According to Lok *et al.,* (2006), upon engagement, both Ag NSs and Ag (+) ions modify the three-dimensional structure of proteins, beak the

disulfide bonds, and obstruct active binding sites, leading to broad functioning issues within the microbe. Another connection between Ag NS bactericidal action and sugar metabolism blockage has been made. As a result of interacting with Ag NS, the enzyme phosphomannose isomerase (in glycolytic cycle) is rendered inactive and results in diminished sugar metabolism (Bhattacharya & Mukherjee, 2008). According to Dakal *et al.,* (2016) study, the Ag NS-DNA interaction may result in DNA denaturation or shearing as well as halting division of cells.

The elimination of endogenous and foreign contaminating bacteria is essential for the successful tissue culture of all plants. The two types of microorganisms that are most frequently found in plant tissues are fungi and bacteria. The tobacco tissue culture treated with Ag NS had the same outcomes (Abdi *et al.*, 2008; Safavi *et al.*, 2011a; Safavi *et al.*, 2011b). When compared to other antibacterial agents, NSs offers long-term residual that is completely safe and works quickly. This technology might significantly reduce the cost of managing plant diseases, and it would undoubtedly enhance profits in the areas where it is used (Shanmugam *et al.*, 2015).

2.2.2 Metal Oxide Nanostructures in Calli Induction and Organogenesis

MO NSs have garnered considerable interest in agricultural and biotechnological studies owing to their potential utility in plant tissue culture, namely in the stimulation of callus formation and organ development (Dikshit *et al.*, 2021; Mohammadinejad *et al.*, 2019). NSs, particularly those comprised of metals have been investigated for their capacity to impact plant growth and development through several processes (Mahendran *et al.*, 2019). MO NSs can promote the process of cell division and proliferation in plant tissues, which is essential for the development of calli. Nanostructures, because to their huge surface area and tiny size, may easily enter plant cells and interact with cellular components, hence influencing cellular processes (Giorgetti *et al.*, 2011; C. Liu *et al.*, 2021). In some cases, the NS can adversely affect the development of the plant segments. For example, the study investigated the impact of various CuO particles on cell division and gene expression in soybean root tips. It was shown that CuO NS had a strong inhibitory effect on the growth of soybean roots, both in terms of exposure duration and concentration (C. Liu *et al.*, 2021). But on the other hand, Willow trees exhibit no acute toxicity when exposed to TiO_2 NS and there was no significant impact on growth, transpiration, or water use efficiency during the

experiment. These findings indicate that NSs may be advantageous for specific types of plants, detrimental to others, and may have no impact on other species. Response varies based on the characteristics of the NSs and the specific plant it is intended to affect (Seeger *et al.*, 2009)**.** Plant responses to NSs vary widely depending on the NSs' unique properties. The effectiveness of these tiny particles in influencing plants is determined by several factors, including their chemical makeup, size, reactivity, surface coating, and most importantly, the amount applied (Doria-Manzur *et al.*, 2023; Hossain *et al.*, 2015; M. Khan *et al.*, 2021; Prasad *et al.*, 2024).

According to research on *Tecomella undulata in vitro* propagation, Ag NS' ethylene-blocking impact increased the proportion of explants that produced shoots, the mean number of new shoots per explant, and plant longevity (Aghdaei *et al.*, 2012). Incorporation of Zn NS and ZnO NS on growth media in Banana *in vitro* culture resulted in the largest percentage of somatic embryogenesis and had the greatest impact on augmenting the regeneration of plantlets with well-formed root systems at 100 mg/L dose (Helaly *et al.*, 2014). Likewise, ZnO NS had a positive influence on the formation of callus and somatic embryos in *in vitro* cultivated *Coffea arabica* leaf explants, as explained by Devasia *et al.,* (2020). Root induction is enhanced by the modulatory action of ZnO and CuO NSs in MS medium of *in vitro* produced regenerates of *Stevia rebaudiana* (Ahmad *et al.*, 2020). Under *in vitro* conditions, drought stress negatively affected all assessed parameters of strawberry plantlets. Mature embryos of barley were grown in MS medium with TiO_2 NS suspension and have the potential to greatly boost callogenesis and calli size (Mandeh *et al.*, 2012).

Mozafari *et al.,* (2018a) treated their plantlets with iron nanostructures (Fe NSs) and salicylic acid and the result of all parameters of strawberry performed better under harsh situations than untreated strawberry plantlets. Additionally, it had a significant impact on the plantlets' assessed characteristics and growth factors.

The impact of M NSs (Ag, Cu, and Au) in *Artemisia absinthium* seeds that were inoculated on MS medium supplemented with different combinations of M NSs suspension was examined by Hussain *et al.,* (2017) reported that the highest seed germination rates were seen for Ag NSs suspensions. In comparison to the application of Cu NSs and Gold (Au) NSs, significant results were found for root length, shoot length, and Seedling Vigour Index (SVI). Both tobacco callus cultures and rooted

tobacco plantlets absorbed the red nano-sized elemental Selenium (nano Se). Organogenesis and root system growth were promoted by Nano Se (265–530 μM concentration range) (Domokos-Szabolcsy *et al.*, 2012). Plant tissue culture provides a valuable platform for exploring the intricate influence of Ag NSs on plant development. The recently discovered synergy with plant growth hormones offers promising avenues for enhancing plant propagation. When the biosynthesized Ag NSs were added to the tissue culture media, they increased the frequency of callus induction, callus renewal, and rhizogenesis. Upon further analysis of the natural hormone levels within regenerating calli, it was shown that the presence of Ag NSs improved the process of regeneration by reducing the levels of ethylene and abscisic acid in the plant tissue (Manickavasagam *et al.*, 2019). However, delving deeper into the underlying mechanisms and potential side effects is paramount for responsible and sustainable utilization of this exciting technology. In *Lamprocapnos spectabilis* 'Valentine,' the growth of shoots and the multiplication ratio are stimulated by the addition of Au NSs to the culture media, particularly at 75 ppm. Further encourage the growth of roots length and its branching (Kulus *et al.*, 2022).

Dehkourdi and Mosavi (2013) examined the impact of nano priming on parsley germination parameters in tissue culture. The addition of nano-anatase (TiO_2 NSs) resulted in significant improvements in various growth parameters of seedlings, including germination percentage, germination rate index, root and shoot length, fresh weight, vigour index, and chlorophyll content. The optimal nano-anatase concentration was 30 mg/mL. CuO NSs showed a significant effect on plant growth parameters for the regeneration of *Oryza sativa* and it has the nutritive properties at the nanoscale (Anwaar *et al.*, 2016). When utilised in nutritional mediums during clonal reproduction of *Mentha longifolia*, Copper and Cobalt NSs boost the plant's shoot quantity, height, internode quantity, growth index, and reproduction coefficient (Talankova-Sereda *et al.*, 2016).

The effects of single or mixed Au and Ag NSs on *Prunella vulgaris* callus growth were examined by (Fazal *et al.*, 2016). In comparison to the control, callus proliferation was increased by the Ag, Ag-Au NSs and NAA. When Au NSs were added to the culture medium, the maximum biomass was obtained.

A study by Ibrahim *et al.,* (2019) investigated the effects of Cu NSs (20–40 nm) on *Ocimum basilicum* plant regeneration by somatic embryogenesis. The outcomes clearly demonstrated that the addition of Cu NSs (5 M) boosted both the average number of regenerated plantlets and the percentage of explants that produced somatic embryos. In plant tissue culture, Titanium trisulphide nano ribbons have an impact on the downy birch and poplar-aspen hybrid. (Zakharova *et al.*, 2021) have discovered that this specific nanomaterial works well both as a sterilising and stimulating agent during the early growth stage and as a rhizogenesis-activating agent during the rooting stage.

Adding 20 mg/L of Cerium oxide (CeO_2) NS and 50-500 mg/L of Indium oxide (In_2O_3) NS to ½ MS medium increased biomass accumulation in *Arabidopsis thaliana* (Ma *et al.*, 2013). Studies show that CeO_2 NSs enhance root elongation and biomass in soybeans when exposed to a concentration range of 500-4000 mg/L. CeO_2 NSs also significantly improve tomato yield at 10 mg/L. CeO_2 NSs alter the nutritional profile and physiology of wheat and enhance biomass and growth in response to different CeO_2 NSs treatments (López-Moreno *et al.*, 2010; Rico *et al.*, 2014).

Aluminum oxide (Al_2O_3) NSs had varied effects on the growth traits and physio-biochemical activities of plants. Abdel Latef *et al.,* (2020) found that a 0.01% concentration of Al_2O_3 NSs had the most significant impact on Egyptian roselle cultivar plants. Similarly, Amist *et al.,* (2017) reported that lower doses of Alumina NSs improved the growth, pigments, sugar, and protein contents of cabbage (*Brassica oleracea* var. *capitata*) seedlings. Si NSs were studied for their effect on cucumber plants under water deficit and salinity stresses. Results showed that 200 mg/Kg of Si NSs significantly improved plant growth and productivity in terms of height, chlorophyll content (Alsaeedi *et al.*, 2019). It was reported that Zirconia (ZrO_2) NSs can enhance the germination of *Berberis vulgaris* and *Eruca sativa* (Jalill *et al.*, 2017).

Fe NSs and TiO_2 NSs have positive effects on plant growth, depending on their concentration. Low concentrations of Iron oxide NSs promote root development and seed germination and enhance chlorophyll content in certain plants, such as *Capsicum annuum, Solanum lycopersicum*, and soybeans. TiO_2 NSs enhance photosynthetic efficiency in *Spinacia oleracea* L., *S. lycopersicum*, and *Cucumis sativus* plant species (Ovais *et al.*, 2020). ZnO NSs or Fe_2O_3 NSs priming for 24 hours improved wheat seed growth, chlorophyll contents, and gas exchange. ZnO NSs also reduced lipid

peroxidation and increased photosynthetic pigments in *Coriandrum sativum* (Prasad *et al.*, 2024; Pullagurala *et al.*, 2018; Rizwan *et al.*, 2019).

2.2.3 Metal Oxide Nanostructures on Enhancement of Secondary Metabolites

All plants produce secondary metabolites, which are challenging to extract and purify since they are frequently unique to a single species or genus under particular environmental conditions. Since ancient times, secondary metabolites have been important in medicine. The poor output of metabolites is a significant barrier to the manufacture of secondary metabolites using plant cell culture technologies (Rao & Ravishankar, 2002; Shilpa *et al.*, 2010). One of the main methods for increasing the supply of secondary metabolites has been the use of elicitors in cell cultures. As per recent investigations, M NSs may be employed as a potential elicitor to boost the synthesis of bioactive plant metabolites, (Prasad *et al.*, 2024; Radman *et al.*, 2003; Rivero-Montejo *et al.*, 2021).

Elicitors can be abiotic stressors and biostimulants, which are products that are designed to enhance plant nutrition, production, and other aspects. Stress is the main trigger for plants to release active secondary metabolites, and a range of elicitors can mimic stress by triggering the plant's active chemical defenses. Secondary signalling messengers that result in transcriptional control of plant secondary metabolism have been suggested by certain authors as being induced by NSs. Significant second messengers (ROS and calcium ions (Ca^{2+})) that cause the up-regulation of transcriptional regulators of secondary metabolites (Anjum *et al.*, 2019; Marslin *et al.*, 2017; Rivero-Montejo *et al.*, 2021).

A study compared the effects of ZnO NSs and TiO_2 NSs on beetroot plants. It found that ZnO NSs significantly impacted plant growth and reduced disease indices more effectively than TiO_2 NSs. This was due to increased Phenylalanine Ammonia Lyase (PAL) activity, leading to the overproduction of coumarin, cinnamic acid, chlorogenic acid and lignin compounds (Siddiqui *et al.*, 2019). Another study found increased gallic acid synthesis in *Hyoscyamus reticulatus* hairy root culture when treated with 100 mg/L of ZnO NSs for 72 hours, resulting in 1.67 mg gallic acid/g fresh weight (Asl *et al.*, 2019). In a study on *Lavandula viridis* and *Thymus lotocephalus*, it was found that high concentrations of ZnO NSs increased rosmarinic acid in *T.*

lotocephalus but reduced total phenolic content in *L. viridis*, showing variation in nanoparticle effects across plant species (Gonçalves *et al.*, 2021).

The most significant secondary metabolite in *Aloe vera* L is called Aloin. The findings demonstrated that nano silver treatment of *Aloe* suspension cell cultures caused the aloin content to rise to 43.7 percent in 48 h following treatment before progressively declining and reaching the control level. A 48 h Nano-TiO_2 treatment produced the most aloin, which was reduced to a lower level at 168 h (Raei *et al.*, 2014). The modulatory effect of CuO NSs (up to a 20 mg/L dosage) and ZnO NSs (up to a 2 mg/L dosage) applied to the MS culture medium of *in vitro* grown regenerants of Candy leaf noticeably triggered biochemical profiling. Total phenolic, total flavonoid content, steviol glycosides concentration and 2,2-diphenyl-1-picryl hydrazyl-free radical scavenging activity were calculated to be the highest (Ahmad *et al.*, 2020). M NSs, specifically Ag, Cu, and Au, showed an increased secondary metabolite production, total phenolic and flavonoid content, antioxidant, superoxide dismutase (SOD) activity, and total protein content (Hussain *et al.*, 2017). Cu and Cobalt (Co) NSs intensified the essential oil production in *Mentha longifolia* (Talankova-Sereda *et al.*, 2016). Likewise, Ag NSs as the elicitor that can induce the production of secondary metabolites of *Catharanthus roseus* L., which incite defence responses. High content of vinblastine was seen in those explants treated with 75 mg/L Ag NSs (Shahin, 2018). The transcription factor WRKY1 in *Momordica charantia*, which is involved in secondary metabolism and growth regulation, was upregulated as a result of the administration of nano Se to the culture medium. These can boost the immune system, development and plant productivity (Rajaee *et al.*, 2020). The Ag-Au NSs in combination with NAA induced maximum accumulation of phenolics and flavonoid content. Moreover, Ag-Au NSs without NAA enhanced antioxidant activity in *Prunella vulgaris* (Fazal *et al.*, 2016).

According to Oukarroum *et al.,* (2013), Ag NSs phytotoxicity was mediated by ROS generation because there was a strong association between the reduction in viable cells and ROS generation at doses of Ag NSs up to 10 mg/mL over the course of a week-long treatment period. Lin and Xing (2008) suggested that lipid peroxidation and particle-dependent ROS production took place on the surface of cellular membranes of ryegrass due to ZnO NS phytotoxicity.

Cell cultures of *H. perforatum* were exposed to Ag, Au, Cu, Pd (Palladium), CeO_2, CuO, TiO_2, and ZnO NSs to study the changes in secondary metabolism. Among the NSs tested, Ag and CuO induced the most significant changes. Ag NSs caused the cellular accumulation of bisxanthone, gancaonin O and fusaroskyrin. Other NSs induced the following compounds the most: hyperxanthone C (Au), apigenin (Cu), emodin (Pd), emodin anthrone (CeO_2), dihydroxydimethoxyxanthone I (CuO), quercetin (TiO_2), and gallic acid (ZnO). Therefore, the types of NSs have varying effects on the secondary metabolites elicitation (Kruszka *et al.*, 2022).

Manganese (Mn) NSs is a less explored NS. Mn_2O_3 (Manganese (III) oxide) NSs, at a concentration of 25 mg/L, promote growth and increase secondary metabolites in *in vitro* culture of *Atropa belladonna* plants by activating antioxidant enzymes (Tian *et al.*, 2018). Exposure of *Corylus avellana* cell suspension culture to 5 mg/L Ag NSs significantly increased taxol production (Jamshidi *et al.*, 2016). The biosynthesized Barium oxide (BaO) NSs have shown strong antibacterial, antioxidant, and anti-inflammatory properties, making them a promising candidate for future therapeutic use (Abdullah *et al.*, 2023).

The application of NSs in medicinal plants as a method to boost biological activity without phytotoxicity was demonstrated by current research as a way to promote the manufacture of bioactive chemicals. However, further research is required on the possible impacts of using nanomaterials as an elicitor on ecosystems and human risk (Rivero-Montejo *et al.*, 2021).

2.2.4 Metal Oxide Nanostructures as Biochemical Alterants

The enzyme 1-aminocyclopropane-1-carboxylic acid (ACC) synthase, a pivotal enzyme in the biosynthesis of the simplest olefin ethylene, is significant in *in vitro* culture conditions and can modulate many facets of the plant life cycle. Transgenic plants with altered ethylene levels, such as tomatoes, can be produced by using ACC synthase and ACC oxidase, which silences the expression of endogenous genes, resulting in slow ripening fruits due to very low level of ethylene (Arshad & Frankenberger, 2012; Prasad *et al.*, 2024). In *in vitro* MS medium with Ag NSs may promote explant lifetime and multiplication in regenerated *Tecomella undulate* (Roxb.) Seem. leaves, enhancing survival and delayed explant senescence, according to gene expression patterns of Acetyl-CoA Synthetase (ACS) gene (Sarmast *et al.*, 2015). When

exposed to saline stress, grape softwood cuttings cultures treated with potassium silicate and iron NSs may significantly increase total protein and free proline levels as well as enzymatic antioxidant activity, hence lowering hydrogen peroxide levels. Iron and potassium silicate have been demonstrated to boost potassium levels and decrease sodium content when exposed to salinity stress. The results of this study suggest that the use of micronutrients in stressful situations is a practical and effective strategy to mitigate the negative effects of saline stress (Mozafari *et al.*, 2018b). Bleeding heart's metabolite profile is altered by *Lamprocapnos spectabilis* 'Valentine' in medium-temperature cultivation with Au NSs, and acclimated plants' longevity and quality were increased (Kulus *et al.*, 2022). One of the most significant issues in plant tissue culture is hyperhydricity (HH). The use of biogenic Ag NSs greatly decreased the proportion of HH in MS medium cultures of *Dianthus chinensis* because of the biological activity of Ag^{+} ions and water controlling mechanisms. Also successfully decreased the amount of hydrogen peroxide (H_2O_2). The genetic stability of Ag NSs - directed HH reversed shoots was observed (Sreelekshmi *et al.*, 2022). The physiology of tobacco plants, including their levels of total soluble sugars, chlorophyll, carotenoid, and flavonoids, was reported to be improved using 20 mg/L of TiO_2 NSs in comparison to untreated controls (Sompornpailin & Chayaprasert, 2020). Carotenoids, chlorophyll A and chlorophyll B are increased in the date palm cultivar Hayani's culture medium when 3.0 ml/L Ag NSs are present. Additionally, the proline, protein, and carbohydrate contents have all increased (Elsayh *et al.*, 2022). The nutraceutical business can profit from MO NSs as they can improve the generation of bioactive metabolic components from medicinal plants in *in vitro* batch cultures (Ahmad *et al.*, 2020). Nickel oxide (NiO) NSs exposure on Chinese cabbage led to enhanced expression of genes related to oxidative stress and phenolic compounds (Chung *et al.*, 2019).

2.2.5 Metal Oxide Nanostructures in Somaclonal Variation

For every micropropagation system, the development of somaclonal variation is a major subject of concern. The term "somaclonal variation" refers to phenotypic and genotypic differences brought by tissue culture. Kokina *et al.,* (2017) investigated how *Linum usitatissimum*'s somaclonal variation was impacted by Au and Ag NSs. Both calli and regenerants grown on media containing Au and Ag NSs had a higher incidence of somaclonal variation. Au and Ag NSs use in tissue culture has expanded recently,

although it's still unclear how NSs cause modifications to the DNA. When used in high amounts, Au NSs (a substance that acts as a mutagen) can cause genetic diversity. The induced metabolic and genetic changes can modify the phenotypic characteristics of *Lamprocapnos spectabilis*, resulting in the development of new cultivars (Kulus *et al.*, 2022). Through cytosine DNA methylation, nano Se supplementation in bitter melon was linked to an epigenetic response, and the treatments elevated genes like PAL and 4-coumarate: CoA-ligase (4CL) (Rajaee *et al.*, 2020). The DNA changes and mutations in four rice genotypes caused by SiO_2 NSs were analyzed and somaclonal variations using RAPD (Random Amplified Polymorphic DNA) and SSR (Simple Sequence Repeat) analyses. Genotype significantly affected callus induction and plant regeneration. The genome template stability percentage (GTS%), reflecting changes in RAPD profiles (DNA based techniques used to evaluate the variation at the DNA sequence level), was the most sensitive endpoint. Two SSR markers generated polymorphism, aiding in rice plant breeding for drought tolerance (Aboulila & Galal, 2019).

2.2.6 Metal Oxide Nanostructures in Genetic Transformation

Plant genetic engineering, a modern innovation in plant science, serves as a significant tool for enhancing yield, crop quality, secondary metabolite levels in medicinal plants, and cultivating crops suited for sustainable agriculture (Cardoso *et al.*, 2019; Niazian, 2019). M NSs can augment the efficacy of genetic transformation in plants by facilitating the absorption and incorporation of exogenous DNA into plant cells (Cunningham *et al.*, 2018).

A new method using NSs for gene transformation in plants accurately transports DNA or RNA, enabling transient or stable transformation. NS-mediated gene transformation gets around the barrier of the plant cell wall (Lv *et al.*, 2020). This process can result in the creation of transgenic plants possessing advantageous characteristics, which can be valuable for enhancing crop quality. A novel method utilizing NS-mediated gene transformation offers a solution to the challenge posed by the plant cell wall, facilitating precise delivery of DNA or RNA into plants for the production of transient or stable transformation (Lv *et al.*, 2020; Mali *et al.*, 2020). For the delivery of nucleic acids in plant cells, several NSs such as mesoporous silica NSs, magnetic NSs, carbon nanotubes, etc., have been used recently (Jat *et al.*, 2020).

Magnetofection is a drug delivery method using magnetic NSs to transfer genes into the cell nucleus. Magnetic NSs Fe_3O_4 and Fe_2O_3 are ideal for various applications due to their thermal stability, large surface area, small size, stability and low toxicity (Lv *et al.*, 2020). Zhao *et al.,* (2012) created a method that uses magnetic NSs to create transgenic seeds. A magnetic field was used to push the plasmid DNA into the pollen after it had been enclosed in magnetic NSs. The resulting transgenic cotton generated seeds with stable inheritance of the transformed DNA.

Research on plants can benefit from leaf protoplast isolation. Standard reference techniques for isolating protoplasts are laborious, damaging cells, generate minimal amounts of material, time consuming, and are prone to microbial contamination. The addition of 10 mg/L Ag NSs to leaf incubation buffer during protoplast isolation produced 3 h of protoplast isolation that produced 34% viable protoplasts. This is the first account of the manufacture of Ag NSs from used plant media, which was used to sterilize explants and quickly isolate protoplasts (Bansod *et al.*, 2015). Through the use of a gene gun, Vijayakumar *et al.,* (2010) showed that carbon-supported Au NSs can transfer DNA into plants such as *Nicotiana tabacum*, *Oryza sativa*, and *Leucaena leucocephala* with minimal damage to the cells and with less Gold and plasmid, thus encouraging plant regeneration and transformation frequency. The authors Torney *et al.,* (2007) demonstrated how mesoporous silica NSs may be used to transport DNA into tobacco protoplasts by endocytosis. They achieved this by utilizing Au-capped mesoporous silica NSs to deliver DNA and chemicals into the callus and leaves using a biolistic gun. Antibiotics used in Agrobacterium-mediated transformation can negatively impact the regeneration potential and genetic stability of regenerated plantlets due to their phytotoxic effects on explants. According to *Agrobacterium tumefaciens* and *A. rhizogenes* growth was entirely inhibited on Luria-Bertani (LB) medium with Ag NSs. The scientists also showed that the co-cultivation of *Tecomella undulata* and tobacco with *Agrobacterium* led to the successful elimination of bacteria with the addition of Ag NSs to the culture medium.

2.2.7 Metal Oxide Nanostructures in Cryopreservation

The process of preserving plant genetic resources for a long term by storing cell lines, tissues, organs, calli, etc. at a temperature of liquid nitrogen (-196°C) is called cryopreservation (Kaviani, 2011). The addition of NSs to the cryoprotectant process

can improve thermal conductivity and viscosity, induce vitrification, suppress devitrification, and enhance solution stability during rewarming (Wang *et al.*, 2015). The unique thermal properties of NSs have significant potential in cryobiology, such as preventing the formation of ice crystals at temperatures below zero (Hou *et al.*, 2018). In addition, NSs also maintain the recovery potential of explants upon introduction to the plant tissue culture medium, protective bead matrix, or to the recovery medium (Tymoszuk & Miler, 2019).

The culture medium and preserving medium of *Pinus radiata* embryogenic cell lines were supplemented with Ag NSs and stored at -80°C, resulting in a 75% recovery rate (Tpu, 2018). Researchers used *in vitro*-derived shoot tips of *Lamprocapnos spectabilis* 'Valentine' and cryopreserved them with Au NSs added either into the preculture medium, the protective bead matrix, or the recovery medium. The study found that adding 10 ppm of Au NSs into the alginate bead matrix improved the recovery level of LN-derived shoot tips (70.0%) compared to the non-NSs-treated cryopreserved control (50.5%). However, adding NSs to the recovery medium had a negative effect on the survival of explants. Moreover, adding Au NSs affected the enzymatic activity in *L. spectabilis.* Adding Au NSs at a lower concentration (10 ppm) into the protective bead matrix can significantly improve the cryopreservation efficiency in *L. spectabilis* without altering the DNA sequence (Kulus & Tymoszuk, 2021).

2.2.8 Secondary Metabolites Biosynthesis and Biomass Accumulation Using NSs

Elicited *in vitro* cultures are valuable sources of secondary metabolites used in various industries. Biomass accumulation and metabolite biosynthesis are two-stage processes. The first stage involves controlling the growth and multiplication of cells/organs, while the second stage focuses on the biosynthesis of metabolites (Murthy *et al.*, 2014).

The highest levels of phenolics and flavonoids production were observed in Ag and Au NSs and NAA-exposed cell suspension cultures of *Prunella vulgaris*, leading to enhanced biomass accumulation (Fazal *et al.*, 2019). Hayat *et al.,* (2021) found that combining Ag and Cu NSs with thidiazuron (TDZ) stimulated biomass accumulation and increased total phenolic and flavonoid contents in callus cultures of *A.*

absinthium. Similar results were observed in callus cultures of *Fagonia indica*, which were stimulated with various concentrations of bio-Ag NSs (Begum *et al.*, 2020).

However, there exists an inverse relationship of biomass accumulation and secondary metabolism. Biomass of plantlets was somehow affected on high concentrations of NSs. Fatima *et al.,* (2020) studied the effects of ZnO, CuO, and CoO NSs on *Artemisia annua* callus culture. They found that high NS concentrations affected callus biomass. The maximum fresh weight of the shoot callus was achieved at 0.01 mg/L NSs concentration. Increasing NS concentration decreased callus biomass but positively affected the induction of secondary metabolites in the plant. The treatment with Ag NSs had an almost insignificant effect on the fresh and dry weight of the biomass of calli. However, the increase in the concentration of Ag NSs was inversely proportional to the contents of the estimated secondary metabolites in the calli of *Balanites aegyptiaca*. The lower concentration of Ag NSs (1 mg/L) resulted in the highest saponin content (70.57 ± 0.00 mg/g dry callus tissues), while the higher concentration (20 mg/L) led to the lowest saponin content (61.22 ± 0.01 mg/g dry callus) (Ebad *et al.*, 2019).

Pharmaceuticals are produced in plants through *in vitro* cultures using a multi-step process that involves both growth and metabolite production phases. Early in the cultivation process, low metabolite production may coexist with high productivity. Later, biomass production may decrease, and metabolite production may increase (Isah *et al.*, 2018).

2.3 BIOSYNTHESIS AND CHARACTERIZATION OF NANOSTRUCTURES

NSs can be synthesized using physical, chemical, or biological (green synthesis) methods. The biological method is the most stable, convenient, faster, eco-friendly and sustainable considering its advantages over other methods. Biological methods include using plants, plant extracts, plant wastes, enzymes, algae, fungi, and microorganisms (Prasad *et al.*, 2019; Ying *et al.*, 2022). Green synthesis involves reducing metal ions and stabilizing them into NSs using plant extracts. Green-synthesized NSs have shown better bioactivities than chemically synthesized ones, due to the presence of plant-derived compounds. These NSs have potential in capturing valuable molecules and drug discovery (Marslin *et al.*, 2018).

Plant mediated synthesis of M NSs is gaining importance owing to its simplicity, rapid rate of synthesis of NSs of diverse morphologies and eco friendliness. The process for synthesizing NSs is similar for microorganisms and plants. Metal salts containing metal ions are reduced to atoms using a reducing agent, forming clusters by nucleation and growing into particles. According to (Shankar *et al.*, 2003) the terpenoids in *Geranium* leaves, contribute to reducing Ag ions. Fourier transform infrared spectroscopy (FTIR) analysis showed that chlorophyll's ester C=O group acts as a reducing agent, and a protein is involved in capping Au NSs synthesized using *Geranium* leaf extract. Similarly, ZnO NSs were synthesized using the root extract of *R. cordifolia* (Prachi *et al.*, 2017) and the extract of *Hydnocarpus alpina* (Ganesh *et al.*, 2019). Nanostructured CuO particles were obtained from *Aloe vera* leaves (Gunalan *et al.*, 2012) and from the aqueous extract of *Cordia sebestena* flowers (Prakash *et al.*, 2018). "Green" methods using plant biomasses or extracts as reducing agents are gaining interest in synthesizing M NSs (Punjabi *et al.*, 2015).

Mittal *et al.,* (2014) investigated the formation of Ag NSs using *Syzygium cumini* fruit extract. They conducted solvent partition and found that the ethyl acetate fraction yielded the most Ag NSs. They isolated two non-polar fractions that produced a good yield of Ag NSs. FTIR, GC-MS and HR-MS analysis, revealed flavonoids as the major components responsible for the synthesis of NSs. They hypothesized a mechanism involving the reduction of cationic silver to metallic silver by the flavonoid compounds through a redox reaction. Additionally, biomolecules from the fruit extracts were responsible for the aggregation and stabilization of the Ag NSs.

The unique attributes of M NSs enable them to penetrate plant cells and tissues quickly. Nanostructures can be absorbed by plants in three primary ways: through a foliar spray, through the soil, and using the artificially created nutritional medium. Following penetration of the cell wall, NSs have the potential to be transferred between cells through either the apoplastic or symplastic pathways. Once internalized, NSs have the potential to disrupt the metabolism of plants. In hydroponic settings, the roots and shoots of *Zea mays* plants exhibited the highest concentration of ZnO NSs following their exposure to M NSs. This is probably because Zn^{2+} ions are more soluble in the rhizosphere, plant uptake, and translocation (Lv *et al.*, 2015).

A generalized interpretation of the mechanism of NSs biosynthesis is, involvement of proteins like enzymes and cofactors that have redox potential as well as act as electron shuttles play key role in metal reduction. The different biomolecules in plant extracts act as reducing and stabilizing agents that play a key role in synthesizing NSs. The type and morphology of NSs are influenced by the nature and source of the plant extract, as well as the physical and chemical factors such as metal ion concentration, pH, temperature, and incubation time (Kumar & Seth, 2021).

The characterization of NSs provides the knowledge of NSs morphology, composition, and coating. The various instruments used for NSs' characterization are UV-vis spectroscopy, X-ray diffraction (XRD), Fourier transforms infrared spectroscopy, Energy dispersive spectroscopy X-ray (EDX), Scanning electron microscopy (SEM), and Transmission electron microscopy (TEM) (Joshi *et al.*, 2008).

Spectroscopic techniques provide information about the optical properties, state, nature, and functional groups of NSs. UV-vis spectroscopy is primarily used to characterize NSs and provides insight into particle aggregation and optical properties (Kumar & Seth, 2021). The aqueous leaf extract of *Euphorbia hirta* changed colour from pale yellow to purplish red when 1 mM $HAuCl_4$ (Chloroauric acid) was added, confirming the formation of Au NSs. $HAuCl_4$, with free electrons, produced a Surface Plasmon Resonance (SPR) absorption band at 530 nm in UV-Vis spectra due to the combined vibration of electrons of metals in resonance with the light wave (Annamalai *et al.*, 2013). Din *et al.,* (2018) used *Calotropis gigantea* leaf extract to synthesize Ni and NiO NSs. The UV-vis spectrum showed a sharp exciton absorption peak at 415 nm, indicating the stability of the green-synthesized NiO NSs.

XRD gives information about crystallinity, crystallite size, and phase composition of NSs (Hassellöv *et al.*, 2008). The crystalline nature and average size of biogenic Ag NSs from *Enicostemma axillare* leaf extract was confirmed by the examining of XRD pattern. The XRD spectrum shows prominent peaks at 2q = 38.12, 46.28, 64.04, and 76.84, representing the (111), (200), (220), and (311) Bragg's reflections of the face-centred cubic structure of Silver. The diffraction peaks are broad, indicating a small crystalline size. The lattice constant calculated from this pattern was a = 3.87 Å. The average size of the Ag NSs was estimated to be between 16 and 31 nm (Raj *et al.*, 2018).

FTIR spectra helps to determine the reducing agent and the capping agent responsible for the synthesis and stability of NSs (Shankar & Rhim, 2014). *Suman et al.,* (2013) used FTIR measurements to identify biomolecules in *Morinda citrifolia* root extract responsible for capping and stabilizing Silver NSs. The FTIR spectrum of the NSs showed peaks corresponding to various functional groups such as –OH, C–H, C=O, and C-C, indicating the presence of flavonoids, terpenoids, and proteins. This suggests that these biomolecules are responsible for capping and stabilizing the NSs. In another study *Calotropis gigantea* leaf extract used to synthesize Ni and NiO NSs. The FT-IR spectra of both Ni and NiO NSs did not show a peak around 1000–1100 cm^{-1}, while the peak for the O–H bond got reduced in the Ni NSs FTIR spectrum and almost completely reduced in the NiO NSs FTIR spectrum, suggesting the important role of alcohols and halogens in metal ion reduction. Amines also played a role as a capping agent in the fabrication of Ni-NSs (Din *et al.*, 2018).

Microscopic Techniques generally used to analyze size, shape, and particle aggregation of NSs (Calzolai *et al.*, 2012). This technique requires no standard as in other techniques above. The SEM gives the images to identify the size and shape of metal NSs by scanning sample surface with a high-energy beam of electrons and gives a two-dimensional imaging. In a study, ZnO NSs were synthesized using *Thymbra Spicata* plant extract. The researchers observed homogeneously distributed Zn NSs with sizes between 6.5 nm and 7.5 nm (Gur *et al.*, 2022). In another study, ZnO NSs created with extracts of *Elaeagnus angustifolia* flowers displayed irregular and almost spherical morphology in SEM images (Singh *et al.*, 2016).

Energy Dispersive X-ray Spectroscopy (EDX) used in conjunction with SEM, this technique identifies the composition of a sample, improving quality control and process optimization (Joshi *et al.*, 2008). Muthukrishnan *et al.,* (2015) produced Ag NSs from leaf extracts of *in vitro*-raised plants of *Ceropegia thwaitesii,* and the EDX analysis confirmed the presence of Ag NSs with strong signal energy peaks in the range of 2.5–3.5 keV.

TEM is the most efficient and widely used technique for the characterization of NSs (Sharma *et al.*, 2019). The TEM images give an idea about the size, aggregation and orientation of NSs (Sang & Lebeau, 2014). TEM analysis of *Calotropis gigantea* mediated TiO_2 NSs showed particles having spherical and diamond shapes with an

average diameter of 160–220 nm (Marimuthu *et al.*, 2013). Sharma *et al.,* (2015) synthesized CuO NSs from the aqueous extract of *C. gigantea* leaves and conducted TEM analysis. The analysis revealed the spherical shape of CuO NSs with a particle size of up to 20 nm.

DTG is an analytical technique that measures weight loss of a material as a function of temperature, to determine the kinetic parameters of organic materials (El-Sayed *et al.*, 2014). The TGA and DTG data for organic compounds from *Trigonella foenum-graecum* and Onion peel extract show that these compounds reduce Fe^{3+} and Au ions to form stabilized nanoparticles. The TGA-DTG curves indicate weight loss up to 530 °C, mainly due to the evaporation of water and residual organic molecules. (Patra *et al.*, 2016; Radini *et al.*, 2018).

Raman spectroscopy is a non-destructive technique that reveals the chemical composition, structure, and size of MO NSs without specific preparation. By illuminating the sample with laser light and measuring the scattered light, Raman spectra provide information on the vibrational modes of the molecules, helping to identify the types of chemical bonds present (Chourpa *et al.*, 2005; Fernandez-Garcia *et al.*, 2004; Testa-Anta *et al.*, 2019b). The Raman spectrum of biosynthesized CeO_2 NSs shows a Ce-O stretching band at 459 cm^{-1} (Miri & Sarani, 2018). Se NSs produced by *Azospirillum thiophilum* displayed a strong Raman band at 250 cm^{-1} in the lower frequency region, corresponding to the A_1 stretching mode of the Se–Se bond, indicating the presence of amorphous Selenium (Tugarova *et al.*, 2018).

2.4 PHYTOCHEMICAL INVESTIGATION OF MEDICINAL PLANTS AND SCREENING FOR BIOACTIVITY

The wide variety of phytochemicals found in plants can indicate their pharmacological activities (Koche *et al.*, 2016). While modern techniques are used to detect these phytochemicals, traditional tests are still valuable for initial screening. After extracting the crude or active fraction from source plants, simple and inexpensive analyses can be used to identify the phytochemical composition of secondary metabolites, including alkaloids, amino acids, carbohydrates, coumarins, flavonoids, glycosides, saponins, reducing sugars, steroids, tannins, terpenoids, quinones, and volatile oils (Banu & Cathrine, 2015; Florence *et al.*, 2015; Sasidharan *et al.*, 2011).

The quantification of detected phytochemical groups validates the initial screening analysis (Rajani & Kanaki, 2008).

Spectrophotometric methods are used to determine the Total Phenolic Content (TPC), Total Flavonoid Content (TFC) and antioxidative activity. Multi-development High-Performance Thin Layer Chromatography (HPTLC) enabled chemical fingerprinting that can be used to differentiate between species (Ibragic *et al.*, 2021). Additionally, biochemical and target-based Liquid Chromatography-Mass Spectrometry (LC-MS) analysis are conducted to identify and quantify various phytochemicals (Choudhury *et al.*, 2020). Raman spectroscopy is utilised to rapidly identify and characterize phytochemicals present in plants without laborious sample preparation (Gunawardana *et al.*, 2022).

2.4.1 Phytochemical Screening

The preliminary phytochemical screening of the secondary metabolites presents in the whole plant extract of *R. cordifolia* was done by Kannan *et al.,* (2009). Humbare *et al.,* (2022) showed positive for alkaloids, glycosides, saponins, tannins, flavonoids, phenols, terpenes, carotenoids and quinones. Chandrashekar *et al.,* (2018) reported the major phytochemicals such as combined anthraquinones, free anthraquinones, alkaloids, steroids, flavones, flavonoids, phenols, saponins, tannins, proteins, and glycosides in methanolic root extract of *R. cordifolia*. Jeruto *et al.,* (2011) conducted phytochemical screening following the methods proposed by Harborne in 1984 and 1973. All plants were found to contain alkaloids, terpernoids, saponins and flavonoids except for the absence of saponins in root extracts of *R. cordifolia* and *C. myricoides* and flavonoids in leave extracts of *L. calostachys* and *A. remota*.

M. S. Khan *et al.,* (2021) analyzed the TPC and TFC in different fractions of *R. cordifolia*. The results show that the TPC in methanolic extract, ethyl acetate fraction, and n-butanol fraction of *R. cordifolia* have 99.732 ± 0.938, 207.306 ± 0.730, and 119.120 ± 0.893 (µg/mg GAE), respectively. The TFC values for the same fractions are 96.564 ± 0.996, 195.224 ± 0.940, and 76.848 ± 0.519 (µg/mg QE), respectively. Another study analyzed the phytochemical composition of *Rubia tinctorum* extracts, finding phenols, alkaloids, coumarin, flavonoids, and tannins in both root and aerial part extracts. The root extracts are rich in phenolic compounds (118.38 mg GAE/g) and

flavonoids (45.29±0.04 mg GAE/g), while the aerial part extract has the highest levels of tannins (134.1±0.1 mg GAE/g) (Houari *et al.*, 2022).

Quantitative phytochemical assay done on eggplant (*Solanum melongena*) seedlings treated with NS (NiO, CuO, and ZnO) and untreated seedlings. The TPC in all NS treatments was higher than in the control eggplants. TPC values increased with NS concentration up to 500 mg/L, then declined at 1000 mg/L. ZnO treatment had the highest TPC content at 180 µg/g, followed by NiO at 130 µg/g and CuO at 120 µg/g. Similarly, TFC was higher in all NS-treated samples compared to the control. TFC levels increased with NS concentration up to 500 mg/L, then decreased at 1000 mg/L. ZnO treatment had the highest TFC content at 302 µg/g, followed by NiO at 200 µg/g and CuO at 185 µg/g at 500 mg/L (Baskar *et al.*, 2018). Saeed *et al.,* (2021) found that green-synthesized ZnO NSs enhanced the accumulation of phenolic (12.3 mg/mg DW) and flavonoid (2.8 mg/mg DW) contents in callus cultures of *Silybum marianum*.

2.4.2 Chromatographic Analysis

Chromatography is an important biophysical technique that enables the separation, identification, and purification of the components of a mixture for qualitative and quantitative analysis. Chromatography is a method used to separate compounds based on their size, shape, charge and binding capacity with the stationary phase (Coskun, 2016). Chromatographic techniques, such as Gas Liquid Chromatography (GLC), Thin Layer Chromatography (TLC), High Performance Thin Layer Chromatography (HPTLC), High Performance Liquid Chromatography (HPLC), and Column Chromatography (CC), are commonly used to separate and purify various phytoconstituents (Patil *et al.*, 2020; Ramraje *et al.*, 2020). TLC is a rapid, flexible, and easy separation technique that provides initial qualitative data on the phytochemical composition (Waksmundzka-Hajnos *et al.*, 2022). The basis of solid-liquid adsorption chromatography lies in the interaction between a thin layer of adsorbent and the chosen solvent (Sherma & Fried, 2003). HPTLC, a solid-liquid adsorption chromatography technique, offers improved separation, repeatability, and sensitive phytochemical detection compared to TLC methods. This is due to the interaction between a thin layer of adsorbent and the chosen solvent techniques (Gbaguidi *et al.*, 2005). HPTLC has been widely used as a quality control tool for the phytochemical evaluation of herbal drugs (Darekar *et al.*, 2009). One major advantage of HPTLC is its capability to

simultaneously analyze multiple samples using a small amount of mobile phase (Banu & Nagarajan, 2014).

Marker-based standardization is an essential method for standardizing herbal drugs. A marker compound is a chemically defined constituent of a herbal drug used for quality control and assurance of the finished product (Momin *et al.*, 2011). Shalini and Ilango, (2022) performed HPTLC densitometric analysis of selected Indian medicinal plants and polyherbal mixture to evaluate the presence of lupeol, rutin and shatavarin IV markers. Darekar *et al.,* (2009) suggested using HPTLC as a technique for the routine quality control of *Hemidesmus indicus* root powder. They employed 2-hydroxy-4-methoxybenzaldehyde as a marker. According to Momin *et al.,* (2011) catechin, a significant component of *Acacia nilotica*, can standardize herbal dental gels using the HPTLC method.

Rajopadhye *et al.,* (2011) quantified the amount of piperine in the fruits of *Piper* species, which are commonly used in traditional Indian medicine formulations. They used HPTLC analysis methods to determine that the highest quantity of piperine was found in the fruits of *Piper nigrum*, while the least amount was present in *Piper betle*. Similarly, Srivastav *et al.,* (2024) quantified Gallic acid and Quercetin markers of *Neolamarckia cadamba*, and conducted phytochemical profiling using HPTLC analysis methods.

2.4.3 Spectroscopic Analysis

The combination of chromatographic and mass spectrometric techniques provides information about compounds' structure and molecular weights, depending on the mass analyser used. Liquid chromatography coupled with mass spectrometry has been established as a powerful tool for analysing secondary metabolites in plant extracts (Wu *et al.*, 2013). Raman spectroscopy is a powerful laser technique for identifying analytes and providing detailed vibrational information (Dijkstra *et al.*, 1999).

2.4.3.a LC-MS Analysis

Liquid Chromatography-Mass Spectrometry (LC-MS) is an analytical technique that couple's high resolution chromatographic separation with sensitive and specific mass spectrometric detection (Lim & Lord, 2002). Liquid chromatography coupled to mass spectrometry is preferred for detecting unknown metabolites in crude extracts or complex mixtures (Bowen & Northen, 2010).

Eugenia calycina is a Brazilian fruit used to treat diabetes. The LC-MS-based targeted quantitative analysis showed high phenolic content in its leaves, pulp, and

seeds, with ellagic acid as the main compound. The fruit has high potential as a plant-based food due to its phytochemical profile and phenolic content (Araujo *et al.*, 2020). The extract from *Humboldtia sanjappae* was analyzed using HR-LCMS-Q-TOF, revealing the presence of flavonoids (Naringenin, Luteolin, Pomiferin) and phenols (Epicatechin, Maritemin). Its rich content of polyphenols and flavonoids indicates potential for developing new antibiotics (Sidhic *et al.*, 2023). Rahimmalek *et al.,* (2023) used LC-MS to identify polyphenolic compounds and flavonoids in *Kelussia odoratissima* Mozaff. leaves. The main phenolic compounds found were p-coumaric acid, ferulic acid, caffeic acid, chlorogenic acid, acetyl phloroglucinol, vanillic acid, m-coumaric acid, and 4-methylsiringol. The main flavonoid components were 3-hydroxyflavone, flavone, quercetin, rutin, neohesperidin, polydatin, and diosmin. Chlorogenic acid, neohesperidin, and diosmin were found to be the most abundant. An ethanolic crude extract from *Juniperus chinensis* leaves was analyzed using UPLC-QTOF-MS and UPLC-MS/MS. Ten compounds were identified, including six major bioactive components: isoquercetin, quercetin-3-O-α-l-rhamnoside, hinokiflavone, amentoflavone, podocarpusflavone A, and matairesinoside. The levels of quercetin-3-O-α-l-rhamnoside and amentoflavone in the extract were 203.78 and 69.84 mg/g, respectively (Lim *et al.*, 2023).

2.4.3.b Raman Spectroscopic Analysis

Raman spectroscopy is an optical technique used to analyze the structure and composition of tissues and cells at the molecular level. It is valuable for analyzing plant tissues and identifying compounds in plant cells (Saletnik *et al.*, 2021). It provides unique spectral patterns for organic compounds and functional groups. The intensity of the bands can be used to calculate relative concentration (Gierlinger & Schwanninger, 2007). Live or intact biological material can be analyzed using Raman spectroscopy before it undergoes other destructive techniques (Gunawardana *et al.*, 2022).

Maize seedlings exposed to Ag NSs showed accumulation of Ag NSs in the root epidermis, cortex, and shoot phloem. The Raman signal intensity highly correlated with nanoparticle content (Yilmaz *et al.*, 2021). The Raman spectrum obtained from the poppy milk presents very clearly characteristic morphine bands (peaks at 631, 1620, and 1642 cm^{-1}) (Schulz *et al.*, 2004). Urlaub *et al.,* (1998) analyzed the structure and spatial distribution of naphtylisoquinoline alkaloids in fresh plant material of a tropical liana (*Ancistrocladis heyneanus*) using micro-FT-Raman spectroscopy.

2.4.4 Antioxidant Activity

Different pharmacological assays could predict the potential pharmacological effects of the various phytochemicals (Shaikh & Patil, 2020). The antioxidant potential of *R. cordifolia* was studied and found to have excellent free radical scavenging activities in Ferric Reducing Antioxidant Power (FRAP), 2,2-azino-bis-3-ethylbenzothiazoline-6-sulphonic acid (ABTS), and Diphenyl Picryl Hydrazyl (DPPH) assays (Barlow *et al.*, 2015).

The antioxidant profile of *R. cordifolia* was evaluated using different fractions, and all fractions showed strong antioxidant scavenging effects. The ethyl acetate fraction exhibited the highest activity, followed by the n-butanol fraction, methanolic extract, aqueous fraction, and n-hexane fraction. The IC50 values for these fractions were 48.52, 44.88, 38.19, 36.86, and 34.9 µg/mL, respectively (M. S. Khan *et al.*, 2021). The antioxidant activity of hydromethanolic extracts from the root and aerial parts of *Rubia tinctorum* was investigated. The aerial part extracts showed the highest antioxidant activity for DPPH (83.23%) and FRAP (1.51±0.22) (Houari *et al.*, 2022).

NSs can cause oxidative stress in plants by interacting with cellular components, leading to the formation of ROS. Phenolic compounds, flavonoids, and antioxidant enzymes help mitigate this stress (Corral-Diaz *et al.*, 2014; Kumar *et al.*, 2018).

The DPPH assay was conducted on eggplant (*S. melongena*) seedlings treated with NS (NiO, CuO, and ZnO) and untreated seedlings. The results showed that NS-treated plants had lower radical scavenging values than control plants. ZnO NSs demonstrated higher DPPH activity than NiO and CuO NSs. Additionally, DPPH activity was more pronounced at lower concentrations of ZnO NS-treated seedlings. All NSs reported lower DPPH activity at higher concentrations, with NiO at 1000 mg/L showing the least antioxidant capacity compared to CuO and ZnO NS treatments (Baskar *et al.*, 2018). Metal NSs (Ag, Cu, and Au) significantly affected the radical scavenging activity in *A. absinthium*. Plantlets treated with Au NSs showed the highest DPPH activity (29.21%) compared to other NSs and the control, while Ag NSs reduced the antioxidant activity compared to the other NSs and the control (Hussain *et al.*, 2017).

CHAPTER – 3

MATERIALS AND METHODS

3.1 CHEMICALS AND GLASSWARE USED IN THE STUDY

3.2 GREEN SYNTHESIS AND CHARACTERIZATION OF NANOSTRUCTURES

3.3 STANDARDIZATION OF PROTOCOL FOR SHOOT MULTIPLICATION OF *R. CORDIFOLIA*

3.4 COMPARATIVE PHYTOCHEMICAL ANALYSIS OF *IN VITRO* RAISED STEM, LEAF AND ROOT OF *R. CORDIFOLIA* FOR IDENTIFYING BEST EXTRACTION SOLVENT AND PLANT PART.

3.5 ANALYSIS OF THE GREEN SYNTHESISED NANOSTRUCTURES AS ELICITORS

3.6 STATISTICAL ANALYSIS

The materials used and methodologies adopted for investigating biomass accumulation and secondary metabolite production in *in vitro* cultures of *Rubia cordifolia* during nanostructure elicitation are detailed below (**Figure 1**).

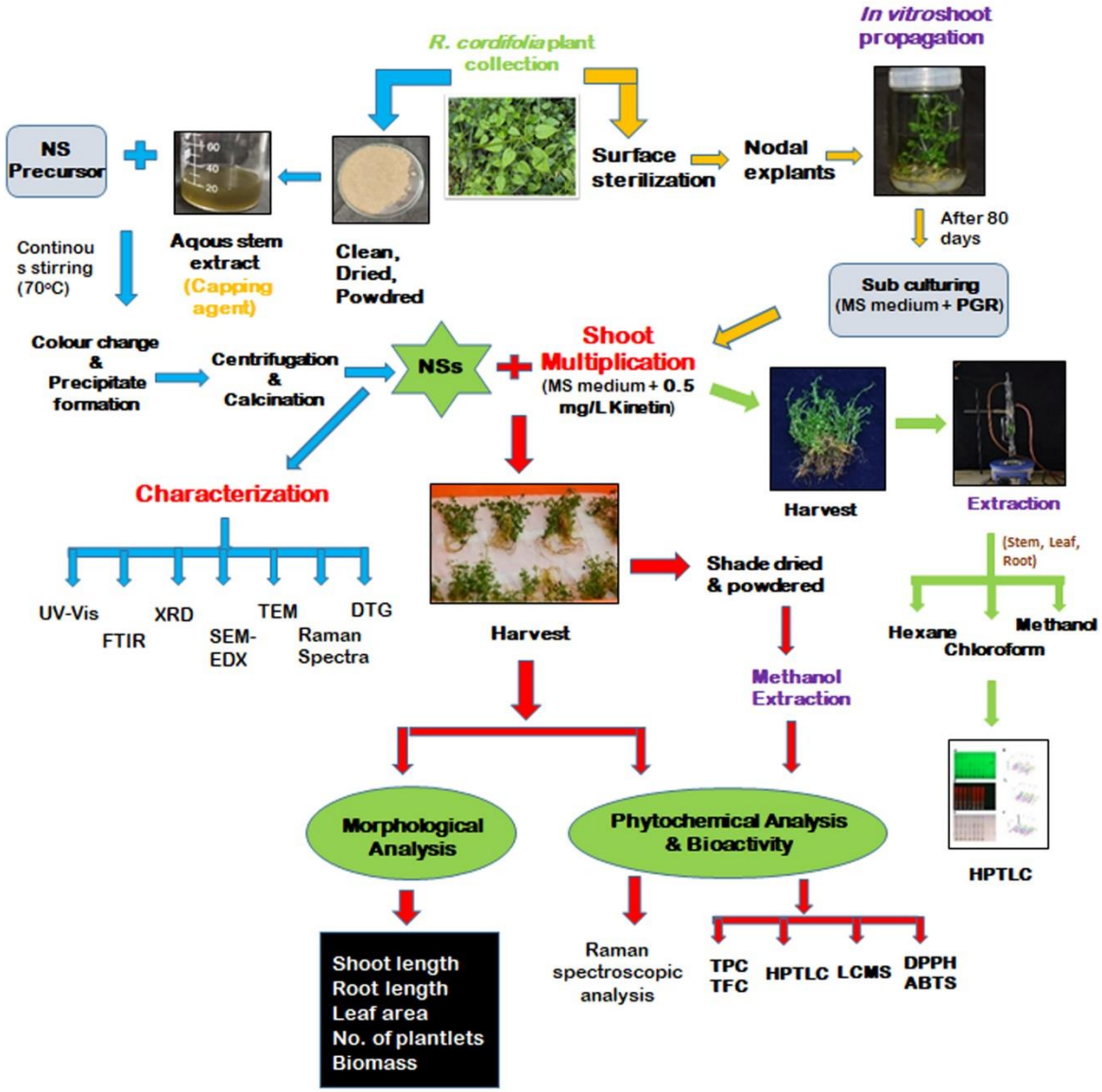

Figure 1: Schematic Representation of Materials and Methods

3.1 CHEMICALS AND GLASSWARE USED IN THE STUDY

Solvents like methanol and ethanol, as well as all other chemicals utilized in this study, were of standard analytical grade and sourced from Merck and HiMedia in India. For the *in vitro* culture studies and other experiments conducted in this research, glassware from the brand Borosil was used.

3.2 GREEN SYNTHESIS AND CHARACTERIZATION OF NANOSTRUCTURES

The following materials were used and methodologies was adopted to synthesise and characterize ZnO and CuO NSs from *R. cordifolia* plant extract.

3.2.1 Green Synthesis

ZnO and CuO NSs were synthesized using *R. cordifolia* plant extract as a reducing and capping agent, with Zinc nitrate Hexahydrate for ZnO and Copper(II) sulfate pentahydrate for CuO as precursor molecules.

3.2.2 Collection of Plant Materials

The fresh and healthy *R. cordifolia* L. **(Plate 1)** plant was collected in January 2020 from Pookode, Wayanad district, Kerala, India. It was identified at St. Joseph's College (Autonomous), Devagiri, and the specimens have been deposited with a voucher No. 9201 in the 'Dev' Herbarium.

3.2.3 Preparation of Aqueous Stem Extract

Fresh stems were washed with running cool and tap water, followed by the clear distilled water. The cleaned stems were shade-dried before being milled into powder and stored. The 20 g of powdered stems were boiled in 500 mL distilled water for 30 minutes at 70-80ºC using a water bath. After cooling, the dark brown extract was filtered using Whatman filter paper to remove insoluble fractions and macromolecules. The aqueous stem extract (ASE) was preserved at a temperature of 4°C, in the refrigerator until needed. The phytochemicals in the extract served as both reducing and capping agents (Ahmed *et al.*, 2016).

3.2.4 Characterization

TEM, SEM-EDX, FT-IR, XRD, and UV-Visible spectroscopy were employed to confirm the production of NSs and to analyse their distribution and sizes.

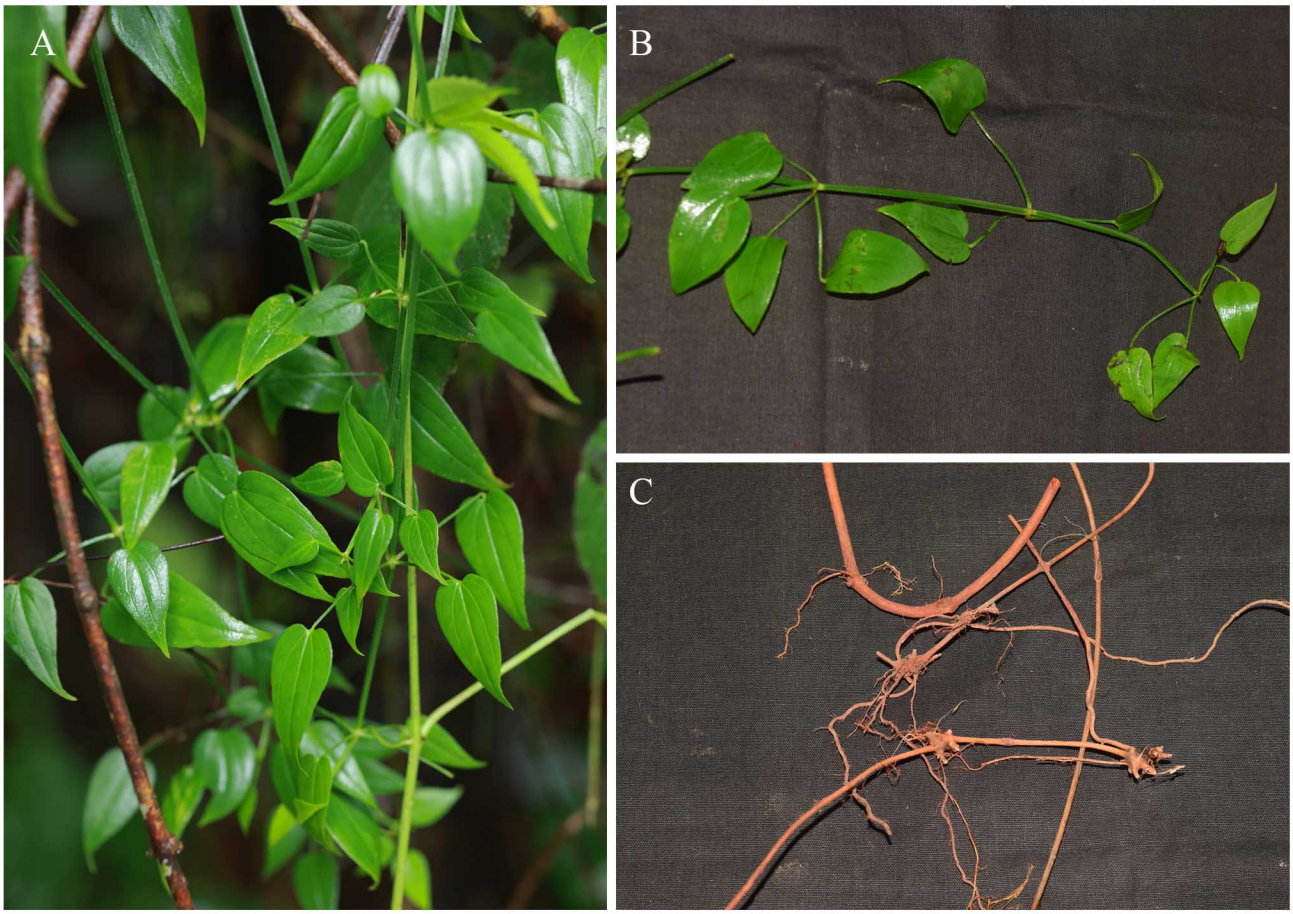

Plate 01: *Rubia cordifolia*. **(A)** Habit, **(B)** Single twig of the plant, **(C)** Roots of the plant.

3.2.4.a UV-Visible Spectroscopy

The preliminary characterization of NSs was done by visual observation of colour change by transmission of laser light. The absorption spectra of the NSs were recorded using a Shimadzu UV-1800 series spectrometer in the 200 – 800 nm range.

3.2.4.b *X-ray Powder Diffraction*

Phase and structure analysis was conducted by recording XRD using a Bruker AXS D8 Advance employing a Coupled Two Theta/Theta type scan at 1.5406 A^0 wavelength, a voltage of 40 kV and a current of 35 mA.

3.2.4.c Fourier Transform Infrared Spectroscopy

The interaction between plant extract and NSs was analyzed by FTIR in the diffuse reflectance mode. FTIR spectra from 4000 to 400 cm^{-1} have been recorded in the transmission mode using a Thermo Nicolet Avatar 370 FT-IR spectrometer operating with a resolution of 4 $cm^{-1.}$ The dried NS powder was mixed with KBr for the FTIR study and formed into pellets. FTIR measurements were carried out to identify the possible biomolecules responsible for reducing the metal oxide ions and the capping of the reduced NSs.

3.2.4.d Scanning Electron Microscopy

A scanning electron microscope with energy-dispersive X-ray spectroscope (SEM-EDAX) analysis was used to analyse the surface topography and morphology of materials and biological samples EDAX for elemental detection. The samples were analysed using Jeol 6390LA/ OXFORD XMX N at 20 kV accelerating voltage, with a 4 nm (30 kV) resolution and a magnification of 500 to 10,000. Chemical analysis of the samples was performed using an EDX analyser.

3.2.4.e Transmission Electron Microscopy

The morphology and size distribution of the samples were determined using TEM. Transmission electron microscopy studies of composites were carried out on Jeol JEM-2100 TEM with a LaB_6 source operating at an accelerating voltage of 200 kV. The system provides a lattice resolution of 0.14 nm and a point-to-point resolution of 0.23 nm. The system also records a Selected Area Electron Diffraction (SAED) pattern for identifying the crystal lattice parameters and structure.

3.2.4.f Differential Thermogravimetric Analysis

Differential Thermogravimetric Analysis (DTG) was carried out to evaluate decomposition features of the composites of the NSs on a STA7200 Thermal Analysis System, Hitachi. The samples (1 mg) were heated from room temperature to 500 °C using alumina crucibles with a heating rate of 10 °C/min under nitrogen flow rate of 100 mL/min).

3.3 STANDARDIZATION OF PROTOCOL FOR SHOOT MULTIPLICATION OF *R. CORDIFOLIA*

3.3.1 Plant Material Collection

The mother plant *R. cordifolia* L. was collected from Pookode in the Wayanad district of Kerala, India. The nodal sections of the source plant were excised and used as explants for the *in vitro* studies.

3.3.2 Preparation of Culture Media

The cultures were multiplied in Murashige and Skoog medium (MS medium) with growth regulators to propagate *R. cordifolia*. MS medium contains micronutrients, macronutrients, vitamins, and iron. These components were sourced from Hi-Media and Sigma.

Each component is prepared as a stock solution according to the medium's nutrient composition, using distilled water and then stored in a refrigerator. Additionally, the medium was supplemented with 3% w/v sucrose. To achieve a semi-solid consistency, 0.8% (w/v) agar was added as a gelling agent (**Table 1**).

The pH of the medium was adjusted to 5.8 using 0.1N HCl or 0.1N NaOH before dispensing a known volume of medium into culture vessels. For instance, 20 mL/tube (15 and 25mm) and 40mL/370mL containers were used for cultures. The culture vessels were sealed with non-absorbent cotton and polypropylene screw caps, and then wrapped with aluminium foil or parafilm tapes.

Table 1: Composition of Murashige and Skoog medium

Components		**Concentration (g/L)**
Macronutrients (10X)		
Ammonium nitrate	NH_4NO_3	16.5g
Potassium nitrate	KNO_3	19g
Calcium chloride	$CaCl_2.2H_2O$	4.4g
Potassium orthophosphate	KH_2PO_4	1.7g
Magnesium sulfate	$MgSO_4.7H_2O$	3.7g
Micronutrients (200X)		
Boric acid	H_3BO_3	0.620g
Manganese sulfate	$MnSO_4.4H_2O$	2.230g
Potassium iodide	KI	0.083g
Zinc sulfate	$ZnSO_4.7H_2O$	0.860g
Sodium molybdate	$Na_2MoO_4.2H_2O$	0.025g
Copper sulfate	$CuSO_4.5H_2O$	0.0025g
Cobalt chloride	$CoCl_2.6H_2O$	0.0025g
Vitamins (100X)		
Myo-inositol	$C_6H_{12}O_6$	2g
Thiamine HCl	$C_{12}H_{17}CIN_4OS.HCl$	0.002g
Nicotinic acid	$C_6H_5NO_2$	0.01g
Pyridoxine HCl	$C_8H_{11}NO_3.HCl$	0.01g
Glycine	$C_2H_5NO_2$	0.04g
Iron source (50X)		
Sodium EDTA	Na_2EDTA	0.3725g
Ferrous sulfate	$FeSO_4.7H_2O$	0.2785g
Sucrose		30g
Agar		8g

3.3.3 Culture Vessels

The cultures were initiated in 15 and 25 mm culture tubes plugged with non-absorbent cotton and multiplied and propagated in 370 mL glass containers with polypropylene screw caps, and each was sealed air-tight with parafilm.

3.3.4 Distilled Water

Distilled water was prepared in a Borosil double distillation unit with quartz glass.

3.3.5 Laminar Air Flow Chamber

The multiplication and sub-culturing were carried out in a laminar airflow chamber equipped with a HEPA filter of 0.3 µm mesh size and a UV light source (MICRO-FILT INDIA Pvt Ltd). The inoculation process was performed on the chamber's sterilized stainless-steel platform.

3.3.6 Autoclave Unit

The automated sterilization unit (Modern Scientific Industries, Bombay) was utilized to sterilize culture media, glass vessels, forceps, and scalpels. It was able to maintain a temperature of 120°C at 15 Pa pressure.

3.3.7 Preparation of Stock Solutions for Plant Growth Regulators

A 0.1 mg/mL cytokinin and BAP stock solutions were prepared by dissolving 25 mg of cytokinin and BAP in a 500 mL beaker with the addition of 1M HCl and 250 mL of distilled water. The solution was then transferred to labelled containers and stored in the refrigerator. Whereas NAA were dissolved first in few drops of NaOH or KOH solution. After that quickly add 250 mL of distilled water and stored at low temperature.

Table 2: Concentrations and combinations of PGRs used for Shoot multiplication

Sl. No.	Plant growth regulators (PGRs)				
	IAA (mg/L)	**NAA (mg/L)**	**KINETIN (mg/L)**	**BA (mg/L)**	**IBA (mg/L)**
1.	-	-	-	-	-
2.	0.5	-	-	-	-
3.	1	-	-	-	-
4.	1.5	-	-	-	-
5.	-	0.5	-	-	-
6.	-	1	-	-	-
7.	-	1.5	-	-	-
8.	-	-	0.5	-	-
9.	-	-	1	-	-
10.	-	-	1.5	-	-
11.	-	-	2	-	-
12.	-	-	-	0.5	-
13.	-	-	-	1	-
14.	-	-	-	1.5	-
15.	-	-	-	2	-
16.	-	-	-	-	1
17.	-	-	-	-	1.5
18.	-	-	-	-	2
19.	-	-	0.5	1	-
20.	-	-	1	0.5	-

Indole 3 acetic acid (IAA), Naphthalene acetic acid (NAA), Kinetin, Benzyl adenine (BA), Indole-3-butyric acid (IBA) and the combination of BA and Kinetin were used as the plant growth regulators. IBA, IAA and NAA were used in three different concentrations such as 0.5mg/L, 1mg/L and 1.5mg/L. Whereas BA and Kinetin were in 0.5mg/L, 1mg/L, 1.5mg/L and 2 mg/L (**Table 2**). Explant cultured in MS medium without any plant growth regulators was used as the control. The best medium for shoot

and root multiplication were analyzed based on the length of shoot and root, number of shoots and the amount of fresh weight and dry weight (DW).

3.3.8 Preparation of Sterilant (Mercuric chloride)

$HgCl_2$ was used for surface sterilization of the explant. A 0.1% stock solution was made by dissolving 0.5 g in 500 mL of distilled water and stored in a container inside the Laminar Air Flow chamber.

3.3.9 Inoculation

The collected explants underwent three rounds of washing: 15 minutes under running tap water, 5 minutes under detergent extran, and a final thorough washing in distilled water. After 5 minutes of surface sterilization in 0.1% mercuric chloride, the explants were cleaned in distilled water. After trimming to the proper size, nodal explants were grown in MS basal medium (Murashige & Skoog, 1962). The developed shoots were then subcultured on MS medium with different concentrations of growth regulators to identify the best culture media for shoot multiplication after 80 days.

3.3.10 Shoot Multiplication and Subculturing

To initiate the shoot multiplication process for further studies, nodal cultures of *R. cordifolia* were placed in MS medium supplemented with 0.5 mg/l Kinetin. The MS medium was prepared in 370 mL glass containers with polypropylene screw caps. The healthy nodal explants selected from the source culture were washed with sterile water multiple times, finely trimmed, and then inoculated onto the medium under sterilized conditions. The inoculated cultures were capped, sealed airtight with parafilm, and kept in the culture room. The temperature in the culture room was maintained at 24±1°C, with a humidity of 60-70%, and a 16/8 light/dark hour photoperiod with approximately 1000-2000 lux provided by cool white fluorescent tubes. Both growth and contamination were monitored in the cultures. Cultures that were tainted were extracted, cleaned, and discarded. Regular sub-culturing in optimal MS media maintains cultures and prevents browning and drying.

3.3.11 Harvest

After eighty days, the cultures were harvested. The plants were taken out, and significant morphological changes were recorded. The length of the shoots, roots, area of the leaves, and fresh weight of each plantlet were measured. The plantlets were then

dried, and their dry weight was recorded. After statistical analysis, the culture media with the best PGR was selected as the shoot multiplication media for further studies.

3.3.12 Hardening

Wholly developed *in vitro*-grown plantlets were removed from the culture jars, cleaned of agar using sterile distilled water, and then placed in paper cups filled with autoclaved sand: soil (1:1). To preserve humidity and keep the plants from drying out, the cups were covered with clear polythene bags. After ten days, the polythene bag was taken off. The plantlets were then moved to the potting mixture-filled garden pots.

3.4 COMPARATIVE PHYTOCHEMICAL ANALYSIS OF *IN VITRO* RAISED STEM, LEAF AND ROOT OF *R. CORDIFOLIA* FOR IDENTIFYING BEST EXTRACTION SOLVENT AND PLANT PART

Various solvents with different polarities such as Hexane, Chloroform and Methanol were selected based on their ability to solubilize different classes of bioactive compounds present in *in vitro* grown *R. cordifolia*.

3.4.1 Preparation of Plant Extract

Harvested plant materials were sorted into leaves, shoots, and roots, washed with sterilized distilled water, and air-dried at room temperature for seven days. These dried plant materials were then homogenized to a fine coarse powder using an electric blender and then stored in airtight containers until further use. Various organic solvents viz. Hexane, Chloroform and Methanol were used for extractions. 5 g of homogenized coarse powders of leaf, stem, and root were extracted by using Soxhlet apparatus and concentrated to 5mL using water bath. Thus the final aliquots were stored at 4^{o}C in labelled sterile bottles (**Figure 2**).

Hexane, chloroform, and methanol are effective extraction solvents due to their low vapour pressure, non-flammability, and stability. Hexane is used for nonpolar extractions, chloroform serves as a nonpolar solvent, and methanol is ideal for polar extractions (Grima *et al.*, 2013; Shikov *et al.*, 2022).

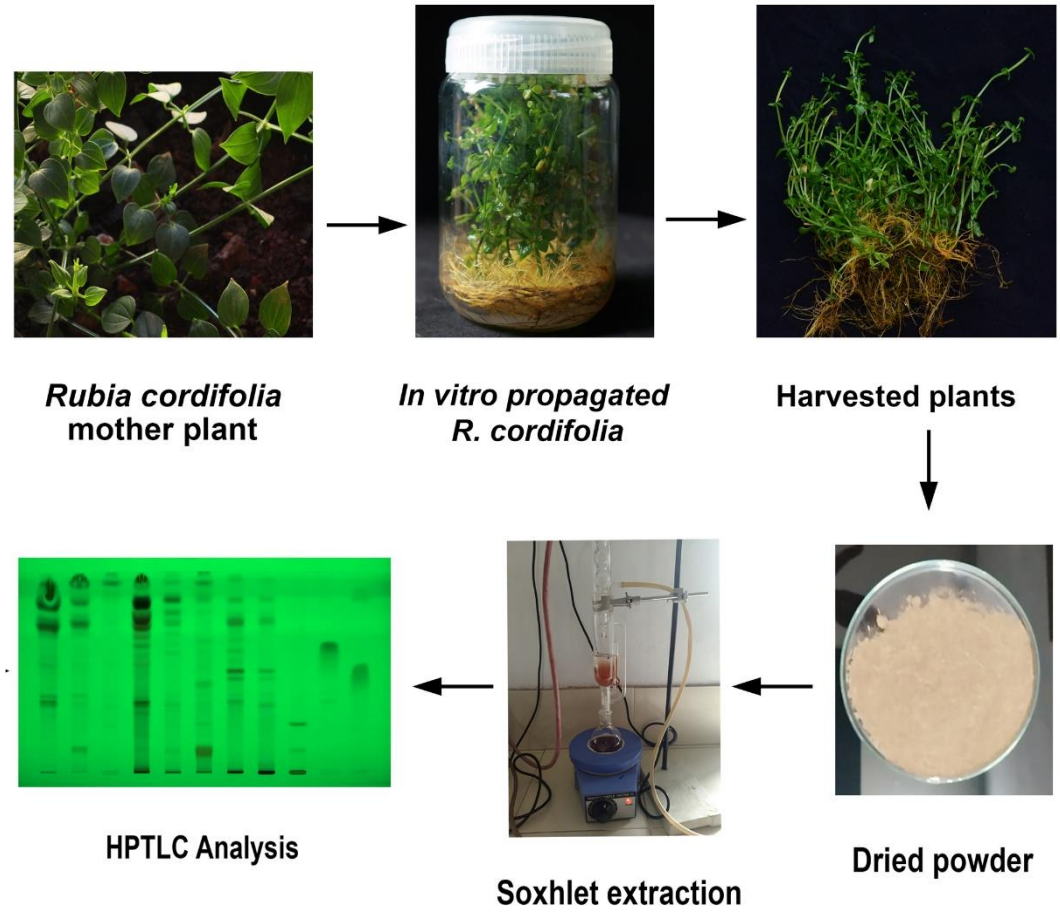

Figure 2: Procedure for extraction and solvent standardization of *R. cordifolia*.

The process involves heating a solvent in the flask, which evaporates and condenses in the condenser. The condensed solvent then percolates through the solid sample, dissolving desired compounds. The solvent, now containing the extracted substances, siphons back into the flask, where it is repeatedly recycled. This method is highly effective for extracting soluble compounds from complex matrices (Alamgir & Alamgir, 2018; Raks *et al.*, 2018).

3.4.2 HPTLC (High-Performance Thin Layer Chromatography)

HPTLC profile for various extractions of *in vitro* propagated *R. cordifolia* plant parts was used to determine the quality and quantity of chemical contents (Kurian *et al.,* 2020). Aluminium backed pre-coated Merk silica gel plate 60 F 254 plate (20×10 cm) was used as the stationary phase. The various extractions of the *R. cordifolia* plant extracts were applied on the plate, using CAMAG Linomat 5 connected to Camag

HPTLC system. Using 100 µl syringe 10 µl of test solutions were applied on a pre-coated silica gel 60 F254 TLC plate of uniform thickness of 0.2 mm plate in the form of bands with 8 mm width. The sample loaded plate was placed in a twin trough development chamber with mobile phase systems. The plates were viewed under UV light at 254 and 365 nm after a brief drying period. They were then sprayed with Anisaldehyde Sulfuric (ANS) reagent heated at 60^{o}C for 5 min until the formation of spots, which were visualized at 550 nm. The Camag TLC scanner 3 was used to perform densitometric scanning of the plates at 254, 366, and 550 nm.

3.5 ANALYSIS OF THE GREEN SYNTHESISED NANOSTRUCTURES AS ELICITORS

The following materials were used and methodologies was adopted to investigate the changes of bioactive molecular components and biomass in NSs treated *in vitro* cultures of *R. cordifolia* culture.

3.5.1 Preparation of Culture Media and Inoculation

In the *in vitro* experiment, ZnO NSs and CuO NSs were used as the elicitors. To prepare a stock solution of NSs for *in vitro* use, add 50 mg of NSs (ZnO and CuO) and 500 mg of agar-agar to 200 mL of distilled water. Mix the solution and then sonicate it using a sonicator to create a well-dispersed colloidal solution. The sonication process breaks down any aggregates and ensures that the NSs are uniformly distributed throughout the solution. Agar-agar acts as a stabilizing additive, forming a gel-like matrix around the particles, which helps prevent agglomeration. This stabilizing effect ensures high dispersion and maintains the stability of the NS colloidal solution for further *in vitro* applications (Balandin *et al.*, 2015).

In a broad spectrum treatment, healthy cultures were sub-cultured in MS medium with 0.5 mg/L Kinetin and with different concentrations of ZnO NSs (0.1 mg/L, 1 mg/L, 10 mg/L, 100 mg/L). Similarly, cultures grown in MS medium with 0.5 mg/L Kinetin were treated with different concentrations of CuO NSs (0.1 mg/L, 1 mg/L, 10 mg/L, 100 mg/L) (**Table 3**). A narrow spectrum treatment of cultures was treated with different concentrations of ZnO NSs (0.2 mg/L, 0.4 mg/L, 0.6 mg/L, and 0.8 mg/L) and CuO NS (0.2 mg/L, 0.4 mg/L, 0.6 mg/L, and 0.8 mg/L) (**Table 4**). For all treatments, NSs were added to the culture medium before adjusting the pH to 5.8. The cultures were incubated

for 80 days, and then harvested to evaluate biomass and secondary metabolite enhancement.

Table 3: Concentrations of abiotic stress used in the broad spectrum treatment

Sl. No.	Broad spectrum treatment with biogenic NSs	Code
1	Control	RC
2	0.1 mg/L ZnO NSs	RZn1
3	1 mg/L ZnO NSs	RZn2
4	10 mg/L ZnO NSs	RZn3
5	100 mg/L ZnO NSs	RZn4
6	0.1 mg/L CuO NSs	RCu1
7	1 mg/L CuO NSs	RCu2
8	10 mg/L CuO NSs	RCu3
9	100 mg/L CuO NSs	RCu4

Table 4: Concentrations of abiotic stress used in the narrow spectrum treatment

Sl. No.	Narrow spectrum treatment with biogenic NSs	Code
1	Control	RC
2	0.2 mg/L ZnO NSs	SZn1
3	0.4 mg/L ZnO NSs	SZn2
4	0.6 mg/L ZnO NSs	SZn3
5	0.8 mg/L ZnO NSs	SZn4
6	0.2 mg/L CuO NSs	SCu1
7	0.4 mg/L CuO NSs	SCu2
8	0.6 mg/L CuO NSs	SCu3
9	0.8 mg/L CuO NSs	SCu4

3.5.2 Harvesting of *In Vitro* Raised Plants

The cultures were observed for 80 days before being harvested for further analysis. After harvesting, the samples underwent morphological and Raman spectroscopic analysis to assess their characteristics. Following these analyses, the cultures were washed, shade-dried, ground into a fine powder, and stored in labelled containers for phytochemical analysis and bioactivity screening.

3.5.3 Phytochemical Investigation and Screening for Bioactivity

To investigate the effect of NS accumulation in *in vitro* NSs-treated *R. cordifolia* plants, the collected plant powders were subjected to methanolic extraction. 5 g of each powdered sample was extracted with methanol using Soxhlet apparatus for 4 hours at 40°C. The resulting methanolic extract was then collected and stored for subsequent phytochemical analysis.

Methanol is highly polar, and in biochemical analysis, it is used as a solvent for extracting polar as well as likely polar compounds from plants. Anthraquinone is soluble in methanol; hence, in these experiments, methanol was used as the extraction solvent (Abubakar & Haque, 2020; Diaz-Munoz *et al.*, 2018).

3.5.3.a Phytochemical Analysis

The TPC and TFC of methanolic extract of *in vitro* NSs treated plants were determined using spectroscopic methods.

Total Phenolic Content (TPC) and Total Flavonoid Content (TFC)

TPC was assessed using the Folin–Ciocalteu reagent assay (Singleton & Rossi, 1965). An aliquot extracts or standard solution of gallic acid (20, 40, 60, 80 and 100 µg/mL) was added to a 25 mL volumetric flask. A reagent blank was prepared using distilled water. 0.2 mL of Folin-Ciocalteu phenol reagent was added to the mixture and shaken. After 5 min, 2 mL of 7% Na_2CO_3 solution was added to the mixture. The volume was then made up to 5 mL by adding distilled water. After incubation for 30 min at room temperature, the absorbance against the reagent blank was determined at 550 nm with a spectrophotometer. Total phenolics content was expressed as mg Gallic Acid Equivalents (GAE).

TFC was measured using the aluminium chloride colorimetric assay as described by Zhishen *et al.,* (1999), with slight modifications. An aliquot of extracts and standard solutions of Quercetin (300, 500, 700, 900 and 1100 µg/mL) was added to a 25 mL

volumetric flask. To this, 0.3 mL of 5% $NaNO_2$ was added, followed by 0.3 mL of 10% $AlCl_3$ after 5 min. After another 5 min, 2 mL of 1M NaOH was added and the volume was made up to 10 mL with distilled water. The solution was mixed thoroughly and after 10 min incubation, absorbance was measured against the blank at 520 nm. The total flavonoid content was expressed in terms of mg Quercetin Equivalents (QE).

High Performance Thin Layer Chromatography (HPTLC) Studies

Chromatographic analysis was done on the methanolic extract of treated and untreated plants to understand the secondary metabolite changes, especially the anthraquinone dyes. The quantity and intensity of bands observed in the HPTLC profile of various methanolic fractions of plant extracts, both treated and untreated with NSs reveal differences in chemical compositions (Kurian *et al.*, 2020).

The stationary phase was Aluminium backed pre-coated Merk silica gel plate 60 F_{254} plate (15×10 cm**).** Methanol fractions of the treated and untreated *R. cordifolia* plant extracts, along with the marker compounds (Alizarin and Purpurin), were applied to the plate with nine tracks using the Camag automatic TLC sampler and connected to the Camag HPTLC system. Using 25µl syringe 10µl of test solutions were applied on a pre-coated silica gel 60 F_{254} TLC plate of uniform thickness of 0.2 mm plate in the form of bands with width 8mm. Develop the plate in a twin trough chamber to a 20 x 10 cm distance using the Toluene: Ethyl Acetate: Fomic Acid (7:3:0.3) solvent systems according to TLC analysis. After that, the plate was derivatized with the ANS (Anisaldehyde Sulfuric acid) reagent. The plate was examined under UV light at wavelengths of 254 nm and 366 nm. Additionally, after ANS derivatization, the plate was visualized at 550 nm. The Camag TLC scanner was used to perform densitometric scanning of the plates at 254, 366, and 550 nm.

High Resolution Liquid Chromatograph Mass Spectrometer (HR-LCMS)

The methanol fractions of the treated and untreated *R. cordifolia* plant extracts were prepared using LC-MS grade solvents and filtered to prepare the stock solution, 10mg/5mL.

The Agilent 1290 UHPLC system (Agilent Technologies, Santa Clara, CA, USA) was used to perform the HR-LCMS-Q-TOF analysis. The LC-MS analysis was carried out according to the previous methods by House *et al.,* (2020). Precisely, 10 µL of the extract was injected into the system, and the run was carried out using water (0.1%

formic acid v/v) (A) and methanol (B) as solvents. The gradient elution mode was used as follows: First 1 min 95% A and 5% B, next 20 min 100% B, 26-30 min 100% B, 30-31 min 95% A and 5% B, 31-35 min 95% A and 5% B. The pressure was 1200 bar, and the flow rate was adjusted to 0.3 mL/min.

Raman Spectroscopy

After 80 days of *in vitro* culture, the NSs treated and untreated plants underwent Raman spectroscopy to identify the fate of NSs applied inside the plant system. Raman spectroscopy is a non-destructive technique that can provide insights, into the dimensions, morphology, and chemical composition of MO NSs (Testa-Anta *et al.*, 2019a). In this study, Raman spectroscopy was employed to verify the impact of NMs on *in vitro* cultured *R. cordifolia* plants by examining the presence of Purpurin and Alizarin dyes, within the plant. The data was recorded using 532 nm (100 mW) green laser with LabRAM HR Evolution Raman spectrometer. The whole plantlets in the cultures as well as the marker compounds (Alizarin and Purpurin) were used for Raman analysis.

3.5.3.b Antioxidant Activity

The antioxidant properties of the methanolic extracts from *in vitro* NSs treated plants were evaluated by assessing their ability to neutralize radicals such as Diphenyl Picryl Hydrazyl (DPPH) (D. Liu *et al.*, 2020) and 2,2-azino-bis-3-ethylbenzothiazoline-6-sulphonic acid (ABTS) (Konaté *et al.*, 2010) could be neutralized. These techniques help, in assessing the capability of the samples being tested to neutralize or reduce these radicals providing insights, into their antioxidant properties (Lai *et al.*, 2010; D. Liu *et al.*, 2020).

Then, the percentage of DPPH or ABTS scavenged was calculated using the equation,

Scavenging DPPH or ABTS (%) = (1 – Absorbance detected /Absorbance reference) x 100.

The percentage of scavenged DPPH or ABTS was plotted versus the concentration of antioxidants and the concentration of antioxidant required to obtain 50% inhibition (50% inhibition concentration or f) was obtained from the graph (Tang & Liu, 2007).

A stock solution of 2.02 mg DPPH in 30 mL methanol was prepared. A working solution was prepared by mixing 10 mL stock solution with 45 mL methanol, resulting in an absorbance of 1.01 units at 520 nm. A series of plant extracts were combined with 2 mL of the DPPH solution for 30 minutes in the dark, then measured at 520 nm absorbance.

To perform the ABTS assay, 7 mM ABTS and 2.45 mM potassium persulfate stock solutions were mixed in equal quantities and allowed to react for 12 hours at room temperature in the dark. The resulting solution was diluted with methanol to obtain an absorbance of 0.70 ± 0.02 units at 734 nm using a spectrophotometer. Plant extracts were then allowed to react with the ABTS solution for 7 minutes in the dark, and the absorbance was measured at 734 nm using a spectrophotometer.

3.6 STATISTICAL ANALYSIS

All experiments were performed in triplicates. The mean and standard deviation of the data were used for interpretation. For the statistical analysis of the experimental data, the two-way ANOVA followed by Tucker Kramer multiple comparison tests with a 5% confidence level was chosen, and One-Way ANOVA and Duncan's multiple range test at $P \leq 0.05$ level were done using IBM SPSS (Ver. 25) for biomass assay. Each experimental value was compared with the value of the respective untreated control group.

CHAPTER – 4

RESULTS AND DISCUSSION

4.1 GREEN SYNTHESIS AND CHARACTERIZATION OF NANOSTRUCTURES

Green nanotechnology, or the creation of nanostructures (NSs) using biological processes, notably plant extracts, is a developing field of study. Today, combining nanosystems with plant tissue culture is essential for bioactive component manufacturing, genetic engineering, crop improvement, and mass reproduction (Bhandari *et al.*, 2022; Smith, 2011).

This study resulted in an inexpensive, environmental friendly, and simple method for developing ZnO and CuO NSs using *R. cordifolia* as the reducing and stabilising agent. The characterization of the generated ZnO and CuO NSs have been confirmed using the methods of UV-Vis, FT-IR, XRD, SEM-EDX, TEM, DTG, IR spectroscopy and Raman spectroscopy. These synthesised metal oxide NSs are used as a stress elicitor in *in vitro* cultures of *R. cordifolia*.

4.1.1 Green Synthesis of ZnO NSs and CuO NSs

The synthesis of ZnO NSs was carried out by gradually adding 20 mL of ASE to 80 mL of 91 mM Zinc nitrate Hexahydrate. After an hour of continuous stirring at 70°C, 1 N; NaOH was added to the reaction mixture to raise the pH to 11. The development of ZnO NSs was identified by the appearance of an off-white colour. The finished product underwent centrifugation at 5,000 rpm for 15 minutes after cooling at ambient temperature. For additional purification, three more centrifugations were conducted using distilled water. After being dried in a hot air oven at 70°C, the off-white powder was calcinated in a muffle furnace for three hours at 500°C. The resulting white powder was stored in an airtight glass container for future use (**Figure 3**).

CuO NSs was prepared by dropwise addition of 25 mL of the ASE to 75 mL of 10 mM Copper (II) sulfate pentahydrate, with continuous stirring at 80ºC for 1 h. This was followed by addition of 1 N NaOH to bring the pH level to 10. The appearance of CuO NSs was indicated by a colour change from green to bluish-green. The precipitate was purified further by centrifugation at 10,000 rpm for 10 minutes after being allowed to cool at ambient temperature. The formed CuO NSs were washed thoroughly with distilled water by centrifugation and dried at 80°C in a hot air oven. The synthesized sample was subjected to a 2 h calcination process at 400°C and the resulting black powder was stored in an airtight glass container (**Figure 3**).

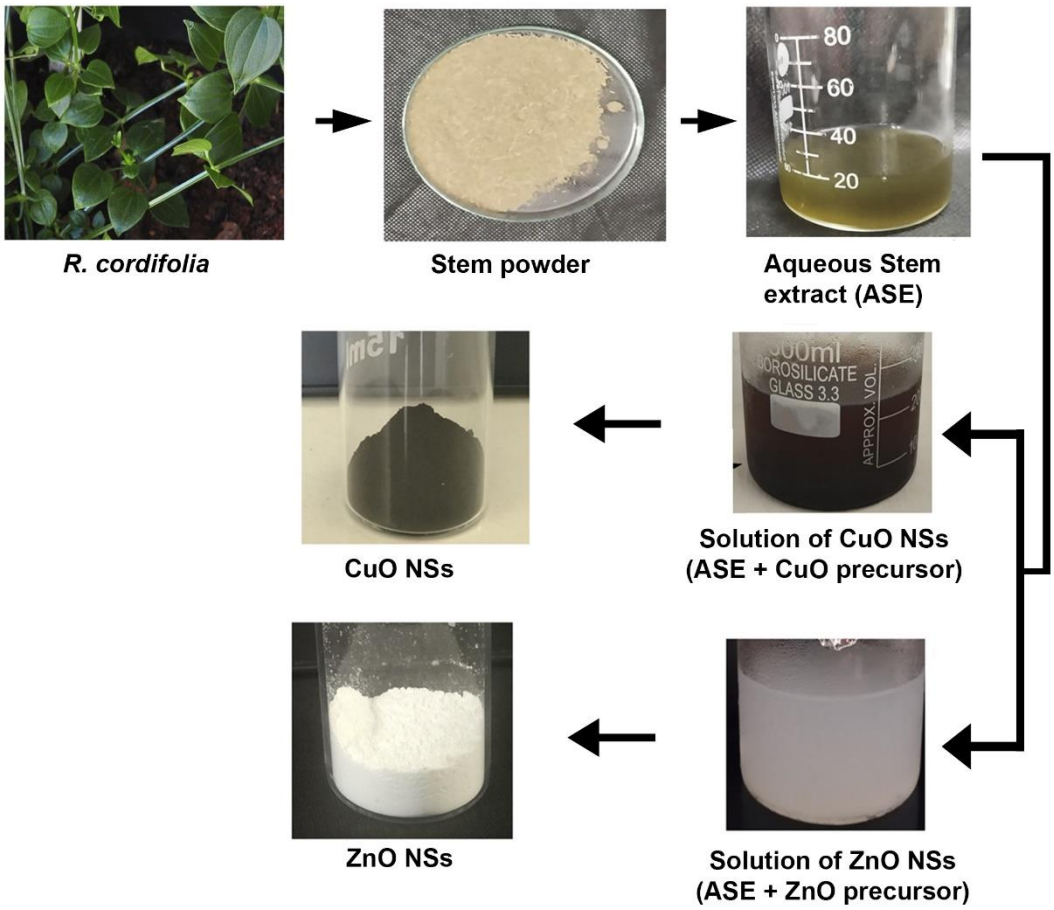

Figure 3: Preparation of nanostructures from aqueous stem extract of *R. cordifolia*

4.1.2 Characterization of Green Synthesised Nanostructures

4.1.2.a UV–Visible Spectroscopic Analysis

The colour change of *R. cordifolia* stem extract solution from light brown to white and brownish-black following 1 h of the addition of ($Zn(NO_3)_2$. $6H_2O$) and $CuSO_4.5H_2O$, respectively, was used to evaluate the green synthesis of ZnO and CuO NSs. UV-Vis spectra of the resulting NSs were acquired in the 200–800 nm wavelength range and the absorption spectra are displayed in **Plate 2**. The maximum absorbance of ZnO and CuO NSs exhibited distinct peaks at 370 nm and 285 nm, respectively 420, and 340 nm, respectively (**Plate 2 A and 2 B**). Similar results were reported with previous research using *R. cordifolia* leaf extract to synthesize ZnO NSs at 374 nm (Sisubalan *et al.*, 2018). Qu *et al.,* (2011) recorded the UV absorption spectra for synthesized ZnO at 370 nm. Extracts from Chamomile flowers and leaves of *Cassia auriculata* supported the formation of CuO NSs in the 285–320 nm range (Duman *et*

al., 2016; Shi *et al.*, 2017). UV-Vis spectral analysis demonstrates the understanding of how MO NSs are generated through the SPR phenomenon (a unique characteristic optical phenomenon of metallic NSs) (Al-Kordy *et al.*, 2021). When SPR is stimulated, visible radiation is absorbed, resulting in nanostructures displaying various colours. The colour of the solution also changes depending on the size of the NSs. Therefore, the creation of NSs is highly dependent on the UV-Vis absorption spectrum (Sarina *et al.*, 2013).

4.1.2.b FT-IR Spectral Analysis

The presence of active phytochemicals and/or biomolecules in the plant extract is confirmed by the FTIR spectrum, and these substances serve as natural reducing and/or stabilising agents for the synthesis of NSs (Manyasree *et al.*, 2017; Nagore *et al.*, 2021). The FT-IR spectrum of the green synthesised ZnO and CuO NSs (**Plate 2 C and 2 D**) to identify the functional groups of biomolecules involved in ZnO and CuO NSs formation. The stretching vibration of the hydroxyl functional group (O-H) present on the surface of NSs or adsorbed water on the sample is indicated by broad and sharp peaks at 3435 cm^{-1} and 3427 cm^{-1}, in the FT-IR spectrum of green synthesised ZnO and CuO NSs, respectively. This is due to absorption of high moisture by nano-crystalline materials with high surface-to-volume ratios (Varughese *et al.*, 2020). Metal oxides typically produce absorption peaks between the ranges of 900 and 400 cm^{-1} (Mink *et al.*, 1995). The typical Zn-O vibration was identified as a strong and intense band that was positioned between 911 cm^{-1} and 417 cm^{-1} (**Plate 2 C**). The bands observed at about 492 cm^{-1} in **Plate 2 D** can be attributed to the Cu-O stretching vibration. Similar stretching vibrations were observed by Sundar *et al.,* (2018) in their experiment on the biosynthesis of CuO nanowires using *Sapindus mukorossi* fruit extract. The peaks at 1631 cm^{-1}, 1629 cm^{-1}, 1521 cm^{-1}, 1331 cm^{-1}, and 1384 cm^{-1} are contributed by carbonyl and alkyl group vibrations. Our results are consistent with earlier research using ZnO NSs synthesized from *Solanum torvum* and *Laurus nobilis* leaf extract (Ezealisiji *et al.*, 2019; Fakhari *et al.*, 2019) and CuO NSs synthesized from *Syzygium guineense* leaf extract and a gram-negative bacteria *Aeromonas hydrophila* (Desalegn *et al.*, 2021; Jayakodi & Shanmugam, 2020).

4.1.2.c X-Ray Powder Diffraction Analysis

To identify the phase of a crystalline substance, XRD is a quick analytical technique and also provides information on unit cell dimensions. Strong diffraction peaks at 31.8, 34.5, 36.3, 56.6, and 63.01^{o}C of 2θ were observed in the XRD spectra of green synthesized ZnO NSs, which corresponds to the (110), (002), (101), (110), and (220) crystal planes (**Plate 2 E**). These results significantly agreed with the ICSD file 094002 (a=b=3.24 c=5.20) and were indexed as the hexagonal- wurtzite structure. Similar results were reported by Ismail *et al.,* (2018) and Vanathi *et al.,* (2014).

A succession of diffraction peaks at 32.63, 35.67, 38.78, 48.88, 61.69, 68.16, and 75.32° was seen in the XRD spectra of biogenic CuO NSs (**Plate 2 F**) and was attributed to the (110), (002), (111), (-202), (202), (113), (311), and (220) planes of monoclinic CuO NSs. The formation of CuO NSs is further evidenced by diffraction peaks (between 2θ = 35 and 39°). The current findings, therefore, agree with earlier reports on the synthesis of CuO NSs (Brazlauskas & Kitrys, 2008; Nezamzadeh-Ejhieh & Amiri, 2013). The acquired XRD data of biogenic CuO NSs closely matched the spectra of crystalline monoclinic CuO NSs (ICSD-69757). The lattice parameters for synthesised CuO NSs were a = 4.692, b = 3.428, and c = 5.137.

Using Debye - Scherrer's formula (1916 and 1917), $D=k\lambda/\beta\cos\theta$ (Sarma & Sarma, 2015), the average size of the NSs were determined as 17.9 nm and 28.35 nm for ZnO NSs and CuO NSs respectively Where D is the particle size (nm) of NSs, k is a constant to 0.94, λ is the wavelength of X-ray radiation (1.5406 A^{o}), β is the full length at half maximum (FWHM) of the peak (in radians), and 2θ is the Bragg's angle (degree) (**Table 5**). The sturdy and unambiguous peak confirms the high purity and crystallinity of the biogenic NSs (Bindu & Thomas, 2014). No distinguishing peaks were visible for other contaminants.

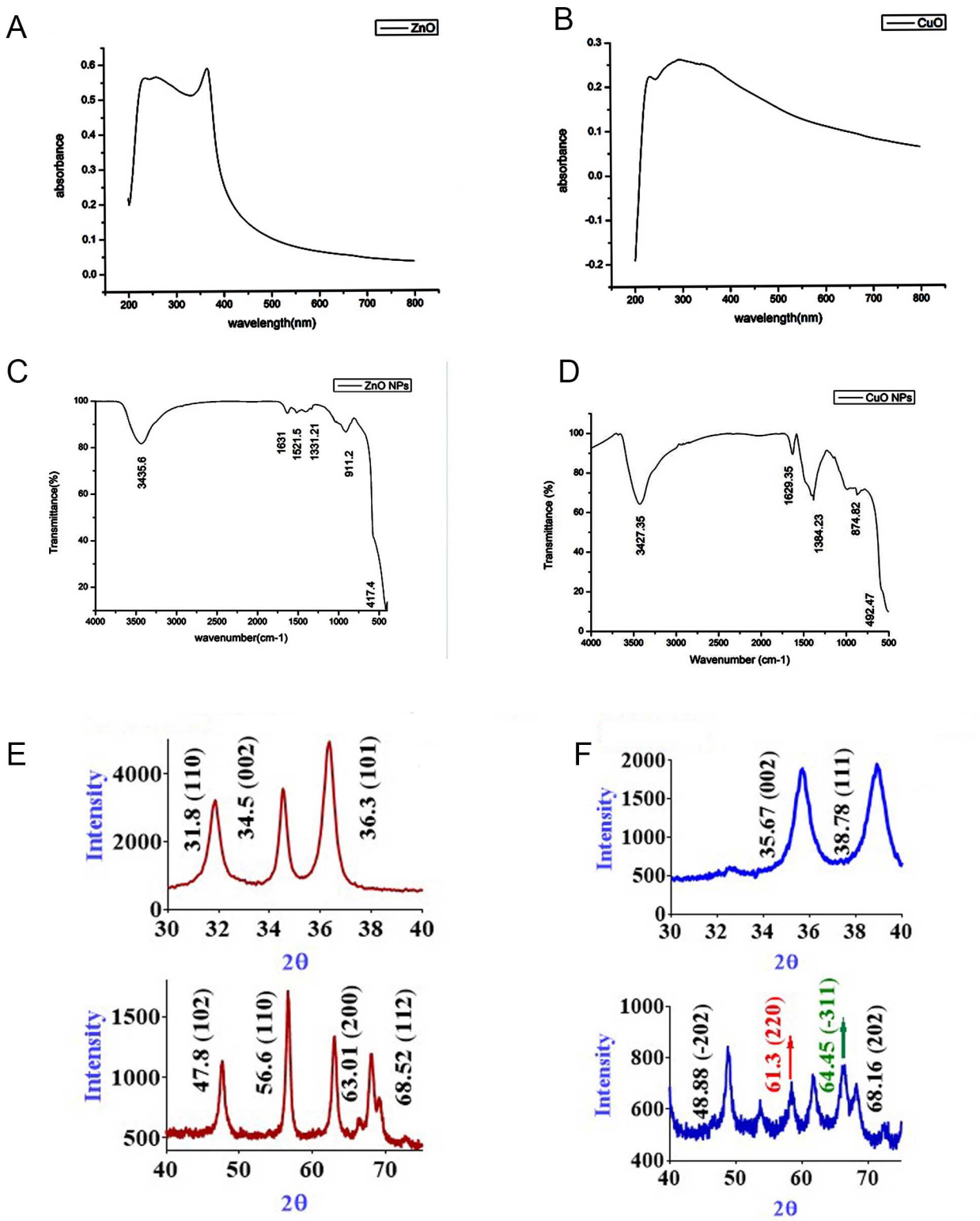

Plate 02: Characterization of green synthesised nanostructures.
(A) UV-Vis spectra of ZnO NSs, **(B)** UV-Vis spectra of CuO NSs, **(C)** FT-IR spectra of ZnO NSs, **(D)** FT-IR spectra of CuO NSs, **(E)** XRD spectra of ZnO NSs, **(F)** XRD spectra of CuO NSs.

Table 5: The average size of green synthesised ZnO and CuO NSs from *R. cordifolia* using Debye - Scherrer's formula

Abiotic Stress	Scherrer constant (K)	Wavelength (λ) (A^o)	Peak position (2θ) (degree)	FWHM (β) (degree)	Size (D) (nm)	Average size (D) (nm)
			31.863	0.479	18.007	
			34.525	0.341	25.470	
			36.336	0.491	17.778	
			56.648	0.642	14.676	
			63.014	0.692	14.058	
			33.434	0.244	33.982	
			35.64	0.336	24.825	
			38.849	0.395	21.317	
			42.514	0.256	33.284	

4.1.2.d Scanning Electron Microscopy

As shown in **Plate 3 A**, the green synthesized ZnO NSs were tetrahedral in shape and some appeared as clusters of small crystal units in the SEM micrographs. The clustering is considered to be caused by the polarity and electrostatic forces of the ZnO NSs. Vidya *et al.,* (2013) and Muhammad *et al.,* (2019) reported comparable SEM analysis results of ZnO NSs synthesized using *Calotropis gigantea* and *Papaver somniferum*. The micrographs of biogenic CuO NSs showed irregularly shaped particles, with a non-smooth, round shape and some appear as tetrahedron clusters (**Plate 3 B**). Comparable observations were found in the research conducted by Ibrahim *et al.,* (2018). They prepared CuO NSs from an aqueous Spinach extract and analysed using SEM. They appeared as irregular spherical particles with a predominant tetrahedron structure.

4.1.2.e Energy-Dispersive X-Ray Spectroscopic Analysis

The elemental makeup of the biogenic nanomaterials was confirmed through the analysis of the EDX plot of the SEM images showing the presence of high purity of the

necessary phase of Zinc and Oxygen, in ZnO NSs as shown in **Plate 3**. The ZnO NSs contained 75.45% Zinc and 20.92% Oxygen (**Plate 3 A**). These findings were supported by Janaki *et al.,* (2015) research on green synthesis of ZnO NSs from dry ginger rhizome extract powder. They confirmed the correct identification of ZnO based on 85.30% Zinc and 13.51% Oxygen content. Likewise, **Plate 3 B** shows the presence of Copper and Oxygen in CuO NSs**.** The composition of CuO NSs consisted of approximately 72.59% Copper and 27.41% Oxygen. The results were supported by a study conducted by Aminuzzaman *et al.,* (2017) in which CuO NSs were synthesized from banana peel extract, and EDX analysis confirmed the presence of Copper (Cu 63.59 wt%) and Oxygen (O 27.06 wt %) in the sample.

4.1.2.f Transmission Electron Microscopic Analysis

TEM analysis is the most common method to determine the size and shape distribution of the NSs. The particle size of ZnO NSs (**Plate 3 C and 3 D**) was determined to be between 6 to 20 nm and is hexagonal in shape. These observations closely consistent with Dallatu *et al.,* (2020). The TEM images of CuO NSs (**Plate 3 F and 3 G**) revealed the formation of spherical CuO NSs, with the size range between 9 to 32 nm. The variation in size distribution was mainly due to the clustering of NSs (Das *et al.*, 2019). This is in close agreement with the results calculated from powder XRD data using the Debye-Scherrer formula (**Table 5**). The Selected Area Electron Diffraction **(**SAED) pattern provided additional evidence of the crystalline structure of NSs. The bright spots in the diffraction rings are related to the crystalline nature of synthesized ZnO NSs (**Plate 3 E**) and CuO NSs (**Plate 3 H**). Similar observations related to CuO and ZnO NSs were reported Narasaiah *et al.,* (2017) and Abderrahman, (2004) respectively, in their study.

Plant extracts are often used in NS synthesis because they contain various organic compounds that can act as reducing agents, helping to reduce metal ions into their metallic form. These organic compounds can also act as stabilising agents, helping to prevent the metal oxides from agglomerating or clumping together. The resulting metal oxide nanoclusters can have many applications, including in catalysis, sensing, and energy storage. The biomolecules in the plant extract include proteins, enzymes, and organic compounds, which can act as nucleation sites for the metal oxide nanocrystals. These biomolecules provide a surface for the metal ions to attach and form clusters.

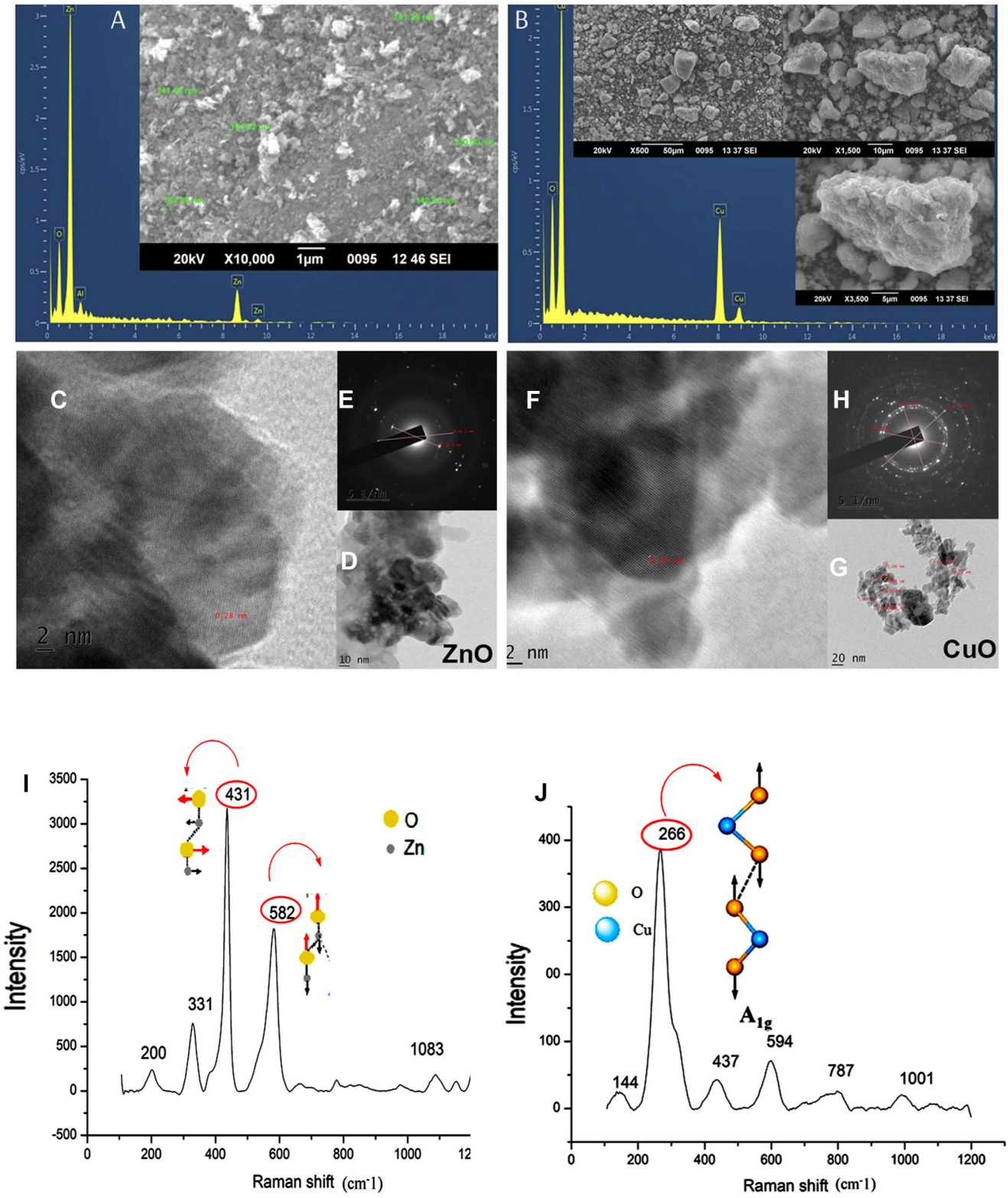

Plate 03: Characterization of green synthesised nanostructures.
(A) EDX and SEM (inset) of ZnO NSs, **(B)** EDX and SEM (inset) of CuO NSs; **(C, D & E)** TEM and SAED pattern of ZnO NSs, **(F, G &H)** TEM and SAED pattern of CuO NSs; **(I)** Raman spectral analysis of ZnO NSs, **(J)** Raman spectral analysis of CuO NSs.

The use of plant extracts as a source of reducing and stabilising agents is a promising approach for the synthesis of metal oxide nanoclusters, as it offers a more nature-friendly and sustainable alternative to traditional chemical methods (Jeevanandam *et al.*, 2016; Shafey, 2020; Vasantharaj *et al.*, 2019).

4.1.2.g Raman Spectroscopy

The Raman spectra of the samples are in the range of 100 cm^{-1} to 1400 cm^{-1}, highlighting the Raman-active modes of green synthesised ZnO and CuO NSs (**Plate 3 I and 3 J**). The ZnO NS has a wurtzite crystal structure with two atoms per primitive cell. Group theory predicts four Raman-active modes: A_1, E_1, and $2E_2$. The A_1 and E_1 modes are infrared active and can be split into longitudinal optical (LO) and transverse optical (TO) components. Nonpolar E_2 modes correspond to the vibrations of oxygen atoms and the Zinc sub-lattice. In the Raman spectrum of pure ZnO NS, the E_2 mode (optical mode) appears at 436 cm^{-1}, while the E_1(LO) mode is observed at 582 cm^{-1}, indicating the c-axis orientation in wurtzite ZnO (Morozov *et al.*, 2015; Song *et al.*, 2019).

The Raman spectra of CuO NS were observed with significant peaks at 266 cm^{-1}, 473 cm^{-1}, and 594 cm^{-1}, which correspond to the A_{1g}, B_{1g}, and B_{2g} modes of Copper oxide (**Plate 3 J**). The CuO NS exhibit the A_{1g} mode of O-Cu-O bending at a stretching frequency of 266 cm^{-1}. Both calcined and uncalcined samples display this A_1g mode, indicating the formation of CuO NSs prior to the calcination step. Additionally, there is a peak at 600 cm^{-1}, which may be attributed to a minor Cu_2O phase. No other peaks suggest the presence of additional Copper oxide phases, confirming the high quality and monophasic nature of the CuO samples (Deng *et al.*, 2016; Tran & Nguyen, 2014; Velliyan & Rajendran, 2021). Furthermore Xu *et al.* (1999), found that the intensity of Raman peaks in CuO nanocrystals varies with grain size, with smaller grains showing stronger and sharper peaks that shift to lower wavenumbers.

4.1.2.h Differential Thermogravimetric Analysis

Thermal stability of the biosynthesised NSs was determined using Differential Thermogravimetric Analysis (DTG). These are the powerful techniques for identification of thermal degradation stages of compounds and nature of hydration of water. **Plate 4 A** shows the weight-loss percentage as a function of temperature for the

dried sample before calcination. A sharp weight loss peak occurred between 200 and 240 °C in green synthesized ZnO and CuO NSs, indicating significant attributed to the loss of moisture and organic residue, which attached on surface of NSs. No further weight loss was observed after 240 °C, as complete decomposition left only pure ZnO and CuO nanostructures as the final residue. Total Percentage weight loss from ZnO and CuO NSs was 9% (at 230ºC) and 47%. (at 206ºC) respectively. In a study by Akhlaghi *et al.,* (2020), Cobalt oxide nanostructures were synthesized using ethanolic extract of fenugreek leaves, with DTG analysis revealing a rapid weight loss of 6.93% above 800 °C. Green synthesized ZnO and Ag–ZnO nanostructures using *Silybum marianum* undergo TGA-DTG analysis, showing weight loss between 135°C and 350°C. (Hameed *et al.*, 2019). Thermal analysis (TG/DTA) of CuO nanoparticles showed that the mass loss between 39-140°C is likely due to lattice water. This is supported by a broad DTA peak at 100°C. The second mass loss stage corresponds to organic residues on the catalyst's surface. Once these residues were removed, no further weight loss occurred, indicating the formation of CuO nanoparticles. Thus, the surface-bound carbonaceous material appears to protect CuO nanoparticles from oxidation (Tanna *et al.*, 2016)

4.1.2.i Influence of the Calcination Process on ZnO and CuO Nanostructures Analyzed by IR Spectroscopy

IR spectroscopy is a valuable method for analyzing multi-component materials, providing insights into their phase composition and interactions among phytochemicals. The IR spectra in **Plate 4 B and 4 C** reveal the organic and inorganic properties of green synthesized ZnO and CuO NSs before and after calcination, focusing on the range of 200–1200 cm^{-1}. The calcined NSs show vibrations between 266–600 cm^{-1}, related to metal–oxygen stretching, with no broad peaks above 1000 cm^{-1}. Calcination effectively decomposed phytochemicals, as indicated by DTG results, eliminating broad absorption bands from carboxylic groups and leaving only the spectra of pure ZnO and CuO NSs.

Shifts in wave numbers suggest improved crystallinity with increased temperature, confirming the successful biosynthesis of these NSs. Infrared studies aimed to determine metal–oxygen interactions. Generally, metal oxides have absorption bands below 1000 cm^{-1} due to interatomic vibrations (Morozov *et al.*, 2015), with

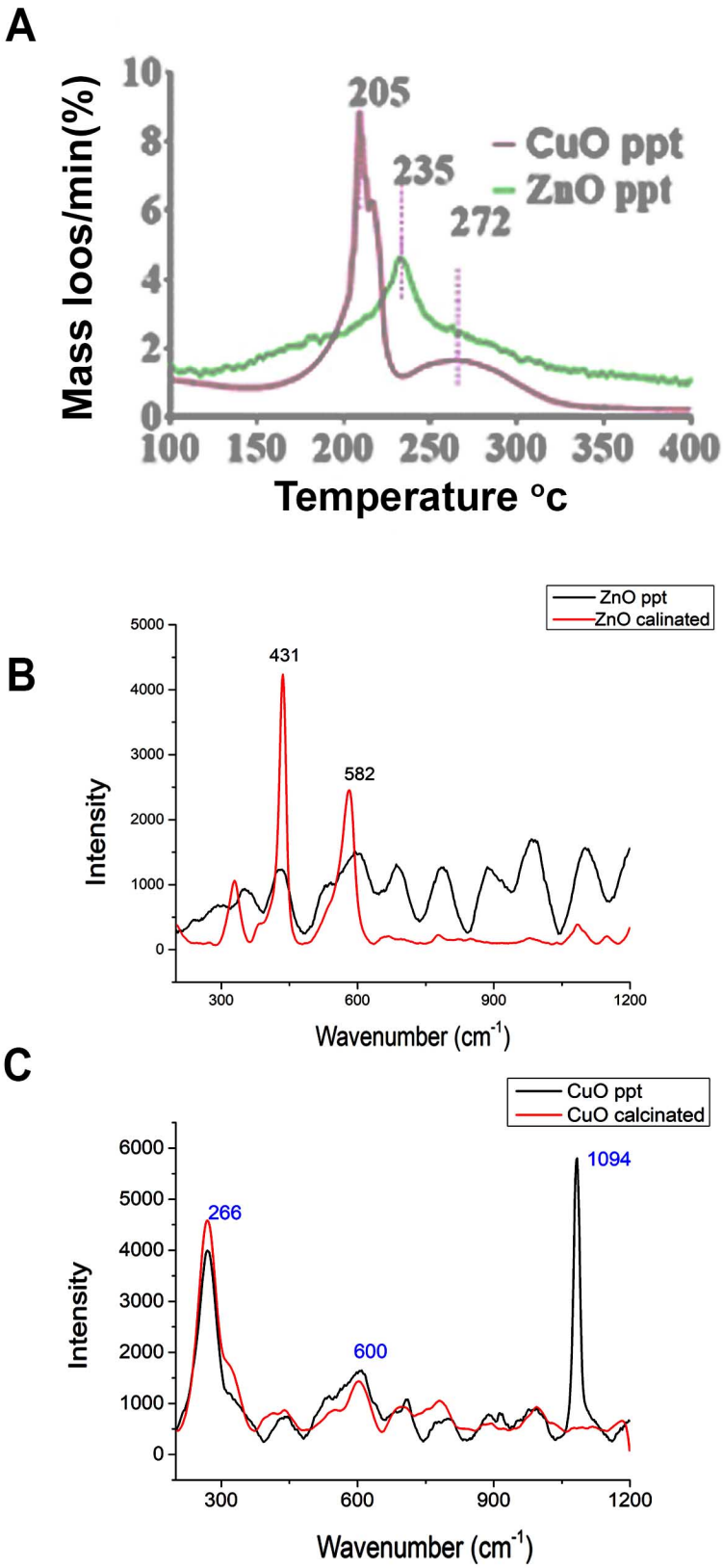

Plate 04: Characterization of green synthesised nanostructures.
(A) DTG of ZnO and CuO precipitate (before calcination), **(B)** IR band of ZnO NSs before and after calcination, **(C)** IR band of CuO NSs before and after calcination.

similar vibrational modes for Cu-O and Zn-O noted in previous studies (Alibe *et al.*, 2017; Sagadevan *et al.*, 2019).

Nanostructures have unique properties and features that make them useful for numerous applications. It is crucial to extensively characterize them, especially for biomedical applications, to ensure they are suitable. The most commonly used techniques for this purpose include UV-Vis, FT-IR, XRD, SEM-EDX, TEM, DTG, IR spectroscopy and Raman spectroscopy. These techniques are employed to study nanostructure size, shape, structure, and surface properties (Altammar, 2023; Mughal *et al.*, 2021).

4.2 STANDARDIZATION OF PROTOCOL FOR SHOOT MULTIPLICATION OF *R. CORDIFOLIA*

Nodal segments of *R. cordifolia* were used as the explant in this study. Using nodal explants for organogenesis represents a highly effective technique for plant propagation. This approach achieves rapid and successful results by culturing nodal segments on MS media enriched with different PGRs in different concentrations. The effectiveness of this method is primarily attributed to axillary buds as well as the presence of highly active meristematic tissue within the nodal explants, which play a crucial role in enhancing plant propagation (Suwal *et al.*, 2020).

The collected plant material of *R. cordifolia* was cultured in MS basal media and they were periodically sub-cultured after attaining maximum growth. This culture was used for the *in vitro* propagation of the study material in MS media with different concentrations of plant growth regulators and the resulting morphological changes after 80 days were analysed. Axillary bud break and the emergence of shoots from nodal explant were noticed in the first week. Rooting was observed about one week after the segments were placed, but the specific timing varied depending on the plant growth regulators used (**Table 6**).

The length of shoots of control plants (MS medium free of PGRs) were 5.02±0.38 cm. The shoots and roots developed directly from the nodes without any callus formation. A substantial amount of multiple shoots (8.428±0.07) was observed. Numerous thin roots with length 3.46±0.66 cm were also seen. The fresh weight and dry weight were 0.14±0.07g and 0.02±0.009 respectively (**Plate 5 T**).

It was observed that the nodal explants cultured in Kinetin containing MS media showed a significant shoot and root development. Both shoot and root formed simultaneously from the nodal explant itself without any callus formation. Few of them produced callus with root only. Among the Kinetin concentrations, 0.5mg/L showed maximum shoot growth (9.7±0.34 cm) and root growth (8.24±0.36 cm), when compared to all other concentrations and control. Broad leaves were noticed here. Roots were numerous and clustered. Maximum shoot multiplication (8.692±0.03) and branching was also observed compared to all other concentrations and control. A single small shoot with numerous thin roots were seen in Kinetin 1 mg/L and Kinetin1.5mg/L (**Plate 5 A-D**)**.** Similar outcomes were showed by a study conducted by Bansal *et al.,*

(2024). According to them, *R. cordifolia* nodal explants have shown a great deal of potential for regeneration, and the use of cytokinin like Kinetin and 2-isopentenyladenine for shoot induction has worked incredibly well. The best option was to augment MS medium with 1.0 mg/L of Kinetin, which produced (12.14 ± 1.58) shoots and (29.78 ± 1.93) axillary buds but in the above study 1mg/L Kinetin showed more root development than shoots. According to Sangeetha *et al.,* (2014), cytokinin-supplemented medium was found to be essential for shoot regeneration in the Cucurbitaceae family same as that observed in case of *R. cordifolia.*

In case of BA treatment, the length of the shoot was small, but shoot multiplication was found to be greater. Shoot and roots were developed from the callus. Among all other BA concentrations, 1mg/L showed the second-highest shoot multiplication (6.29±0.06). A slight colour difference from dark green to yellowish green was noticed. The leaves were bent downwards and were wavy in nature when compared to control. Plants were short and stout but with a considerable thickness. Also, the roots were few but have greater thickness (**Plate 5 E-H**). Similar study shows that among cytokinin concentrations tested, BA was more effective in inducing multiple shoot formation than Kinetin in nodal explants of *R. cordifolia* (Radha *et al.*, 2011). MS medium augmented with additives and 2.0 mg/L BAP was recorded optimum for shoot bud induction from the nodal meristems of *Oldenlandia corymbosa* (Revathi *et al.*, 2018). The most gratifying effect on encouraging the proliferation of many shoots through direct organogenesis in *R. cordifolia* has been demonstrated by studies conducted by Swaroopa Ghatge *et al.,* (2011) and Radha *et al.,* (2011) where the results were same as that of present study.

When MS media fortified with IAA, shoot development occurred first and roots were developed at a later period. Organogenesis was observed to occurs directly from the explant without callus formation. In the case of IAA 0.5 mg/L, less number of shoots were formed from the explant**.** The length of the shoot (6.78±0.39 cm) was much higher when compared to other concentrations of IAA. Only a few shoots were developed in IAA 1mg/L, they were short, whereas in IAA 1.5mg/L, no roots were formed in most of the cultures (**Plate 5 I-K**). De Klerk et al., (1997) reported that the strong inhibition of root formation was occurred at supraoptimal auxin concentrations.

MS medium treated with NAA showed only root formation. Roots were developed from the callus. The maximum root formation was observed in NAA 1.5mg/L (2.8±0.42 cm). The small shoots developed from the axillary buds when grown in a medium containing 0.5 mg/L of NAA. No shoot formation occurs in the rest of the NAA treatments (**Plate 5 L-N**). The same results were noted in a work conducted by Radha *et al.,* (2011), where nodal explants of *R. cordifolia* cultivated in conditions containing BA and NAA developed a compact red callus on their cut ends.

In case of IBA treatment, the length of the shoot and multiplication was found to be substantially lower. But the thickness of shoots was comparatively high and the leaves are very broad. Among all other IBA concentrations, 0.5 mg/L showed maximum shoot multiplication (1.087±0.03) and length (1.2±1.54) (**Plate 5 O-Q**). An experiment conducted by Shahab *et al.,* (2013) assessed the effects of different levels of IBA on Alstonia cuttings. The results showed that stem diameter was significantly influenced by IBA treatment. The results showed that cuttings treated with 10% IBA had the largest stem diameter at 14.44 mm, while those without IBA treatment measured 8.53 mm.

When MS medium containing a combination of BA and Kinetin was used, comparatively less growth was observed. MS media containing Kinetin 0.5 mg/L and BA 1 mg/L as well as MS media containing BA 0.5 mg/L and Kinetin 1 mg/L were the two combinations used. In a combination of BA 1mg/L and Kinetin 0.5mg/L, Shoots and roots were originated from the callus. In certain cultures, leaves develop straight from the callus and were grouped in a clustered fashion without internodes. Roots were not formed here (**Plate 5 R and 5 S**). The outcome was consistent with the finding of Saha *et al.,* (2007), the regeneration capacity of Bottle gourd, when treated with combinations of BA and Kinetin, was very low, and the emergence of shoot buds was delayed. BA promoted ethylene production, but the combined effect of Kinetin and BA decreased ethylene production and contributed to a higher frequency of regeneration from cotyledon explants of Bottle gourd (*Lagenaria siceraria*). Whereas when a combination of BA 0.5mg/L and Kinetin 1mg/L is used, two types of plants were developed. One type was with shoots only having short stem and small leaves and another one was with roots only which were formed from the callus**.**

Among the growth regulators tested, Kinetin was more effective in inducing multiple shoot and root formation than other treatments. when Kinetin alone was used,

Plate 05: *In vitro* cultures of *R. cordifolia* in MS media containing various concentrations of plant growth regulators.
(A) 0.5 mg/L Kinetin, **(B)** 1 mg/L Kinetin, **(C)** 1.5 mg/L Kinetin, **(D)** 2 mg/L Kinetin, **(E)** 0.5 mg/L BA, **(F)** 1 mg/L BA, **(G)** 1.5 mg/L BA, **(H)** 2 mg/L BA, **(I)** 0.5 mg/L IAA, **(J)** 1 mg/L IAA, **(K)** 1.5 mg/L IAA, **(L)**0.5 mg/L NAA, **(M)** 1 mg/L NAA, **(N)** 1.5 mg/L NAA, **(O)** 0.5 mg/L IBA, **(P)** 1 mg/L IBA, **(Q)** 1.5 mg/L IBA, **(R)** 0.5 mg/L Kinetin+1 mg/L BA, **(S)** 0.5 mg/L BA+1 mg/L Kinetin, **(T)** MS basal (control).

better results were obtained only at certain optimum concentration. The highest frequency of shoot formation was recorded in nodes in an optimum concentration of 0.5 mg/L Kinetin with an average number of 2-3 shoots per node, with a mean shoot length of 9.7±0.34 cm. The quality of shoots and the overall growth response in terms of average number of nodes per shoot was better in this concentration.

When the number of shoots of all plants were compared, the plants grown in different BA concentrations showed the better results. BA showed a significant increase in area of leaf than control. The maximum area of leaf was observed in BA 2mg/L (1.488±0.47 cm^2). All other concentrations showed lesser area of leaf. Among these, NAA containing medium had no leaf formation**.**

While analyzing the fresh and dry weight of each sample, it was observed that the medium with 0.5mg/L Kinetin had maximum fresh weight (3.64±0.14 g) and dry weight (0.26±0.02) which were higher than the control (3.17±0.25 g and 0.24±0.04 g respectively).

A simple and dynamic protocol was developed for the micropropagation of *R. cordifolia* by testing various concentrations of growth regulators. Kinetin 0.5 mg/L to be the satisfactory media for the multiplication of shoots, roots and biomass production. Hence, the *in vitro* propagation of nodal segments of *R. cordifolia* using plant growth regulators was identified to be a rapid and cost-effective technique for the large scale production of this plant.

4.2.1 Hardening

Plantlets grown *in vitro* were successfully transferred to *ex-vitro* conditions, where they thrived and remained healthy (**Plate 6**). Their shoots flourished in the field, and their leaves became more vibrant. The plants produced through micropropagation closely resembled the mother plants in both structure and function.

Table 6: Effect of PGRs on shoot multiplication from nodal segments of *R. cordifolia* in MS medium

Sl. No.	PGRs					Morphological Traits				
	KIN (mg/L)	IAA (mg/L)	BA (mg/L)	NAA (mg/L)	IBA (mg/L)	Length of shoot (cm)	Length of root (cm)	No. of shoots	Fresh weight (g)	Dry weight (g)
1.	-	-	-	-	-	8.22±0.75	4.84±0.75	7.428±0.07	3.17±0.25	0.24±0.04
2.	0.5	-	-	-	-	9.7±0.34	8.24±0.36	8.692±0.03	3.64±0.14	0.26±0.02
3.	1	-	-	-	-	5.08±0.49	4.04±0.35	4.16±0.05	0.053±0.02	0.06±0.04
4.	1.5	-	-	-	-	3.24±0.28	3.5±0.78	3.098±0.04	0.05±0.01	0.01±0.00
5.	2	-	-	-	-	4.42±0.52	4.2±0.81	4.178±0.03	0.11±0.02	0.02±0.00
6.	-	0.5	-	-	-	6.78±0.39	3.24±0.46	3.262±0.11	0.29±0.04	0.04±0.01
7.	-	1	-	-	-	3.1±0.37	2.74±0.41	4.072±0.01	0.27±0.05	0.04±0.01
8.	-	1.5	-	-	-	0.82±0.50	1.64±0.58	3.01±0.0	0.08±0.03	0.02±0.01
9.	-	-	0.5	-	-	2.04±0.22	1.48±0.50	3.064±0.01	0.03±0.00	0.01±0.00
10.	-	-	1	-	-	4.24±0.33	1.7±0.32	6.29±0.06	0.09±0.01	0.02±0.00
11.	-	-	1.5	-	-	4.02±0.48	2.88±0.54	1.144±0.04	0.14±0.03	0.02±0.00
12.	-	-	2	-	-	4.28±0.32	1.58±0.62	2.588±0.47	0.14±0.02	0.06±0.04

13.	-	-	-	0.5	-	0.06±0.04	0.7±0.18	0±0.0	0.18±0.01	0.03±0.01
14.	-	-	-	1	-	0±0.0	1.38±0.25	0±0.0	0.30±0.06	0.05±0.02
15.	-	-	-	1.5	-	0±0.0	2.8±0.42	0±0.0	0.47±0.05	0.14±0.03
16.	-	-	-	-	0.5	1.2±1.54	1.6±0.86	1.087±0.03	0.03±0.00	0.01±0.00
17.	-	-	-	-	1	0.8±1.37	2.5±1.06	1.060±0.11	0.09±0.01	0.02±0.01
18.	-	-	-	-	1.5	0.4±1.05	1.5±0.57	0.30±0.02	0.04±0.03	0.02±0.00
19.	0.5	-	1	-	-	1±0.42	0.56±0.56	2.07±0.0	0.06±0.01	0.01±0.02
20.	1	-	0.5	-	-	0.88±0.51	1.02±0.44	1.044±0.03	0.06±0.01	0.03±0.02

Data in each column represents mean ± standard deviation. According to Duncan's multiple range test, significant differences are denoted as $p \leq 0.05$ (Duncan, 1955).

Plate 06: Acclimatization of *in vitro* cultured *R. cordifolia*.
(A) Habit, **(B)** Culture established in medium containing 0.5 mg/L Kinetin, **(C)** Acclimatized plantlets in sterile soil at lab conditions, **(D)** Well established plantlet in Garden pot.

4.3 COMPARATIVE PHYTOCHEMICAL ANALYSIS OF *IN VITRO* RAISED STEM, LEAF AND ROOT OF *R. CORDIFOLIA* FOR IDENTIFYING BEST EXTRACTION SOLVENT AND PLANT PART

This study aimed to optimize a solvent system to maximize the extraction yield of bio active compounds (Alizarin and Purpurin) from *in vitro* propagated *R. cordifolia* using three solvent systems (methanol, hexane and chloroform) and to validate the method using HPTLC for qualitative analysis. The study revealed quantitative and qualitative differences between extraction solvent and different parts of the plant.

4.3.1 HPTLC Profiling

The various parts (leaf, stem and root) of the *in-vitro* propagated *R. cordifolia* plant were separately extracted using hexane, chloroform and methanol to obtain a total of nine extracts. The HPTLC profile was developed for each extract as well as for two standard markers (Alizarin and Purpurin). The solvent systems for these extractions were standardized. Differences were observed in the number of bands and area percentage of the HPTLC profile developed for the different extractions of *in vitro* grown *R. cordifolia* and their marker compounds. These differences indicate variations in the qualitative and quantitative chemical constituents. HPTLC allows for the clear separation of Alizarin and Purpurin, making it easier to compare the effectiveness of different extraction solvents (Valianou *et al.*, 2009).

The optimal solvent system for separating all 9 extracts and 2 anthraquinone markers was a combination of Toluene, Ethyl Acetate and Formic Acid in the ratio of 7:3:0.3. The developed chromatographic plate was viewed under 254 nm and 366 nm, followed by derivatization using ANS reagent and visualized at 550 nm. The developed HPTLC profile for the standard markers shows specific bands with a high area percentage at R_f 0.64 for Alizarin and R_f 0.52 for Purpurin.

The three *R. cordifolia* leaf extracts showed a total of 19 bands at 254 nm. Bands at R_f 0.19, 0.35, 0.52, and 0.64 were common to hexane, chloroform and methanol extracts. The three bands with the highest area percentage were all from the methanol extract. In the methanol extract, there are 12 bands, with a unique band at R_f 0.77 showing the highest area percentage (26.88%). In the hexane and chloroform extracts, the highest area percentage was found in a common band at R_f 0.74, with 35.55% and 33.86% respectively. Compared with standard marker bands, the Alizarin and Purpurin

bands were observed in all the thee extracts. The methanol extraction exhibited a high area percentage for both Alizarin (5.02%) and Purpurin (15.74%) (**Plate 7 A and 7 B; Table 7**).

Table 7: Comparative HPTLC analysis of Hexane, Chloroform and Methanol extracts of *in vitro R. cordifolia* plant parts (leaf, stem and root) at 254 nm.

Sl.No.	R_f	Area % at 254 nm		
		Hexane	Chloroform	Methanol
		Leaf		
1.	0.01	0.11	-	-
2.	0.08	0.11	-	-
3.	0.10	0.51	0.64	-
4.	0.19	0.61	1.58	0.85
5.	0.24	-	-	2.02
6.	0.35	14.96	14.75	16.88
7.	0.38	5.68	-	4.79
8.	0.41	-	1.73	-
9.	0.43	2.15	-	2.48
10.	0.47	-	-	9.26
11.	0.52	6.32	1.81	15.74
12.	0.54	-	2.53	-
13.	0.58	-	1.16	4.19
14.	0.64	3.93	1.76	5.02
15.	0.69	-	3.16	4.11
16.	0.74	35.55	33.86	-
17.	0.77	-	-	26.88
18.	0.84	12.14	30.21	-
19.	0.90	18.02	-	7.77
20.	0.94	-	1.25	-
		Stem		
1.	0.03	0.54	-	0.63
2.	0.07	-	-	0.62
3.	0.11	6.65	1.98	-

4.	0.18	-	0.70	1.48
5.	0.21	-	-	1.68
6.	0.24	1.35	-	2.79
7.	0.27		2.51	3.48
8.	0.29	2.57	-	-
9.	0.31	-	3.49	-
10.	0.34	6.26	10.60	16.29
11.	0.39	6.73	4.42	5.35
12.	0.47	-	-	5.37
13.	0.52	3.45	3.21	14.49
14.	0.55	2.71	1.69	-
15.	0.60	2.73	3.82	-
16.	0.64	-	1.73	1.71
17.	0.71	5.34	2.17	4.08
18.	0.76	37.04	13.03	24.21
19.	0.81	-	13.75	-
20.	0.86	14.85	36.88	-
21.	0.89	-	-	9.49
22.	0.91	-	-	8.34
23.	0.95	9.78	-	-
		Root		
1.	0.01	-	0.10	-
2.	0.09	-	19.70	5.87
3.	0.18	-	0.95	-
4.	0.21	-	1.03	-
5.	0.24	4.38	3.19	27.37
6.	0.28	-	1.35	5.00
7.	0.34	12.54	7.5	-
8.	0.37	-	-	6.01
9.	0.39	8.69	3.90	-
10.	0.44	-	11.64	-

11.	0.47	-	-	3.96
12.	0.52	11.94	8.87	6.19
13.	0.64	6.92	4.78	8.45
14.	0.67	-	6.30	12.16
15.	0.72	2.80	1.00	-
16.	0.77	3.05	0.43	-
17.	0.82	2.31	1.20	2.36
18.	0.86	-	-	-
19.	0.90	11.42	12.99	22.64
20.	0.97	35.96	14.83	-

At 366 nm, 21 compounds were detected, six of which were present in all three extracts. The common bands had the highest area percentages at R_f 0.77, 0.64, and 0.48 for the methanol extract, and at R_f 0.41 and 0.35 for the hexane extract, while the area percentage for R_f 0.30 was approximately the same for all three extracts. Comparison with markers: The Alizarin bands are present in all three extracts, while the Purpurin band is absent in the hexane extract. The highest area percentage (area%) is for both marker bands (Purpurin - 11.18% and Alizarin – 7.79%) in the methanol extract (**Plate 7 C and 7 D; Table 8**).

Table 8: Comparative HPTLC analysis of Hexane, Chloroform and Methanol extracts of *in vitro R. cordifolia* plant parts (leaf, stem and root) at 366nm.

Sl.No.	**R_f**	**Area % at 366 nm**		
		Hexane	**Chloroform**	**Methanol**
		Leaf		
1.	0.01	-	0.07	-
2.	0.11	-	0.19	-
3.	0.19	0.74	2.72	-
4.	0.23	-	-	3.04
5.	0.25	-	3.44	1.77
6.	0.30	4.87	5.27	4.07
7.	0.35	15.29	10.80	8.22
8.	0.38	-	-	2.25

9.	0.41	4.21	3.11	2.89
10.	0.48	-	2.16	8.67
11.	0.52	3.47	1.48	11.18
12.	0.55	4.61	3.73	5.86
13.	0.59	3.55	1.83	-
14.	0.64	4.81	6.62	7.79
15.	0.69	-	4.34	8.43
16.	0.73	16.38	9.56	-
17.	0.77	5.71	17.65	21.90
18.	0.85	21.91	27.03	-
19.	0.88	14.46	-	13.28
20.	0.94	-	-	0.20
21.	0.98	-	-	0.44
		Stem		
1.	0.03	0.38	-	-
2.	0.08	-	-	0.25
3.	0.10	3.99	0.59	-
4.	0.14	-	0.39	0.86
5.	0.19	0.35	-	-
6.	0.22	0.87	2.66	3.73
7.	0.30	3.61	5.62	5.94
8.	0.34	7.31	4.75	4.69
9.	0.38	-	-	1.42
10.	0.42	-	2.01	1.76
11.	0.47	-	1.84	6.86
12.	0.49	0.83	-	-
13.	0.52	1.83	2.47	11.37
14.	0.56	-	-	1.73
15.	0.59	0.72	-	2.29
16.	0.61	-	5.36	-
17.	0.64	2.63	6.54	7.27

18.	0.71	3.34	4.64	2.13
19.	0.75	21.51	11.81	18.89
20.	0.81	3.72	13.98	3.95
21.	0.88	48.91	37.33	24.16
22.	0.95	-	-	1.69
23.	0.98	-	-	1.03
		Root		
1.	0.09	-	19.70	7.94
2.	0.21	-	4.81	-
3.	0.24	10.33	3.53	32.22
4.	0.30	8.13	9.89	5.57
5.	0.32	23.52	-	-
6.	0.34	-	2.64	-
7.	0.37	-	-	6.62
8.	0.44	-	10.41	-
9.	0.58	-	4.04	-
10.	0.61	-	2.32	-
11.	0.64	-	5.86	17.32
12.	0.73	-	-	10.35
13.	0.75	19.77	3.10	-
14.	0.82	3.7	6.05	-
15.	0.88	34.48	27.65	9.87
16.	0.96	-	-	10.11

A total of 25 bands were found to be present in the ANS derivatized hexane HPTLC plates visualized at 550 nm. There were ten common bands among the three extracts. At the R_f values of 0.09, 0.26, 0.56, 0.69 for the hexane extract, 0.13, 0.18, 0.45 for the methanol extract, and R_f 0.76, 0.85 for the chloroform extract were found to have the maximum area percentages of the bands. The bands in the methanol and chloroform extract were about equal at R_f 0.29. The specific marker bands were only seen in methanol extract (**Plate 7 E and 7 F; Table 9**).

Table 9: Comparative HPTLC analysis of Hexane, Chloroform and Methanol extracts of *in vitro R. cordifolia* plant parts (leaf, stem and root) at 550 nm.

Sl.No.	R_f	Area % at 550 nm		
		Hexane	Chloroform	Methanol
		Leaf		
1.	0.01	0.24	0.09	-
2.	0.02	-	0.07	0.08
3.	0.09	4.99	0.82	2.50
4.	0.13	4.31	2.54	6.71
5.	0.18	3.62	4.22	5.85
6.	0.23	-	1.66	-
7.	0.26	5.48	3.44	3.70
8.	0.29	3.25	4.23	4.27
9.	0.34	-	13.91	6.08
10.	0.35	13.12	-	8.48
11.	0.41	-	0.70	-
12.	0.45	2.72	1.30	6.91
13.	0.52	-	-	11.05
14.	0.56	15.79	9.91	11.63
15.	0.61	-	-	1.70
16.	0.64	-	-	12.39
17.	0.69	27.11	16.56	6.84
18.	0.73	-	3.80	-
19.	0.76	2.50	16.64	7.12
20.	0.81	-		0.93
21.	0.85	3.78	18.64	2.76
22.	0.90	13.09	-	-
23.	0.93	-	0.85	-
24.	0.95	-	-	1.00
25.	0.97	-	0.61	-

		Stem		
1.	0.02	4.58	-	0.16
2.	0.04	-	-	0.53
3.	0.08	-	-	0.91
4.	0.10	4.63	-	-
5.	0.13	4.41	12.57	5.80
6.	0.17	-	5.11	4.41
7.	0.18	4.17	-	-
8.	0.19	-	6.43	4.27
9.	0.23	-	4.56	3.59
10.	0.27	1.28	4.35	4.28
11.	0.29	-	3.30	3.69
12.	0.31	5.33	-	-
13.	0.33	8.83	12.49	16.05
14.	0.38	-	1.55	1.50
15.	0.42	-	0.48	-
16.	0.47	0.25	-	1.58
17.	0.52	2.03	2.19	7.10
18.	0.57	21.04	10.77	12.65
19.	0.64	19.56	10.30	18.39
20.	0.71	8.20	3.31	5.24
21.	0.74	6.10	-	-
22.	0.76	-	1.86	6.90
23.	0.78	2.68	-	-
24.	0.81	-	6.07	-
25.	0.87	4.15	11.83	2.74
26.	0.95	2.27	2.80	0.21
27.	0.97	0.49	-	-
		Root		
1.	0.03	-	1.07	-
2.	0.09	-	6.23	-

3.	0.13	17.51	11.98	29.44
4.	0.19	7.65	8.78	8.55
5.	0.24	3.75	5.09	8.50
6.	0.28	5.50	10.18	8.39
7.	0.34	12.36	10.72	10.39
8.	0.39	4.66	1.24	2.78
9.	0.45	-	0.27	-
10.	0.46	1.84	0.24	-
11.	0.52	4.09	3.10	4.37
12.	0.57	22.25	20.38	16.76
13.	0.64	11.07	8.73	9.51
14.	0.71	3.26	1.52	-
15.	0.74	-	0.61	-
16.	0.79	1.75	1.89	0.95
17.	0.87	-	1.29	-
18.	0.96	4.32	6.66	0.36

HPTLC profile was developed for the three extracts of *R. cordifolia* stem and the developed plate was visualized at different wavelengths. At 254 nm, 23 compounds were observed, with five common bands at R_f 0.34, 0.39, 0.52, 0.71, and 0.76. The bands at R_f 0.39, 0.71, and 0.76 show the highest area% in the hexane extracts, while the bands at R_f 0.34 and 0.52 show the highest area% in the methanol extract. The Purpurin band was present in all three extracts, with the highest area% in the methanol extract. The Alizarin band was only present in the chloroform and methanol extract (**Plate 7 A and 7 B; Table 7**).

The three different stem extracts were visualized at 366 nm and were found to contain a total of 22 compounds. Ten bands were found to be shared among the three extracts. Amid that, the highest area percentages were observed at R_f 0.34, 0.75, and 0.88 in the hexane extract, at R_f 0.52, 0.71, and 0.81 in the chloroform extract, and R_f 0.22, 0.30, 0.47, and 0.64 in the methanol extract. The unique marker compound bands were seen in the methanol extract, with a high area percentage of 11.37% for Purpurin and 7.27% for Alizarin (**Plate 7 C and 7 D; Table 8**).

The HPTLC plate of the stem extract showed 25 compounds when derivatized with ANS and observed at 550 nm. Ten bands were consistently present in all three extracts. Among these, R_f values of 0.57, 0.64, and 0.71 had the highest area percentage in the hexane extract compared to the other two extracts. In the chloroform extract, R_f values of 0.13, 0.17, 0.27, 0.87, and 0.95 had the highest area percentage, whereas in the methanol extract, R_f values of 0.33, 0.51, and 0.76 had the highest area percentage. The marker compound bands were present in all extracts, with Purpurin (7.10%) showing the highest area percentage in the methanol extract and Alizarin showing approximately the same area percentage in the hexane and methanol extracts (19.56% and 18.39% respectively) (**Plate 7 E and 7 F; Table 9**).

The HPTLC studies were used to develop the chromatogram of the three different extracts of *R. cordifolia* root extract at different wavelengths. When visualized at 254 nm, the HPTLC plate revealed around 20 compounds. Five common bands were present in all three extracts. Among these, four bands (R_f 0.24, 0.64, 0.82, and 0.90) had high area percentages in the methanol extraction, while the remaining band with high area percentage (R_f 0.52) was in the hexane extract. The marker compound bands were present in all three extracts, with the highest area percentage of Purpurin (11.94%) in the hexane extract and Alizarin (8.45%) in the methanol extract (**Plate 7 A and 7 B; Table 7**).

A total of 15 compounds were observed in the root extracts under 366 nm light. Three common bands with the highest area percentage were detected at R_f 0.24 in methanol, R_f 0.30 in chloroform, and R_f 0.88 in the hexane extract. Only the Alizarin band was visible at this wavelength, and it was not present in the hexane extract. The Alizarin band with a high area% was found in the methanol extract (**Plate 7 C and 7 D; Table 8**).

After ANS derivatization, the HPTLC chromatogram at 550 nm revealed 18 compounds with nine common bands across three extracts. High area percentages were found in specific bands: four in hexane (R_f 0.34, 0.39, 0.57, 0.65), three in methanol (R_f 0.13, 0.24, 0.52), and one in chloroform (R_f 0.28). while the remaining one band (R_f 0.19) was shared between methanol and chloroform extracts. The marker bands were seen in all the three extracts. Purpurin had a high area percentage (4.09%) in

methanol, while Alizarin (11.0%) was in the hexane extract (**Plate 7 E and 7 F; Table 9**).

The HPTLC analysis compared hexane, chloroform, and methanol extracts of *in vitro R. cordifolia* plant parts. The results showed that the highest number of phyto-constituents was present in the methanol extract (45) and chloroform extract (46) in the case of the leaf. In the case of the stem, the highest number of compounds was found in the methanol extract (52), and in the case of the root, it was in the chloroform extract (47). The hexane extract consistently showed the least number of compounds in all cases.

Similar studies showed that methanol is a polar solvent that effectively extracts hydrophilic compounds such as Alizarin and Purpurin (Duval *et al.*, 2016). A study by Ahmad *et al.,* (2024) found that methanol extraction from the roots of *R. cordifolia* resulted in significant quantities of both Alizarin and Purpurin, which were quantified using HPTLC. On the other hand, hexane is a non-polar solvent, making it more suitable for dissolving lipid-soluble compounds rather than phenolic compounds like Alizarin and Purpurin (Danlami *et al.*, 2015). Another study by Ibraheim, (2002) showed that hexane extraction led to minimal recovery of anthraquinones, indicating its inefficacy in extracting polar phytochemicals from the plant. Chloroform, with intermediate polarity between methanol and hexane, may effectively extract certain secondary metabolites, although it may not be as efficient as methanol for extracting anthraquinones.

The HPTLC analysis compared the hexane, chloroform and methanol extracts of *in vitro R. cordifolia* plant parts and marker compounds. The highest area percentage of Alizarin was found in the methanol extract compared to the chloroform and hexane extracts of the leaf and root at all three different wavelengths. Meanwhile, the highest area percentage of the stem was found in the methanol extract at 366 nm. The highest area percentage of Purpurin was also found in the methanol extract compared to the chloroform and hexane extract in the case of the leaf and stem at all three wavelengths, while in the case of the root, it was highest in the hexane extract at 254 nm (**Figure 4**).

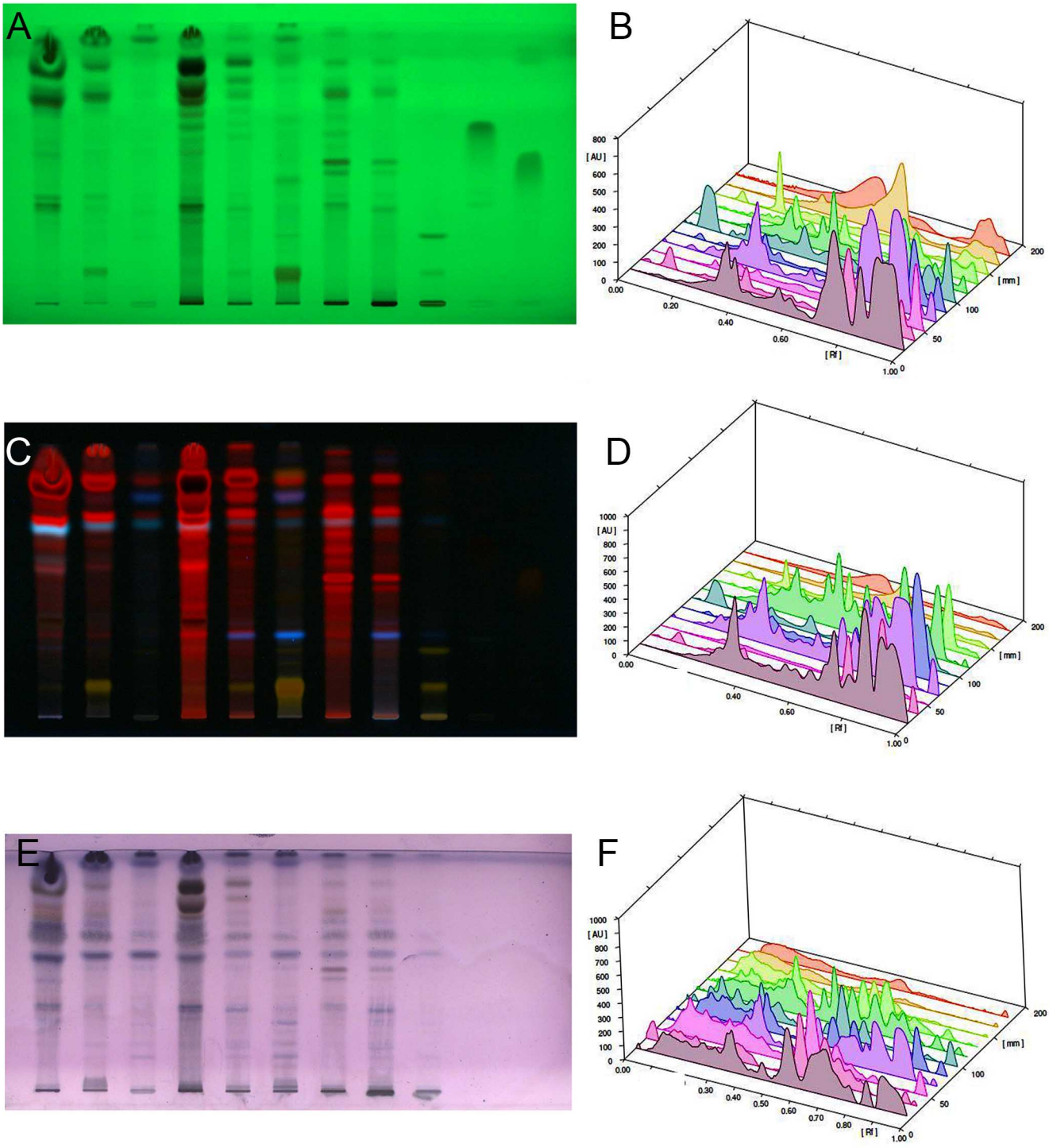

Plate 07: HPTLC Profile of Hexane, Chloroform and Methanol extracts of *in vitro* grown *R. cordifolia* plant parts (leaf, stem and root).
(A & B) HPTLC chromatogram and densitometric scanning image under 254 nm, **(C & D)** HPTLC chromatogram and densitometric scanning image under 366 nm, **(E & F)** HPTLC chromatogram and densitometric scanning image under 550 nm after derivatization; (**Tracks:** 1 - Hexane leaf, 2 - Hexane stem, 3 - Hexane root, 4 - Chloroform leaf, 5 - Chloroform stem, 6 - Chloroform root, 7 - Methanol leaf, 8 - Methanol stem, 9 - Methanol root, 10 - Alizarin, 11 – Purpurin).

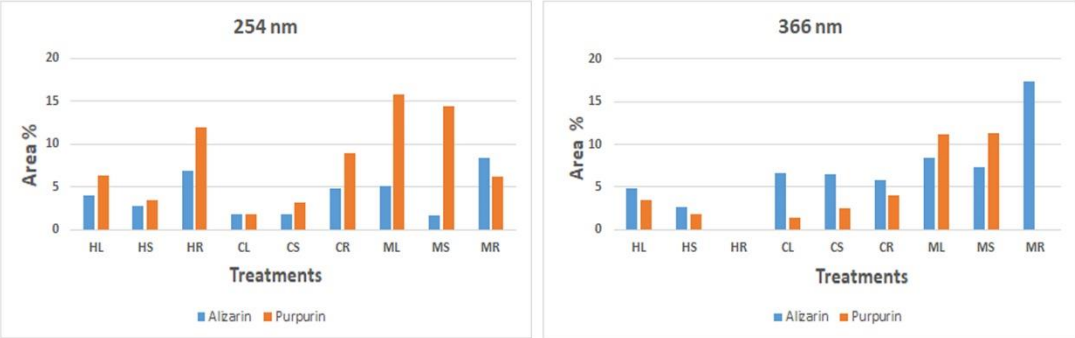

Figure 4: **The HPTLC analysis of *R. cordifolia* grown *in vitro,* extracted using different solvents; HL-Hexane leaf, HS-Hexane stem, HR-Hexane root, CL-Chloroform leaf, CS-Chloroform stem, CR-Chloroform root, ML-Methanol leaf, MS-Methanol stem, MR-Methanol root**

Many researchers prefer using methanol as an extracting solvent for anthraquinone compounds due to its ability to extract more compounds. Absolute methanol is commonly used as the solvent to solubilize anthraquinone pigments (Dabiri *et al.*, 2005). Bányai *et al.,* (2006) used a methanolic extract of lyophilized hairy roots to determine the quantities of the anthraquinones Alizarin and Purpurin in genetically transformed hairy root cultures of *Rubia tinctorum* L. According to Wang *et al.,* (2008), the percent recovery of anthraquinones was found to be highly dependent on the type of solvent, with acetone > acetonitrile > methanol > ethanol. Gong *et al.,* (2005) used methanol to collect aloe-emodin, emodin, chrysophanol, physcion, and rhein from rhubarb.

The HPTLC analysis compared the three different extracts of leaves, stems and roots of the *in vitro R. cordifolia* plant, along with marker compounds. All three parts of the plant contain both marker compounds. However, the root extract had the highest area percentage of Alizarin, while the stem extract had the least. Regarding Purpurin, the hexane and chloroform extracts of the root contained a higher area percentage, while in case of the leaf and stem, the high area% was in the methanol extract. According to Meena *et al.,* (2010) the roots from *R. cordifolia* produced the highest amounts of Alizarin and Purpurin. On the other hand, *R. cordifolia* leaves and stem also showed presence of anthraquinones (Deshkar *et al.*, 2008).

The study by Wang *et al.,* (2023) examined the possible synthetic sites of anthraquinone in *R. cordifolia*. They observed that Purpurin was synthesized in the stems and roots. Previous studies have indicated that the roots and rhizomes of *R. cordifolia* contain high concentrations of secondary metabolites, such as Purpurin and Alizarin. At the same time, the aerial parts have minimal amounts of anthraquinones. *R. cordifolia* is a medicinal plant known for its anti-inflammatory, anticancer, and anti-platelet aggregation properties, attributed to various secondary metabolites, including anthraquinones and naphthoquinones, found in its roots (Kaur *et al.*, 2010; Wang *et al.*, 2024).

In summary, the study revealed quantitative and qualitative differences between extraction solvents and different parts of the plant. Standardizing the best solvent is essential to obtaining an optimal level of bioactive compounds, especially for industries focusing on economic benefits. The study results show that Alizarin and Purpurin were significantly higher in methanolic extraction, and the whole plant can be used for the extraction of these dyes.

4.4 ANALYSIS OF THE GREEN SYNTHESISED NANOSTRUCTURES AS ELICITORS ON MORPHOGENIC RESPONSES

This study aims to assess the impact of different concentrations of ZnO and CuO NSs on various aspects of plant growth, such as shoot length, root length, leaf area, the number of plantlets and biomass. The treatments were compared to a control group to determine their effects on plant growth.

4.4.1 Broad Spectrum Treatment

In the current study, nodal segments of *R. cordifolia* were cultured in MS media supplemented with different concentrations of ZnO and CuO NSs (0.1 mg/L, 1 mg/L, 10 mg/L, and 100 mg/L). Growth occurred in all concentrations except for the highest (100 mg/L NSs) concentration. The control group was placed in MS medium with 0.5 mg/L Kinetin. After 80-day growth period, the plants were harvested, and various growth parameters were analyzed to evaluate the morphogenic response in the *in vitro* cultures of *R. cordifolia* (**Plate 8 and Table 10**).

Table 10: Effects of broad spectrum treatments of NSs in morphogenic responses of *in vitro* cultures of *R. cordifolia*.

Sl. No.	Broad spectrum Treatments of NSs	Avg. shoot length (cm) (Mean±SE)	Avg. Root length (cm) (Mean±SE)	Avg. leaf area (cm^2) (Mean±SE)	Avg. no. of plantlets (Mean±SE)	Fresh Weight (g)	Dry Weight (g)
1.	Control	11.2 ± 0.75^{ab}	8.88 ± 0.89^{a}	0.626 ± 0.13^{b}	4.2 ± 0.37^{a}	4	0.31
2.	0.1 mg/L ZnO	9.1 ± 0.6^{cd}	7.7 ± 0.8^{ab}	0.774 ± 0.15^{b}	3.8 ± 0.37^{a}	1.62	0.19
3.	1mg/L ZnO	7.98 ± 0.08^{d}	5.5 ± 0.52^{b}	0.718 ± 0.06^{b}	4.6 ± 0.24^{a}	1.31	0.15
4.	10mg/L ZnO	8.3 ± 0.66^{d}	6.92 ± 0.56^{ab}	0.654 ± 0.05^{b}	3.6 ± 0.51^{ab}	1.12	0.12
5.	0.1mg/L CuO	10.26 ± 0.91^{bc}	8.92 ± 1.41^{a}	0.62 ± 0.05^{b}	2.6 ± 0.4^{b}	1.03	0.14
6.	1mg/L CuO	12.94 ± 0.49^{a}	6.38 ± 0.24^{ab}	1.328 ± 0.22^{a}	4.2 ± 0.37^{a}	1	0.16
7.	10mg/L CuO	7.62 ± 0.29^{d}	6.42 ± 0.63^{ab}	0.562 ± 0.05^{b}	3.6 ± 0.24^{ab}	1	0.12

Means within a column followed by the same letters are not significantly ($p \leq 0.05$) different as determined by Duncan's Multiple Range test.

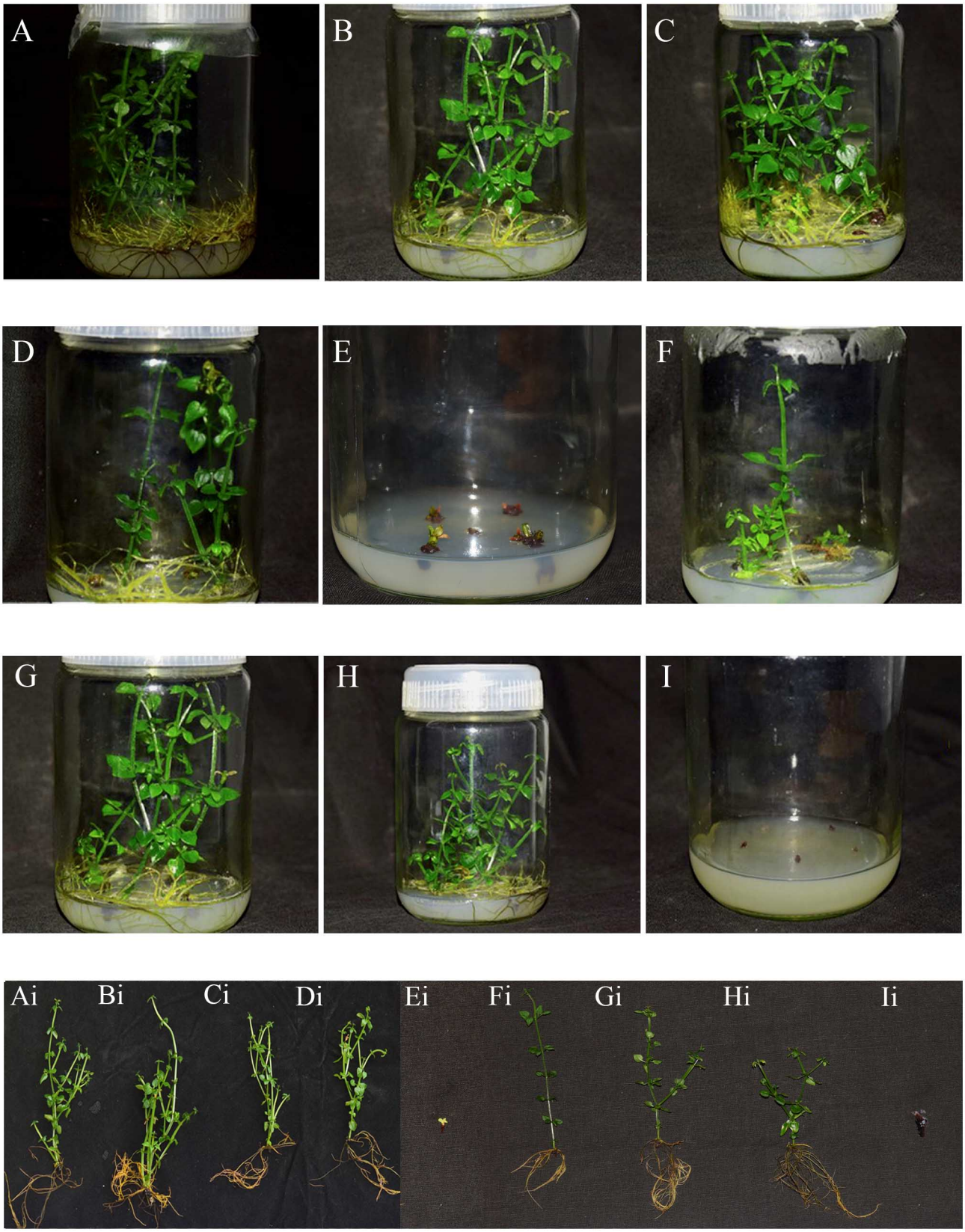

Plate 08: *In vitro* cultures of *R. cordifolia* in MS media containing various concentrations of green synthesised nanostructures.
(A) MS basal (control), **(B)** 0.1 mg/L ZnO NSs, **(C)** 1 mg/L ZnO NSs, **(D)** 10 mg/L ZnO NSs, **(E)** 100 mg/L ZnO NSs, **(F)** 0.1 mg/L CuO NSs, **(G)** 1 mg/L CuO NSs, **(H)** 10 mg/L CuO NSs, **(I)** 100 mg/LCuO NSs; **(Ai - Ii)** Individual plants from different *in vitro* cultures of *R. cordifolia.*

4.4.1.a Shoot Length

The highest shoot length was observed in the plants treated with 1 mg/L CuO NS (12.94±0.49 cm), which was significantly greater than the other treatments. These shoots were long and had multiple branches. The control group also had a high shoot length (11.2±0.75 cm) with numerous branches. On the other hand, the shortest shoot lengths were observed in the plants treated with 1 mg/L ZnO NS (7.98±0.08 cm) and 10 mg/L CuO NS (7.62±0.29 cm). Plantlets treated with 0.1 mg/L CuO NS showed a single shoot with minimal branching (**Figure 5**).

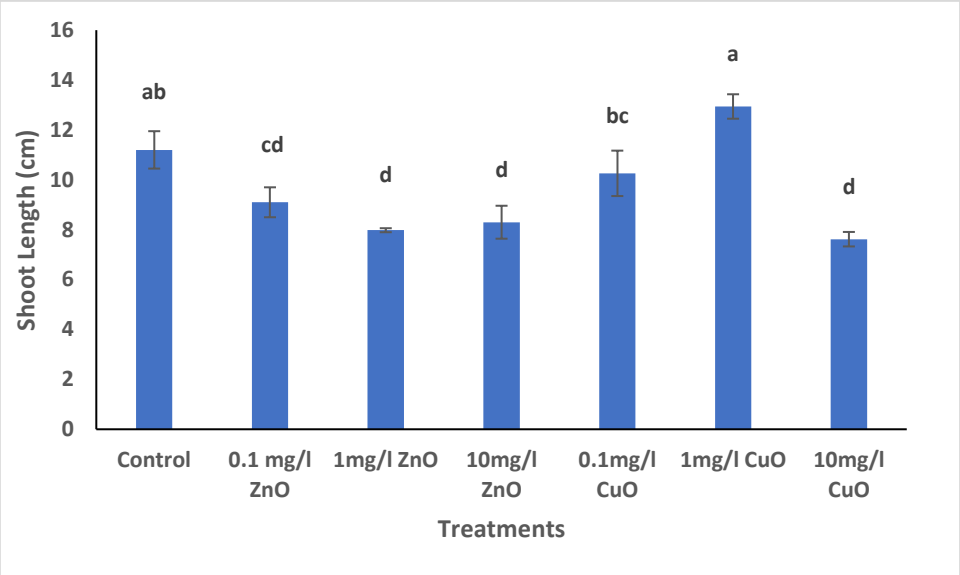

Figure 5: Effects of broad spectrum NSs on the length of shoots in *in vitro* cultures of *R. cordifolia* ($p \leq 0.05$) corresponding to Duncan's Multiple Range tests.

4.4.1.b Root Length

The control group exhibited the longest roots (8.88±0.89 cm) with vigorous branching, while the 1 mg/L ZnO NS treatment resulted in the shortest roots (5.5±0.52 cm). 0.1 mg/L CuO NS treatment also showed long roots (8.92±1.41 cm) similar to control. The root length was relatively similar across ZnO and CuO NS treatments, except for the 1 mg/L CuO NS treatment, which yielded slightly shorter roots compared to the control (**Figure 6**).

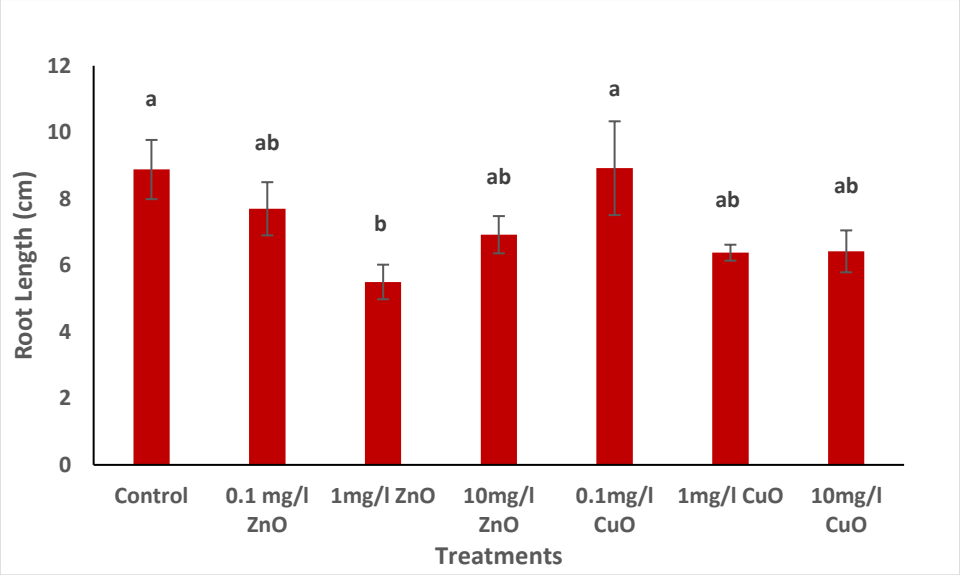

Figure 6: Effects of broad spectrum NSs on the length of roots in *in vitro* cultures of *R. cordifolia* ($p \leq 0.05$) corresponding to Duncan's Multiple Range tests.

4.4.1.c Leaf Area

The largest leaf area was found in the 1 mg/L CuO NS treatment (6.38±0.24 cm^2), which was significantly higher than other treatments. The leaf areas in ZnO NS treatments were similar but lower compared to the control (**Figure 7**).

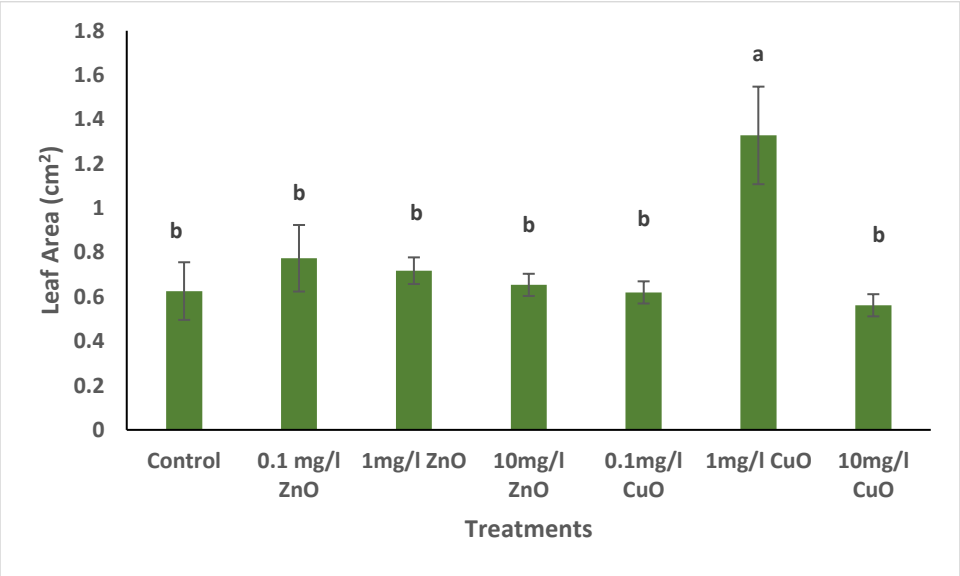

Figure 7: Effects of broad spectrum NSs on the area of leaves in *in vitro* cultures of *R. cordifolia* ($p \leq 0.05$) corresponding to Duncan's Multiple Range tests.

4.4.1.d Number of Plantlets

The highest number of plantlets were observed in the 1 mg/L ZnO NS treatment (4.6±0.24), which was comparable to the control. In contrast, the 0.1 mg/L CuO NS treatment resulted in the lowest number of plantlets (2.6±0.4). The number of plantlets in the other treatments was similar to that of the control (**Figure 8**).

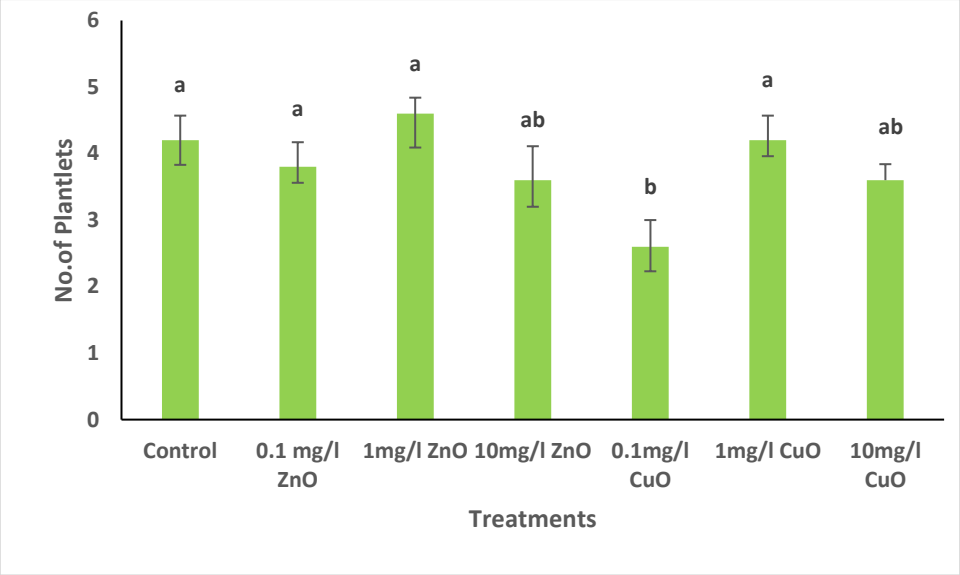

Figure 8: Effects of broad spectrum NSs on the no. of plantlets in *in vitro* cultures of *R. cordifolia* ($p \leq 0.05$) corresponding to Duncan's Multiple Range tests.

4.4.1.e Biomass

The study investigated the impact of different concentrations of ZnO NSs and CuO NSs on the fresh and dry weights of the sample. The control treatment showed the highest fresh weight (4.00 g) and dry weight (0.31 g) among all treatments. Fresh weight decreased as the concentrations of ZnO and CuO NSs increased. The highest fresh weight was observed with 0.1 mg/L ZnO NS (1.62 g), while the lowest was with 10 mg/L ZnO NS and 10 mg/L CuO NS (1.12 g and 1.00 g, respectively). Dry weight also decreased with increasing concentrations of ZnO and CuO NSs. The control had the highest dry weight (0.31 g), while the lowest dry weight was recorded at 10 mg/L ZnO NS and 10 mg/L CuO NS (0.12 g each). ZnO NS generally resulted in lower fresh and dry weights than CuO NS at similar concentrations. In conclusion, ZnO and CuO NS treatments reduced fresh and dry weights compared to the control, with ZnO NS causing a more pronounced effect (**Figure 9**).

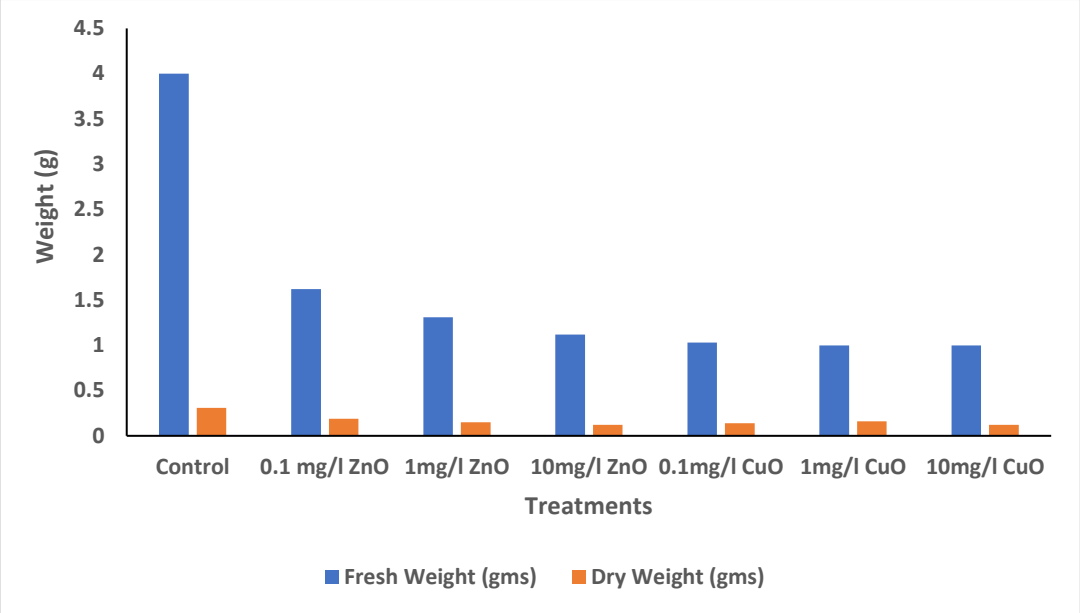

Figure 9: Effects of broad spectrum NSs on the total biomass production in *in vitro* cultures of *R. cordifolia*

4.4.2 Narrow Spectrum Treatment

In the narrow spectrum treatment, nodal segments from *R. cordifolia* were cultured on MS media supplemented with different concentrations of ZnO and CuO NSs (0.2 mg/L, 0.4 mg/L, 0.6 mg/L, and 0.8 mg/L). The control group was placed in MS medium with 0.5 mg/L Kinetin. After 80-day growth period, the plants were harvested, and various growth parameters were analysed to evaluate the morphogenic response in the *in vitro* cultures of *R. cordifolia* (**Plate 9 and Table 11**).

4.4.2.a Shoot Length

The control group had the longest shoot length at 11.2 cm, while the shortest was observed in the 0.6 mg/L ZnO NS treatment at 7.3 cm. ZnO NS treatments generally resulted in reduced shoot lengths compared to the control group, with significant decreases noted at higher concentrations. CuO NS treatments also led to reduced shoot length, with the lowest value recorded at 0.6 mg/L CuO NS at 5.34 cm (**Figure 10**).

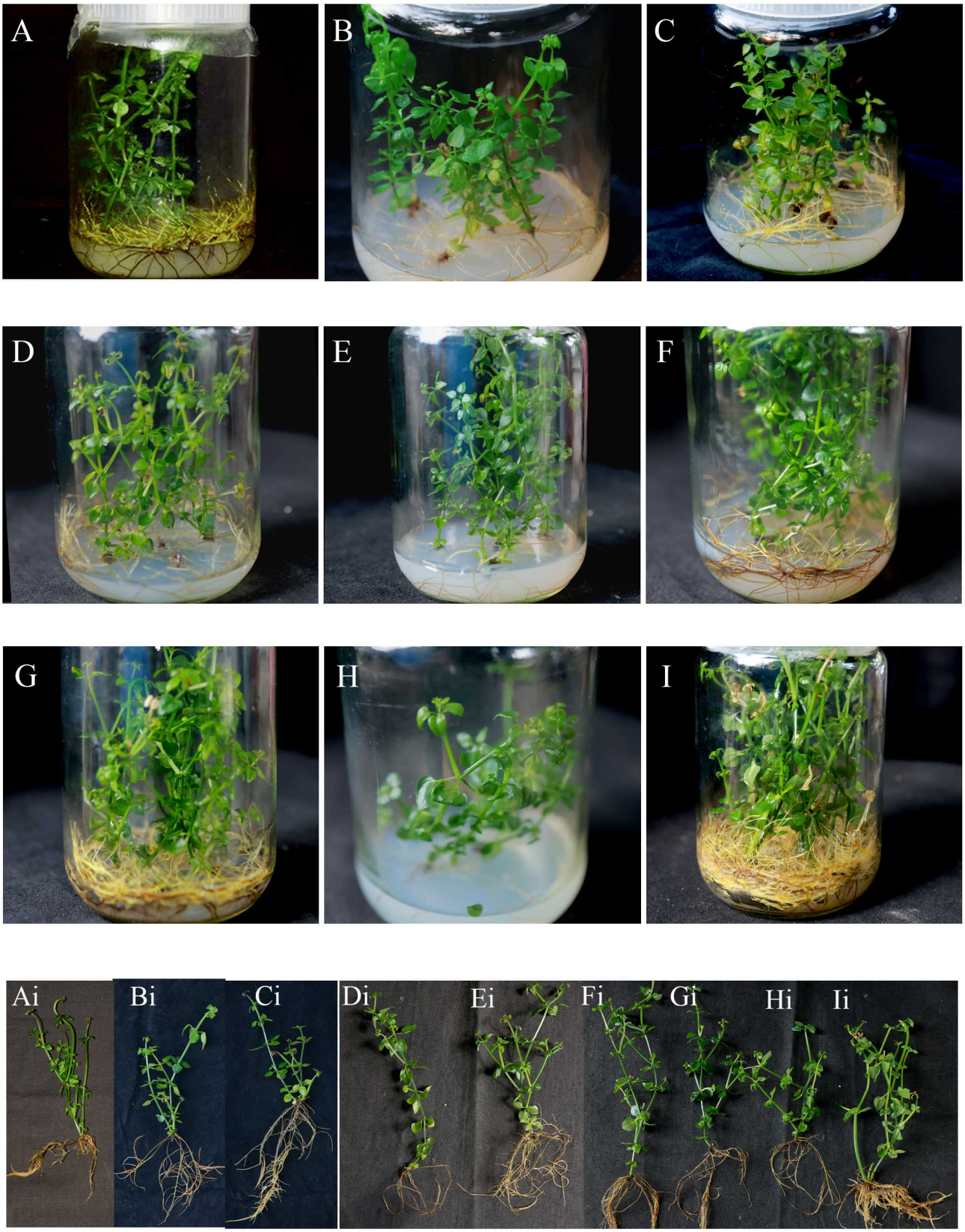

Plate 09: *In vitro* cultures of *R. cordifolia* in MS media containing various concentrations of green synthesised nanostructures.
(A) MS medium+0.5mg/L Kinetin (Control), **(B)** 0.2 mg/L ZnO NSs, **(C)** 0.4 mg/L ZnO NSs, **(D)** 0.6 mg/L ZnO NSs, **(E)** 0.8 mg/L ZnO NSs, **(F)** 0.2 mg/L CuO NSs, **(G)** 0.4 mg/L CuO NSs, **(H)** 0.6 mg/L CuO NSs, **(I)** 0.8 mg/L CuO NSs; **(Ai - Ii)** Individual plants from different *in vitro* cultures of *R. cordifolia.*

Table 11: Effects of narrow spectrum treatments of NSs in morphogenic responses of *in vitro* cultures of *R. cordifolia*

Sl. No.	Narrow Spectrum Treatments of NSs	Avg. shoot length (cm) (Mean±SE)	Avg. Root length (cm) (Mean±SE)	Avg. leaf area (cm^2) (Mean±SE)	Avg. no. of plantlets (Mean±SE)	Fresh Weight (g)	Dry Weight (g)
1.	Control	11.2 ± 0.75^{a}	8.88 ± 0.89^{a}	0.626 ± 0.13^{bc}	4.2 ± 0.37^{abc}	4	0.31
2.	0.2 mg/L ZnO	10.7 ± 0.95^{ab}	5.5 ± 0.52^{c}	1.224 ± 0.16^{a}	3.8 ± 0.37^{c}	1.68	0.18
3.	0.4 mg/L ZnO	10.68 ± 0.89^{ab}	4.94 ± 1.23^{c}	1.08 ± 0.25^{ab}	4.6 ± 0.24^{abc}	1.45	0.14
4.	0.6 mg/L ZnO	7.3 ± 0.53^{cd}	6.36 ± 0.61^{bc}	0.832 ± 0.07^{abc}	3.8 ± 0.2^{c}	0.63	0.13
5.	0.8 mg/L ZnO	10.24 ± 1.11^{ab}	8.08 ± 0.68^{ab}	0.776 ± 0.09^{abc}	4.6 ± 0.24^{abc}	0.79	0.12
6.	0.2 mg/L CuO	8.96 ± 0.61^{abc}	5.6 ± 0.43^{c}	0.92 ± 0.18^{abc}	5 ± 0^{a}	0.83	0.12
7.	0.4 mg/L CuO	8.42 ± 0.33^{bc}	6.36 ± 0.56^{bc}	0.788 ± 0.11^{abc}	4.8 ± 0.2^{ab}	0.83	0.13
8.	0.6 mg/L CuO	5.34 ± 0.32^{d}	5.66 ± 0.52^{c}	0.464 ± 0.05^{bc}	4 ± 0.31^{bc}	0.24	0.05
9.	0.8 mg/L CuO	10.14 ± 0.67^{ab}	8.28 ± 0.85^{ab}	1.028 ± 0.12^{ab}	3.8 ± 0.37^{c}	0.71	0.19

Means within a column followed by the same letters are not significantly ($p < 0.05$) different as determined by Duncan's Multiple Range test.

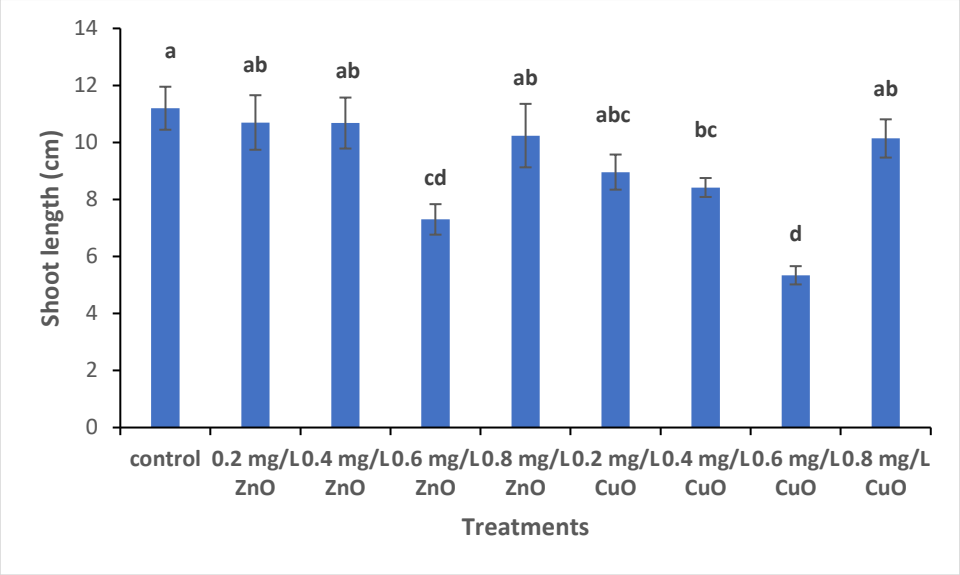

Figure 10: Effects of narrow spectrum NSs on the length of shoots in *in vitro* cultures of *R. cordifolia* ($p \leq 0.05$) corresponding to Duncan's Multiple Range tests

4.4.2.b Root Length

The control group exhibited the longest root length at 8.88 cm, while ZnO NS treatments significantly reduced root length, particularly at concentrations of 0.4 mg/L and 0.6 mg/L. CuO NS treatments had varying effects on root length, with no significant differences noted between the control and lower CuO NS concentrations (0.2 mg/L and 0.4 mg/L) (**Figure 11**).

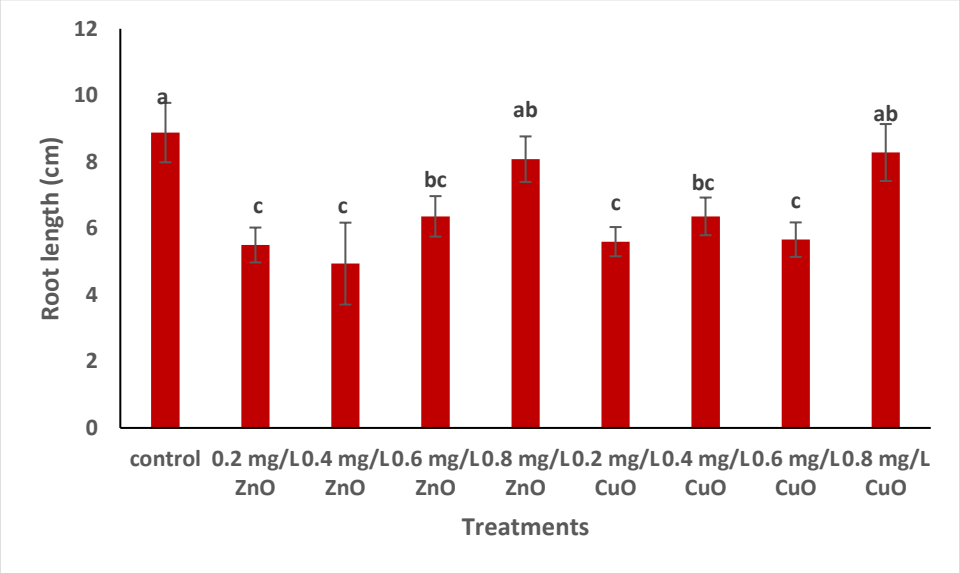

Figure 11: Effects of narrow spectrum NSs on the length of roots in *in vitro* cultures of *R. cordifolia* ($p \leq 0.05$) corresponding to Duncan's Multiple Range tests

4.4.2.c Leaf Area

The largest leaf area was observed in the 0.2 mg/L ZnO NS treatment at 1.224 cm^2, while the smallest was in the 0.6 mg/L CuO NS treatment at 0.464 cm^2. ZnO NS treatments tended to increase leaf area at lower concentrations but decreased at higher concentrations. CuO NS treatments showed a similar trend, with reduced leaf area at higher concentrations (**Figure 12**).

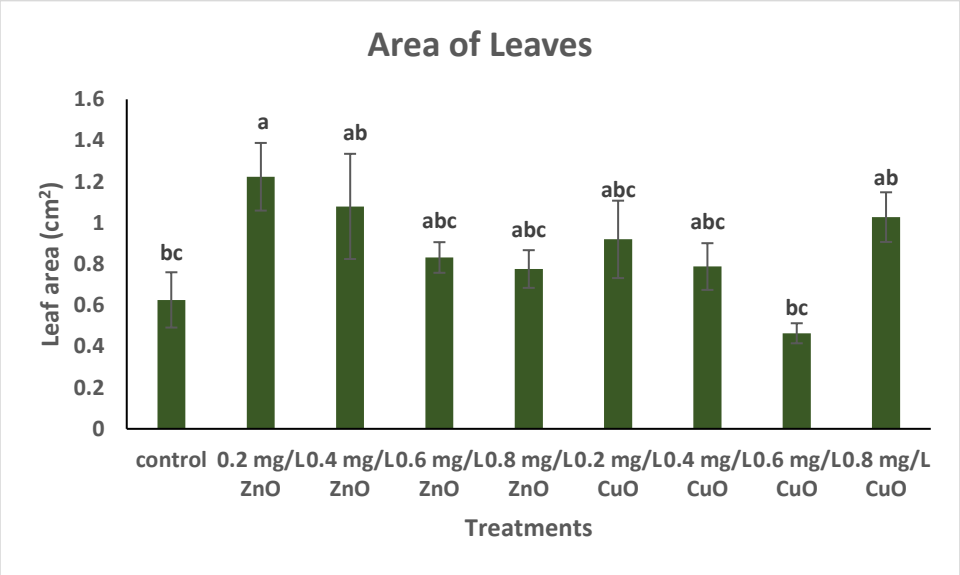

Figure 12: Effects of narrow spectrum NSs on the area of leaves in *in vitro* cultures of *R. cordifolia* ($p \leq 0.05$) corresponding to Duncan's Multiple Range tests

4.4.2.d Number of Plantlets

The control group and the 0.2 mg/L CuO NS treatment yielded the highest number of plantlets (4.2 and 5, respectively). Both ZnO and CuO NS treatments generally resulted in fewer plantlets, with significant reductions observed in the 0.2 mg/L ZnO NS and 0.8 mg/L CuO NS treatments (**Figure 13**).

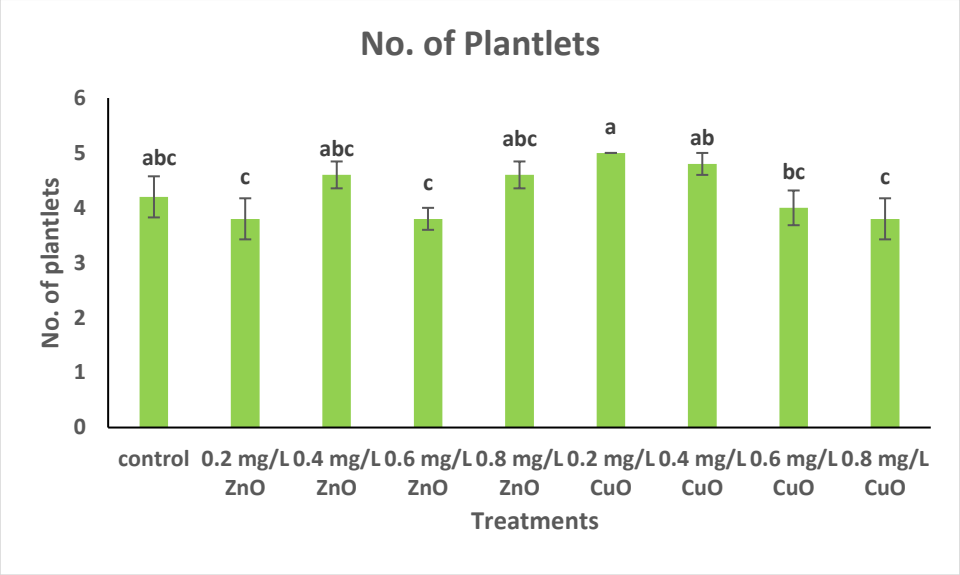

Figure 13: Effects of narrow spectrum NSs on the no. of plantlets in *in vitro* cultures of *R. cordifolia* ($p \leq 0.05$) corresponding to Duncan's Multiple Range tests.

4.4.2.e Biomass

The control treatment exhibited the highest fresh weight (4.00 g), indicating optimal growth without NS addition. ZnO NS treatments significantly reduced fresh weight compared to the control. The reduction is noticeable with higher concentrations, particularly at 0.6 mg/L (0.63 g) and 0.8 mg/L (0.79 g). CuO NS treatments also resulted in decreased fresh weight, with the lowest value at 0.6 mg/L CuO NS (0.24 g). The fresh weight at 0.2 mg/L and 0.4 mg/L CuO NS (0.83 g) was comparable but still significantly lower than the control. Dry weight followed a similar trend to fresh weight, with the control having the highest dry weight (0.31 g). ZnO NS treatments resulted in a notable decrease in dry weight. The lowest dry weight was observed at 0.8 mg/L ZnO NS (0.12 g). CuO NS treatments led to variable dry weights. While 0.6 mg/L CuO NS had the lowest dry weight (0.05 g), the 0.8 mg/L CuO NS treatment had a higher dry weight (0.19 g) compared to some ZnO NS treatments (**Figure 14**).

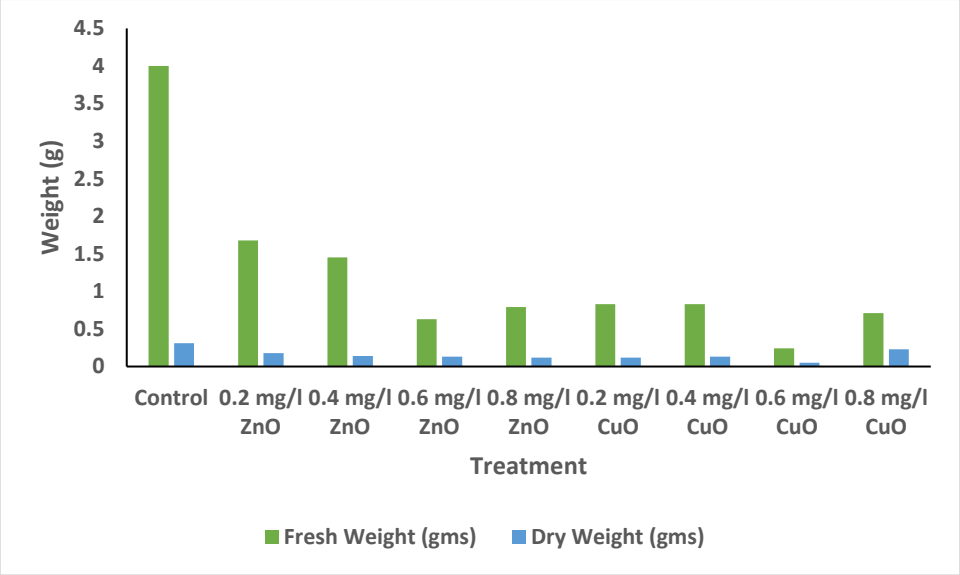

Figure 14: Effects of narrow spectrum NSs on the total biomass production in *in vitro* cultures of *R. cordifolia.*

The current investigation demonstrated the significant influence of biogenic CuO and ZnO NSs on the morphological traits of *in vitro R. cordifolia*. MO NSs have gained considerable interest in agricultural and biotechnological studies due to their potential utility in plant tissue culture, particularly in the stimulation of callus formation and organ development (Dikshit *et al.*, 2021; Mohammadinejad *et al.*, 2019). M NSs can promote the process of cell division and proliferation in plant tissues, which is essential for the development of calli. Due to their large surface area and small size, NSs may easily enter plant cells and interact with cellular components, thus influencing cellular processes (Giorgetti *et al.*, 2011; C. Liu *et al.*, 2021).

In the two treatments it was found that different concentrations of ZnO and CuO NSs affect plant growth in varying ways. Comparing the two treatments, the broad spectrum treatment exhibited higher shoot length, leaf area, and number of plantlets compared to the narrow spectrum treatment of *R. cordifolia*, particularly with CuO NS (1 mg/L and 0.1 mg/L) treatments. All growth parameters were higher in the CuO NS treatment and equal to or greater than the control. CuO NSs significantly influenced plant growth parameters in *Oryza sativa*, exhibiting nutritive properties at the nanoscale (Anwaar *et al.*, 2016). When utilized in nutritional mediums during clonal reproduction of *Mentha longifolia*, Cu and Co NSs boost the plant's quantity of shoot, height, internode quantity, growth index, and reproduction coefficient (Talankova-Sereda *et al.*,

2016). Ibrahim *et al.,* 2019 investigated the effects of Cu NSs on *Ocimum basilicum* plant regeneration by somatic embryogenesis. The outcomes clearly demonstrated that adding Cu NSs (5 M) boosted the average number of regenerated plantlets and the percentage of explants that produced somatic embryos. Root induction was enhanced by the modulatory action of ZnO and CuO NSs in MS medium of *in vitro* produced regenerates of *Stevia rebaudiana* (Ahmad *et al.*, 2020). The application of Cu NS is reported to boost the growth of rice, wheat, maize, basil and tomatoes (Babu *et al.*, 2022; Do *et al.*, 2021; Jyothi & Hebsur, 2017). Cu played a vital role in the production of regulatory proteins, as well as in mitochondrial respiration and hormone signalling, which finally resulted in the enhancement of plant growth parameters (Mir *et al.*, 2021).

The narrow spectrum treatment showed varied results, with CuO and ZnO NS showing higher values in some treatments, while the control group had the highest values in most cases. CuO and ZnO NS-treated *Amaranthus hybridus* plants showed improved growth parameters, but ZnO NS treatment had a better influence. ZnO NSs exert a beneficial effect on auxin production, which stimulates cell division and mineral absorption, hence promoting plant development (Salam *et al.*, 2022). Zinc is vital in seed germination, plant growth, and development and is involved in the synthesis of protein and plant hormones (auxin), cell growth, and stress resistance (Francis *et al.*, 2022).

In this study on biomass, the control group exhibited higher levels of biomass compared to the treatment groups. However, the broad spectrum treatment showed greater biomass production than the narrow spectrum treatment in the cultivation of *in vitro R. cordifolia*. In the case of *Vigna radiata*, exposure to higher levels of CuO NSs (200 and 500 mg/L) resulted in a significant reduction in overall biomass (Gopalakrishnan *et al.*, 2014). Ali *et al.,* (2019) conducted research on *in vitro* cultures of *Caralluma tuberculata* elicited with Ag NSs (90 µg/L), which led to an overall decrease in plant biomass but a significant increase in total flavonoid content, total phenols, PAL, and fresh weight of plants.

In conclusion, the present study showed that biogenic CuO and ZnO NSs have a significant impact on the morphological characteristics of *in vitro* cultures of *R. cordifolia*. The use of CuO NS (1 mg/L and 0.1 mg/L) generally resulted in an enhanced

growth parameters compared to the control and other treatments for *R. cordifolia*. However, NS treatment had an inverse effect on biomass production.

4.4.3 Inhibitory Effect of NSs on Plant Growth

On the basis of morphological studies, the effects of both the ZnO and CuO NSs were studied on plant growth and are shown in **Plate 8**. Specifically, as observed in **Plate 8 E and 8 I**, the highest concentration treatment (100 mg/L) of ZnO and CuO NSs exhibited a significant inhibitory effect on plant growth as compared to untreated (**Plate 8 A**) and lower concentrations of ZnO NSs (**Plate 8 B-D**) and CuO NSs (**Plate 8 F-H**). Metal NSs, at higher concentrations, can lead to issues like stunted growth, cell damage, and even death. A study on *Solanum melongena* (eggplant) revealed that different NSs at different concentrations affect seedling growth (Baskar *et al.*, 2018). Similar observations were also seen in *Abelmoschus esculentas* (Baskar *et al.*, 2021). In *Vigna radiata* exposure to higher levels of CuO nanomaterials (200 and 500 mg/L) caused a notable reduction in shoot length and overall biomass (Gopalakrishnan *et al.*, 2014). Ibrahim *et al.,* (2022) found that the growth of *Triticum aestivum* was improved by lower concentrations of CuO NSs but inhibited by higher quantities. Conversely, multiple studies have shown that elevated levels of CuO can indeed have a detrimental effect on plant development (Alhaithloul *et al.*, 2023; Kacziba *et al.*, 2023). Similar to other plant species this inhibitory effect in *R. cordifolia* growth may be due to the physiological disruptions caused by higher concentrations of NSs (Baskar *et al.*, 2018; Baskar *et al.*, 2021).

Lee *et al*., (2013) investigated the phytotoxicity of ZnO NS on buckwheat seedlings, finding that higher concentrations inhibited root elongation and biomass accumulation, leading to oxidative stress and increased antioxidant enzyme activities. Another study examined the impact of TiO_2 NS on *Nigella arvensis*, revealing that concentrations of 1000 mg/L or more reduced chlorophyll and carotenoid synthesis and increased hydrogen peroxide levels, indicating oxidative stress (Frazier *et al*., 2023). Research on green pea plants compared bare and hybrid ZnO NSs, showing that bare ZnO significantly inhibited root and shoot elongation and impacted seed nutritional quality (Mukherjee *et al*., 2016). Lastly, a study of seven MO NSs on maize and rice found that CuO and ZnO reduced root length significantly, especially in maize, while other metal oxides like TiO_2 and SiO_2 showed minimal toxicity (Yang *et al*., 2015).

4.5 ANALYSIS OF THE GREEN SYNTHESISED NANOSTRUCTURES AS ELICITORS ON SECONDARY METABOLITES

An alternative to traditional whole plant culture for the production of significant secondary metabolites is the use of *in vitro* techniques. A variety of techniques, including hairy root cultures, callus cultures, organ cultures, and cell suspension cultures, are commonly used in bioreactors for the industrial synthesis of secondary metabolites. One promising approach for improving secondary metabolites is the use of NSs as stress elicitors, in *in vitro* cultures (Humbal & Pathak, 2023; Ozyigit *et al.*, 2023; Wawrosch & Zotchev, 2021).

In this experiment, the nodal segments of *in vitro* propagated *R. cordifolia* were placed in MS medium with elicitors such as ZnO and CuO NSs. Both these NSs has already been used as a potential elicitor in enhancing the synthesis of diverse secondary metabolites in *in vitro* shoot cultures (Inam *et al.*, 2023). After being exposed to these elicitors for 80-days, they were harvested, and the methanol extracts of the dried samples were analysed using various quantitative and qualitative phytochemical analysis like HPTLC, TPC, TFC, LC-MS and antioxidant assay.

4.5.1 HPTLC Analysis

The analysis of the impact of ZnO and CuO NSs on the *in vitro* production of secondary metabolites in *R. cordifolia*, evaluated through HPTLC for the standard anthraquinone compounds Purpurin and Alizarin, reveals distinct variations in the effectiveness of different treatments. This was confirmed by analyzing through band formation and area percentage in HPTLC analysis.

The results from the first and second treatments provide insights into how different NSs affect the production of these compounds, which are indicative of the plant's secondary metabolic pathways.

4.5.1.a Broad Spectrum Treatment of NSs

The elicitation of NSs was conducted in *in vitro* cultures of *R. cordifolia* by applying varying concentrations of ZnO and CuO NSs to the culture medium. The following treatment concentrations were used in this study: 0.1 mg/L, 1 mg/L, 10 mg/L, and 100 mg/L. The MS medium with 0.5 mg/L Kinetin was used as the control. The treatment resulted in growth for all three concentrations except the highest (100 mg/L

NSs). Therefore, the methanol extracts of 0.1 mg/L, 1 mg/L, and 10 mg/L were analyzed using HPTLC (**Plate 10**).

The HPTLC analysis using the standard markers, identified the compound with R_f values 0.48 and 0.62 at both 366 nm and 254 nm as Purpurin and Alizarin respectively (**Table 12 and 13**).

The current study observed 15 prominent bands in the HPTLC analysis at 366 nm. The 2-D graphical representation of NS-treated cultures showed a notable increase in peak areas. Each R_f in the chromatogram of the plant methanol extract represents a different compound. R_f values of 0.23, 0.26, 0.31, 0.48, 0.62, and 0.83 were present across all treatments. Except for 0.83, all R_f values had a higher area percentage in the 0.1 mg/L CuO NS (RCu1) treatment than the control. The control treatment displayed only one R_f value (0.55) with a higher area percentage than the other treatments. The R_f values of 0.83 and 0.31 indicate significantly high area percentages across all treatments. Among these values, 0.83 demonstrates a notably higher area percentage, particularly in the ZnO NS treatment, especially in the RZn2 condition. In contrast, for the R_f value of 0.31, the area percentage increases with higher concentrations of CuO NS. Furthermore, the R_f value of 0.23 shows a higher area percentage in the RCu1 treatment than all other treatments. The R_f 0.55 is only observed in the CuO treatment and control, but not in the ZnO treatments.

Fifteen prominent bands were identified in the HPTLC analysis at 254 nm. The R_f values of 0.23, 0.29, 0.48, 0.62, and 0.99 were present in all treatment groups as well as the control. However, the R_f values of 0.60, 0.41, and 0.70 were only detected in the control group. The R_f value of 0.95 exhibited the highest area percentage in the RZn1 treatment and the lowest in the RCu1 treatment. For the R_f value of 0.83, the area percentage increased in the ZnO treatments as the concentration decreased (**Table 13**).

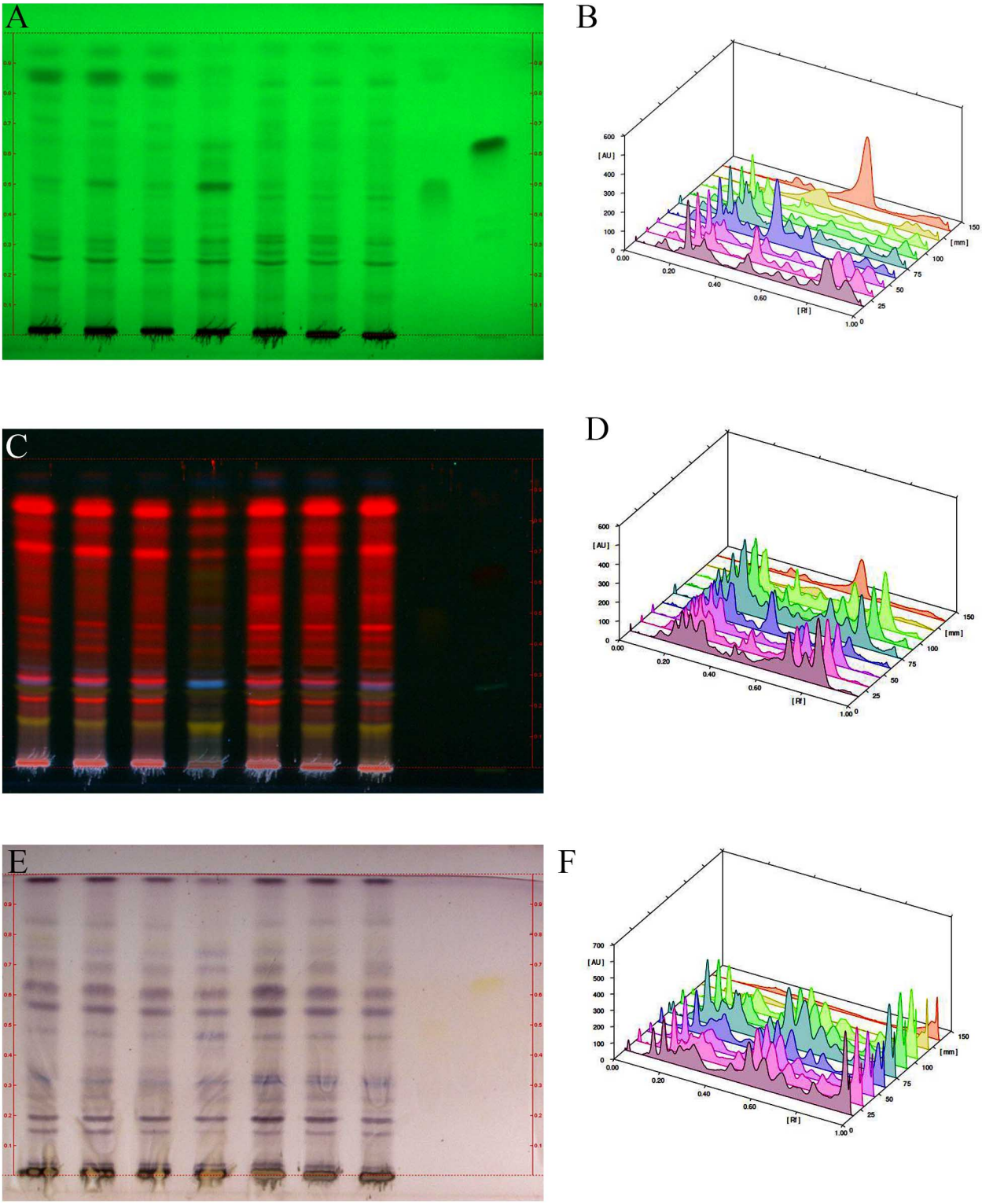

Plate 10: HPTLC Profile of methanol extracts of *in vitro* grown *R. cordifolia* treated with broad spectrum NSs. **(A & B)** HPTLC chromatogram and densitometric scanning image under 254 nm, **(C & D)** HPTLC chromatogram and densitometric scanning image under 366 nm, **(E & F)** HPTLC chromatogram and densitometric scanning image under 550 nm after derivatization; (**Tracks:** 1 - 0.1 mg/L, 2 - 1 mg/L, 3 - 10 mg/L, 4 - 0.1 mg/L, 5 - 1 mg/L, 6 - 10 mg/L, 7 - Control, 8 - Purpurin, 9 – Alizarin).

Table 12: **The compound with R_f values and area percentages of methanolic extracts of broad spectrum NSs induced *in vitro* cultures of *R. cordifolia* visualized at 254 nm.**

Sl. No.	R_f	Control	RZn1 (0.1 mg/L ZnO NS)	RZn2 (1 mg/L ZnO NS)	RZn3 (10 mg/L ZnO NS)	RCu1 (0.1 mg/L CuO NS)	RCu2 (1 mg/L CuO NS)	RCu3 (10 mg/L CuO NS)
1.	0.06	0.39	-	-	-	-	-	-
2.	0.12	5.23	-	-	-	2.95	-	4.64
3.	0.23	16.15	13.33	11.61	14.03	12.29	12.96	16.20
4.	0.26	3.36	-	4.03	5.61	-	8.43	8.45
5.	0.29	18.38	13.27	8.67	13.17	8.59	11.19	9.97
6.	0.41	3.87	-	-	-	-	-	-
7.	0.45	7.05	-	-	-	-	3.38	3.58
8.	0.48	8.05	9.62	16.59	8.33	27.54	7.17	5.94
9.	0.62	7.81	5.30	4.02	6.04	11.26	7.25	10.88
10.	0.70	5.63	-	-	-	-	-	-
11.	0.83	11.36	24.57	22.62	20.25	-	5.26	7.82
12.	0.95	11.78	14.21	-	-	4.12	9.86	11.25
13.	0.99	0.94	0.56	0.49	0.86	0.70	0.83	0.92

Table 13: **The compound with R_f values and area percentages of methanolic extracts of broad spectrum NSs induced *in vitro* cultures of *R. cordifolia* visualized at 366 nm.**

Sl. No.	R_f	Control	RZn1 (0.1 mg/L ZnO NS)	RZn2 (1 mg/L ZnO NS)	RZn3 (10 mg/L ZnO NS)	RCu1 (0.1 mg/L CuO NS)	RCu2 (1 mg/L CuO NS)	RCu3 (10 mg/L CuO NS)
1.	0.15	2.80	-	2.98	4.57	7.24	-	-
2.	0.20	4.47	6.78	5.88	7.56	-	10.58	9.89
3.	0.23	5.10	7.50	7.03	7.94	10.51	5.01	5.27
4.	0.26	6.57	12.25	8.76	14.04	9.20	9.97	10.51
5.	0.31	15.54	10.09	10.61	12.13	15.52	17.36	18.49
6.	0.36	2.13	2.29	-	2.26	3.51	3.04	2.58
7.	0.41	3.73	1.33	-	2.08	2.75	3.07	2.74
8.	0.45	7.12	2.39	3.23	2.83	19.21	4.70	4.46
9.	0.50	5.36	-	3.71	-	-	5.38	4.29
10.	0.55	5.26	-	-	-	3.06	3.36	2.27
11.	0.62	2.76	-	3.67	-	-	-	-
12.	0.70	13.61	-	14.02	-	-	10.04	10.65
13.	0.77	5.71	8.32	10.15	-	4.51	6.76	5.92
14.	0.83	18.60	19.81	21.18	16.48	8.14	11.77	14.03
15.	0.97	1.25	-	0.36	-	0.85	1.98	1.89

In the broad spectrum analysis, the results demonstrated that the different NSs variably affected the production of Purpurin and Alizarin. For Purpurin, the RZn2 treatment yielded the highest area percentage (7.65%), suggesting an increased production compared to the control (5.36%). Conversely, for Alizarin, the RZn2 treatment also showed a higher area percentage (5.05%), indicating that RZn2 positively influenced the production of both Purpurin and Alizarin. The RCu1 treatment

resulted in the highest area percentage for Purpurin (19.21%) and Alizarin (8.11%), indicating a more pronounced effect on Purpurin and Alizarin production.

4.5.1.b Narrow Spectrum Treatments of NSs

The HPTLC results from the broad spectrum treatment showed that the best outcome was achieved with the 0.1 mg/L CuO treatment, which resulted in a high area percentage of marker compounds. A narrow spectrum treatment was conducted to confirm the optimal concentration level of NSs for enhancing secondary metabolites, with concentrations ranging from 0.1 mg/L to 1 mg/L. The concentrations used in the second trial were 0.2 mg/L, 0.4 mg/L, 0.6 mg/L, and 0.8 mg/L. The MS medium with 0.5 mg/L Kinetin was also used as the control (**Plate 11**).

The recent study identified 17 prominent bands in the HPTLC analysis at 366 nm, demonstrating a significant increase in the production of various secondary metabolites. The control group displayed only 10 bands. The highest number of bands was found in the treatment with 0.4 mg/L CuO NS. R_f values of 0.17, 0.20, 0.24, 0.30, 0.49, 0.63, 0.84, and 0.90 were present in almost all treatments. The control treatment only had one R_f value (0.63), with a higher area percentage than the other treatments (**Table 14 and 15**).

Table 14: **The compound with R_f values and area percentages of methanolic extracts of narrow spectrum NSs induced *in vitro* cultures of *R. cordifolia* visualized at 254 nm.**

Sl. No.	R_f	Control	SZn1 (0.2 mg/L ZnO NS)	SZn2 (0.4 mg/L ZnO NS)	SZn3 (0.6 mg/L ZnO NS)	SZn4 (0.8 mg/L ZnO NS)	SCu1 (0.2 mg/L CuO NS)	SCu2 (0.4 mg/L CuO NS)	SCu3 (0.6 mg/L CuO NS)	SCu4 (0.8 mg/L CuO NS)
1.	0.04	0.82	1.43	-	-	1.49	0.94	-	-	1.49
2.	0.08	1.85		3.61	3.32	2.51	1.98	3.61	3.32	2.51
3.	0.16	5.08	18.54	18.01	15.97	10.74	11.75	18.01	15.97	10.74
4.	0.24	8.53	-	12.01	7.53	5.10	4.32	12.01	7.53	5.10
5.	0.29	8.13	20.02	5.73	6.68	9.18	6.31	5.73	6.68	9.18
6.	0.54	10.05	2.37	9.92	12.93	5.55	7.34	9.92	12.93	5.55
7.	0.69	26.71	-	11.89	11.02	16.35	19.59	11.89	11.02	16.35

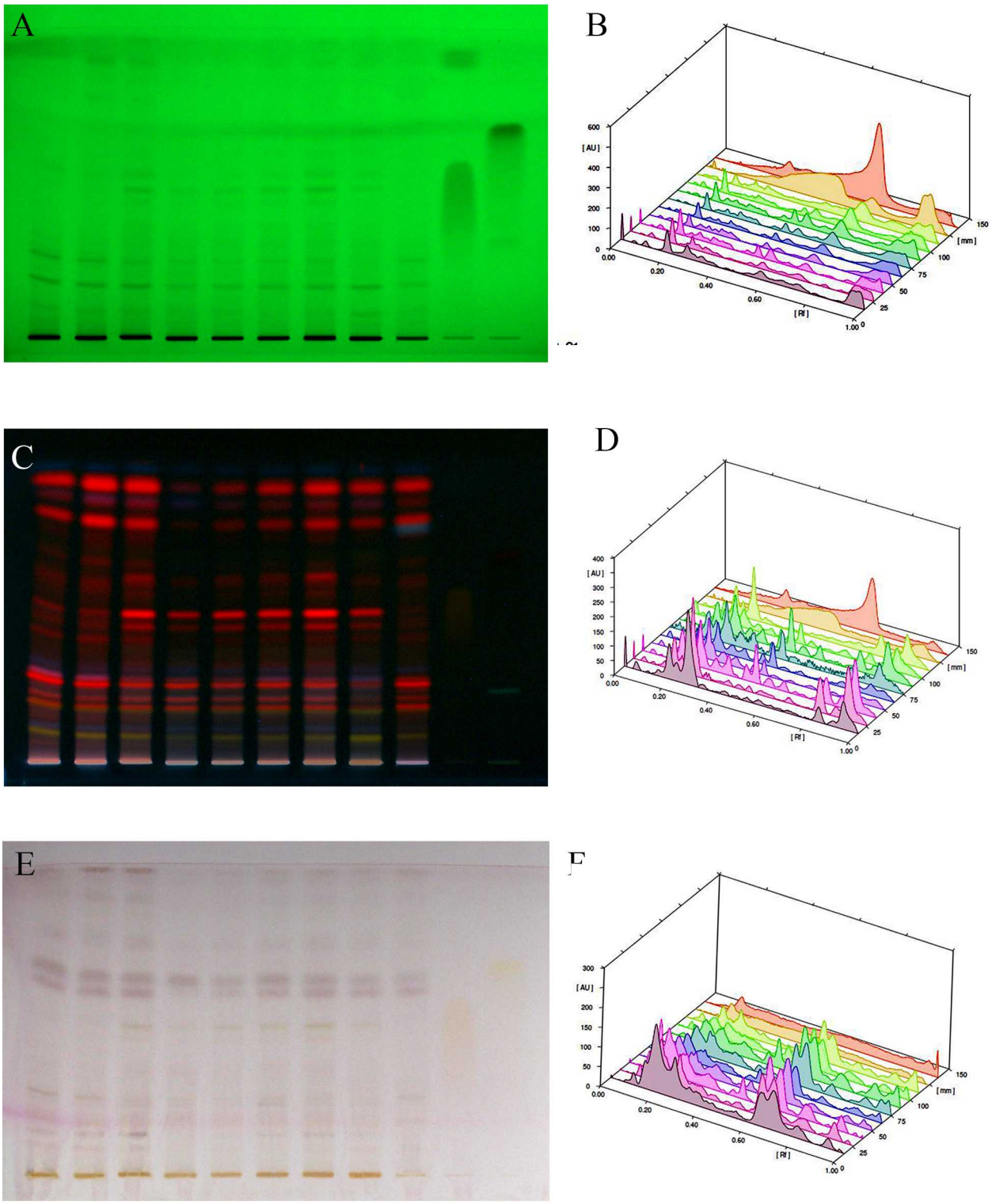

Plate 11: HPTLC Profile of methanol extracts of *in vitro* grown *R. cordifolia* treated with narrow spectrum NSs.
(A & B) HPTLC chromatogram and densitometric scanning image under 254 nm, **(C & D)** HPTLC chromatogram and densitometric scanning image under 366 nm, **(E & F)** HPTLC chromatogram and densitometric scanning image under 550 nm after derivatization; (**Tracks**: 1 - 0.2 mg/L, 2 - 0.4 mg/L, 3 - 0.6 mg/L, 4 - 0.8 mg/L, 5 - 0.2 mg/L, 6 - 0.4 mg/L, 7 - 0.6 mg/L, 8 - 0.8 mg/L, 9 - Control, 10 - Purpurin, 11 - Alizarin).

8.	0.81	10.17	-	2.79	-	-	-	2.79	-	-
9.	0.85	-	-	-	-	-	-	-	3.02	6.28
10.	0.91	13.83	-	23.52	11.26	20.59	21.04	23.52	11.26	20.59
11.	0.97	14.83	20.80	-	-	-	-	-	-	-

Table 15: **The compound with R_f values and area percentages of methanolic extracts of narrow spectrum NSs induced *in vitro* cultures of *R. cordifolia* visualized at 366 nm.**

Sl. No.	R_f	Control	SZn1 (0.2 mg/L ZnO NS)	SZn2 (0.4 mg/L ZnO NS)	SZn3 (0.6 mg/L ZnO NS)	SZn4 (0.8 mg/L ZnO NS)	SCu1 (0.2 mg/L CuO NS)	SCu2 (0.4 mg/L CuO NS)	SCu3 (0.6 mg/L CuO NS)	SCu4 (0.8 mg/L CuO NS)
1.	0.04	-	-	-	0.87	1.88	2.17	1.17	0.66	4.96
2.	0.06	1.40	2.96	1.13	-	-	-	0.33	-	1.09
3.	0.13		2.51	1.67	-	--	-	2.16	-	2.60
4.	0.17	13.53	-	11.22	10.85	19.13	13.42	10.69	10.93	9.86
5.	0.20	5.27	18.49	4.04	5.67	11.62	7.11	7.04	6.28	8.03
6.	0.24	23.76	8.47	-	15.75	26.01	17.20	16.02	15.42	11.33
7.	0.27	3.08	47.18	24.76	4.66	9.71	7.45	8.75	3.53	4.46
8.	0.30	-	-	1.09	-	8.15	7.26	8.25	4.93	3.64
9.	0.36	-	2.30	-	-	-	-	1.12	-	-
10.	0.39	-	2.60	1.51		3.74	5.76	4.80	5.60	3.35
11.	0.44	-	-	1.57	8.91	7.04	10.41	8.88	11.43	8.38
12.	0.49	3.95	2.07	2.11	3.24	-	2.23	2.11	3.75	2.90
13.	0.63	6.15	2.72	2.15	3.02	-	2.43	2.72	2.15	-
14.	0.78	12.54	-	14.33	9.49	-	3.81	4.96	9.36	6.44
15.	0.84	4.92	8.06	3.84	4.47	6.11	3.84	2.74	4.28	3.68
16.	0.90	25.39	2.65	27.73	21.70	-	9.33	12.69	19.44	24.53
17.	0.96	-	-	-	-	6.62	7.57	2.22	-	-

In the narrow spectrum treatment, the control (RC) shows Purpurin with an area percentage of 3.95% and Alizarin with an area percentage of 6.15%. The ZnO NS-based

treatments (SZn1, SZn2, SZn3, SZn4) and CuO NS-based treatments (SCu1, SCu2, SCu3, SCu4) all show a general decrease in Purpurin and Alizarin production. Interestingly, the SZn4 treatment shows a complete absence of Purpurin and Alizarin.

In comparison, the broad spectrum treatment generally displays more variability and higher maximum values in Purpurin production, with RCu1 significantly exceeding the other treatments. Additionally, the broad spectrum treatment shows higher Alizarin production than the narrow treatment. The highest value in the broad spectrum treatment (RCu1) exceeds that observed in the narrow spectrum treatment (RC control). On the other hand, the narrow spectrum treatment has a narrower range of Purpurin and Alizarin production, with the highest value (RC) being much lower than the broad spectrum treatment.

After analysing the results, it is evident that the broad spectrum treatment had a more significant impact on the production of both Purpurin and Alizarin. In particular, the RCu1 treatment showed substantial increases in the production of these secondary metabolites. As a result of these findings, the broad spectrum treatment was selected for further phytochemical analysis and studies.

The HPTLC spectra indicate that the levels of Purpurin and Alizarin were 5.36% and 2.76%, respectively, in the control group (RC). These levels increased to 4 times their original amount in plants treated with 0.1 mg/L of CuO NS (RCu1). In previous studies, the impact of NSs on the production of secondary metabolites has been demonstrated in various plants. Fatima *et al.,* (2020) found that applying 0.1 mg/L CuO NSs in the callus culture of *Artemisia annua* L. increased total phenolic content accumulation. Gonçalves *et al.,* (2021) found that treating *Thymus leptocephalus* extracts with ZnO and Fe_3O_4 NSs led to an increase in total phenolic and rosmarinic acid contents. CuO NSs are considered to be abiotic stress inducers that have a positive impact on the enhanced quantity of anthraquinone markers in *R. cordifolia* plants. This positive effect is initially observed, but once the threshold of 10 mg/L of CuO nanomaterials is crossed, a sudden decline is observed due to the continued addition of CuO nanomaterials (100 mg/L) to the growth medium. Javed *et al.,* (2017) reported that CuO NSs play a beneficial role, mainly due to the release of Cu ions from the nanomaterials, which are absorbed by the cells and play a significant role in plant

biochemistry. Consequently, significant variations in plant biomass and anthraquinone markers were observed.

4.5.2 Total Phenolic and Flavonoid Contents

The investigation aimed to evaluate the NSs treatment on overall phenolic and flavonoid contents in *in vitro* culture. In **Figure 15 A, 15 B and Table 16**, no statistically significant differences were observed in the TPC among treatments. However, statistically significant variations were noted in TFC ($p \leq 0.001$). When considering the percentage changes in TPC and TFC, treatment RCu1 showed a 69.26% increase in TPC and a 92.78% increase in TFC compared to the control. The observed percentage increase in terms of TPC can be attributed to different mechanisms proposed in several studies. One proposed mechanism is that metal NSs could trigger stress in plants, which could lead to an increase in the biosynthesis of phenolic compounds as a defensive mechanism (Mosa *et al.*, 2018; Pratyusha, 2022).

Table 16: Total phenolic and flavonoid contents of *in vitro* plants treated with various concentrations of NSs.

Treatments	TPC		TFC	
	µg GAE/mg of Extract	% Increase	µg QE/mg of Extract	% Increase
RC	12.31 ± 0.17	0.00	82.08 ± 7.48	0.00
RZn1	15.47 ± 0.35	25.70	94.89 ± 13.39	15.60
RZn2	13.06 ± 0.03	6.11	81.19 ± 6.31	-1.09
RZn3	14.25 ± 0.00	15.76	81.42 ± 12.76	-0.81
RCu1	20.83 ± 0.77	69.26	158.24 ± 22.86***	92.78
RCu2	11.74 ± 0.17	-4.57	132.58 ± 21.93**	61.53
RCu3	16.53 ± 0.43	34.30	154.52 ± 10.82**	88.25

Data are represented as mean ± SD, Differences between the mean value of components in the different extracts were taken to be statistically significant at $p \leq 0.001$. *indicates significant variation with respect to RC. ** indicates higher significant variation with respect to RC and *** indicates highest significant variation with respect to that of RC.

4.5.3 Antioxidant activity

The antioxidant activity of NSs on *R. cordifolia* was evaluated using the DPPH and ABTS scavenging tests. As observed in **Figure 15 C, 15 D and Table 17** except for the RCu2 treatment, all other treatment groups showed a significant decrease in IC50 values for both DPPH and ABTS assay, as compared to the untreated group, showing antioxidant property of both ZnO NSs and CuO NSs. However, compared to untreated and all other treatment groups, RCu1 showed the lowest IC50 values representing highest DPPH radical and $ABTS^{+}$ radical scavenging activity. The enhanced phenolics and flavonoids content in RCu1 group might be the reason for the increased antioxidant activity seen in the extract. The antioxidant capabilities of phenolics and flavonoids are believed to contribute to a broad range of pharmacological activities (Gutiérrez-Grijalva *et al.*, 2017).

Table 17: Antioxidant activity of *in vitro* plants treated with various concentrations of NSs expressed as IC50 values (µg/mL).

Treatments	DPPH Assay		ABTS Assay	
	IC50	% Decrease	IC50	% Decrease
RC	1091.75 ± 7.2	0	467.76 ± 3.94	0
RZn1	984.252 ± 0.00	9.84	354.80 ± 4.91*	24.14
RZn2	1041.888 ± 15.2	4.56	376.67 ± 2.98*	19.47
RZn3	944.2946 ± 2.7*	13.50	367.65 ± 1.08*	21.40
RCu1	499.3867 ± 8.2***	54.25	214.91 ± 0.23***	54.05
RCu2	1417.807 ± 44.2	-29.86	712.76 ± 2.54	-52.37
RCu3	934.1364 ± 34.9*	14.446	335.74 ± 4.40*	28.22

Data are represented as mean ± SD, Differences between the mean value of components in the different extracts were taken to be statistically significant at $p \leq 0.001$. *indicates significant variation with respect to RC. ** indicates higher significant variation with respect to RC and *** indicates highest significant variation with respect to that of RC.

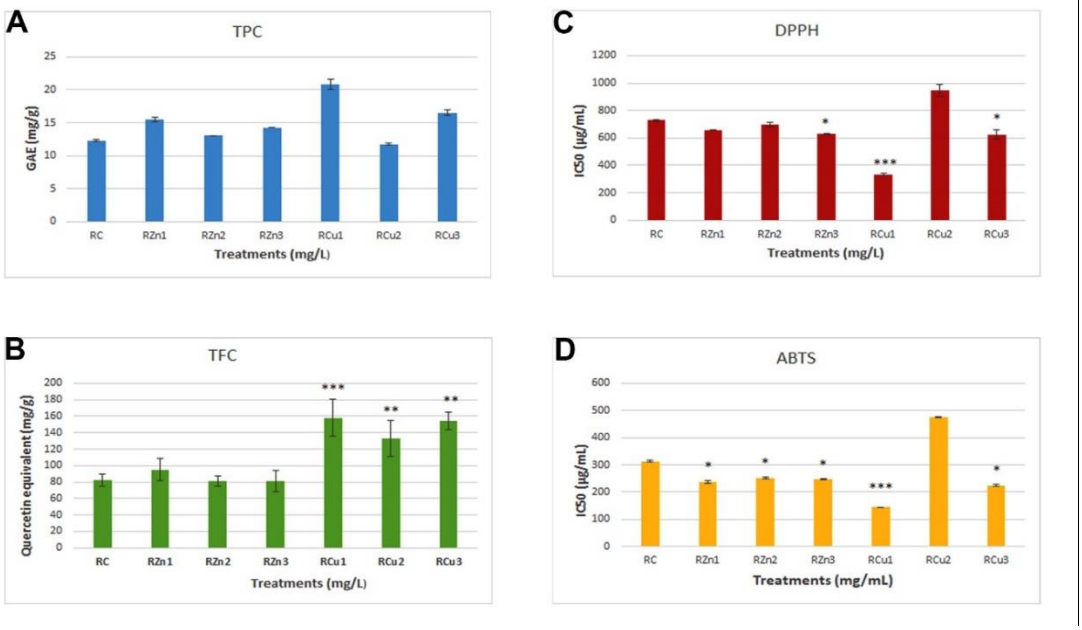

Figure 15: Estimation of phytochemical and antioxidant activity of NSs treated extract. (A) TPC (B) TFC (C) DPPH (D) ABTS analysis; (RC-control, RZn1-0.1mg/L ZnO NSs, RZn2-1 mg/L ZnO NSs, RZn3-10 mg/L ZnO NSs, RCu1-0.1mg/L CuO NSs, RCu2-1 mg/L CuO NSs, RCu3-10 mg/L CuO NSs)

4.5.4 Phytochemical Profiling Using HR-LCMS

Among all the NS treatment groups, RCu1 (0.1mg/L CuO NSs) showed the most promising results with respect to enhanced secondary metabolites, phenolic and flavonoid contents and antioxidant property. Subsequently, the methanolic extracts of untreated group (RC) and treated group (RCu1) was subjected to HR-LCMS analysis to understand the qualitative difference of the extract in terms of phytochemical components (**Plate 12 A and 12 B).** Based on the fragmentation pattern from LC–MS, phytocompounds belonging to several different classes were identified and represented in **Table 18 and 19**.

The LC-MS analysis revealed the presence of several compounds, which were common in both the treated (0.1 mg/L CuO NSs) and untreated group (control). Compounds like morindaparvin A, cinnamodial, limonoate, euphornin, ganoderic acid F and Norethindrone acetate were present in both groups indicating that the nanomaterial treatment did not impact these compounds. Flavonoids such as aurapentol, sinesietin, oroxylin A and luteolin 7 O glucuronide were only found in the control samples. On the other hand, several flavonoids such as, (+) sophorol, betavulgarin, 3-O-

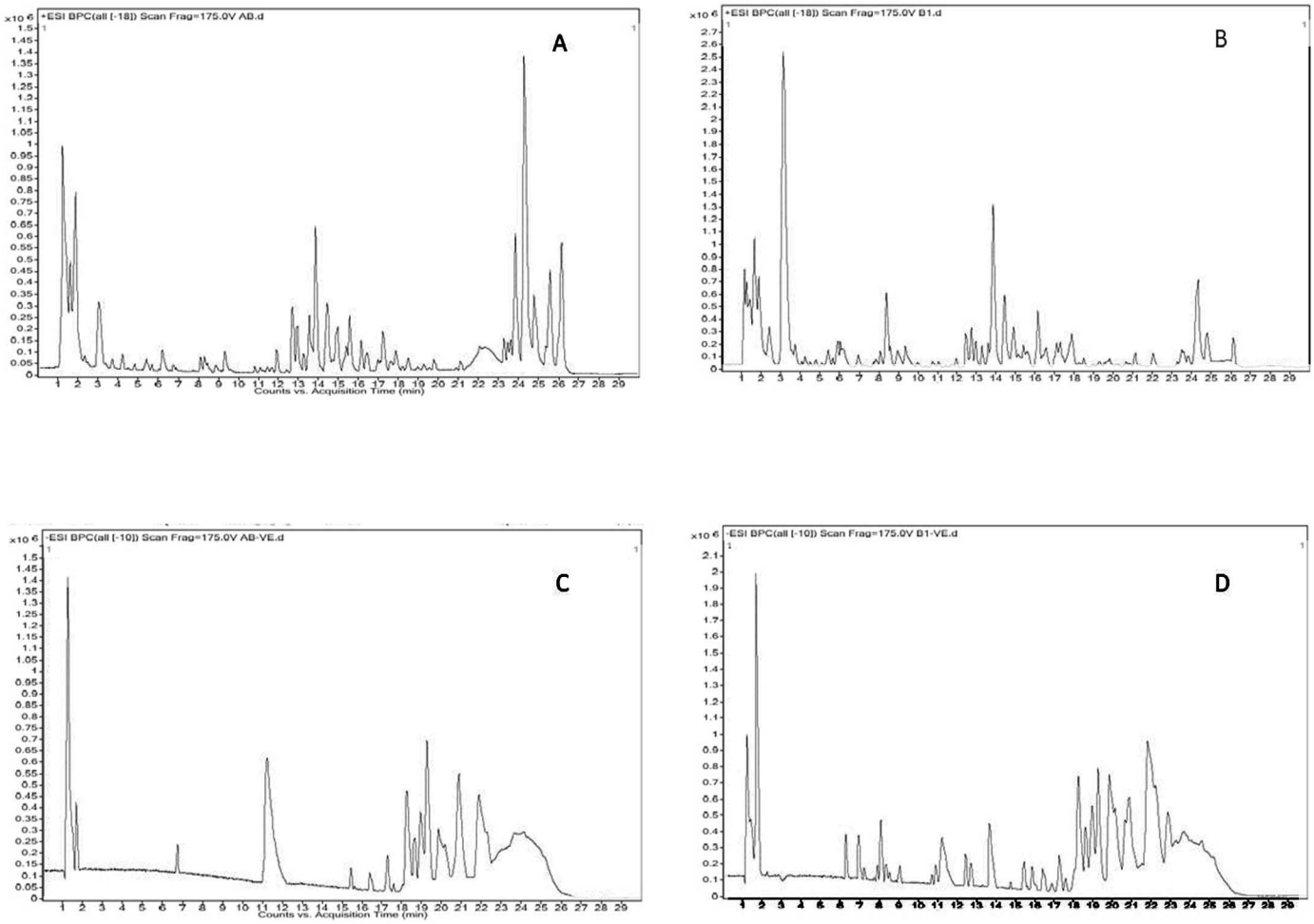

Plate 12: LC-MS Chromatogram of methanolic extracts of NS treated *in vitro* grown *R. cordifolia.* **(A)** Control +ve, **(B)** 0.1 mg/L CuO NS +ve, **(C)** Control -ve, **(D)** 0.1 mg/L CuO NS -ve.

methylcoumestrol, catechin, myricitrin, tricin 5 glucoside, luteolin 4' O glucoside, tectorigenin were detected in the treated plants but not in the control samples. The influence of 0.1mg/L CuO NS treatment on the production or accumulation of these flavonoids are visible from these results. Variations in tannins and alkaloids were also clear. between the treated and untreated plants. Tannins such as gibberellin A75, ganoderic acid Mc, halstoctacosanolide A and 3-O-p-trans-coumaroylalphitolic acid were identified solely in the control group.

These differences in the secondary metabolites indicates the effect of CuO NS on *in vitro* culture of *R. crodifolia.* It is well known that flavonoids are known for their antioxidant effects (Shen *et al.*, 2022). Hence, the accumulation of more flavonoids in treated samples explains the reason behind the increased antioxidant capacity of the treated sample. The RCu1 treatment has shown enhanced antioxidant activity based on DPPH and ABTS assays. The presence of compounds like betavulgarin, catechin, myricitrin, etc. might be the reason for enhancement of the antioxidant potential (Ahangarpour *et al.*, 2018; Grzesik *et al.*, 2018; Wootton-Beard & Ryan, 2011) of the extract derived from the treated plants.

Oxidative stress plays a role, in the development of chronic diseases like cancer, diabetes and heart conditions. Plant extracts with antioxidant properties can combat these diseases linked to oxidative stress (Sidhic *et al.*, 2023). *R. cordifolia* is widely used to treat health issues including inflammation (Patil *et al.*, 2009; Shen *et al.*, 2018) cancer (Ghosh *et al.*, 2010) and diarrhoea (Gong *et al.*, 2017). Inflammatory conditions may lead to an increase in reactive species production (Fialkow *et al.*, 2007). The use of extracts, with antioxidant properties is supported by their ability to protect from oxidative stress. Hence, the antioxidant rich extract helps to reduce inflammatory processes associated with disease development (Biswas, 2016).

Incorporating antioxidant-rich extracts into treatment plans offers an approach to reducing inflammation associated with various health conditions. This integration enhances well-being and shows promise in improving clinical outcomes by mitigating symptoms slowing disease advancement and boosting the effectiveness of current treatments. The diverse benefits of antioxidants extend beyond inflammation control in protecting disease processes present a holistic strategy, for managing several illnesses effectively.

Table 18: LC−MS analysis and chemical composition of control (RC)

Sl. No.	RT	m/z a	m/z b	Name of the Compound	Fragments	Mol. Wt.	Chemical Formula	Structure
1.	6.782	461.0749	461.0725	Luteolin 7-O-glucuronide	255.0304 417.0514	462.082	$C_{21}H_{18}O_{12}$	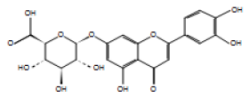
2.	11.03	283.0259	283.0248	Rhein	239.0353	284.0329	$C_{15}H_8O_6$	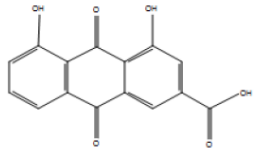
3.	11.203	239.0363	239.035	Alizarin	239.0364	240.0435	$C_{14}H_8O_4$	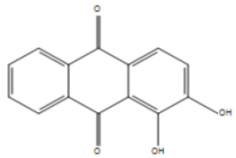

4.	18.501	615.3176	615.3175	Avermectin B1b aglycone	163.0405 255.2336 453.3385	570.319	C_{33} H_{46} O_8	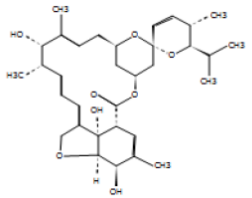
5.	18.543	653.3648	653.3556	L-Urobilin	163.0414 267.6570 453.3361 617.3858	594.3487	C_{33} $H_{46}N_4O_6$	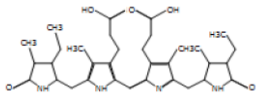
6.	18.661	617.3843	617.3848	3-O-p-trans-Coumaroylalphitolic acid	163.0411 255.2357 453.3390	618.3919	C_{39} H_{54} O_6	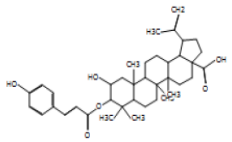
7.	18.81	647.3988	647.3953	trans-3-Feruloylcorosolic acid	134.0380 193.0515 453.3380 573.3580	648.4058	C_{40} H_{56} O_7	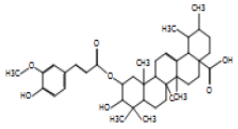

8.	18.847	683.3748	683.3648	26-Glucosyl-1,3,11,22-tetrahydroxyergosta-5,24-dien-26-oate	134.0370 193.0510 453.3394 573.3639 647.3973	638.3741	$C_{34}H_{54}O_{11}$	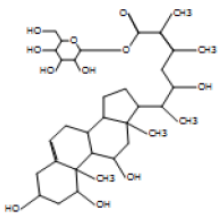
9.	19.85	843.5331	843.5264	Halstoctacosanolide A	164.9852 225.0083 283.2703 559.2583	844.5393	$C_{48}H_{76}O_{12}$	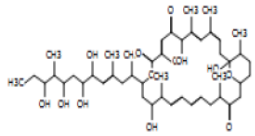
10.	20.388	309.1754	309.1707	Valdiate	149.0974	310.1826	$C_{17}H_{26}O_5$	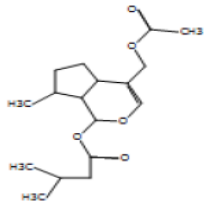

11.	23.735	339.2023	339.1966	Norethindrone acetate	183.0130	340.2091	C_{22} H_{28} O_3	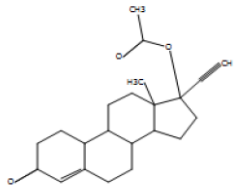
12.	24.036	339.2021	339.1966	17-Hydroxy-3-oxo-17alpha-pregna-1,4-diene-21- carboxylic acid, gamma-lactone	183.0121	340.209	C_{22} H_{28} O_3	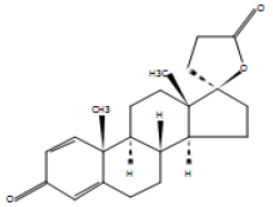
13.	1.424	260.1118	260.1129	Osmaronin	260.1073	259.1044	C_{11} H_{17} N O_6	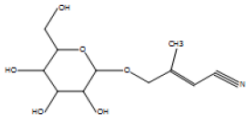
14.	6.78	301.0328	301.0343	Psuedopurpurin	213.0160 283.0231	300.0257	C_{15} H_8 O_7	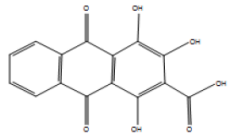

15.	8.539	253.0485	253.0495	Morindaparvin A;	253.0476	252.0412	$C_{15}H_8O_4$	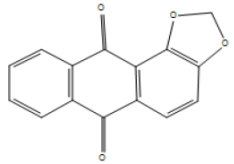
16.	9.175	331.1522	331.1516	Cinnamodial	165.0684	308.1631	$C_{17}H_{24}O_5$	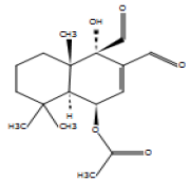
17.	9.37	324.0853	324.0842	Citrusinie I	220.0742 292.0587	301.0961	$C_{16}H_{15}NO_5$	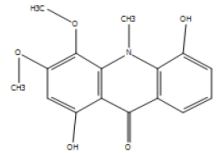
18.	12.401	285.0779	285.0757	Oroxylin A	139.0537	284.0704	$C_{16}H_{12}O_5$	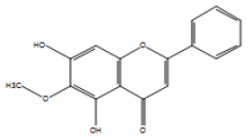

19.	13.579	283.0951	283.0941	(S)-Auraptenol	239.0693	260.1059	C_{15} H_{16} O_4	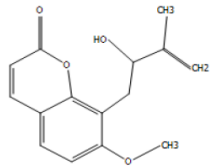
20.	13.688	313.1058	313.1046	5,6-Dihydro-11-methoxyyangonin	227.0679	290.1165	C_{16} H_{18} C_5	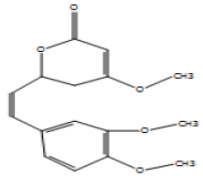
21.	13.892	403.1371	403.1363	Gibberellin A75	127.0388 183.0282 373.0887	380.1478	C_{19} H_{24} O_8	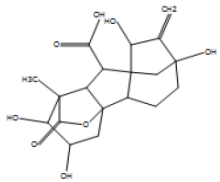
22.	14.94	373.127	373.1282	Sinensetin	183.0275 343.0791	372.1197	C_{20} H_{20} O_7	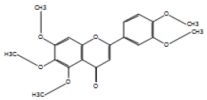

23.	17.662	507.2253	507.2225	Limonoate	238.1215	506.2179	C_{26} H_{34} O_{10}	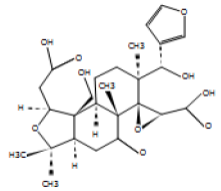
24.	19.19	631.3957	631.3841	Ganoderic acid Mc	177.0548 374.2578 585.3543	630.3888	C_{36} H_{54} O_9	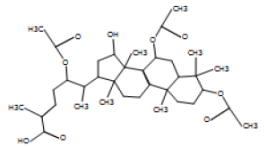
25.	22.002	607.2522	607.2527	4Z,15E-Bilirubin IXa	308.1035 447.2132 547.2286	584.263	C_{33} H_{36} N_4 O_6	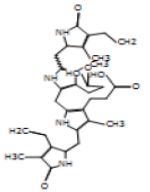
26.	22.111	640.2803	640.2752	Demethyl desacetyl-rifamycin S	215.0799 275.1153 341.1673 406.2099 493.2199 579.2550	639.273	C_{34} H_{41} N O_{11}	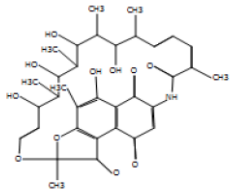

27.	24.195	669.1734	669.1637	Leucodelphinidin 3-[galactosyl-(1->4)-glucoside]	229.0858 564.1535	646.1827	$C_{27}H_{34}O_{18}$	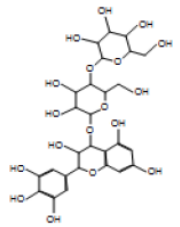
28.	24.372	593.2737	593.2721	Ganoderic acid F	181.0756 262.1314 338.1608 460.2225 505.2208 533.2518 563.2294	570.2845	$C_{32}H_{42}O_9$	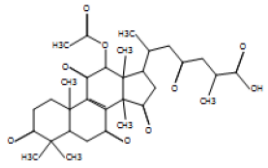
29.	24.393	621.268	621.2684	Hematoporphyrin	308.2931 474.2012 561.2458	598.2805	$C_{34}H_{38}N_4O_6$	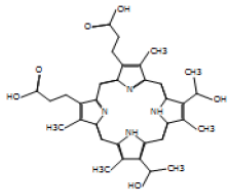

30.	25.213	749.6169	749.6231	Plastoquinone-9	189.0898 393.3467	748.6099	C_{53} H_{80} O_2	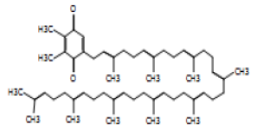
31.	25.491	623.285	623.2752	O-Methylsomniferine	170.0938 233.1041 341.1484 407.2215 485.2317 545.2511 573.2476 605.2714	622.2774	C_{37} H_{38} N_2 O_7	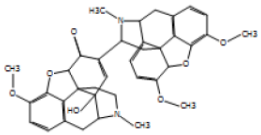
32.	25.964	653.2949	654.2909	Rifamycin W-hemiacetal	250.1103 479.2408 557.2627	652.2873	C_{35} H_{43} N O_{11}	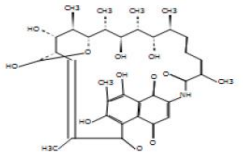
33.	26.044	607.2904	607.2878	Euphornin	180.1007 337.1399 460.2238 547.2666	584.3009	C_{33} H_{44} O_9	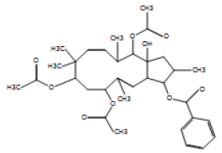

Table 19: LC−MS analysis and chemical composition of 0.1 mg/L CuO NS (RCu1)

Sl. No.	RT	m/z a	m/z b	Name of the Compound	Fragments	Mol. Wt.	Chemical Formula	Structure
1.	1.288	473.1654	473.1664	6-Feruloylglucose 2,3,4-trihydroxy-3-methylbutylglycoside	327.1323 444.9288	474.1723	$C_{21}H_{30}O_{12}$	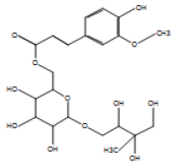
2.	6.337	477.107	477.1038	Pedaliin	299.0209	478.1141	$C_{22}H_{22}O_{12}$	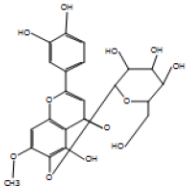
3.	6.984	463.0914	463.0882	Myricitrin	300.0282 463.0893	464.0985	$C_{21}H_{20}O_{12}$	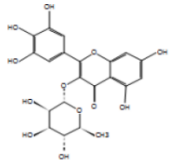

4.	7.022	491.1228	491.1195	Tricin 5-glucoside	313.0371 491.1218	492.1297	C_{23} H_{24} O_{12}	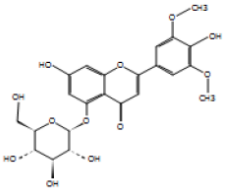
5.	8.112	447.0966	447.0933	Luteolin 4'-O-glucoside	255.0313	448.1037	C_{21} H_{20} O_{11}	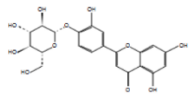
6.	8.461	563.1434	563.1406	Kaempferol 3-rhamnoside 7-xyloside	251.0360 529.2691	564.1503	C_{26} H_{28} O_{14}	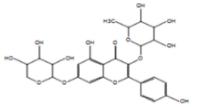
7.	11.359	283.0274	283.0248	Rhein	239.0366	284.0346	C_{15} H_{8} O_{6}	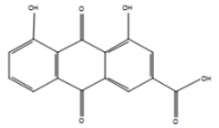

8.	12.776	299.0571	299.0561	Tectorigenin	267.0316	300.0643	C_{16} H_{12} O_6	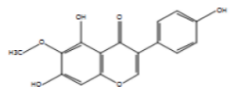
9.	13.673	269.0481	269.0455	Genistein	197.0619	270.0553	C_{15} H_{10} O_5	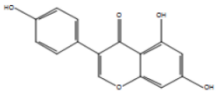
10.	18.673	617.3891	617.3848	3-O-p-trans-Coumaroylalphitolic acid	163.0415 337.2546 453.3403	618.3963	C_{39} H_{54} O_6	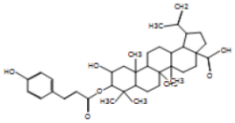
11.	18.737	595.2938	595.2913	Salannin	152.9968 279.2341	596.3007	C_{34} H_{44} O_9	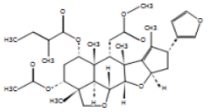
12.	18.8	647.4004	647.3953	trans-3-Feruloylcorosolic acid	134.0382 193.0519 453.3403 573.3618	648.4079	C_{40} H_{56} O_7	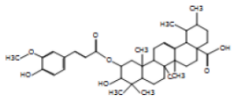

13.	20.16	431.2242	431.2241	Usambarensine	278.2235	432.2314	C_{29} H_{28} N_4	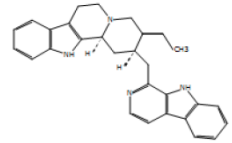
14.	20.409	309.1766	309.1707	Valdiate	183.0136	310.1837	C_{17} H_{26} O_5	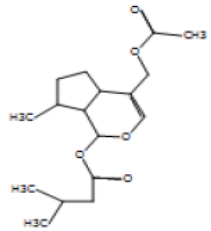
15.	20.808	571.2932	571.2913	Ganoderic acid H	152.9957 255.2341 315.0470	572.3004	C_{32} H_{44} O_9	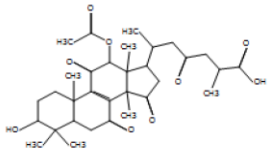
16.	24.852	339.2025	339.1966	Norethindrone acetate	183.0129	340.2093	C_{22} H_{28} O_3	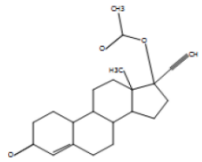

17.	1.374	260.1117	260.1129	Osmaronin	196.0944	259.10 42	C_{11} H_{17} N O_6	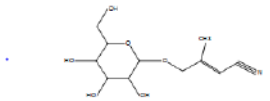
18.	1.696	262.1275	262.1285	Lotaustralin	118.0837 140.0004 167.0685 201.0857 244.1105	261.1202	C_{11} H_{19} N O_6	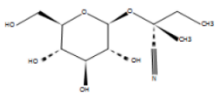
19.	5.37	268.1033	268.1027	Miraxanthin-III	169.0748	267.0891	C_9 H_{17} N O_8	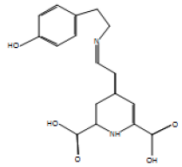
20.	5.935	290.1011	290.1023	Acronycidine	159.0430 272.0856	289.0937	C_{15} H_{15} N O_5	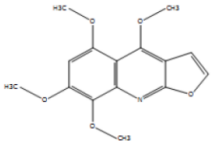

21.	7.067	409.1111	409.1105	1-O-Sinapoylglucose	232.0347 327.1563	386.1219	$C_{17}H_{22}O_{10}$	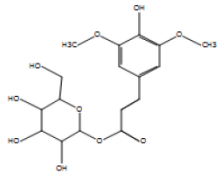
22.	8.493	253.0486	253.0495	Morindaparvin A	151.0524	252.0412	$C_{15}H_8O_4$	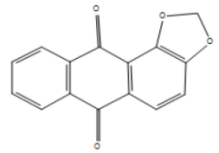
23.	8.647	241.0482	241.0495	1,4-Dihydroxyanthraquinone	241.0490	240.0411	$C_{14}H_8O_4$	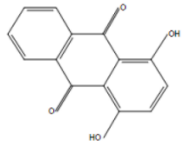
24.	9.095	301.0693	301.0707	(+)-Sophorol	283.0581	300.062	$C_{16}H_{12}O_6$	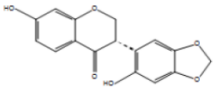

25.	9.177	313.0695	313.0707	Betavulgarin	270.0498	312.0622	$C_{17}H_{12}O_6$	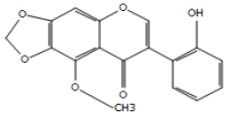
26.	9.274	331.1521	331.1516	Cinnamodial	212.0445 270.0511	308.163	$C_{17}H_{24}O_5$	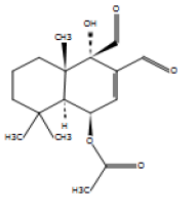
27.	9.416	324.0854	324.0842	Citrusinine I	180.0798 220.0745 236.0683 264.0638 292.0597	301.0962	$C_{16}H_{15}NO_5$	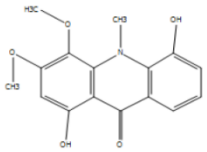
28.	9.479	384.1064	384.1078	Lilaline	269.0429	383.0992	$C_{20}H_{17}NO_7$	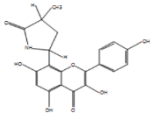

29.	9.656	283.059	283.0601	3-O-Methylcoumestrol	283.0590	282.0517	$C_{16}H_{10}O_5$	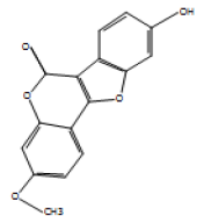
30.	10.809	271.0588	271.0601	Morindone	256.0349	270.0516	$C_{15}H_{10}O_5$	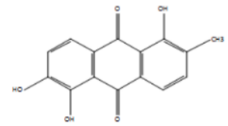
31.	10.94	261.0743	261.0733	1-(2,4,5-Trimethoxyphenyl)-1,2-propanedione	163.0018 231.0271	238.0851	$C_{12}H_{14}O_5$	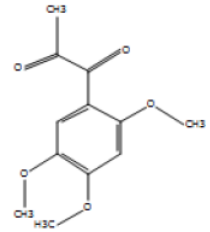

32.	11.115	313.0692	313.0683	Catechin	270.0504	290.08	C_{15} H_{14} O_6	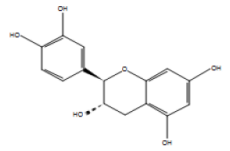
33.	11.158	345.0951	345.0969	Santin	270.0504	344.0878	C_{18} H_{16} O_7	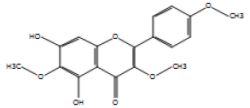
34.	13.931	403.1367	403.1363	Gibberellin	183.0286 373.0900	380.1475	C_{19} H_{24} O_8	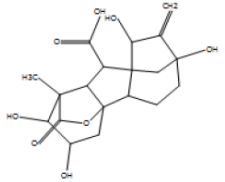
35.	17.642	507.225	507.2225	Limonoate	238.1211 316.1080 433.2202	506.2177	C_{26} H_{34} O_{10}	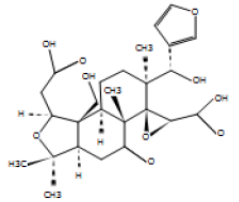

36.	23.502	625.2793	625.2702	Kanokoside D	262.1430 479.2409	624.272	C_{27} H_{44} O_{16}	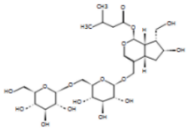
37.	23.535	669.1742	669.1637	Leucodelphinidin 3-	159.1147 508.1267 564.1541	646.1834	C_{27} H_{34} O_{18}	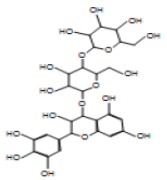
38.	24.246	593.2739	593.2758	Pheophorbide a	207.0862 460.2217 533.2512	592.2666	C_{35} H_{36} N_4 O_5	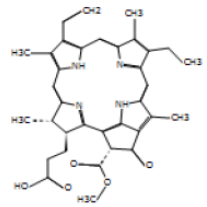
39.	24.582	593.2732	593.2721	Ganoderic acid F	229.0806 461.2298 533.2520	570.2838	C_{32} H_{42} O_9	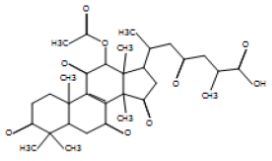

40.	24.735	653.1801	653.1841	(R)-Rutaretin 1'-(6"-sinapoylglucoside)	183.0820 520.1287 578.1337	630.19	C_{31} H_{34} O_{14}	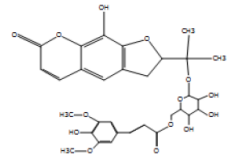
41.	26.212	607.2894	607.2878	Euphornin	285.1240 460.2229 547.2703	584.3	C_{33} H_{44} O_9	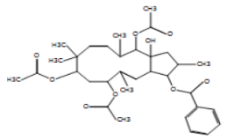

4.5.5 Raman Spectroscopic Analysis

Raman spectroscopy is a fast and non-destructive method used to capture the molecular vibrations of cellular metabolites found in a sample. Raman spectroscopy involves the use of laser light to stimulate molecules, causing them to emit light at a new optical frequency. This new frequency, called Stokes radiation, is shifted downward from the incident laser frequency by an amount equal to the molecules' vibrational frequencies, and is then detected using a spectrometer. In this study, Raman spectroscopy was employed to determine how plants react to stress induced by NSs. Whole root and leaf samples from live plants that were exposed to CuO NS and ZnO NS treatments (0.1mg/L CuO NS and 0.1 mg/L ZnO NS) for 80 days *in vitro* were analyzed using Raman spectroscopy, along with control samples. In addition, green-synthesized NS powder and standard markers (Alizarin and Purpurin) also underwent Raman spectroscopy for comparison. The study focused on detecting the presence of NSs in cells and identifying variations in the peaks of anthraquinone pigments (Alizarin and Purpurin), chlorophyll, carotenoids, and anthocyanins.

4.5.5.a Raman Spectroscopy of NS Treated Leaf Samples of In Vitro Grown R. cordifolia

Distinct narrow peaks at 1,019 and 1,193 cm^{-1} were observed for carotenoids in the spectra of control plants. These peaks were found to be enhanced under abiotic stress caused by ZnO and CuO compared to the control. Furthermore, the Raman spectra of chlorophyll exhibited strong bands in the 1516 cm^{-1} range, which correspond to the C=C stretching vibrations of the conjugated double bonds in the porphyrin ring of the chlorophyll molecule. These bands were also enhanced under abiotic stress caused by ZnO and CuO NSs compared to the control (**Plate 13 D**).

After subjecting plants to abiotic stress by ZnO and CuO NSs, the Raman peaks of anthocyanin at 574, 590, and 696 cm^{-1} were suppressed (**Plate 13 C**). Similar results were published by Altangerel *et al.,* (2017) when *Coleus* plants were subjected to abiotic stress conditions and examined using Raman spectroscopy, distinct narrow peaks at 1,007-1,157 cm^{-1} were observed for carotenoids, while Raman peaks at 539-733 cm^{-1} for anthocyanins were clearly distinguished. This study indicated a negative correlation between carotenoids and anthocyanins during stressed conditions. Raman spectroscopy was also performed on Algae, revealing peaks in the range of 1100-1600

cm^{-1} for chlorophyll (Parab & Tomar, 2012). Furthermore, in a study by Adil *et al.,* (2022), it was found that the application of ZnO NSs on wheat plants led to an increase in chlorophyll A and B contents.

The application of NSs was found to be positively correlated with an increase in chlorophyll and carotenoid content in *R. cordifolia* plants. The lowest levels of chlorophyll and carotenoid pigments were observed in the control group, while the highest values were recorded with the application of NSs as an *in vitro* treatment. This study emphasizes the positive impact of NSs on chlorophyll concentrations in *in vitro R. cordifolia* plants. Similarly, in a study by Alhaithloul *et al.,* (2023), the highest chlorophyll concentrations, photosynthetic parameters, and gas exchange attributes were observed with the application of 100 mg/L of CuO NSs as a foliar treatment in *T. aestivum* plants compared to the control. Both ZnO and CuO NSs help in the synthesis of chlorophyll, which promotes plant growth. Past studies have shown that a lack of Cu and Zn can lead to a decrease in chlorophyll content, resulting in chlorotic symptoms and a significant reduction in plant growth. (Francis *et al.*, 2022).

The results above are similar to those found by Mahdi *et al.,* (2020). When CuO NSs were applied to wheat shoots, they had a positive impact on photosynthetic pigments, with the maximum value of chlorophyll b and total pigments. However, the same treatment had a slight negative effect on carotenoid content when compared to the control. Hernández-Hernández *et al.,* (2018), observed an increase in the content of photosynthetic parameters after the application of Cu NSs (100 ppm) to tomato plants under salinity conditions. The positive effect of CuO NSs may be due to Cu being recognized as an important component for controlling plant growth and development, including chlorophyll formation and seed production (Mahdi *et al.*, 2020).

4.5.5.b Raman Spectroscopy of NS Treated Root Samples of In Vitro Grown R. cordifolia

In this study, the whole root specimen from NS treatment and untreated groups were subjected to Raman spectroscopy for the detection of presence of NSs inside the plant cell and for the variation in anthraquinone pigments (Alizarin and Purpurin).

As shown in **Plate 13 A**, Raman spectra of the root sample following 0.1 mg/L CuO NS treatment showed a band at 600 cm^{-1} representing Cu_2O NSs instead of CuO band at 266 cm^{-1} (Aghdam *et al.*, 2019). This indicates the reduction of CuO to Cu_2O

under physiological conditions of the plant. While no such bands were observed in the control. Likewise, the ZnO NS treated sample (0.1 mg/L) shows the Raman Signatures of ZnO NS at 431 cm^{-1} and 582 cm^{-1}. This proves the percolation of ZnO NS from the medium to the root structure.

Further the spectral analysis showed enhancement of the anthraquinone pigments (Alizarin and Purpurin) in NS treated root sample corresponding to bands between 1200 cm^{-1} and 1260 cm^{-1} in comparison with the control. CuO NS treated root sample shows intense peak of anthraquinone than ZnO NS treated root sample (**Plate 13 B**). Shadi *et al.,* (2004) reported a semi-quantitative analysis of Alizarin and Purpurin using Surface-Enhanced Resonance Raman spectroscopy (SERRS). The detection limits for Alizarin were calculated to be 4 ppm (632.8 nm excitation) and 39 ppm (514.5 nm excitation) for vibrational bands at 1265 cm^{-1} and 1334 cm^{-1}, respectively. For Purpurin, 42 ppm (514.5 nm excitation) and 8 ppm (632.8 nm excitation) were determined for the vibrational bands at 1330 cm^{-1} and 1070 cm^{-1}, respectively. A study conducted on the evaluation of the effect of Ag NSs derived from *Syzygium aromaticum* flowers, on stem cultures of *Rubia tinctorum* showed the highest concentrations of anthraquinones in the cultures treated with 30 mg/L of bio-Ag NSs (Nartop *et al.*, 2023).

Natural dyes from plants offer a range of colours and lasting functional properties such as UV protection, deodorizing, antibacterial, and antioxidant effects. Importantly the antibacterial, antioxidant and anti-inflammatory properties are attributed to the presence of anthraquinone components, in the root extracts. Being a natural dye with biodegradability gives them wide acceptance in the textile industry (Do *et al.*, 2023; Schmidt-Przewoźna & Kicińska-Jakubowska, 2023).

Our study supports the adoption of this approach in laboratories to enhance plant growth in the textile and dye industries. Elicitation is a method that involves introducing agents to boost plant defense mechanisms and enhance metabolite production (Narayani & Srivastava, 2017). These approaches notably aid habitat conservation and reduce the harvesting of wild species. The impact of NSs, on living organisms remains somewhat ambiguous. Numerous research studies have examined the presence of NSs and their impact, on *in vitro* systems considering both abiotic and biotic factors as triggers, which makes them worthy for further studies (Salih *et al.*, 2021).

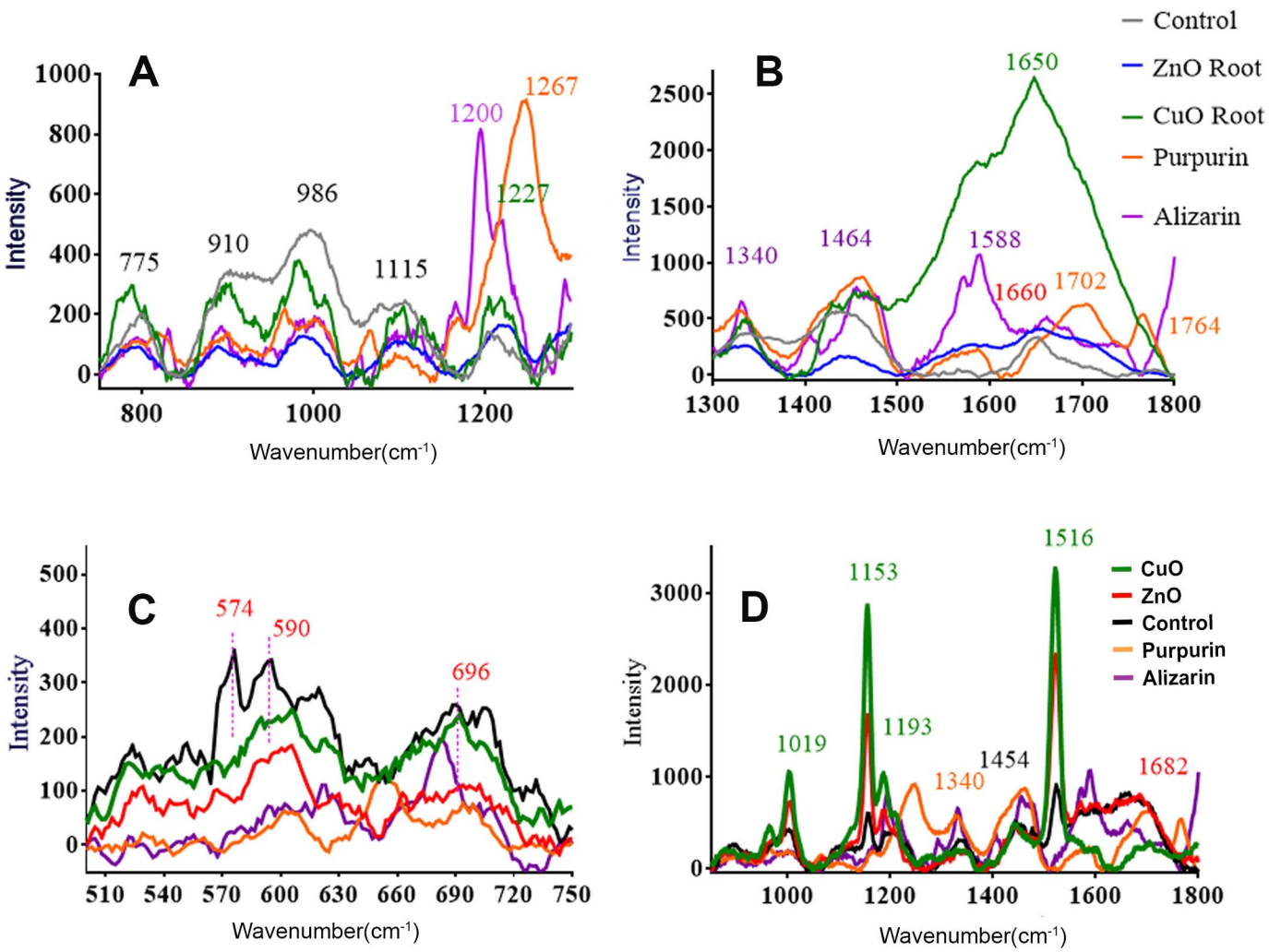

Plate 13: Comparitive Raman spectral analysis of nano structures treated and untreated *in vitro* grown *R. cordifolia* and marker compounds.
(A & B) Root samples, **(C & D)** Leaf samples.

The uptake and movement of MO NSs in plants are influenced by their unique characteristics, including high surface area to volume ratio, small size, high reactivity, and their ability to facilitate electron exchange (Inam *et al.*, 2023).

The uptake of NSs by plants was found to be higher at low concentrations of NSs due to lesser aggregation. However, at high concentrations, there is an increased chance for aggregate formation, making it difficult for the NSs to pass through the cell wall pores. As a result, NS uptake and accumulation are reduced. A similar result was observed by López-Moreno *et al.,* (2010) in the uptake and accumulation of ZnO NSs by *Glycine max* seedlings.

NSs can penetrate plants in three main ways: through foliar spray, through the soil, or using artificially created nutritional mediums. In order to enter plant tissue, MO NSs need to overcome the plant cell wall, which can be achieved through openings in the wall or by altering the size of existing pores (Ma *et al.*, 2015). NS internalization of the cell membrane into the cytosol or other organelles occurs through various mechanisms, such as endocytosis, induction of new pores via ion carrier substances, or specific membrane-bound transporter proteins (Tripathi *et al.*, 2017b). Once inside the plant, NSs can be transferred between cells through either the apoplastic or symplastic pathways (W. Liu *et al.*, 2020).

The internalization of NSs inside plant cells may disrupt the primary and specialized metabolism of plants, potentially due to the generation of ROS or other mechanisms (Gao *et al.*, 2023). Studies have shown that when *Zea mays* plants were exposed to MO NSs in hydroponic conditions, there was a significant accumulation of ZnO NSs in the roots and shoots, likely due to increased solubility and translocation of Zn^{2+} ions (Lv *et al.*, 2015). Roots absorbed Zn due to Zn^{2+} released from ZnO NSs. The accumulated Zn was in the form of $ZnSO_4$. ZnO NSs adsorbed on root surfaces and moved into the root cortex due to rapid cell division and elongation of the root tips. As a result, the ZnO NSs were mainly detected in the epidermis, cortex, vascular system, and root tip cells. The ZnO NSs entered the vascular system through the gaps of the casparian strips at the location of the primary and lateral root junction (A. Singh *et al.*, 2018).

Plants have the ability to uptake, transport, and convert CuO NSs. These particles can enter the root epidermis, exodermis, and cortex, and eventually reach the endodermis. When plants take up CuO NSs, these particles can dissolve in the plant

cells due to the acidic pH, promoting the dissolution of CuO NSs. The dissolved Cu is then either precipitated in the plants by citrate or phosphate ligands or bound to amino acids before being translocated within the plants (Peng *et al.*, 2015). Similar biotransformation of CuO NSs was also observed in the case of wheat (Dimkpa *et al.*, 2013). The reduction of CuO to Cu_2O observed in this study is in agreement with Wang *et al.,* (2011), who observed that some CuO NSs were reduced to Cu_2O in the intracellular environment of *Microcystis aeruginosa*. In an experiment conducted by Peng *et al.,* (2015) on rice plants under hydroponic conditions, the scanning transmission X-ray microscopy (STXM) revealed that Cu in the root cells is present in the form of Cu-citrate, while in the intercellular space, it exists as CuO NSs.

4.5.6 Biomass and Secondary Metabolites

As comparing the present and previous sub chapters, it reveals a relationship between biomass and the production of secondary metabolites in *in vitro* cultures of *R. cordifolia* in relation to NS. In the above discussion, the HPTLC results showed that NSs had an impact on the anthraquinone dye content of *in vitro* cultures of *R. cordifolia*. **Figure 16 A** illustrates that the dye content was higher in the 0.1 mg/L CuO (RCu1) treatment group compared to the other treatments and the untreated group (RC). By scanning the chromatograms and evaluating them under 366 nm UV, two bands at R_f values of 0.48 and 0.62, corresponding to Purpurin and Alizarin were identified (as shown in **Figure 16 B**). In **Figure 16 C**, it is evident that both dye contents were highest in the RCu1 treatment group compared to RC and all other treatments. We calculated that the area percentage of Purpurin and Alizarin were in a ratio of 1:4 in both RC and RCu1 treatments.

Similarly, in the previous chapter, the impact of various concentrations of green synthesized ZnO and CuO NSs on the biomass (Fresh and Dry weight) of *in vitro*-grown *R. cordifolia* was evaluated. As represented in the graph (**Figure 16 D**), a significant decrease in the biomass was observed in treated plants compared to the untreated group. The biomass was drastically affected at high concentrations of both the NSs.

In comparison to the control group, the HPTLC analysis revealed that plants treated with 0.1 mg/L CuO NSs with high area% of Purpurin and Alizarin had significantly higher levels of anthraquinones. Specifically, the treated plants showed 19.21% of Purpurin and 8.11% of Alizarin, compared to 5.36% and 2.6% in the control

plants, respectively. However, the fresh weight of the treated plants was significantly lower at 1.03 g and 0.14g, respectively compared to 4 g and 0.31g respectively in the untreated control plants. As a result, the biomass-to-metabolite production ratio was 3:1 in the control group and 1:4 in the NS-treated group. The obtained results indicated that inhibition of plant growth and development may correlate with high metabolism and production of secondary metabolites (Murthy *et al.*, 2014).

Similar results were seen in a study that investigated the effects of different concentrations of jasmonic acid on *Panax ginseng* adventitious root cultures. Though ginsenoside content was increased by 5.2-fold, a decrease in both fresh and dry biomass of roots was observed with an increase in jasmonic acid concentration (Yu *et al.*, 2002). A multi-step process that includes growth and metabolite production stages can be used to produce plant derived pharmaceuticals grown *in vitro* culture. High productivity and low metabolite production can coexist early in the cultivation process with a subsequent increase in the metabolite production and overall decrease in biomass (Isah *et al.*, 2018).

The method of direct shoot organogenesis is used to promote *in vitro* shoot growth of *R. cordifolia*. The presence of NSs stimulates growth and metabolic pathways for the production of active constituents (Bernela *et al.*, 2023). Mineral nutrients are the essential components of tissue culture media, and the response of the explant depends on the type and concentration of the nutrients. Various Copper-containing enzymes involved in electron transport, protein, and carbohydrate biosynthesis also play a role in plant regeneration (Awasthi *et al.*, 2022; Niedz *et al.*, 2007). However, the critical threshold level of each component is crucial. Copper has been studied as a stimulatory component for the induction of *in vitro* culture in many plant species, as well as for its high regeneration capacity, including *Ocimum basilicum* L., *Triticum aestivum* L., *Vinga radiata* L., and *Lactuca sativa* L. (Ibrahim *et al.*, 2019; Iqbal *et al.*, 2022; Malik *et al.*, 2021; Pelegrino *et al.*, 2020). These findings indicate that CuO NSs also stimulate *in vitro* shoot regeneration and the production of secondary metabolites.

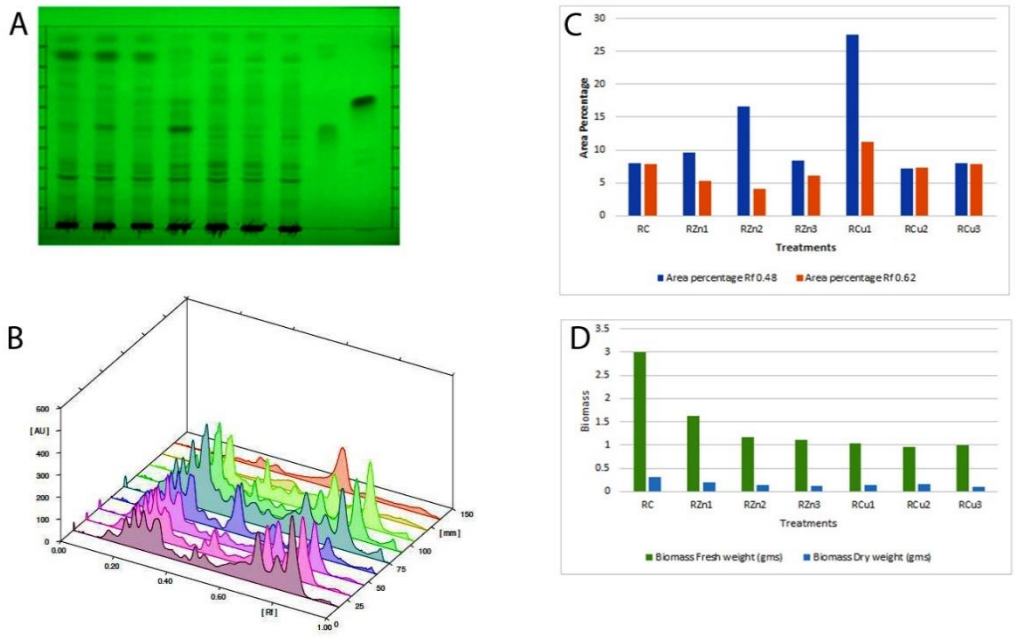

Figure 16: A comparison of secondary metabolite production and biomass. (A) HPTLC chromatogram (Track 1-RZn1, 2-RZn2, 3-RZn3, 4-RCu1, 5-RCu2, 6-RCu3, 7-RC, 8-Purpurin, 9-Alizarin) (B) HPTLC densitometric scanning image under 366 nm of methanol extract of nanostructures treated and untreated *R. cordifolia* (C) The HPTLC area percentage of Purpurin and Alizarin in treated extracts and (D) Biomass of NSs treated and untreated *R. cordifolia*

In previous research, it has been suggested that NSs may have an impact on plant secondary metabolism and signalling pathways, but the specific mechanism of this modulation is still not fully understood (Inam *et al.*, 2023). It is believed that when plants are exposed to NSs, it may lead to elevated levels of ROS, cytoplasmic Ca^{2+}, and activation of MAPK cascades as part of the plant's early response. When exposed to NSs such as Ag, ZnO, Al_2O_3, etc., plants exhibit complex physiological and biochemical responses. These NSs induce the production of ROS in plants through various mechanisms. Upon NS exposure, ROS like hydrogen peroxide (H_2O_2) and superoxide anion (O^{2-}) accumulate due to NADPH oxidase activation at the plasma membrane, triggering downstream signalling pathways involving MAPKs, which regulate gene expression for defense responses (Humbal & Pathak, 2023; Thwala *et al.*, 2013; Zhao *et al.*, 2012).

A mutant of *Arabidopsis thaliana* lacking NADPH oxidase (RBOH) showed a significantly lower amount of ROS formation in response to Ag NSs, indicating that the enzymes attached to the plasma membrane are responsible for mediating the accumulation of ROS in cells (Mittler, 2017; Sosan *et al.*, 2016). According to Jiang *et al.,* (2017), It has been suggested that ions released from NSs, rather than intact particles, are the source of ROS activation. Internalized Ag in *Spirodela polyrhiza* has the same potential to produce ROS whether it comes from exposure to Ag ions or Ag NSs. Similarly, other studies have demonstrated that ZnO, CuO, and CeO_2 dissolve into the corresponding ions (Zn^{2+}, Cu^{2+}, Ce^{4+}) (Bradfield *et al.*, 2017; Ebbs *et al.*, 2016).
NS exposure also disturbs the ion balance within plant cells. NS-induced stress responses depend critically on the influx and efflux of Ca^{2+}, which are mediated by channels and pumps. Increased levels of cytosolic Ca^{2+} stimulate various signalling pathways and transcription factors, affecting the expression of genes linked to the generation of secondary metabolites and stress adaption (Sosan *et al.*, 2016). Plants use both non-enzymatic (glutathione) and enzymatic (superoxide dismutase, catalase, and ascorbate peroxidase) antioxidant mechanisms to counteract oxidative damage caused by NSs. These systems are essential for cellular survival and function under stress, as they work to detoxify ROS and maintain redox balance inside cells (Sewelam *et al.*, 2016; Tripathi *et al.*, 2017a).

In a recent study by Iqbal *et al.,* (2022), nanostructures of ZnO and CuO synthesized with *Nigella sativa* extracts were utilized to enhance the phytochemicals in three varieties of *in vitro* cultures of *Vigna radiata*. At a concentration of 0.5 mg/L for each type of nanostructures, all three classes of mung beans showed increased phenolic content, with enhancements of 26%, 25.6%, and 22.7%, respectively. Furthermore, a 50%, 37.5%, and 25% increase in glycoside production was observed in the three varieties of beans. CuO NSs are used to stimulate the production of secondary metabolites in plants. When *Withania somnifera* was treated with CuO NSs for 20 days, the shoots showed 27.215 ± 0.73 mg/g DW of phenolic compounds, while the roots contained 26.455 ± 0.365 mg/g DW (O. S. Singh *et al.*, 2018). A callus culture of *Echinacea purpurea* was exposed to a range of ZnO NS concentrations. Optimum outcomes were observed at 75 mg/L, resulting in 23.25 mg/g dry weight of flavonoids. However, higher concentrations led to phytotoxicity, inhibiting further synthesis (Karimi *et al.*, 2018). In a recent study by Asadollahei *et al.,* (2023), it was found that

exposing *Lavandula stoechas* to Nano-CuO stress at concentrations of 0, 25, 50, and 100 mg/L led to an increase in phytochemicals. The highest total flavonoid content of 0.68 mg/g fresh weight was observed at 50 mg/L after a 5-day exposure period. Additionally, 36.51 mg/g fresh weight of anthocyanins and 0.29 mg/g fresh weight of flavonols were reported. Furthermore, another study by Nazir *et al.,* (2021) explored the effects of CuO and MnO NSs on *Ocimum basilicum*. The research indicated that at 10 mg/L, CuO NSs led to the highest accumulation of flavonoids (9.1 mg/g DW) and stimulated peroxidase and superoxide dismutase more effectively than MnO NSs.

Chung *et al.,* (2019a) found that the yield of gymnemic acid II in the cell suspension cultures of *Gymnema sylvestre* increased significantly. The highest yield occurred after treating the cultures with 3 mg/L of CuO NSs for 48 hours, resulting in a nine-fold increase in the amount of gymnemic acid II compared to untreated cultures. Gymnemic acid is a triterpene saponin with potential anti-diabetic applications (Li *et al.*, 2019). Nekoukhou *et al.,* (2023) investigated the impact of different concentrations of CuO NSs and chelated-CuO NSs on the production and yield of secondary metabolites such as geraniol, neral, geranial, and geranyl acetate in *Dracocephalum moldavica*. They found promising results at 80 mg/L of CuO NSs compared to 160 mg/L of conventionally chelated-CuO NSs. Another recent study by Asadollahei *et al.,* (2023) discussed the potential effect of CuO NSs as elicitors on the essential oils and terpenoid components in *Lavandula stoechas.* The results showed a significant increase in essential components such as lavandulol (21.68%), germacrene D (9.33%), 1,8-cineole (17.21%), and E-nerlidol (8.11%). The study demonstrated the significant potential of CuO NSs for use in the production of secondary metabolites for industrial and medicinal purposes.

Research has demonstrated the potential use of CuO NSs in medicinal plants to enhance biological activity without phytotoxicity and promote the production of bioactive chemicals. However, further studies are needed to understand the potential impacts of using nanomaterials as elicitors on ecosystems and human health.

CHAPTER - 5

SUMMARY AND CONCLUSION

R. cordifolia L. is a medicinally and industrially important plant and belonging to the Rubiaceae family. It contains alkaloids, terpenoids, and flavonoids. *R. cordifolia* is a source of anthraquinone-based dye widely used in dyeing industries. Purpurin and Alizarin are the paramount dyes derived from the root extract of *R. cordifolia* and are widely used in dying and pharmaceutical industries as bioactive compounds.

Plant secondary metabolites are a source of many high-value chemical compounds that find applications in pharmaceuticals, cosmetics, flavours, fragrances, insecticides, and dyes. Therefore, research in the field of secondary metabolite production is essential to meeting human needs. *In vitro* techniques are an alternative to traditional whole plant culture for the production of significant secondary metabolites. The synthesis of biogenic NSs using plant extracts is a growing area of research. Combining nanosystems with plant tissue culture is now essential for the manufacturing of bioactive components, genetic engineering, crop improvement, and mass reproduction. Nanostructured metal oxides such as ZnO and CuO NSs are particularly important in *in vitro* plant culture. The production of ZnO and CuO NSs has been an important focus due to their potential use in nanotechnologies.

The present study has developed an environmental friendly, cost-effective, energy-efficient, and stable method for creating ZnO and CuO NSs using stem extract from *R. cordifolia.* The various organic compounds in the stem extract can act as reducing or stabilizing agents, aiding in the reduction of metal ions into their NS form. The structural features of the produced ZnO and CuO NSs have been confirmed using UV-Vis, FT-IR, XRD, SEM-EDX, TEM, Raman spectroscopy, and DTG analysis methods.

The maximum absorption peaks for green synthesized ZnO and CuO NSs were observed at 370 nm and 285 nm, respectively, in the UV-Vis spectra. The FTIR spectrum confirmed the presence of active phytochemicals and biomolecules involved in the reduction or stabilization of the NSs. Zn-O and Cu-O stretching vibrations were strong and intense, and the XRD pattern showed the average crystalline size of the nanomaterials. The sizes were calculated as 17.9 nm for ZnO NSs and 28.35 nm for CuO NSs using the Debye-Scherrer's formula. The XRD patterns indicated a hexagonal-wurtzite structure for ZnO and a monoclinic structure for CuO. Whereas, SEM micrograph shows a tetrahedron CuO and ZnO clusters. TEM observations were correlated with the XRD data. The ZnO NSs have a hexagonal shape and a particle size

ranging from 6 to 20 nm, while CuO NSs have a spherical structure with a size range between 9 to 32 nm. The elemental composition of the biogenic NSs was confirmed by analyzing the EDX plot of the SEM images, which displayed a high purity of NSs.

The development of a protocol for organogenesis was a crucial step. Different concentrations of growth regulators were used, alone or in combination, to achieve this. Nodal explants cultured in MS basal medium produced contamination-free plants, which were utilized for further studies. MS medium supplemented with various concentrations and combinations of IAA, NAA, Kinetin, BA, and a combination of BA and Kinetin were used as the plant growth regulators. Among the PGRs, it was found that Kinetin at 0.5 mg/L was the most effective for the multiplication of shoots, roots, and biomass production.

In order to standardize the best solvent system for the extraction of bioactive compounds, especially Purpurin and Alizarin, and to identify the suitable plant part for isolation of these compounds, extractions from the cultures of *in vitro R. cordifolia* plant parts (leaf, stem, root) were conducted using solvents such as hexane, chloroform, and methanol to obtain three different extracts of each sample. Disparities were observed regarding the number of bands and band intensity of the HPTLC profiles developed. The maximum area percentage of Alizarin and Purpurin was found to be present in the methanol fraction. Furthermore, the three parts of *in vitro R. cordifolia* showed the presence of these compounds with a maximum area percentage.

This study aims to examine how NS elicitors affect the growth and production of secondary metabolites in *in vitro R. cordifolia* cultures. In this experiment, *R. cordifolia* plantlets grown in a standard MS medium were exposed to two different sets of concentrations of biogenic ZnO and CuO NSs. The broad spectrum treatment used four concentrations (0.1 mg/L, 1 mg/L, 10 mg/L, and 100 mg/L) of ZnO NSs and CuO NSs. The narrow spectrum treatment used concentrations of 0.2 mg/L, 0.4 mg/L, 0.6 mg/L, and 0.8 mg/L. Control cultures without NSs were also maintained. After 80 days, the plants were harvested, and their morphogenic traits were measured. The harvested plants were then shade-dried and powdered, and 5 g of each sample was extracted in methanol using a Soxhlet apparatus. The concentrated methanol extracts were analyzed using HPTLC, TPC, TFC, DPPH, ABTS and HR-LCMS to identify the secondary metabolites qualitatively. Secondary metabolite enhancement was observed in *R. cordifolia* plants treated with NS elicitors.

The study found that ZnO and CuO NSs affect plant growth differently. CuO NS had a more significant positive impact on various growth parameters than ZnO NSs. Specifically, plants treated with 1 mg/L and 0.1 mg/L concentrations of CuO NSs showed significant improvements in shoot length, leaf area, and the number of plantlets, surpassing those observed in the control group. However, the biomass production in plants treated with these NSs was lower than that of the control group. Additionally, higher concentrations of ZnO and CuO NSs (100 mg/L) were found to hinder growth. Therefore, while NSs can positively influence specific growth attributes, they seem to have a negative impact on overall biomass accumulation.

The HPTLC assessment of both treated and untreated methanol extracts showed that ZnO and CuO NSs had an impact on enhancing the presence of Alizarin and Purpurin in *in vitro R. cordifolia*. The experiments demonstrated that these compounds accumulated more in the treated plants. Specifically, shoots grown in 0.1 mg/L CuO NSs treatment showed the best results, with Purpurin at 19.21% and Alizarin at 8.11% in terms of anthraquinone accumulation.

There was a clear relationship between the amount of biomass and the secondary metabolites when plants were exposed to NSs treatment. Comparing the 0.1 mg/L CuO NSs with high area% of Purpurin and Alizarin and the control, the HPTLC analysis showed that the treated plants had significantly higher levels of anthraquinones, precisely 19.21% of Purpurin and 8.11% of Alizarin, compared to 5.36% and 2.6% in control plants, respectively. On the other hand, the fresh weight and dry weight of the treated plants was significantly lower at 1.03 g and 0.14g, respectively compared to 4 g and 0.31 g respectively in the untreated control plants. This resulted in a biomass-to-metabolite production ratio of 3:1 in the control group and 1:4 in the NS-treated group. These findings suggest a trade-off between the accumulation of plant material and the synthesis of secondary metabolites in response to NS treatment.

The total phenolic content, flavonoid contents, and antioxidant activity of NSs treated *in vitro* cultured *R. cordifolia* were analyzed to study the effect of NSs on the phytochemical constituents and antioxidant activity of *R. cordifolia*. In all ZnO and CuO NS treatments and controls, the percentage increase in TPC and TFC was highest with 0.1 mg/L CuO NSs. The antioxidant activity was also highest with 0.1 mg/L CuO, as indicated by its low IC50 value.

Based on the results from the HPTLC, phytochemical, and antioxidant activity analyses, it is clear that the treatment with 0.1 mg/L CuO NS has a more beneficial effect on *in vitro R. cordifolia* plants than other treatments. As a result, we conducted further analysis using HR-LCMS techniques to identify any qualitative differences in phytochemical components between the methanolic extracts of the untreated and treated groups (0.1 mg/L CuO NS) of *R. cordifolia*.

LC-MS analysis revealed common compounds in both groups, indicating minimal impact from nanomaterial treatment. However, the control samples found only flavonoids like aurapentol, sinesietin, oroxylin A, and luteolin 7 O glucuronide. On the other hand, several flavonoids such as (+) sophorol, betavulgarin, 3-O-methylcoumestrol, catechin, myricitrin, tricin 5 glucoside, luteolin 4' O glucoside, and Tectorigenin were detected in the treated plants but not in the control samples.

Variations in tannins and alkaloids also showed differences between the treated and untreated plants. Tannins such as gibberellin A75, ganoderic Acid Mc, halstoctacosanolide A, and 3-O-p-trans-coumaroylalphitolic acid were identified solely in the control group. These differences in secondary metabolites indicate the effect of CuO NS on *in vitro* culture of *R. cordifolia*. The accumulation of more flavonoids in treated samples explains the increased antioxidant capacity of the treated sample.

Raman spectroscopy was utilised to assess how *R. cordifolia* respond to stress induced by ZnO and CuO NSs *in vitro*. Leaf and root samples exposed to these NSs (0.1 mg/L) were analysed. The study found that stress from NSs enhanced chlorophyll and carotenoid content while anthocyanin level was reduced. Peaks of anthraquinone pigments (Alizarin and Purpurin) in the roots were more substantial in NS-treated plants, especially CuO treatments. Raman spectra revealed the uptake of NSs with CuO reduced to Cu_2O inside the plant. The findings indicate that NSs positively affect chlorophyll synthesis and plant growth, but varying effect was observed on secondary metabolites.

The study introduces an eco-friendly, cost-effective method for synthesizing ZnO and CuO metal oxide nanostructures from *R. cordifolia* stem extract. The NS elicited *in vitro* studies found that lower NS concentrations (0.1 mg/L and 1 mg/L) increased secondary metabolite production in plants, particularly CuO NSs. However, higher concentrations (100 mg/L) diminished plant growth and metabolite production. This highlights the impact of NS concentration on plant phytochemical composition

and antioxidant potential. The research suggests that treating plants with 0.1 mg/L of CuO NS can enhance the synthesis of bioactive compounds with potential applications in the pharmaceutical and textile industries.

CHAPTER - 6

RECOMMENDATIONS

In the current study conducted in *R. cordifolia* it is found that NSs can enhance the production of secondary metabolites, specifically the anthraquinone dyes such as Purpurin and Alizarin. It is recommended to implement this pilot study to assess the practical aspects of using NSs in commercial settings, including scalability.
The following recommendations are suggested as future line of work.

- The range of NSs studies can be expanded (Silver, Titanium, Gold, etc.).
- Investigate the molecular mechanism by which NSs influence biomass accumulation and secondary metabolite synthesis.
- Scaling up studies – Transition from *in vitro* cultures to bioreactor system.
- Investigate synergistic effect of NSs with Plant growth regulators.
- Explore the possibility of engineering metabolite pathways in *Rubia* to work for targeted metabolite enhancement.

CHAPTER - 7

REFERENCES

Abdel Latef, A. A., Zaid, A., Abu Alhmad, M. F., & Abdelfattah, K. E. (2020) The impact of priming with Al_2O_3 nanoparticles on growth, pigments, osmolytes, and antioxidant enzymes of Egyptian Roselle (*Hibiscus sabdariffa* L.) cultivar. *Agronomy,* 10 (5): 681.

Abderrahman, S. M. (2004) Mitodepressive effect of *Rubia cordifolia* extract on the bone marrow cells of mice. *Cytologia,* 69 (3): 307-311.

Abdi, G., Salehi, H., & Khosh-Khui, M. (2008) Nano silver: a novel nanomaterial for removal of bacterial contaminants in valerian (*Valeriana officinalis* L.) tissue culture. *Acta Physiologiae Plantarum*, 30: 709-714.

Abdullah, Rahman, A. U., Faisal, S., Almostafa, M. M., Younis, N. S., & Yahya, G. (2023) Multifunctional spirogyra-hyalina-mediated barium oxide nanoparticles (BaONPs): synthesis and applications. *Molecules*, 28 (17): 6364.

Aboulila, A. A., & Galal, O. A. (2019) Evaluation of silica nanoparticles (SiO_2NP) and somaclonal variation effects on genome template stability in rice using RAPD and SSR markers. *Egyptian Journal of Genetics and Cytology,* 48 (1): 1-16.

Abubakar, A. R., & Haque, M. (2020) Preparation of medicinal plants: Basic extraction and fractionation procedures for experimental purposes. *Journal of Pharmacy and Bioallied Sciences,* 12 (1): 1-10.

Adeel, S., Habib, N., Kanwal, A., Shah, Z. A., Hosseinnezhad, M., Batool, F., & Qayyum, M. A. (2022) Rejuvenation of Natural Dyes from Medicinal-Based Plants. *Textile Dyes and Pigments: A Green Chemistry Approach,*12: 345-363.

Adejoke, H. T., Louis, H., Amusan, O. O., & Apebende, G. (2019) A review on classes, extraction, purification and pharmaceutical importance of plants alkaloid. *Journal of Medicinal and Chemical Sciences,* 2 (4): 130-139.

Adil, M., Bashir, S., Bashir, S., Aslam, Z., Ahmad, N., Younas, T., . . . Elshikh, M. S. (2022) Zinc oxide nanoparticles improved chlorophyll contents, physical parameters and wheat yield under salt stress. *Frontiers in Plant Science,* 13: 93-101.

Adwankar, M. K., & Chitnis, M. P. (1982) *In vivo* anti-cancer activity of RC-18a plant isolate from *Rubia cordifolia*, linn, against a spectrum of experimental tumour models. *Chemotherapy,* 28 (4): 291-293.

Afolayan, A., & Adebola, P. (2004) *In vitro* propagation: A biotechnological tool capable of solving the problem of medicinal plants decimation in South Africa. *African Journal of Biotechnology,* 3 (12): 683-687.

Aghdaei, M., Salehi, H., & Sarmast, M. (2012) Effects of silver nanoparticles on *Tecomella undulate* (Roxh.) Seem. *Micropropagation. Advances in Horticultural Science,* 26 (1): 21-24.

Aghdam, H. D., Bellah, S. M., & Malekfar, R. (2019) Surface-enhanced Raman scattering studies of Cu/Cu_2O Core-shell NPs obtained by laser ablation. *Spectrochimica Acta Part A: Molecular and Biomolecular Spectroscopy*, 223: 117-137.

Ahangarpour, A., Oroojan, A. A., Khorsandi, L., Kouchak, M., & Badavi, M. (2018) Antioxidant effect of myricitrin on hyperglycemia-induced oxidative stress in C_2C1_2 cell. *Cell Stress and Chaperones*, 23 (4): 773-781.

Ahmad, M. A., Javed, R., Adeel, M., Rizwan, M., Ao, Q., & Yang, Y. (2020) Engineered ZnO and CuO nanoparticles ameliorate morphological and biochemical response in tissue culture regenerants of candyleaf (*Stevia rebaudiana*). *Molecules*, 25 (6): 28-36.

Ahmad, R., Fatima, Z., Ali, S., Dhaneshwar, S., & Ahmad, S. (2024) HPTLC Method Development and Validation for Simultaneous Quantification of Purpurin and Alizarin in *Rubia cordifolia* L. Roots and their Marketed Preparations. *Pharmacognosy Research*, 16 (3): 652-661.

Ahmed, S., Ahmad, M., Swami, B. L., & Ikram, S. (2016) Green synthesis of silver nanoparticles using *Azadirachta indica* aqueous leaf extract. *Journal of Radiation Research and Applied Science*, 9 (1): 1-7.

Akhlaghi, N., Najafpour-Darzi, G., & Younesi, H. (2020) Facile and green synthesis of cobalt oxide nanoparticles using ethanolic extract of *Trigonella foenumgraceum* (Fenugreek) leaves. *Advanced Powder Technology*, 31 (8): 3562-3569.

Al-Kordy, H. M., Sabry, S. A., & Mabrouk, M. E. (2021) Statistical optimization of experimental parameters for extracellular synthesis of Zinc oxide nanoparticles by a novel haloalaliphilic Alkalibacillus sp. W7. *Scientific Reports*, 11 (1): 10924-10928.

Alamgir, A., & Alamgir, A. (2018) Methods of Qualitative and Quantitative Analysis of Plant Constituents. Therapeutic Use of Medicinal Plants and their Extracts: Volume 2: *Phytochemistry and Bioactive Compounds*, 22: 721-804.

Alfei, S. (2020) Nanotechnology applications to improve solubility of bioactive constituents of foods for health-promoting purposes: *Nano-food Engineering*, 1:189-257.

Alhaithloul, H. a. S., Ali, B., Alghanem, S. M. S., Zulfiqar, F., Al-Robai, S. A., Ercisli, S., . . . Ali, Q. (2023) Effect of green-synthesized copper oxide nanoparticles on growth, physiology, nutrient uptake, and cadmium accumulation in *Triticum aestivum* (L.). *Ecotoxicology and Environmental Safety*, 268: 115701-115711.

Ali, A., Mohammad, S., Khan, M. A., Raja, N. I., Arif, M., Kamil, A., & Mashwani, Z. U. R. (2019) Silver nanoparticles elicited in vitro callus cultures for accumulation of biomass and secondary metabolites in *Caralluma tuberculata*. *Artificial Cells, Nanomedicine, and Biotechnology*, 47 (1): 715-724.

Alibe, I. M., Matori, A. K., Saion, E., Ali, A. M., & Zaid, M. H. M. (2017) The influence of calcination temperature on structural and optical properties of ZnO nanoparticles via simple polymer synthesis route. *Science of Sintering*, 49 (3): 263-275.

Alsaeedi, A., El-Ramady, H., Alshaal, T., El-Garawany, M., Elhawat, N., & Al-Otaibi, A. (2019) Silica nanoparticles boost growth and productivity of cucumber under water deficit and salinity stresses by balancing nutrients uptake. *Plant Physiology and Biochemistry*, 139: 1-10.

Altammar, K. A. (2023) A review on nanoparticles: characteristics, synthesis, applications, and challenges. *Frontiers in Microbiology*, 14: 115-135.

Altangerel, N., Ariunbold, G. O., Gorman, C., Alkahtani, M. H., Borrego, E. J., Bohlmeyer, D., . . . Scully, M. O. (2017) *In vivo* diagnostics of early abiotic plant stress response via Raman spectroscopy. *Proceedings of the National Academy of Sciences*, 114 (13): 3393-3396.

Álvarez, S. P., Tapia, M. a. M., Vega, M. E. G., Ardisana, E. F. H., Medina, J. A. C., Zamora, G. L. F., & Bustamante, D. V. (2019) Nanotechnology and plant tissue culture. *Plant Nanobionics: Advances in the Understanding of Nanomaterials Research and Applications*, 1: 1333-370.

Aminuzzaman, M., Kei, L. M., & Liang, W. H. (2017). Green synthesis of copper oxide (CuO) nanoparticles using banana peel extract and their photocatalytic activities. In *AIP conference proceedings*, AIP Publishing. 1828 (1).

Amist, N., Singh, N., Yadav, K., Singh, S., & Pandey, J. (2017) Comparative studies of Al^{3+} ions and Al_2O_3 nanoparticles on growth and metabolism of cabbage seedlings. *Journal of Biotechnology*, 254: 1-8.

Anjum, S., Anjum, I., Hano, C., & Kousar, S. (2019) Advances in nanomaterials as novel elicitors of pharmacologically active plant specialized metabolites: Current status and future outlooks. *RSC Advances*, 9 (69): 40404-40423.

Annamalai, A., Christina, V., Sudha, D., Kalpana, M., & Lakshmi, P. (2013) Green synthesis, characterization and antimicrobial activity of Au NPs using *Euphorbia hirta* L. leaf extract. *Colloids and Surfaces B: Biointerfaces*, 108: 60-65.

Anwaar, S., Maqbool, Q., Jabeen, N., Nazar, M., Abbas, F., Nawaz, B., . . . Hussain, S. Z. (2016) The effect of green synthesized CuO nanoparticles on callogenesis and regeneration of *Oryza sativa* L. *Frontiers in Plant Science*, 7: 1330-1338.

Arab, M. M., Yadollahi, A., Shojaeiyan, A., Shokri, S., & Ghojah, S. M. (2014) Effects of nutrient media, different cytokinin types and their concentrations on *in vitro* multiplication of G× N15 (hybrid of almond× peach) vegetative rootstock. *Journal of Genetic Engineering and Biotechnology*, 12 (2): 81-87.

Araujo, N. M. P., Arruda, H. S., Dos Santos, F. N., De Morais, D. R., Pereira, G. A., & Pastore, G. M. (2020) LC-MS/MS screening and identification of bioactive compounds in leaves, pulp and seed from *Eugenia calycina* Cambess. *Food Research International*, 137: 109-119.

Arshad, M., & Frankenberger, J. W. T. (2012). *Ethylene: Agricultural Sources and Applications*, Springer science and Business media.

Asadollahei, M. V., Tabatabaeian, J., Yousefifard, M., Mahdavi, S. M. E., & Nekonam, M. S. (2023) Impact of elicitors on essential oil compositions and phytochemical constituents in *Lavandula stoechas* L. *Plant Physiology and Biochemistry*, 194: 722-730.

Asl, K. R., Hosseini, B., Sharafi, A., & Palazon, J. (2019) Influence of nano-zinc oxide on tropane alkaloid production, h6h gene transcription and antioxidant enzyme activity in *Hyoscyamus reticulatus* L. hairy roots. *Engineering in Life Sciences*, 19 (1): 73-89.

Awasthi, S., Chauhan, R., & Srivastava, S. (2022). The importance of beneficial and essential trace and ultratrace elements in plant nutrition, growth, and stress tolerance. In *Plant Nutrition and Food Security in the Era of Climate Change*, Elsevier. Pp. 27-46.

Azad, M., Yokota, S., Begum, F., & Yoshizawa, N. (2009) Plant regeneration through somatic embryogenesis of a medicinal plant, *Phellodendron amurense* Rupr. *In Vitro Cellular Developmental Biology-Plant*, 45: 441-449.

Babu, S., Singh, R., Yadav, D., Rathore, S. S., Raj, R., Avasthe, R., . . . Yadav, B. (2022) Nanofertilizers for agricultural and environmental sustainability. *Chemosphere*, 292: 133-143.

Balachandran, P., Ibrahim, M. A., Zhang, J., Wang, M., Pasco, D. S., & Muhammad, I. (2021) Crosstalk of cancer signaling pathways by cyclic hexapeptides and anthraquinones from *Rubia cordifolia*. *Molecules*, 26 (3): 735.

Balandin, G., Suvorov, O., Shaburova, L., Podkopaev, D., Frolova, Y. V., & Ermolaeva, G. (2015) The study of the antimicrobial activity of colloidal solutions of silver nanoparticles prepared using food stabilizers. *Journal of Food Science and Technology*, 52: 3881-3886.

Bansal, S., Sharma, M. K., Joshi, P., Malhotra, E. V., Latha, M., & Malik, S. K. (2024) An efficient direct organogenesis protocol for *in vitro* clonal propagation of *Rubia cordifolia* L. *Industrial Crops and Products*, 208: 117-127.

Bansod, S., Bawskar, M., & Rai, M. (2015) *In vitro* effect of biogenic silver nanoparticles on sterilisation of tobacco leaf explants and for higher yield of protoplasts. *IET Nanobiotechnology*, 9 (4): 239-245.

Banu, K. S., & Cathrine, L. (2015) General techniques involved in phytochemical analysis. *International Journal of Advanced Research in Chemical Science*, 2 (4): 25-32.

Banu, R., & Nagarajan, N. (2014) TLC and HPTLC fingerprinting of leaf extracts of *Wedelia chinensis* (Osbeck) Merrill. *Journal of Pharmacognosy and Phytochemistry*, 2 (6): 29-33.

Bányai, P., Kuzovkina, I., Kursinszki, L., & Szőke, É. (2006) HPLC analysis of alizarin and purpurin produced by *Rubia tinctorum* L. hairy root cultures. *Chromatographia,* 63: S111-S114.

Bao, H. G., Tung, H. T., Van, H. T., Bien, L. T., Khai, H. D., Mai, N. T. N., . . . Nhut, D. T. (2022) Copper nanoparticles enhanced surface disinfection, induction and maturation of somatic embryos in tuberous begonias (*Begonia* × *tuberhybrida* Voss) cultured *in vitro*. *Plant Cell, Tissue and Organ Culture*, 151 (2): 385-399.

Barlow, R., Barnes, D., Campbell, A. M., Nigam, P. S., & Owusu-Apenten, R. K. (2015) Antioxidant, anticancer and antimicrobial, effects of *Rubia cordifolia* aqueous root extract. *Journal of Advances in Biology & Biotechnology,* 5(1): 1-8.

Baskar, V., Nayeem, S., Kuppuraj, S. P., Muthu, T., & Ramalingam, S. (2018) Assessment of the effects of metal oxide nanoparticles on the growth, physiology and metabolic responses in *in vitro* grown eggplant (*Solanum melongena*). *3 Biotech*, 8: 1-12.

Baskar, V., Safia, N., Sree Preethy, K., Dhivya, S., Thiruvengadam, M., & Sathishkumar, R. (2021) A comparative study of phytotoxic effects of metal oxide (CuO, ZnO and NiO) nanoparticles on *in-vitro* grown *Abelmoschus esculentus*. *Plant Biosystems-An International Journal Dealing with all Aspects of Plant Biology*, 155 (2): 374-383.

Begum, S., Zahid, A., Khan, T., Khan, N. Z., & Ali, W. (2020) Comparative analysis of the effects of chemically and biologically synthesized silver nanoparticles on biomass accumulation and secondary metabolism in callus cultures of *Fagonia indica*. *Physiology and Molecular Biology of Plants,* 26: 1739-1750.

Bernela, M., Seth, M., Kaur, N., Sharma, S., & Pati, P. K. (2023) Harnessing the potential of nanobiotechnology in medicinal plants. *Industrial Crops and Products,* 194: 116-126.

Bhagya, N., Chandrashekar, K., Karun, A., & Bhavyashree, U. (2013) Plantlet regeneration through indirect shoot organogenesis and somatic embryogenesis in *Justicia gendarussa* Burm. f., a medicinal plant. *Journal of Plant Biochemistry and Biotechnology,* 22: 474-482.

Bhandari, S., Sinha, S., Nailwal, T. K., & Thangadurai, D. (2022) An approach for enhancement of plant system in terms of tissue culture. In *Biogenic Nanomaterials*. Apple Academic Press. 163-192.

Bhatla, S. C., & Lal, M. A. (2023) Secondary metabolites. In *Plant Physiology, Development and Metabolism*, Springer. 765-808.

Bhatt, N. S., & Deshpande, M. (2015) Pharmacognostic studies on identity of Manjishtha-Rubia cordifolia Linn-an Ayurvedic plant. *IOSR Journal of Pharmacy,* 5 (3): 06-12.

Bhattacharya, R., & Mukherjee, P. (2008) Biological properties of "naked" metal nanoparticles. *Advanced Drug Delivery Reviews,* 60 (11): 1289-1306.

Bindu, P., & Thomas, S. (2014) Estimation of lattice strain in ZnO nanoparticles: X-ray peak profile analysis. *Journal of Theoretical and Applied Physics*, 8: 123-134.

Biswas, S. K. J. O. M., & Longevity, C. (2016) Does the interdependence between oxidative stress and inflammation explain the antioxidant paradox?. *Oxidative Medicine and Cellular longevity*, 2016 (1): 569-578.

Bizzo, H. R., Silveira, D., & Gimenes, M. A. (2012) Tânia da S. Agostini-Costa1, Roberto F. Vieira1, Humberto R. Dâmaris Silveira3 and Marcos A. Gimenes1. *Chromatography and its Applications*, 131.

Boominathan, S., V, K., & Balakrishanan, S. (2022) Optimization of process parameters on color strength and antimicrobial activities of cotton fabric dyed with *Rubia cordifolia* extract. *Journal of Natural Fibers*, 19 (7): 2414-2428.

Bourgaud, F., Gravot, A., Milesi, S., & Gontier, E. (2001) Production of plant secondary metabolites: a historical perspective. *Plant Science*, 161 (5): 839-851.

Bowen, B. P., & Northen, T. R. (2010) Dealing with the unknown: metabolomics and metabolite atlases. *Journal of the American Society for Mass Spectrometry*, 21: 1471-1476.

Bradfield, S. J., Kumar, P., White, J. C., & Ebbs, S. D. (2017) Zinc, copper, or cerium accumulation from metal oxide nanoparticles or ions in sweet potato: yield effects and projected dietary intake from consumption. *Plant Physiology and Biochemistry*, 110: 128-137.

Bramwell, D. (1990) The role of *in vitro* cultivation in the conservation of endangered species. *Conservation T'echniques in Botanic Gardens*, 15: 3-15.

Brazlauskas, M., & Kitrys, S. (2008) Synthesis and properties of CuO/zeolite sandwich type adsorbent-catalysts. *Chinese Journal of Catalysis*, 29 (1): 25-30.

Cai, Sun, M., Xing, J., & Corke, H. (2004) Antioxidant phenolic constituents in roots of *Rheum officinale* and *Rubia cordifolia*: Structure− radical scavenging activity relationships. *Journal of Agricultural and Food Chemistry*, 52 (26): 7884-7890.

Calzolai, L., Gilliland, D., & Rossi, F. (2012) Measuring nanoparticles size distribution in food and consumer products: a review. *Food Additives and Contaminants: Part A*, 29 (8): 1183-1193.

Cardoso, J. C., Oliveira, M. E. B. D., & Cardoso, F. D. C. (2019) Advances and challenges on the *in vitro* production of secondary metabolites from medicinal plants. *Horticultura Brasileira*, 37 (2): 124-132.

Cardoso, J. C., Sheng Gerald, L. T., & Teixeira Da Silva, J. A. (2018) Micropropagation in the twenty-first century. *Plant Cell Culture Protocols*, 17-46.

Chandrashekar, B., Prabhakara, S., Mohan, T., Shabeer, D., Bhandare, B., Nalini, M., . . . Rao, H. H. (2018) Characterization of *Rubia cordifolia* L. root extract and its evaluation of cardioprotective effect in Wistar rat model. *Indian Journal of Pharmacology*, 50 (1): 12-21.

Chang, L. C., Chávez, D., Gills, J. J., Fong, H. H., Pezzuto, J. M., & Kinghorn, A. D. (2000) Rubiasins A–C, new anthracene derivatives from the roots and stems of *Rubia cordifolia*. *Tetrahedron Letters*, 41 (37): 7157-7162.

Chourpa, I., Douziech-Eyrolles, L., Ngaboni-Okassa, L., Fouquenet, J. F., Cohen-Jonathan, S., Soucé, M., . . . Dubois, P. (2005) Molecular composition of iron oxide nanoparticles, precursors for magnetic drug targeting, as characterized by confocal Raman microspectroscopy. *Analyst*, 130 (10): 1395-1403.

Choudhury, P., Dutta, K. N., Singh, A., Malakar, D., Pillai, M., Talukdar, N. C., . . . Devi, R. (2020) Assessment of nutritional value and quantitative analysis of bioactive phytochemicals through targeted LC-MS/MS method in selected scented and pigmented rice varietals. *Journal of Food Science*, 85 (6): 1781-1792.

Chung, I.-M., Rajakumar, G., Subramanian, U., Venkidasamy, B., & Thiruvengadam, M. (2019a) Impact of copper oxide nanoparticles on enhancement of bioactive compounds using cell suspension cultures of *Gymnema sylvestre* (Retz.) R. Br. *Applied Sciences*, 9 (10): 2165.

Chung, I.-M., Venkidasamy, B., & Thiruvengadam, M. (2019b) Nickel oxide nanoparticles cause substantial physiological, phytochemical, and molecular-level changes in Chinese cabbage seedlings. *Plant Physiology and Biochemistry*, 139: 92-101.

Corral-Diaz, B., Peralta-Videa, J. R., Alvarez-Parrilla, E., Rodrigo-García, J., Morales, M. I., Osuna-Avila, P., . . . Gardea-Torresdey, J. L. (2014) Cerium oxide nanoparticles alter the antioxidant capacity but do not impact tuber ionome in *Raphanus sativus* (L). *Plant Physiology and Biochemistry*, 84: 277-285.

Coskun, O. (2016) Separation techniques: chromatography. *Northern Clinics of Istanbul*, 3 (2): 156.

Costa, T., Vieira, R. F., Bizzo, H. R., Silveira, D., & Gimenes, M. A. (2012) Secondary metabolites. *Chromatography and Its Applications*,131-162.

Crozier, A., Jaganath, I. B., & Clifford, M. N. (2006a) Phenols, polyphenols and tannins: an overview. *Plant Secondary Metabolites: Occurrence, Structure and Role in The Human Diet*,1: 1-25.

Crozier, A., Clifford, M. N., & Ashihara, H. (2006b) Plant secondary metabolites. *Occurrence, Structure and Role in the Human Diet*, Blackwell Publishers.

Cunningham, F. J., Goh, N. S., Demirer, G. S., Matos, J. L., & Landry, M. P. (2018) Nanoparticle-mediated delivery towards advancing plant genetic engineering. *Trends in Biotechnology*, 36 (9): 882-897.

Dabiri, M., Salimi, S., Ghassempour, A., Rassouli, A., & Talebi, M. (2005) Optimization of microwave-assisted extraction for alizarin and purpurin in Rubiaceae plants and its comparison with conventional extraction methods. *Journal of Separation Science*, 28 (4): 387-396.

Dakal, T. C., Kumar, A., Majumdar, R. S., & Yadav, V. (2016) Mechanistic basis of antimicrobial actions of silver nanoparticles. *Frontiers in Microbiology*, 7: 1831.

Dallatu, Y., Shallangwa, G., & Africa, S. (2020) Synthesis and growth of spherical ZnO nanoparticles using different amount of plant extract: characterization and morphology of structures. *Journal of Applied Sciences and Environmental Management*, 24 (12): 2147-2151.

Danlami, J. M., Arsad, A., & Zaini, M. a. A. (2015) Characterization and process optimization of castor oil (*Ricinus communis* L.) extracted by the soxhlet method using polar and non-polar solvents. *Journal of the Taiwan Institute of Chemical Engineers*, 47: 99-104.

Darekar, R. S., Khetre, A. B., Singh, S. M., & Damle, M. C. (2009) HPTLC quantitation of 2-hydroxy-4-methoxybenzaldehyde in *Hemidesmus indicus* R. Br. root powder and extract. *JPC–Journal of Planar Chromatography–Modern TLC*, 22 (6): 453-456.

Das, D., Ghosh, R., & Mandal, P. (2019) Biogenic synthesis of silver nanoparticles using S1 genotype of *Morus alba* leaf extract: characterization, antimicrobial and antioxidant potential assessment. *SN Applied Sciences*, 1: 1-16.

Das, S., Ghosh, S., Bakshi, A., Khanna, S., Bindhani, B. K., Parhi, P. K., & Kumar, R. (2023) Nanotechnology and Plant Biotechnology: The Current State of Art and Future Prospects. *Biological Applications of Nanoparticles*, 101-120.

De Klerk, G.-J., Brugge, J. T., & Marinova, S. (1997) Effectiveness of indoleacetic acid, indolebutyric acid and naphthaleneacetic acid during adventitious root formation *in vitro* in Malus 'Jork 9'. *Plant Cell, Tissue and Organ Culture*, 49 (1): 39-44.

Dehkourdi, E. H., & Mosavi, M. (2013) Effect of anatase nanoparticles (TiO_2) on parsley seed germination (*Petroselinum crispum*) *in vitro*. *Biological Trace Element Research*, 155: 283-286.

Delgado-Montemayor, C., Cordero-Pérez, P., Salazar-Aranda, R., & Waksman-Minsky, N. (2015) Models of hepatoprotective activity assessment. *Medicina Universitaria*, 7 (69): 222-228.

Deng, Y., Handoko, A. D., Du, Y., Xi, S., & Yeo, B. S. (2016) In situ Raman spectroscopy of copper and copper oxide surfaces during electrochemical oxygen evolution reaction: identification of CuIII oxides as catalytically active species. *Acs Catalysis*, 6 (4): 2473-2481.

Desalegn, T., Murthy, H., Ravikumar, C., & Nagaswarupa, H. (2021) Green synthesis of CuO nanostructures using *Syzygium guineense* (Willd.) DC plant leaf extract and their applications. *Journal of Nanostructures*, 11 (1): 81-94.

Deshkar, N., Tilloo, S., & Pande, V. (2008) A comprehensive review of *Rubia cordifolia* Linn. *Pharmacognosy Reviews*, 2 (3): 124.

Dev, S. (1997) Ethnotherapeutics and modern drug development: the potential of Ayurveda. *Current Science*, 73 (11): 909-928.

Devasia, J., Muniswamy, B., & Mishra, M. K. (2020) Investigation of ZnO Nanoparticles on *In Vitro* Cultures of Coffee (*Coffea arabica* L.). *International Journal of Nanoscience and Nanotechnology*, 16 (4): 271-277.

Devi Priya, M., & Siril, E. (2014) Traditional and modern use of indian madder (*Rubia cordifolia* L.): an overview. *International Journal of Pharmaceutical Sciences Review and Research*, 25 (1): 154-164.

Diaz-Munoz, G., Miranda, I. L., Sartori, S. K., De Rezende, D. C., & Diaz, M. A. (2018) Anthraquinones: an overview. *Studies in Natural Products Chemistry*, 58: 313-338.

Dijkstra, R. J., Bader, A. N., Hoornweg, G. P., Brinkman, U. A. T., & Gooijer, C. (1999) On-line coupling of column liquid chromatography and Raman spectroscopy using a liquid core waveguide. *Analytical Chemistry*, 71 (20): 4575-4579.

Dikshit, P. K., Kumar, J., Das, A. K., Sadhu, S., Sharma, S., Singh, S., . . . Kim, B. S. (2021) Green synthesis of metallic nanoparticles: Applications and limitations. *Catalysts*,11 (8): 902.

Dimkpa, C. O., Latta, D. E., Mclean, J. E., Britt, D. W., Boyanov, M. I., & Anderson, A. J. (2013) Fate of CuO and ZnO nano-and microparticles in the plant environment. *Environmental Science and Technology*, 47 (9): 4734-4742.

Din, M. I., Nabi, A. G., Rani, A., Aihetasham, A., & Mukhtar, M. (2018) Single step green synthesis of stable nickel and nickel oxide nanoparticles from *Calotropis gigantea*: catalytic and antimicrobial potentials. *Environmental Nanotechnology, Monitoring and Management*, 9: 29-36.

Do E. S. P. A., Caixeta Oliveira, H., Fernandes Fraceto, L., & Santaella, C. (2021) Nanotechnology potential in seed priming for sustainable agriculture. *Nanomaterials*, 11 (2): 267-272.

Do, K. L., Su, M., Mushtaq, A., Ahsan, T., & Zhao, F. (2023) Functionalization of silk with chitosan and *Rubia cordifolia* L. dye extract for enhanced antimicrobial and ultraviolet protective properties. *Textile Research Journal*, 93 (15-16): 3777-3789.

Domokos-Szabolcsy, E., Marton, L., Sztrik, A., Babka, B., Prokisch, J., & Fari, M. (2012) Accumulation of red elemental selenium nanoparticles and their biological effects in *Nicotinia tabacum*. *Plant Growth Regulation*, 68: 525-531.

Doria-Manzur, A., Sharifan, H., & Tejeda-Benitez, L. (2023) Application of zinc oxide nanoparticles to promote remediation of nickel by *Sorghum bicolor*: Metal ecotoxic potency and plant response. *International Journal of Phytoremediation*, 25 (1): 98-105.

Dosseh, C., Tessier, A., & Delaveau, P. (1981) *Rubia cordifolia* roots. II. New quinones. Planta Medica, 43 (2): 141-147.

Duman, F., Ocsoy, I., & Kup, F. O. (2016) Chamomile flower extract-directed CuO nanoparticle formation for its antioxidant and DNA cleavage properties. *Materials Science and Engineering: C*, 60: 333-338.

Duncan, D. B. (1955) Multiple range and multiple F tests. *Biometrics*, 11 (1): 1-42.

Duval, J., Pecher, V., Poujol, M., & Lesellier, E. (2016) Research advances for the extraction, analysis and uses of anthraquinones: A review. *Industrial Crops and Products*, 94: 812-833.

Ebad, F. A., Hussein, E. A., & Aref, M. S. (2019) Effect of treatment with some nanoparticles on morphology, growth and some active secondary metabolites in callus culture of *Balanites aegyptiaca* (L.). *Egyption Journal of Biotechnology*, 58: 107 - 122.

Ebbs, S. D., Bradfield, S. J., Kumar, P., White, J. C., & Ma, X. (2016) Projected dietary intake of zinc, copper, and cerium from consumption of carrot (*Daucus carota*) exposed to metal oxide nanoparticles or metal ions. *Frontiers in Plant Science*, 7: 188-195.

El-Sayed, S. A., Mostafa, M. J. E. C., & Management (2014) Pyrolysis characteristics and kinetic parameters determination of biomass fuel powders by differential thermal gravimetric analysis (TGA/DTG). *Energy conversion and management*, 85: 165-172.

Elsayh, S. A., Arafa, R. N., Ali, G. A., Abdelaal, W., Sidky, R. A., & Ragab, T. I. (2022) Impact of silver nanoparticles on multiplication, rooting of shoots and biochemical analyses of date palm Hayani cv. by *in vitro*. *Biocatalysis and Agricultural Biotechnology*, 43: 102-115.

Eom, T., Kim, E., & Kim, J.-S. (2020) *In vitro* antioxidant, antiinflammation, and anticancer activities and anthraquinone content from *Rumex crispus* root extract and fractions. *Antioxidants*, 9 (8): 726-732.

Ezealisiji, K. M., Siwe-Noundou, X., Maduelosi, B., Nwachukwu, N., & Krause, R. W. M. (2019) Green synthesis of zinc oxide nanoparticles using *Solanum torvum* (L) leaf extract and evaluation of the toxicological profile of the ZnO nanoparticles–hydrogel composite in Wistar albino rats. *International Nano Letters*, 9: 99-107.

Fakhari, S., Jamzad, M., Kabiri Fard, H. J. G. C. L., & Reviews (2019) Green synthesis of zinc oxide nanoparticles: a comparison. *Green Chemistry Letters and Reviews*, 12 (1): 19-24.

Fatima, K., Abbas, S., Zia, M., Sabir, S., Khan, R., Khan, A., . . . Zaman, R. (2020) Induction of secondary metabolites on nanoparticles stress in callus culture of *Artemisia annua* L. *Brazilian Journal of Biology*, 81: 474-483.

Fay, M. F. (1992) Conservation of rare and endangered plants using *in vitro* methods. *In Vitro Cellular and Developmental Biology-Plant*, 28: 1-4.

Fazal, H., Abbasi, B. H., Ahmad, N., & Ali, M. (2016) Elicitation of medicinally important antioxidant secondary metabolites with silver and gold nanoparticles in callus cultures of *Prunella vulgaris* L. *Applied Biochemistry and Biotechnology*, 180: 1076-1092.

Fazal, H., Abbasi, B. H., Ahmad, N., Ali, M., Shujait Ali, S., Khan, A., & Wei, D.-Q. (2019) Sustainable production of biomass and industrially important secondary metabolites in cell cultures of selfheal (*Prunella vulgaris* L.) elicited by silver and gold nanoparticles. *Artificial Cells, Nanomedicine, and Biotechnology*, 47 (1): 2553-2561.

Fernandez-Garcia, M., Martinez-Arias, A., Hanson, J. C., & Rodriguez, J. A. (2004). Nanostructured oxides in chemistry: characterization and properties. *Chemical Reviews*, 104 (9): 4063-4104.

Fialkow, L., Wang, Y., & Downey, G. P. (2007) Reactive oxygen and nitrogen species as signaling molecules regulating neutrophil function. *Free Radical Biology and Medicine*, 42 (2): 153-164.

Florence, A., Sukumaran, S., Joselin, J., Brintha, T., & Jeeva, S. (2015) Phytochemical screening of selected medicinal plants of the family Lythraceae. *Bioscience Discovery*, 6 (2): 73-82.

Francis, D. V., Sood, N., & Gokhale, T. (2022) Biogenic CuO and ZnO nanoparticles as nanofertilizers for sustainable growth of *Amaranthus hybridus*. *Plants*, 11 (20): 2776-2778.

Frazier, E. A., Patil, R. P., Mane, C. B., Sanaei, D., Asiri, F., Seo, S. S., & Sharifan, H. (2023) Environmental exposure and nanotoxicity of titanium dioxide nanoparticles in irrigation water with the flavonoid luteolin. *RSC advances*, 13(21): 14110-14118.

Ganesh, M., Lee, S. G., Jayaprakash, J., Mohankumar, M., & Jang, H. T. (2019) *Hydnocarpus alpina* Wt extract mediated green synthesis of ZnO nanoparticle and screening of its anti-microbial, free radical scavenging, and photocatalytic activity. *Biocatalysis and Agricultural Biotechnology*, 19: 101-129.

Gao, M., Chang, J., Wang, Z., Zhang, H., & Wang, T. (2023) Advances in transport and toxicity of nanoparticles in plants. *Journal of Nanobiotechnology*, 21 (1): 75-82.

Gao, M., Yang, J., Wang, Z., Yang, B., Kuang, H., Liu, L., . . . Yang, C. (2016) Simultaneous determination of purpurin, munjistin and mollugin in rat plasma by ultra-high performance liquid chromatography-tandem mass spectrometry: Application to a pharmacokinetic study after oral administration of *Rubia cordifolia* L. extract. *Molecules*, 21 (6): 717-720.

Gbaguidi, F., Muccioli, G., Accrombessi, G., Moudachirou, M., & Quetin-Leclercq, J. (2005) Densitometric HPTLC quantification of 2-azaanthraquinone isolated from *Mitracarpus scaber* and antimicrobial activity against *Dermatophilus congolensis*. *JPC-Journal of Planar Chromatography-Modern TLC*, 18 (105): 377-379.

George, E. F., & Sherrington, P. D. (1984) *Plant Propagation by Tissue Culture*: Exegetics Ltd. 709.

Ghosh, S., Das Sarma, M., Patra, A., & Hazra, B. (2010) Anti-inflammatory and anticancer compounds isolated from *Ventilago madraspatana* Gaertn., *Rubia cordifolia* Linn. and *Lantana camara* Linn. *Journal of Pharmacy and Pharmacology*, 62 (9): 1158-1166.

Gierlinger, N., & Schwanninger, M. (2007) The potential of Raman microscopy and Raman imaging in plant research. *Spectroscopy*, 21 (2): 69-89.

Giorgetti, L., Castiglione, M. R., Bernabini, M., & Geri, C. (2011) Nanoparticles effects on growth and differentiation in cell culture of carrot (*Daucus carota* L.). *Agrochimica*, 55 (1): 45-53.

Gnanaraj, M., Sivamaruthi, B. S., Mohamed, S. S., Sisubalan, N., Basha, M. H. G., & Chaiyasut, C. (2024) Optimization of conditions to achieve a high content of alizarin and purpurin in the adventitious roots of *Rubia cordifolia* L. *Journal of Applied Biology and Biotechnology*, 10(22): 1-9.

Gonçalves, S., Mansinhos, I., Rodríguez-Solana, R., Pereira-Caro, G., Moreno-Rojas, J. M., & Romano, A. (2021) Impact of metallic nanoparticles on *in vitro* culture, phenolic profile and biological activity of two Mediterranean Lamiaceae species: *Lavandula viridis* L'Hér and *Thymus lotocephalus* G. López and R. Morales. *Molecules*, 26 (21): 6427.

Gong, X. P., Sun, Y.-Y., Chen, W., Guo, X., Guan, J. K., Li, D. Y., & Du, G. (2017) Anti-diarrheal and anti-inflammatory activities of aqueous extract of the aerial part of *Rubia cordifolia*. *BMC Complementary and Alternative Medicine*, 17: 1-9.

Gong, Y. X., Li, S. P., Wang, Y. T., Li, P., & Yang, F. Q. (2005) Simultaneous determination of anthraquinones in Rhubarb by pressurized liquid extraction and capillary zone electrophoresis. *Electrophoresis*,26 (9): 1778-1782.

Gopalakrishnan, N., M, P., Kim, S. H., & Chung, I. M. (2014) Copper oxide nanoparticle toxicity in mung bean (*Vigna radiata* L.) seedlings: physiological and molecular level responses of *in vitro* grown plants. *Acta Physiologiae Plantarum*, 36: 2947-2958.

Grima, E. M., González, M. J. I., & Giménez, A. G. (2013). Solvent extraction for microalgae lipids. *Algae for biofuels and energy*, 187-205.

Grzesik, M., Naparło, K., Bartosz, G., & Sadowska-Bartosz, I. (2018) Antioxidant properties of catechins: Comparison with other antioxidants. *Food Chemistry*, 241: 480-492.

Gunalan, S., Sivaraj, R., & Venckatesh, R. (2012) *Aloe barbadensis* Miller mediated green synthesis of mono-disperse copper oxide nanoparticles: optical properties. *Spectrochimica Acta Part A: Molecular and Biomolecular Spectroscopy*, 97: 1140-1144.

Gunawardana, S., Gunasekara, C., & Sirimuthu, N. (2022) Raman spectroscopy in phytochemical analysis. *Sri Lankan Journal of Applied Sciences*, 1 (1): 01-10.

Gupta, P., Srimal, R., Verma, N., & Tandon, J. (1999) Biological activity of *Rubia cordifolia* and isolation of an active principle. *Pharmaceutical Biology*, 37 (1): 46-49.

Gur, T., Meydan, I., Seckin, H., Bekmezci, M., & Sen, F. (2022) Green synthesis, characterization and bioactivity of biogenic zinc oxide nanoparticles. *Environmental Research*, 204: 111-120.

Gusain, P., Uniyal, D., & Joga, R. (2021). Conservation and sustainable use of medicinal plants. In *Preparation of Phytopharmaceuticals for the Management of Disorders*, Elsevier. 409-427.

Gutiérrez-Grijalva, E. P., Picos-Salas, M. A., Leyva-López, N., Criollo-Mendoza, M. S., Vazquez-Olivo, G., & Heredia, J. B. (2017) Flavonoids and phenolic acids from oregano: Occurrence, biological activity and health benefits. *Plants*, 7 (1): 2-8.

Hameed, S., Khalil, A. T., Ali, M., Numan, M., Khamlich, S., Shinwari, Z. K., & Maaza, M. (2019). Greener synthesis of ZnO and Ag–ZnO nanoparticles using *Silybum marianum* for diverse biomedical applications. *Nanomedicine*, 14 (6): 655-673.

Hamilton, A. C. (2004) Medicinal plants, conservation and livelihoods. *Biodiversity & Conservation*, 13: 1477-1517.

Hasan, S. (2015) A review on nanoparticles: their synthesis and types. *Research Journal of Recent Science*, 2277: 2502-2509.

Hassellöv, M., Readman, J. W., Ranville, J. F., & Tiede, K. (2008) Nanoparticle analysis and characterization methodologies in environmental risk assessment of engineered nanoparticles. *Ecotoxicology*, 17: 344-361.

Hayat, K., Ali, S., Ullah, S., Fu, Y., & Hussain, M. (2021) Green synthesized silver and copper nanoparticles induced changes in biomass parameters, secondary metabolites production, and antioxidant activity in callus cultures of *Artemisia absinthium* L. *Green Processing and Synthesis*, 10 (1): 61-72.

He, S.-S., Liu, C.-Z., & Saxena, P. K. (2007) Plant regeneration of an endangered medicinal plant *Hydrastis canadensis* L. *Scientia Horticulturae*, 113 (1): 82-86.

Helaly, M. N., El-Metwally, M. A., El-Hoseiny, H., Omar, S. A., & El-Sheery, N. I. (2014) Effect of nanoparticles on biological contamination of *'in vitro'* cultures and organogenic regeneration of banana. *Australian Journal of Crop Science*, 8 (4): 612-624.

Hernández-Hernández, H., González-Morales, S., Benavides-Mendoza, A., Ortega-Ortiz, H., Cadenas-Pliego, G., & Juárez-Maldonado, A. (2018) Effects of chitosan–PVA and Cu nanoparticles on the growth and antioxidant capacity of tomato under saline stress. *Molecules*, 23 (1): 178-182.

Hossain, Z., Mustafa, G., & Komatsu, S. (2015) Plant responses to nanoparticle stress. *International Journal of Molecular Sciences*, 16 (11): 26644-26653.

Hou, Y., Sun, Z., Rao, W., & Liu, J. (2018) Nanoparticle-mediated cryosurgery for tumor therapy. *Nanomedicine: Nanotechnology, Biology and Medicine*, 14 (2): 493-506.

Houari, F. Z., Erenler, R., & Hariri, A. (2022) Biological activities and chemical composition of *Rubia tinctorum* (L) root and aerial part extracts thereof. *Acta Biologica Colombiana*, 27 (3): 403-414.

House, N. C., Puthenparampil, D., Malayil, D., & Narayanankutty, A. (2020) Variation in the polyphenol composition, antioxidant, and anticancer activity among different *Amaranthus* species. *South African Journal of Botany*, 135: 408-412.

Huang, H. (2011) Plant diversity and conservation in China: planning a strategic bioresource for a sustainable future. *Botanical Journal of the Linnean Society*, 166 (3): 282-300.

Humbal, A., & Pathak, B. (2023) Harnessing nanoparticle-mediated elicitation in plant tissue culture: a promising approach for secondary metabolite production. *Plant Cell, Tissue and Organ Culture*, 155 (2): 385-402.

Humbare, R. B., Sarkar, J., Kulkarni, A. A., Juwale, M. G., Deshmukh, S. H., Amalnerkar, D., . . . Kamble, S. C. (2022) Phytochemical characterization, antioxidant and anti-proliferative properties of *Rubia cordifolia* L. extracts prepared with improved extraction conditions. *Antioxidants*, 11 (5): 1006-1009.

Hussain, M., Raja, N. I., Mashwani, Z.-U.-R., Iqbal, M., Sabir, S., & Yasmeen, F. (2017) *In vitro* seed germination and biochemical profiling of *Artemisia absinthium* exposed to various metallic nanoparticles. *Journal of Botechnology*, 7: 1-8.

Hussain, M. S., Fareed, S., Ansari, S., Rahman, M. A., Ahmad, I. Z., & Saeed, M. (2012) Current approaches toward production of secondary plant metabolites. *Journal of Pharmacy and Bioallied Sciences*, 4 (1): 10-20.

Ibragic, S., Barbini, S., Oberlerchner, J. T., Potthast, A., Rosenau, T., & Böhmdorfer, S. (2021) Antioxidant properties and qualitative analysis of phenolic constituents in Ephedra spp. by HPTLC together with injection port derivatization GC–MS. *Journal of Chromatography B*, 1180: 122-131.

Ibraheim, Z. Z. (2002) Saponins, naphthohydroquinone and anthraquinone glycosides from *Rubia cordifolia* L. *Bulletin of Pharmaceutical Sciences Assiut University*, 25 (1): 85-94.

Ibrahim, A. M., Munshi, G. H., & Al-Harbi, L. M. (2018) Copper (II) oxide nanocatalyst preparation and characterization: green chemistry route. *Bulletin of the National Research Centre*, 42: 1-4.

Ibrahim, A. S., Ali, G. A., Hassanein, A., Attia, A. M., & Marzouk, E. R. (2022) Toxicity and uptake of CuO nanoparticles: evaluation of an emerging nanofertilizer on wheat (*Triticum aestivum* L.) plant. *Sustainability*, 14 (9): 4914-4934.

Ibrahim, A. S., Fahmy, A. H., & Ahmed, S. S. (2019) Copper nanoparticles elevate regeneration capacity of (*Ocimum basilicum* L.) plant via somatic embryogenesis. *Plant Cell, Tissue and Organ Culture*, 136: 41-50.

Inam, M., Attique, I., Zahra, M., Khan, A. K., Hahim, M., Hano, C., & Anjum, S. (2023) Metal oxide nanoparticles and plant secondary metabolism: unraveling the game-changer nano-elicitors. *Plant Cell, Tissue and Organ Culture,* 155 (2): 327-344.

Iqbal, Z., Javad, S., Naz, S., Shah, A. A., Shah, A. N., Paray, B. A., . . . Abdelsalam, N. R. (2022) Elicitation of the *in vitro* cultures of selected varieties of *Vigna radiata* L. with zinc oxide and copper oxide nanoparticles for enhanced phytochemicals production. *Frontiers in Plant Science*, 13: 908-918.

Isah, T., Umar, S., Mujib, A., Sharma, M. P., Rajasekharan, P., Zafar, N., & Frukh, A. (2018) Secondary metabolism of pharmaceuticals in the plant *in vitro* cultures: strategies, approaches, and limitations to achieving higher yield. *Plant Cell, Tissue and Organ Culture,* 132: 239-265.

Ismail, M., Taha, K., Modwi, A., & Khezami, L. (2018) ZnO nanoparticles: Surface and X-ray profile analysis. *Journal of Ovonic Research*, 14 (5): 381-393.

Itokawa, H., Ibraheim, Z. Z., Qiao, Y.-F., & Takeya, K. (1993) Anthraquinones, naphthohydroquinones and naphthohydroquinone dimers from *Rubia cordifolia* and their cytotoxic activity. *Chemical and Pharmaceutical Bulletin*, 41 (10): 1869-1872.

Itokawa, H., Qiao, Y.-F., & Takeya, K. (1990) New arborane type triterpenoids from *Rubia cordifolia* var. pratensis and *R. oncotricha*. *Chemical and Pharmaceutical Bulletin*, 38 (5): 1435-1437.

Jalill, R., Jawad, M., & Abd, A. N. (2017) Plants extracts as green synthesis of zirconium oxide nanoparticles. *Journal of Genetic and Environmental Resources Conservation*, 5 (1): 6-23.

Jamshidi-Kia, F., Lorigooini, Z., & Amini-Khoei, H. (2017) Medicinal plants: Past history and future perspective. *Journal of Herbmed Pharmacology*, 7 (1): 1-7.

Jamshidi, M., Ghanati, F., Rezaei, A., & Bemani, E. (2016) Change of antioxidant enzymes activity of hazel (*Corylus avellana* L.) cells by AgNPs. *Cytotechnology*, 68: 525-530.

Janaki, A. C., Sailatha, E., & Gunasekaran, S. (2015) Synthesis, characteristics and antimicrobial activity of ZnO nanoparticles. *Spectrochimica Acta Part A: Molecular and Biomolecular Spectroscopy,* 144: 17-22.

Jat, S. K., Bhattacharya, J., & Sharma, M. K. (2020) Nanomaterial based gene delivery: a promising method for plant genome engineering. *Journal of Materials Chemistry B*, 8 (19): 4165-4175.

Javed, R., Mohamed, A., Yücesan, B., Gürel, E., Kausar, R., & Zia, M. (2017) CuO nanoparticles significantly influence *in vitro* culture, steviol glycosides, and antioxidant activities of *Stevia rebaudiana* Bertoni. *Plant Cell, Tissue and Organ Culture,* 131: 611-620.

Javed, R., Yucesan, B., Zia, M., & Gurel, E. (2018) Elicitation of secondary metabolites in callus cultures of *Stevia rebaudiana* Bertoni grown under ZnO and CuO nanoparticles stress. *Sugar Tech*, 20: 194-201.

Javed, R., Yucesan, B., Zia, M., & Gurel, E. (2022). Nanoelicitation: a promising and emerging technology for triggering the sustainable *in vitro* production of secondary metabolites in medicinal plants. *In Plant and Nanoparticles.* Springer. 265-280.

Jayakodi, S., & Shanmugam, V. K. (2020) Green synthesis of CuO nanoparticles and its application on toxicology evaluation. *Biointerface Research in Applied Chemistry,* 10 (5): 6343-6353.

Jeevanandam, J., Chan, Y. S., & Danquah, M. K. (2016) Biosynthesis of metal and metal oxide nanoparticles. *ChemBioEng Reviews*, 3 (2): 55-67.

Jeruto, P., Mutai, C., Lukhoba, C., & Ouma, G. (2011) Phytochemical constituents of some medicinal plants used by the Nandis of South Nandi District, Kenya. *Journal of Animal and Plant Sciences*, 9 (3): 1201-1210.

Jiang, H. S., Yin, L. Y., Ren, N. N., Zhao, S. T., Li, Z., Zhi, Y., . . . Gontero, B. (2017) Silver nanoparticles induced reactive oxygen species via photosynthetic energy transport imbalance in an aquatic plant. *Nanotoxicology*, 11 (2): 157-167.

Joshi, M., Bhattacharyya, A., & Ali, S. W. (2008) Characterization techniques for nanotechnology applications in textiles. *Indian Journal of Fibre and Textile Research*, 33: 304-317.

Jyothi, T., & Hebsur, N. (2017) Effect of nanofertilizers on growth and yield of selected cereals-A review. *Agricultural Reviews*, 38 (2): 112-120.

Kacziba, B., Szierer, Á., Mészáros, E., Rónavári, A., Kónya, Z., & Feigl, G. (2023) Exploration the homeostasis of signaling molecules in monocotyledonous crops with different CuO nanoparticle tolerance. *Plant Stress*, 7: 100-110.

Kannan, M., Singh, A., & Narayanan, M. (2009) Phytochemistry and ethanopharmacological studies on *Rubia cordifolia* Linn. (Rubiaceae). *Ethnobotanical Leaflets*, 2009 (2): 338-342.

Karimi, N., Behbahani, M., Dini, G., & Razmjou, A. (2018) Enhancing the secondary metabolite and anticancer activity of *Echinacea purpurea* callus extracts by treatment with biosynthesized ZnO nanoparticles. *Advances in Natural Sciences: Nanoscience and Nanotechnology*, 9 (4): 45-52.

Kaur, P., Chandel, M., Kumar, S., Kumar, N., Singh, B., & Kaur, S. (2010) Modulatory role of alizarin from *Rubia cordifolia* L. against genotoxicity of mutagens. *Food and Chemical Toxicology*, 48 (1): 320-325.

Kaviani, B. (2011) Conservation of plant genetic resources by cryopreservation. *Australian Journal of Crop Science*, 5 (6): 778-800.

Kazmi, A., Khan, M. A., & Ali, H. (2019) Biotechnological approaches for production of bioactive secondary metabolites in *Nigella sativa*: an up-to-date review. *International Journal of Secondary Metabolite*, 6 (2): 172-195.

Khan, M., Khan, M. S. A., Borah, K. K., Goswami, Y., Hakeem, K. R., & Chakrabartty, I. (2021) The potential exposure and hazards of metal-based nanoparticles on plants and environment, with special emphasis on ZnO NPs, TiO_2 NPs, and AgNPs: a review. *Environmental Advances*, 6: 100-128.

Khan, M. S., Aziz, S., Khan, M. Z., Khalid, Z. M., Riaz, M., Ahmed, D., . . . Ahmad, M. S. (2021) Antihyperglycemic effect and phytochemical investigation of *Rubia cordifolia* (Indian Madder) leaves extract. *Open Chemistry*, 19 (1): 586-599.

Kim, D. H., Gopal, J., & Sivanesan, I. (2017) Nanomaterials in plant tissue culture: the disclosed and undisclosed. *RSC Advances*, 7 (58): 36492-36505.

Koche, D., Shirsat, R., & Kawale, M. (2016) An overerview of major classes of phytochemicals: their types and role in disease prevention. *Hislopia*, 9 (1/2): 1-11.

Kokina, I., Mickeviča, I., Jermaļonoka, M., Bankovska, L., Gerbreders, V., Ogurcovs, A., & Jahundoviča, I. (2017) Case study of somaclonal variation in resistance genes Mlo and Pme3 in flaxseed (*Linum usitatissimum* L.) induced by nanoparticles. *International Journal of Genomics*, 1: 167-172.

Konaté, K., Souza, A., Coulibaly, A., Meda, N., Kiendrebeogo, M., Lamien-Meda, A., . . . Nacoulma, O. (2010) *In vitro* antioxidant, lipoxygenase and xanthine oxidase inhibitory activities of fractions from *Cienfuegosia digitata* Cav., *Sida alba* L. and *Sida acuta* Burn f.(Malvaceae). *Pakistan Journal of Biological Sciences*, 13 (22): 1092-1098.

Kossel, A. (1891) Ueber die chemische Zusammensetzung der Zelle. *Du Bois-Reymond's Archiv/Arch Anat Physiol Physiol Abt*, 278: 181-186.

Kruszka, D., Selvakesavan, R. K., Kachlicki, P., & Franklin, G. (2022) Untargeted metabolomics analysis reveals the elicitation of important secondary metabolites upon treatment with various metal and metal oxide nanoparticles in *Hypericum perforatum* L. cell suspension cultures. *Industrial Crops and Products*, 178: 114-124.

Kulus, D., & Tymoszuk, A. (2021) Gold nanoparticles affect the cryopreservation efficiency of *in vitro*-derived shoot tips of bleeding heart. *Plant Cell, Tissue and Organ Culture*, 146 (2): 297-311.

Kulus, D., Tymoszuk, A., Jedrzejczyk, I., & Winiecki, J. (2022) Gold nanoparticles and electromagnetic irradiation in tissue culture systems of bleeding heart: Biochemical, physiological, and (cyto) genetic effects. *Plant Cell, Tissue and Organ Culture*, 149 (3): 715-734.

Kumar, D., & Seth, C. S. (2021) Green-synthesis, characterization, and applications of nanoparticles (NPs): a mini review. *International Journal of Plant and Environment*, 7 (01): 91-95.

Kumar, V., Sharma, M., Khare, T., & Wani, S. H. (2018). Impact of nanoparticles on oxidative stress and responsive antioxidative defense in plants. In *Nanomaterials in Plants, Algae, and Microorganisms*, Elsevier. 393-406.

Kurian, A., Sreelakshmi, P., Thomas, B., & George, S. (2020) Comparative evaluation of phytoconstituents in Nayopayam Kwatha (An Indian polyherbal formulation) and its component Herbs. *International Journal of Botany Studies*, 5 (5): 110-122.

Lai, S.-C., Ho, Y.-L., Huang, S.-C., Huang, T.-H., Lai, Z.-R., Wu, C.-R., . . . Chang, Y.-S. (2010) Antioxidant and antiproliferative activities of *Desmodium triflorum* (L.) DC. *The American Journal of Chinese Medicine*, 38 (02): 329-342.

Lee, S., Kim, S., Kim, S., & Lee, I. (2013) Assessment of phytotoxicity of ZnO NPs on a medicinal plant, *Fagopyrum esculentum*. *Environmental Science and Pollution Research*, 20: 848-854.

Li, Y., Sun, M., Liu, Y., Liang, J., Wang, T., & Zhang, Z. (2019) Gymnemic acid alleviates type 2 diabetes mellitus and suppresses endoplasmic reticulum stress *in vivo* and *in vitro*. *Journal of Agricultural and Food Chemistry,*67 (13): 3662-3669.

Lim, C.-K., & Lord, G. (2002) Current developments in LC-MS for pharmaceutical analysis. *Biological and Pharmaceutical Bulletin*, 25 (5): 547-557.

Lim, D. J., Song, J.-S., Lee, B.-H., Son, Y. K., & Kim, Y. (2023) Qualitative and quantitative analysis of the major bioactive components of *Juniperus chinensis* L. Using LC-QTOF-MS and LC-MSMS and investigation of antibacterial activity against pathogenic bacteria. *Molecules*, 28 (9): 3937.

Lin, D., & Xing, B. (2008) Root uptake and phytotoxicity of ZnO nanoparticles. *Environmental Science and Technology*, 42 (15): 5580-5585.

Liu, C., Yu, Y., Liu, H., & Xin, H. (2021) Effect of different copper oxide particles on cell division and related genes of soybean roots. *Plant Physiology and Biochemistry*, 163: 205-214.

Liu, D., Guo, Y., Wu, P., Wang, Y., Golly, M. K., & Ma, H. (2020) The necessity of walnut proteolysis based on evaluation after *in vitro* simulated digestion: ACE inhibition and DPPH radical-scavenging activities. *Food Chemistry*, 311: 125-129.

Liu, W., Feng, Y., Yu, S., Fan, Z., Li, X., Li, J., & Yin, H. (2021) The flavonoid biosynthesis network in plants. *International Journal of Molecular Sciences*, 22 (23): 12824-12828.

Liu, W., Zeb, A., Lian, J., Wu, J., Xiong, H., Tang, J., & Zheng, S. (2020) Interactions of metal-based nanoparticles (MBNPs) and metal-oxide nanoparticles (MONPs) with crop plants: a critical review of research progress and prospects. *Environmental Reviews*, 28 (3): 294-310.

Loberant, B., & Altman, A. (2010) Micropropagation of plants. *Encyclopedia of Industrial Biotechnology: Bioprocess, Bioseparation, Cell Technology*. Wiley, New York 3499-3515.

Lok, C.-N., Ho, C.-M., Chen, R., He, Q.-Y., Yu, W.-Y., Sun, H., . . . Che, C.-M. (2006) Proteomic analysis of the mode of antibacterial action of silver nanoparticles. *Journal of Proteome Research*, 5 (4): 916-924.

López-Moreno, M. L., De La Rosa, G., Hernández-Viezcas, J. Á., Castillo-Michel, H., Botez, C. E., Peralta-Videa, J. R., & Gardea-Torresdey, J. L. (2010) Evidence of the differential biotransformation and genotoxicity of ZnO and CeO2 nanoparticles on soybean (*Glycine max*) plants. *Environmental Science and Technology*, 44 (19): 7315-7320.

Loyola-Vargas, V. M., & Ochoa-Alejo, N. (2018) An introduction to plant tissue culture: advances and perspectives. *Plant Cell Culture Protocols*,10: 3-13.

Lv, J., Zhang, S., Luo, L., Zhang, J., Yang, K., & Christie, P. (2015) Accumulation, speciation and uptake pathway of ZnO nanoparticles in maize. *Environmental Science: Nano*, 2 (1): 68-77.

Lv, Z., Jiang, R., Chen, J., & Chen, W. (2020) Nanoparticle-mediated gene transformation strategies for plant genetic engineering. *The Plant Journal*, 104 (4): 880-891.

Ma, C., Chhikara, S., Xing, B., Musante, C., White, J. C., & Dhankher, O. P. (2013) Physiological and molecular response of *Arabidopsis thaliana* (L.) to nanoparticle cerium and indium oxide exposure. *ACS Sustainable Chemistry and Engineering*, 1 (7): 768-778.

Ma, C., White, J. C., Dhankher, O. P., & Xing, B. (2015) Metal-based nanotoxicity and detoxification pathways in higher plants. *Environmental Science and Technology*, 49 (12): 7109-7122.

Mahdi, A., El-Saber, M. M., Osman, A., Hassan, A., & Farroh, K. Y. (2020) Toxicological and significant execute of biocompatible CuO nanoparticles and their influences on biochemical and molecular markers of wheat genotypes under saline conditions. *IOSR Journal of Biotechnology and Biochemistry*, 6 (5): 58-74.

Mahendran, D., Geetha, N., & Venkatachalam, P. (2019) Role of silver nitrate and silver nanoparticles on tissue culture medium and enhanced the plant growth and development. *In Vitro Plant Breeding towards Novel Agronomic Traits: Biotic and Abiotic Stress Tolerance*, 20: 59-74.

Mahendran, D., Thiyagarajan, M., Kishor, P. K., & Venkatachalam, P. (2016) Efficient plant regeneration from shoot tip explants of *Gloriosa superba* L.: An endangered anti-cancer medicinal plant. *Plant Cell Biotechnology and Molecular Biology*, 17 (1-2): 31-38.

Mali, S. C., Raj, S., & Trivedi, R. (2020) Nanotechnology a novel approach to enhance crop productivity. *Biochemistry and Biophysics Reports*, 24: 100821-100828.

Malik, W. A., Mahmood, I., Razzaq, A., Afzal, M., Shah, G. A., Iqbal, A., . . . Ahmad, I. (2021) Exploring potential of copper and silver nano particles to establish efficient callogenesis and regeneration system for wheat (*Triticum aestivum* L.). *GM Crops & Food*, 12 (1): 564-585.

Mandeh, M., Omidi, M., & Rahaie, M. (2012) *In vitro* influences of TiO_2 nanoparticles on barley (*Hordeum vulgare* L.) tissue culture. *Biological Trace Element Research*, 150: 376-380.

Manickavasagam, M., Pavan, G., & Vasudevan, V. (2019) A comprehensive study of the hormetic influence of biosynthesized AgNPs on regenerating rice calli of indica cv. IR64. *Scientific Reports*, 9 (1): 8821-8826.

Manyasree, D., Peddi, K. M., & Ravikumar, R. (2017) CuO nanoparticles: synthesis, characterization and their bactericidal efficacy. *International Journal of Applied Pharmaceutics*, 9 (6): 71-74.

Marimuthu, S., Rahuman, A. A., Jayaseelan, C., Kirthi, A. V., Santhoshkumar, T., Velayutham, K., . . . Iyappan, M. (2013) Acaricidal activity of synthesized titanium dioxide nanoparticles using *Calotropis gigantea* against *Rhipicephalus microplus* and *Haemaphysalis bispinosa*. *Asian Pacific Journal of Tropical Medicine*, 6 (9): 682-688.

Marslin, G., Sheeba, C. J., & Franklin, G. (2017) Nanoparticles alter secondary metabolism in plants via ROS burst. *Frontiers in Plant Science*, 8: 832-836.

Marslin, G., Siram, K., Maqbool, Q., Selvakesavan, R. K., Kruszka, D., Kachlicki, P., & Franklin, G. (2018) Secondary metabolites in the green synthesis of metallic nanoparticles. *Materials*, 11 (6): 940-948.

Marston, A. (2007) Role of advances in chromatographic techniques in phytochemistry. *Phytochemistry*, 68 (22-24): 2786-2798.

Matsuura, H. N., & Fett-Neto, A. G. (2015) Plant alkaloids: main features, toxicity, and mechanisms of action. *Plant Toxins*,2 (7): 1-15.

Maurer-Jones, M. A., Gunsolus, I. L., Murphy, C. J., & Haynes, C. L. (2013) Toxicity of engineered nanoparticles in the environment. *Analytical Chemistry*, 85 (6): 3036-3049.

Meena, A., Pal, B., Panda, P., Sannd, R., & Rao, M. (2010) A review on *Rubia cordifolia*: its phyto constituents and therapeutic uses. *Drug Invention Today*, 2 (5): 244-246.

Mélinon, P., Begin-Colin, S., Duvail, J. L., Gauffre, F., Boime, N. H., Ledoux, G., . . . Warot-Fonrose, B. (2014) Engineered inorganic core/shell nanoparticles. *Physics Reports*, 543 (3): 163-197.

Mink, J., Kristof, J., De Battisti, A., Daolio, S., & Németh, C. (1995) Investigation on the formation of RuO2-based mixed oxide coatings by spectroscopic methods. *Surface Science*, 335: 252-257.

Mir, A. R., Pichtel, J., & Hayat, S. (2021) Copper: uptake, toxicity and tolerance in plants and management of Cu-contaminated soil. *BioMetals*, 34 (4): 737-759.

Miri, A., & Sarani, M. (2018) Biosynthesis, characterization and cytotoxic activity of CeO_2 nanoparticles. *Ceramics International*, 44 (11): 12642-12647.

Mischenko, N., Fedoreyev, S., Glazunov, V., Chernoded, G., Bulgakov, V., & Zhuravlev, Y. (1999) Anthraquinone production by callus cultures of *Rubia cordifolia*. *Fitoterapia*, 70 (6): 552-557.

Mittal, A. K., Bhaumik, J., Kumar, S., & Banerjee, U. C. (2014) Biosynthesis of silver nanoparticles: elucidation of prospective mechanism and therapeutic potential. *Journal of Colloid and Interface Science*, 415: 39-47.

Mittler, R. (2017) ROS are good. *Trends in Plant Science*, 22 (1): 11-19.

Mohamad, N. A. N., Arham, N. A., Jai, J., & Hadi, A. (2014) Plant extract as reducing agent in synthesis of metallic nanoparticles: A review. *Advanced Materials Research*, 832: 350-355.

Mohammadinejad, R., Shavandi, A., Raie, D. S., Sangeetha, J., Soleimani, M., Hajibehzad, S. S., . . . Arzani, A. (2019) Plant molecular farming: production of metallic nanoparticles and therapeutic proteins using green factories. *Green Chemistry*, 21 (8): 1845-1865.

Momin, N., Disouza, J., Tatke, P., & Gonsalves, M. (2011) Marker based standardization of novel herbal dental gel. *Research Journal of Topical and Cosmetic Sciences*, 2 (1): 25-29.

Morozov, I. G., Belousova, O. V., Ortega, D., Mafina, M. K., & Kuznetcov, M. V. (2015). Structural, optical, XPS and magnetic properties of Zn particles capped by ZnO nanoparticles. *Journal of Alloys and Compounds*, 633: 237-245.

Mosa, K. A., El-Naggar, M., & Hani, H. (2018) Copper nanoparticles induced genotoxicty, oxidative stress, and changes in superoxide dismutase (SOD) gene expression in cucumber (*Cucumis sativus*) plants. *Frontiers in Plant Science*, 9: 365-375.

Mozafari, A. A., Ghadakchi Asl, A., & Ghaderi, N. (2018b) Grape response to salinity stress and role of iron nanoparticle and potassium silicate to mitigate salt induced damage under *in vitro* conditions. *Physiology and Molecular Biology of Plants*, 24: 25-35.

Mozafari, A. A., Havas, F., & Ghaderi, N. (2018a) Application of iron nanoparticles and salicylic acid in in vitro culture of strawberries (Fragaria× ananassa Duch.) to cope with drought stress. *Plant Cell, Tissue and Organ Culture*, 132: 511-523.

Mughal, B., Zaidi, S. Z. J., Zhang, X., & Hassan, S. U. (2021) Biogenic nanoparticles: Synthesis, characterisation and applications. *Applied Sciences*, 11 (6): 2598.

Muhammad, W., Ullah, N., Haroon, M., & Abbasi, B. H. (2019) Optical, morphological and biological analysis of zinc oxide nanoparticles (ZnO NPs) using *Papaver somniferum* L. *Rsc Advances*, 9 (51): 29541-29548.

Mukherjee, A., Sun, Y., Morelius, E., Tamez, C., Bandyopadhyay, S., Niu, G., ... & Gardea-Torresdey, J. L. (2016) Differential toxicity of bare and hybrid ZnO nanoparticles in green pea (*Pisum sativum* L.): a life cycle study. *Frontiers in plant science*, 6: 1242.

Murashige, T., & Skoog, F. (1962) A revised medium for rapid growth and bio assays with tobacco tissue cultures. *Physiologia Plantarum*, 15 (3): 473-497.

Murch, S., Krishnaraj, S., & Saxena, P. (2000) Tryptophan is a precursor for melatonin and serotonin biosynthesis in *in vitro* regenerated St. John's wort (*Hypericum perforatum* L. cv. Anthos) plants. *Plant Cell Reports*, 19: 698-704.

Murthy, H. N., Joseph, K. S., Paek, K. Y., & Park, S. Y. (2022) Anthraquinone production from cell and organ cultures of Rubia species: An overview. *Metabolites*, 13 (1): 39-42.

Murthy, H. N., Lee, E.-J., & Paek, K.-Y. (2014) Production of secondary metabolites from cell and organ cultures: strategies and approaches for biomass improvement and metabolite accumulation. *Plant Cell, Tissue and Organ Culture*, 118: 1-16.

Muthukrishnan, S., Bhakya, S., Kumar, T. S., & Rao, M. (2015) Biosynthesis, characterization and antibacterial effect of plant-mediated silver nanoparticles using *Ceropegia thwaitesii*–An endemic species. *Industrial Crops and Products*, 63: 119-124.

Nagore, P., Ghotekar, S., Mane, K., Ghoti, A., Bilal, M., & Roy, A. (2021) Structural properties and antimicrobial activities of *Polyalthia longifolia* leaf extract-mediated CuO nanoparticles. *BioNanoScience*, 11: 579-589.

Narasaiah, P., Mandal, B. K., & Sarada, N. (2017). Biosynthesis of copper oxide nanoparticles from *Drypetes sepiaria* leaf extract and their catalytic activity to dye degradation. In *IOP conference series: materials science and engineering*. IOP Publishing. 263 (2): 022012.

Narayani, M., & Srivastava, S. (2017) Elicitation: a stimulation of stress in *in vitro* plant cell/tissue cultures for enhancement of secondary metabolite production. *Phytochemistry Reviews*, 16: 1227-1252.

Nartop, P., Çetin, B. N., & Zaidan, G. (2023) Dose-dependent effects of bio-AgNPs on *Rubia tinctorum* callus and root biomass. *Iranian Journal of Science*, 47 (2): 337-345.

Natarajan, S., Mishra, P., Vadivel, M., Basha, M. G., Kumar, A., & Velusamy, S. (2019) ISSR characterization and quantification of purpurin and alizarin in *Rubia cordifolia* L. populations from India. *Biochemical Genetics*, 57: 56-72.

Nazir, S., Jan, H., Zaman, G., Khan, T., Ashraf, H., Meer, B., . . . Abbasi, B. H. (2021) Copper oxide (CuO) and manganese oxide (MnO) nanoparticles induced biomass accumulation, antioxidants biosynthesis and abiotic elicitation of bioactive compounds in callus cultures of *Ocimum basilicum* (Thai basil). *Artificial Cells, Nanomedicine, and Biotechnology*, 49 (1): 625-633.

Nekoukhou, M., Fallah, S., Pokhrel, L. R., Abbasi-Surki, A., & Rostamnejadi, A. (2023) Foliar enrichment of copper oxide nanoparticles promotes biomass, photosynthetic pigments, and commercially valuable secondary metabolites and essential oils in dragonhead (*Dracocephalum moldavica* L.) under semi-arid conditions. *Science of the Total Environment*, 863: 160-170.

Nezamzadeh-Ejhieh, A., & Amiri, M. (2013) CuO supported Clinoptilolite towards solar photocatalytic degradation of p-aminophenol. *Powder Technology*, 235: 279-288.

Niazian, M. (2019) Application of genetics and biotechnology for improving medicinal plants. *Planta*, 249: 953-973.

Niedz, R. P., Evens, T. J. & Biology-Plant, D. (2007) Regulating plant tissue growth by mineral nutrition. *In Vitro Cellular and Developmental Biology-Plant*, 43: 370-381.

Nyeem, M. B., & Mannan, M. A. (2018) *Rubia cordifolia* phytochemical and Pharmacological evaluation of indigenous medicinal plant: A review. *International Journal of Physiology, Nutrition and Physical Education*, 3 (1): 766-771.

Oseni, O. M., Pande, V., & Nailwal, T. K. (2018) A review on plant tissue culture, a technique for propagation and conservation of endangered plant species. *International Journal of Current Microbiology and Applied Science*, 7 (7): 3778-3786.

Oukarroum, A., Barhoumi, L., Pirastru, L., & Dewez, D. (2013) Silver nanoparticle toxicity effect on growth and cellular viability of the aquatic plant *Lemna gibba*. *Environmental Toxicology and Chemistry*, 32 (4): 902-907.

Ovais, M., Khalil, A. T., Ayaz, M., & Ahmad, I. (2020) Metal oxide nanoparticles and plants. In *Phytonanotechnology.* Elsevier, 123-141.

Ozyigit, I. I., Dogan, I., Hocaoglu-Ozyigit, A., Yalcin, B., Erdogan, A., Yalcin, I. E., . . . Kaya, Y. (2023) Production of secondary metabolites using tissue culture-based biotechnological applications. *Frontiers in Plant Science*, 14: 1132555.

Paduch, R., Kandefer-Szerszeń, M., Trytek, M., & Fiedurek, J. (2007) Terpenes: substances useful in human healthcare. *Archivum Immunologiae et Therapiae Experimentalis*, 55: 315-327.

Pagare, S., Bhatia, M., Tripathi, N., Pagare, S., & Bansal, Y. (2015) Secondary metabolites of plants and their role: Overview. *Current Trends in Biotechnology and Pharmacy*, 9 (3): 293-304.

Pal, D. C., & Jain, S. K. (1998) *Tribal medicine*, Elsevier Publishers. (Vol. 18) pp. 317-320.

Parab, N., & Tomar, V. (2012) Raman spectroscopy of algae: a review. *Journal of Nanomedicine and Nanotechnology*, 3: 24-28.

Pargai, D., Jahan, S., & Gahlot, M. (2020) Functional properties of natural dyed textiles. *Chemistry and Technology of Natural and Synthetic Dyes and Pigments*, 12: 1-19.

Patil, A. R., Ghagare, P. M., Deshmane, B. J., & Kondawar, M. S. (2020) Review on chromatography principal types and it's application. *Research Journal of Pharmaceutical Dosage Forms and Technology*, 12 (1): 27-32.

Patil, R., Mohan, M., Kasture, V., & Kasture, S. (2009) *Rubia cordifolia*: a review. *Advances in Traditional Medicine*, 9 (1): 1-13.

Patra, J. K., Kwon, Y., & Baek, K. H. (2016). Green biosynthesis of gold nanoparticles by onion peel extract: Synthesis, characterization and biological activities. *Advanced Powder Technology*, 27(5): 2204-2213.

Pelegrino, M. T., Kohatsu, M. Y., Seabra, A. B., Monteiro, L. R., Gomes, D. G., Oliveira, H. C., . . . Lange, C. N. (2020) Effects of copper oxide nanoparticles on growth of lettuce (*Lactuca sativa* L.) seedlings and possible implications of nitric oxide in their antioxidative defense. *Environmental Monitoring and Assessment*, 192: 1-14.

Peng, C., Duan, D., Xu, C., Chen, Y., Sun, L., Zhang, H., . . . Yang, J. (2015) Translocation and biotransformation of CuO nanoparticles in rice (*Oryza sativa* L.) plants. *Environmental Pollution*, 197: 99-107.

Prachi, A. M., Patel, R., Singh, N., Negi, D. S., & Rawat, S. (2017) Green synthesis of zinc oxide nanoparticles using *Rubia cordifolia* root extract against different bacterial pathogens. *Indo American journal of Pharmaceutical Research*, 7 (09): 759-765.

Prakash, S., Elavarasan, N., Venkatesan, A., Subashini, K., Sowndharya, M., & Sujatha, V. (2018) Green synthesis of copper oxide nanoparticles and its effective applications in Biginelli reaction, BTB photodegradation and antibacterial activity. *Advanced Powder Technology*, 29 (12): 3315-3326.

Prasad, A. R., Garvasis, J., Oruvil, S. K., & Joseph, A. (2019) Bio-inspired green synthesis of zinc oxide nanoparticles using *Abelmoschus esculentus* mucilage and selective degradation of cationic dye pollutants. *Journal of Physics and Chemistry of Solids*, 127: 265-274.

Prasad, A., Sidhic, J., Sarbadhikary, P., Narayanankutty, A., George, S., George, B. P., & Abrahamse, H. (2024). Role of metal nanoparticles in organogenesis, secondary metabolite production and genetic transformation of plants under *in vitro* condition: a comprehensive review. *Plant Cell, Tissue and Organ Culture*, 158(2): 33.

Pratyusha, S. (2022) Phenolic compounds in the plant development and defense: An overview. *Plant Stress Physiology-Perspectives in Agriculture*, 125-140.

Pullagurala, V. L. R., Adisa, I. O., Rawat, S., Kalagara, S., Hernandez-Viezcas, J. A., Peralta-Videa, J. R., & Gardea-Torresdey, J. L. (2018) ZnO nanoparticles increase photosynthetic pigments and decrease lipid peroxidation in soil grown cilantro (*Coriandrum sativum*). *Plant Physiology and Biochemistry*, 132: 120-127.

Punjabi, K., Choudhary, P., Samant, L., Mukherjee, S., Vaidya, S., & Chowdhary, A. (2015) Biosynthesis of nanoparticles: a review. *International Journal of Pharmaceutical Sciences Review and Research*, 30 (1): 219-226.

Qu, J., Luo, C., & Cong, Q. (2011) Synthesis of multi-walled carbon nanotubes/ZnO nanocomposites using absorbent cotton. *Nano-Micro Letters*, 3: 115-120.

Radha, R., Shereena, S., Divya, K., Krishnan, P., & Seeni, S. (2011) *In vitro* propagation of *Rubia cordifolia* Linn., a medicinal plant of the Western Ghats. *International Journal of Botany*, 7 (1): 90-96.

Radini, I. A., Hasan, N., Malik, M. A., & Khan, Z. (2018). Biosynthesis of iron nanoparticles using *Trigonella foenum-graecum* seed extract for photocatalytic methyl orange dye degradation and antibacterial applications. *Journal of Photochemistry and Photobiology B: Biology*, 183: 154-163.

Radman, R., Saez, T., Bucke, C., & Keshavarz, T. (2003) Elicitation of plants and microbial cell systems. *Biotechnology and Applied Biochemistry*, 37 (1): 91-102.

Raei, M., Angaji, S. A., Omidi, M., & Khodayari, M. (2014) Effect of abiotic elicitors on tissue culture of *Aloe vera*. *International Journal of Biosciences*, 5 (1): 74-81.

Rafieia-Kopaei, M. (2011) Medicinal plants and the human needs. *Journal of Biology*, 35: 635-639.

Rahimmalek, M., Szumny, A., Gharibi, S., Pachura, N., Miroliaei, M., & Łyczko, J. (2023) Chemical Investigations in *Kelussia odoratissima* Mozaff. Leaves Based on Comprehensive Analytical Methods: LC-MS, SPME, and GC-MS Analyses. *Molecules*, 28 (16): 6140.

Rahman, M. U. (2021). Sources of nanomaterials. In *Nanomaterials: Synthesis, Characterization, Hazards and Safety*, Elsevier. 15-29.

Raj, S., Mali, S. C., & Trivedi, R. (2018) Green synthesis and characterization of silver nanoparticles using *Enicostemma axillare* (Lam.) leaf extract. *Biochemical and Biophysical Research Communications*, 503 (4): 2814-2819.

Rajaee Behbahani, S., Iranbakhsh, A., Ebadi, M., Majd, A., & Ardebili, Z. O. (2020) Red elemental selenium nanoparticles mediated substantial variations in growth, tissue differentiation, metabolism, gene transcription, epigenetic cytosine DNA methylation, and callogenesis in bittermelon (*Momordica charantia*); an *in vitro* experiment. *PLoS One*, 15 (7): 235-356.

Rajani, M., & Kanaki, N. S. (2008). Phytochemical standardization of herbal drugs and polyherbal formulations. In *Bioactive molecules and medicinal plants*, Springer. 349-369.

Rajopadhye, A., Upadhye, A., & Mujumdar, A. (2011) HPTLC method for analysis of piperine in fruits of Piper species. *JPC-Journal of Planar Chromatography-Modern TLC*, 24 (1): 57-59.

Raks, V., Al-Suod, H., & Buszewski, B. (2018) Isolation, separation, and preconcentration of biologically active compounds from plant matrices by extraction techniques. *Chromatographia*,81 (2): 189-202.

Ramraje, G. R., Patil, S. D., Patil, P., & Pawar, A. R. (2020) A brief review on: Separation techniques chromatography. *Asian Journal of Pharmaceutical Analysis*, 10 (4): 231-238.

Rani, S. J., Nagarauk, R., & Anuradha, P. (2010) Antibacterial properties of extracts of Indian medicinal plants: *Syzygium alternifolium*, *Phyllanthus niruri* and *Rubia cordifolia*. *Biomedical and Pharmacology Journal*, 3 (1): 123-131.

Rao, G. M. M., Rao, C. V., Pushpangadan, P., & Shirwaikar, A. (2006) Hepatoprotective effects of rubiadin, a major constituent of *Rubia cordifolia* Linn. *Journal of Ethnopharmacology*, 103 (3): 484-490.

Rao, S. R., & Ravishankar, G. (2002) Plant cell cultures: chemical factories of secondary metabolites. *Biotechnology Advances*, 20 (2): 101-153.

Rawal, A. K., Muddeshwar, M. G., & Biswas, S. K. (2004) *Rubia cordifolia*, *Fagonia cretica* linn and *Tinospora cordifolia* exert neuroprotection by modulating the antioxidant system in rat hippocampal slices subjected to oxygen glucose deprivation. *BMC Complementary and Alternative Medicine*, 4 (1): 1-9.

Razdan, M. K. (2002) *An Introduction to Plant Tissue Culture*, Oxford and IBH publishing.

Revathi, J., Manokari, M., & Shekhawat, M. S. (2018) Optimization of factors affecting *in vitro* regeneration, flowering, *ex vitro* rooting and foliar micromorphological studies of *Oldenlandia corymbosa* L.: a multipotent herb. *Plant Cell, Tissue and Organ Culture*, 134 (1): 1-13.

Rico, C. M., Lee, S. C., Rubenecia, R., Mukherjee, A., Hong, J., Peralta-Videa, J. R., & Gardea-Torresdey, J. L. (2014) Cerium oxide nanoparticles impact yield and modify nutritional parameters in wheat (*Triticum aestivum* L.). *Journal of Agricultural and Food Chemistry*, 62 (40): 9669-9675.

Rivero-Montejo, S. D. J., Vargas-Hernandez, M., & Torres-Pacheco, I. (2021) Nanoparticles as novel elicitors to improve bioactive compounds in plants. *Agriculture*, 11 (2): 134-138.

Rizwan, M., Ali, S., Ali, B., Adrees, M., Arshad, M., Hussain, A., . . . Waris, A. A. (2019) Zinc and iron oxide nanoparticles improved the plant growth and reduced the oxidative stress and cadmium concentration in wheat. *Chemosphere*, 214: 269-277.

Roba, K. (2020) The role of terpene (secondary metabolite). *Natural Products Chemistry and Research*, 411: 18-24.

Rushdan, N. a. N. A., Ab Ghani, N., & Rasol, N. E. (2023) Review on anthraquinones isolated from rubiaceae family. *Journal of Science and Mathematics Letters*, 11: 163-174.

Saeed, F., Younas, M., Fazal, H., Mushtaq, S., Rahman, F. U., Shah, M., . . . Hano, C. (2021) Green and chemically synthesized zinc oxide nanoparticles: Effects on *in-vitro* seedlings and callus cultures of *Silybum marianum* and evaluation of their antimicrobial and anticancer potential. *Artificial Cells, Nanomedicine, and Biotechnology*, 49 (1): 450-460.

Safavi, K., Esfahanizadeh, M., Mortazaeinezahad, D. H., & Dastjerd, H. (2011a). The study of nano silver (NS) antimicrobial activity and evaluation of using NS in tissue culture media. In*International conference on life science and technology IPCBEE*, 3(1): 159-161.

Safavi, K., Mortazaeinezahad, F., Esfahanizadeh, M., & Asgari, M. J. (2011b) *In vitro* antibacterial activity of nanomaterial for using in tobacco plants tissue culture. *World Academy of Science, Engineering and Technology*, 55: 372-373.

Saha, S., Mori, H., & Hattori, K. (2007) Synergistic effect of kinetin and benzyl adenine plays a vital role in high frequency regeneration from cotyledon explants of bottle gourd (*Lagenaria siceraria*) in relation to ethylene production. *Breeding Science*, 57 (3): 197-202.

Salam, A., Khan, A. R., Liu, L., Yang, S., Azhar, W., Ulhassan, Z., . . . Gan, Y. (2022) Seed priming with zinc oxide nanoparticles downplayed ultrastructural damage and improved photosynthetic apparatus in maize under cobalt stress. *Journal of Hazardous Materials*, 423: 127-131.

Saletnik, A., Saletnik, B., & Puchalski, C. (2021) Overview of popular techniques of Raman spectroscopy and their potential in the study of plant tissues. *Molecules*, 26 (6): 1537.

Salih, A. M., Al-Qurainy, F., Khan, S., Tarroum, M., Nadeem, M., Shaikhaldein, H. O., . . . Alfarraj, N. S. (2021) Biosynthesis of zinc oxide nanoparticles using *Phoenix dactylifera* and their effect on biomass and phytochemical compounds in *Juniperus procera*. *Scientific Reports,*11 (1): 19136.

Sang, X., & Lebeau, J. M. (2014) Revolving scanning transmission electron microscopy: Correcting sample drift distortion without prior knowledge. *Ultramicroscopy,*138: 28-35.

Sagadevan, S., Vennila, S., Marlinda, A. R., Al-Douri, Y., Rafie Johan, M., & Anita Lett, J. (2019). Synthesis and evaluation of the structural, optical, and antibacterial properties of copper oxide nanoparticles. *Applied Physics A*, 125: 1-9.

Sangeetha, P., Venkatachalam, P. (2014) Induction of direct shoot organogenesis and *in vitro* flowering from shoot tip explants of cucumber (*Cucumis sativus* L. cv.'Green long'). *In Vitro Cellular and Developmental Biology-Plant*, 50: 242-248.

Sanzari, I., Leone, A., & Ambrosone, A. (2019) Nanotechnology in plant science: to make a long story short. *Frontiers in Bioengineering and Biotechnology*, 7: 120-129.

Sarina, S., Waclawik, E. R., & Zhu, H. (2013) Photocatalysis on supported gold and silver nanoparticles under ultraviolet and visible light irradiation. *Green Chemistry*, 15 (7): 1814-1833.

Sarma, H., & Sarma, K. (2015). Structural characterization of cadmium oxide nanoparticles by means of X-ray line profile analysis. *Journal of Basic and Applied Engineering Research,* 2(20): 1773-1780.

Sarmast, M., Niazi, A., Salehi, H., & Abolimoghadam, A. (2015) Silver nanoparticles affect ACS expression in *Tecomella undulatain vitro* culture. *Plant Cell, Tissue and Organ Culture*, 121: 227-236.

Sarmast, M. K., & Salehi, H. (2016) Silver nanoparticles: an influential element in plant nanobiotechnology. *Molecular Biotechnology*, 58: 441-449.

Sasidharan, S., Chen, Y., Saravanan, D., Sundram, K., & Latha, L. Y. (2011) Extraction, isolation and characterization of bioactive compounds from plants' extracts. *African Journal of Traditional, Complementary and Alternative Medicines,* 8 (1): 1-10.

Schmidt-Przewoźna, K., & Kicińska-Jakubowska, A. (2023) *Rubia cordifolia* roots as a raw material for dyeing wool in red colors. *Herba Polonica*, 69 (4): 54-60.

Schulz, H., Baranska, M., Quilitzsch, R., & Schütze, W. (2004) Determination of alkaloids in capsules, milk and ethanolic extracts of poppy (*Papaver somniferum* L.) by ATR-FT-IR and FT-Raman spectroscopy. *Analyst*, 129 (10): 917-920.

Seeger, E. M., Baun, A., Kästner, M., & Trapp, S. (2009) Insignificant acute toxicity of TiO_2 nanoparticles to willow trees. *Journal of Soils and Sediments*, 9: 46-53.

Sengul, A. B., & Asmatulu, E. (2020) Toxicity of metal and metal oxide nanoparticles: a review. *Environmental Chemistry Letters*, 18 (5): 1659-1683.

Sewelam, N., Kazan, K., & Schenk, P. M. (2016) Global plant stress signaling: reactive oxygen species at the cross-road. *Frontiers in Plant Science*, 7: 187-196.

Shadi, I. T., Chowdhry, B. Z., Snowden, M. J., & Withnall, R. (2004) Semi-quantitative analysis of alizarin and purpurin by surface-enhanced resonance Raman spectroscopy (SERRS) using silver colloids. *Journal of Raman Spectroscopy,* 35 (9): 800-807.

Shafey, A. M. E. (2020) Green synthesis of metal and metal oxide nanoparticles from plant leaf extracts and their applications: A review. *Green Processing and Synthesis*, 9 (1): 304-339.

Shahab, M., Ayub, G., Rahman, A., Rashid, A., Jamal, A., & Ali, J. (2013) Assessment of IBA (Indole Butyric Acid) levels and planting time for rooting and growth of Alstonia Cuttings. *Assessment*, 3 (14): 59-67.

Shahin, H. (2018) Enhanced production of secondary metabolites by methyl jasmonate and silver nanoparticles elicitation in tissue culture of *Catharanthus roseus* (Apocynaceae). *Al-Azhar Journal of Pharmaceutical Sciences*, 57 (1): 62-69.

Shahzad, A., Sharma, S., Parveen, S., Saeed, T., Shaheen, A., Akhtar, R., . . . Ahmad, Z. (2017) Historical perspective and basic principles of plant tissue culture. *Plant Biotechnology: Principles and Applications*, 15: 1-36.

Shaikh, J. R., & Patil, M. (2020) Qualitative tests for preliminary phytochemical screening: An overview. *International Journal of Chemical Studies*, 8 (2): 603-608.

Shalini, K., & Ilango, K. (2022) Macroscopical and microscopical analysis of selected Indian medicinal plants and HPTLC method for quantification of chemical markers in a polyherbal formulation. *Journal of Pharmacy and Pharmacognosy Research*, 10 (2): 253-269.

Shankar, S., & Rhim, J.-W. (2014) Effect of copper salts and reducing agents on characteristics and antimicrobial activity of copper nanoparticles. *Materials Letters*, 132: 307-311.

Shankar, S. S., Ahmad, A., & Sastry, M. (2003) Geranium leaf assisted biosynthesis of silver nanoparticles. *Biotechnology Progress*, 19 (6): 1627-1631.

Shanmugam, C., Gunasekaran, D., Duraisamy, N., Nagappan, R., & Krishnan, K. (2015) Bioactive bile salt-capped silver nanoparticles activity against destructive plant pathogenic fungi through *in vitro* system. *RSC Advances*, 5 (87): 71174-71182.

Sharma, J. K., Akhtar, M. S., Ameen, S., Srivastava, P., & Singh, G. (2015) Green synthesis of CuO nanoparticles with leaf extract of *Calotropis gigantea* and its dye-sensitized solar cells applications. *Journal of Alloys and Compounds*, 632: 321-325.

Sharma, P., Pant, S., Dave, V., Tak, K., Sadhu, V., & Reddy, K. R. (2019) Green synthesis and characterization of copper nanoparticles by *Tinospora cardifolia* to produce nature-friendly copper nano-coated fabric and their antimicrobial evaluation. *Journal of Microbiological Methods*, 160: 107-116.

Sharma, R., Bhat, Z. F., Kumar, A., Kumar, S., Bhatti, M. A., & Jayawardena, R. (2021) *Rubia cordifolia* based novel edible film for improved lipid oxidative and microbial stability of meat products. *Journal of Food Processing and Preservation*, 45 (7): e15654-e15660.

Shen, C.-H., Liu, C. T., Song, X. J., Zeng, W. Y., Lu, X. Y., Zheng, Z. L., & Zhan, R. T. (2018) Evaluation of analgesic and anti-inflammatory activities of *Rubia cordifolia* L. by spectrum-effect relationships. *Journal of Chromatography B*, 1090: 73-80.

Shen, N., Wang, T., Gan, Q., Liu, S., Wang, L., & Jin, B. (2022) Plant flavonoids: Classification, distribution, biosynthesis, and antioxidant activity. *Food chemistry*, 383: 132-138.

Sherma, J., & Fried, B. (2003) *Handbook of thin-layer chromatography*, CRC press. 89: 112-129.

Shi, L. B., Tang, P. F., Zhang, W., Zhao, Y. P., Zhang, L. C., & Zhang, H. (2017) Green synthesis of CuO nanoparticles using *Cassia auriculata* leaf extract and *in vitro* evaluation of their biocompatibility with rheumatoid arthritis macrophages (RAW 264.7). *Tropical Journal of Pharmaceutical Research*, 16 (1): 185-192.

Shikov, A. N., Mikhailovskaya, I. Y., Narkevich, I. A., Flisyuk, E. V., & Pozharitskaya, O. N. (2022). Methods of extraction of medicinal plants. In *Evidence-Based Validation of Herbal Medicine*. Elsevier. pp. 771-796.

Shilpa, K., Varun, K., & Lakshmi, B. (2010) An alternate method of natural drug production: eliciting secondary metabolite production using plant cell culture. *Journal of Plant Science*, 5 (3): 222-247.

Shimomura, K., Yoshimatsu, K., Jaziri, M., & Ishimaru, K. (1997) Traditional medicinal plant genetic resources and biotechnology applications. *Plant Biotechnology Plant Genetic Resources for Sustainability Productivity*. Austin, TX: RG Landes Company Academic Press Inc. 209-225.

Shin, S.-H. (1989) Studies on the production of anthraquinone derivatives by tissue culture of Rubia species. *Archives of Pharmacal Research*, 12: 99-102.

Siddique, A., Gaur, A., Bajpai, A., & John, A. (2022) Evaluation of hepatoprotective potential of *Rubia cordifolia* in experimentally (carbon tetrachloride) induced hepatotoxicity in albino rats. *International Journal of Health Sciences*, (IV): 804-814.

Siddiqui, Z. A., Khan, M. R., Abd_Allah, E. F., & Parveen, A. (2019) Titanium dioxide and zinc oxide nanoparticles affect some bacterial diseases, and growth and physiological changes of beetroot. *International Journal of Vegetable Science*, 25 (5): 409-430.

Sidhic, J., George, S., Alfarhan, A., Rajagopal, R., Olatunji, O. J., & Narayanankutty, A. (2023) Phytochemical Composition and Antioxidant and Anti-Inflammatory Activities of *Humboldtia sanjappae* Sasidh. & Sujanapal, an Endemic Medicinal Plant to the Western Ghats. *Molecules*, 28 (19): 6875.

Singh, A., Singh, N., Hussain, I., Singh, H., Yadav, V., & Singh, S. (2016) Green synthesis of nano zinc oxide and evaluation of its impact on germination and metabolic activity of *Solanum lycopersicum*. *Journal of Biotechnology*, 233: 84-94.

Singh, A., Singh, N. Á., Afzal, S., Singh, T., & Hussain, I. (2018) Zinc oxide nanoparticles: a review of their biological synthesis, antimicrobial activity, uptake, translocation and biotransformation in plants. *Journal of Materials Science*, 53 (1): 185-201.

Singh, O. S., Pant, N. C., Laishram, L., Tewari, M., Dhoundiyal, R., Joshi, K., & Pandey, C. (2018) Effect of CuO nanoparticles on polyphenols content and antioxidant activity in Ashwagandha (*Withania somnifera* L. Dunal). *Journal of Pharmacognosy and Phytochemistry*, 7 (2): 3433-3439.

Singleton, V. L., & Rossi, J. A. (1965) Colorimetry of total phenolics with phosphomolybdic-phosphotungstic acid reagents. *American journal of Enology and Viticulture*, 16 (3): 144-158.

Siril, E. (2013) Pharmacognostic studies on Indian madder (*Rubia cordifolia* L.). *Journal of Pharmacognosy and Phytochemistry*, 1 (5): 112-119.

Sisubalan, N., Ramkumar, V. S., Pugazhendhi, A., Karthikeyan, C., Indira, K., Gopinath, K., . . . Basha, M. H. G. (2018) ROS-mediated cytotoxic activity of ZnO and CeO_2 nanoparticles synthesized using the *Rubia cordifolia* L. leaf extract on MG-63 human osteosarcoma cell lines. *Environmental Science and Pollution Research*, 25: 10482-10492.

Smith, G. B. (2011). Green nanotechnology. In*Nanostructured thin films IV*, SPIE. 8104: 9 -22.

Sompornpailin, K., & Chayaprasert, W. (2020) Plant physiological impacts and flavonoid metabolic responses to uptake TiO_2 nanoparticles. *Australian Journal of Crop Science*, 14 (4): 581-587.

Son, J. K., Jung, S. J., Jung, J. H., Fang, Z., Lee, C. S., Seo, C. S., . . . Woo, M. H. (2008) Anticancer constituents from the roots of *Rubia cordifolia* L. *Chemical and Pharmaceutical Bulletin*, 56 (2): 213-216.

Song, Y., Zhang, S., Zhang, C., Yang, Y., & Lv, K. (2019). Raman spectra and microstructure of zinc oxide irradiated with swift heavy ion. *Crystals*, 9(8): 395.

Sosan, A., Svistunenko, D., Straltsova, D., Tsiurkina, K., Smolich, I., Lawson, T., . . . Sokolik, A. (2016) Engineered silver nanoparticles are sensed at the plasma membrane and dramatically modify the physiology of Arabidopsis thaliana plants. *The Plant Journal*, 85 (2): 245-257.

Sreelekshmi, R., Siril, E., & Muthukrishnan, S. (2022) Role of biogenic silver nanoparticles on hyperhydricity reversion in *Dianthus chinensis* L. an *in vitro* model culture. *Journal of Plant Growth Regulation*, 12: 1-17.

Srivastav, A. K., Verma, S., Awasthi, H., & Kumar, S. (2024) HPTLC phytochemical profiling and simultaneous quantification of quercetin and gallic acid in *Neolamarckia cadamba* (Roxb.). *Research Journal of Pharmacy and Technology*, 17 (1): 271-276.

Suman, S. (2017) Plant tissue culture: A promising tool of quality material production with special reference to micropropagation of banana. *Biochemical Cellular Archives*, 17 (1): 1-26.

Suman, T., Rajasree, S. R., Kanchana, A., Elizabeth, S. B. J. C., & Biointerfaces, S. B. (2013) Biosynthesis, characterization and cytotoxic effect of plant mediated silver nanoparticles using *Morinda citrifolia* root extract. *Colloids and Surfaces B: Biointerfaces*, 106: 74-78.

Sundar, S., Venkatachalam, G., & Kwon, S. J. (2018) Biosynthesis of copper oxide (CuO) nanowires and their use for the electrochemical sensing of dopamine. *Nanomaterials*, 8 (10): 823.

Suwal, M. M., Lamichhane, J., & Gauchan, D. P. (2020) Regeneration technique of bamboo species through nodal segments: a review. *Nepal Journal of Biotechnology*, 8 (1): 54-68.

Swaroopa Ghatge, S. G., Subhash Kudale, S. K., & Ghansham Dixit, G. D. (2011) An improved plant regeneration system for high frequency multiplication of *Rubia cordifolia* L.: a rare medicinal plant. *Asian Journal of Biotechnology*, 3 (4): 397-405.

Taiz, L., Zeiger, E., Møller, I. M., & Murphy, A. (2015) *Plant physiology and Development*. (*Ed.* 6), 761.

Talankova-Sereda, T., Liapina, K., Shkopinskij, E., Ustinov, A., Kovalyova, A., Dulnev, P., & Kucenko, N. (2016). The influence of Cu и Co nanoparticles on growth characteristics and biochemical structure of *Mentha longifoliain vitro*. In *Nanophysics, Nanophotonics, Surface Studies, and Applications: Selected Proceedings of the 3rd International Conference Nanotechnology and Nanomaterials (NANO2015)*, Lviv. Ukraine. Springer. 427-436.

Tanna, J. A., Chaudhary, R. G., Sonkusare, V. N., & Juneja, H. D. (2016). CuO nanoparticles: synthesis, characterization and reusable catalyst for polyhydroquinoline derivatives under ultrasonication. *Journal of the Chinese Advanced Materials Society*, 4 (2): 110-122.

Tang, Y.-Z., & Liu, Z.-Q. (2007) Free-radical-scavenging effect of carbazole derivatives on DPPH and ABTS radicals. *Journal of the American Oil Chemists' Society*, 84: 1095-1100.

Tessier, A., Delaveau, P., & Champion, B. (1981) New anthraquinones in *Rubia cordifolia* roots. *Planta Medica*, 41 (4): 337-343.

Testa-Anta, M., Ramos-Docampo, M. A., Comesaña-Hermo, M., Rivas-Murias, B., & Salgueiriño, V. (2019) Raman spectroscopy to unravel the magnetic properties of iron oxide nanocrystals for bio-related applications. *Nanoscale Advances*, 1 (6): 2086-2103.

Theis, N., & Lerdau, M. (2003) The evolution of function in plant secondary metabolites. *International Journal of Plant Sciences*, 164 (S3): S93-S102.

Thirumurugan, D., Cholarajan, A., Raja, S., & Vijayakumar, R. (2018) An introductory chapter: secondary metabolites. *Secondary Metabolites-Sources and Applications*, 1: 13.

Thorpe, T. (2012) History of plant tissue culture. *Plant Cell Culture Protocols*, 22: 9-27.

Thwala, M., Musee, N., Sikhwivhilu, L., & Wepener, V. (2013) The oxidative toxicity of Ag and ZnO nanoparticles towards the aquatic plant *Spirodela punctuta* and the role of testing media parameters. *Environmental Science: Processes and Impacts*, 15 (10): 1830-1843.

Tian, H., Ghorbanpour, M., & Kariman, K. (2018) Manganese oxide nanoparticle-induced changes in growth, redox reactions and elicitation of antioxidant metabolites in deadly nightshade (*Atropa belladonna* L.). *Industrial Crops and Products*, 126: 403-414.

Tiwari, R., & Rana, C. (2015) Plant secondary metabolites: a review. *International Journal of Engineering Research and General Science*, 3 (5): 661-670.

Torney, F., Trewyn, B. G., Lin, V. S.-Y., & Wang, K. (2007) Mesoporous silica nanoparticles deliver DNA and chemicals into plants. *Nature Nanotechnology*, 2 (5): 295-300.

Tpu, T. (2018) Simplified method to store embryogenic cells: Silver nanoparticles and cryoprotectors elimination effect. *Abstracts/Cryobiology*, 85: 134-138.

Tran, T. H., & Nguyen, V. T. (2014). Copper oxide nanomaterials prepared by solution methods, some properties, and potential applications: a brief review. *International Scholarly Research Notices*, (1): 856592.

Tripathi, D. K., Singh, S., Singh, S., Srivastava, P. K., Singh, V. P., Singh, S., . . . Pandey, A. C. (2017a) Nitric oxide alleviates silver nanoparticles (AgNps)-induced phytotoxicity in *Pisum sativum* seedlings. *Plant Physiology and Biochemistry*, 110: 167-177.

Tripathi, D. K., Singh, S., Singh, V. P., Prasad, S. M., Dubey, N. K., & Chauhan, D. K. (2017b) Silicon nanoparticles more effectively alleviated UV-B stress than silicon in wheat (*Triticum aestivum*) seedlings. *Plant Physiology and Biochemistry*, 110: 70-81.

Tripathi, L., & Tripathi, J. N. (2003) Role of biotechnology in medicinal plants. *Tropical Journal of Pharmaceutical Research*, 2 (2): 243-253.

Tripathi, Y., & Sharma, M. (1998) Comparison of the antioxidant action of the alcoholic extract of *Rubia cordifolia* with rubiadin. *Indian Journal of Biochemistry and Biophysics*, 35 (5): 313-316.

Tripathi, Y. B., & Singh, A. V. (2007) Role of *Rubia cordifolia* Linn. in radiation protection. *Indian Journal of Experimental Biology*, 45: 620-625.

Tugarova, A. V., Mamchenkova, P. V., Dyatlova, Y. A., & Kamnev, A. A. (2018). FTIR and Raman spectroscopic studies of selenium nanoparticles synthesised by the bacterium *Azospirillum thiophilum*. *Spectrochimica Acta Part A: Molecular and Biomolecular Spectroscopy*, 192: 458-463.

Tung, H. T., Bao, H. G., Cuong, D. M., Ngan, H. T. M., Hien, V. T., Luan, V. Q., . . . Trieu, L. N. (2021) Silver nanoparticles as the sterilant in large-scale micropropagation of chrysanthemum. *In Vitro Cellular and Developmental Biology-Plant*, 1-10.

Türker, A. U., Yücesan, B., & Gürel, E. (2010) Adventitious shoot regeneration from stem internode explants of *Verbena officinalis* L., a medicinal plant. *Turkish Journal of Biology*, 34 (3): 297-304.

Tymoszuk, A., & Miler, N. (2019) Silver and gold nanoparticles impact on *in vitro* adventitious organogenesis in chrysanthemum, gerbera and Cape Primrose. *Scientia Horticulturae*, 257: 108766.

Urlaub, E., Popp, J., Kiefer, W., Bringmann, G., Koppler, D., Schneider, H., . . . Schrader, B. (1998) FT-Raman investigation of alkaloids in the liana *Ancistrocladus heyneanus*. *Biospectroscopy*, 4 (2): 113-120.

Valianou, L., Karapanagiotis, I., & Chryssoulakis, Y. (2009) Comparison of extraction methods for the analysis of natural dyes in historical textiles by high-performance liquid chromatography. *Analytical and Bioanalytical Chemistry*, 395: 2175-2189.

Vanathi, P., Rajiv, P., Narendhran, S., Rajeshwari, S., Rahman, P. K., & Venckatesh, R. (2014) Biosynthesis and characterization of phyto mediated Zinc oxide nanoparticles: a green chemistry approach. *Materials Letters*, 134: 13-15.

Vankar, P. S., Shukla, D., Wijayapala, S., Samanta, A. K., & Technology, R. (2017) Innovative silk dyeing using enzyme and *Rubia cordifolia* extract at room temperature. *Pigment and Resin Technology*, 46 (4): 296-302.

Varughese, A., Kaur, R., & Singh, P. (2020). Green synthesis and characterization of copper oxide nanoparticles using *Psidium guajava* leaf extract. In *IOP Conference Series: Materials Science and Engineering*, 961(1): 012011.

Vasantharaj, S., Sathiyavimal, S., Senthilkumar, P., Lewisoscar, F., & Pugazhendhi, A. (2019) Biosynthesis of iron oxide nanoparticles using leaf extract of *Ruellia tuberosa*: antimicrobial properties and their applications in photocatalytic degradation. *Journal of Photochemistry and Photobiology B: Biology*, 192: 74-82.

Velliyan, S., & Rajendran, V. (2021). Study on the effect of Ce^{3+} doping on structural, morphological and optical properties of CuO nanoparticles synthesized via combustion technique. *Physica B: Condensed Matter*, 613: 413015.

Verma, A., Kumar, B., Alam, P., Singh, V., & Gupta, S. K. (2016) *Rubia cordifolia*-a review on pharmaconosy and phytochemistry. *International Journal of Pharmaceutical Sciences and Research*, 7 (7): 2720.

Verma, S., & Singh, S. (2008) Current and future status of herbal medicines. *Veterinary World*, 1 (11): 347.

Vidya, C., Hiremath, S., Chandraprabha, M., Antonyraj, M., Gopal, I. V., Jain, A., & Bansal, K. J. (2013) Green synthesis of ZnO nanoparticles by *Calotropis gigantea*. *International Journal of Current Engineering and Technology*, 1 (1): 118-120.

Vijayakumar, P. S., Abhilash, O. U., Khan, B. M., & Prasad, B. L. (2010) Nanogold-loaded sharp-edged carbon bullets as plant-gene carriers. *Advanced Functional Materials*, 20 (15): 2416-2423.

Waksmundzka-Hajnos, M., Hawrył, M., Hawrył, A., & Jożwiak, G. (2022). Thin Layer Chromatography in Phytochemical Analysis. In *Handbook of Bioanalytics*, Springer. 1-31.

Wang, L., Li, D., Bao, C., You, J., Wang, Z., Shi, Y., & Zhang, H. (2008) Ultrasonic extraction and separation of anthraquinones from *Rheum palmatum* L. *Ultrasonics Sonochemistry*, 15 (5): 738-746.

Wang, S., Hua, H., Wu, L., Li, X., & Zhu, T. (1992) Studies on anthraquinones from the roots of *Rubia cordifolia* L. *Yao xue xue bao= Acta Pharmaceutica Sinica*, 27 (10): 743-747.

Wang, T., Zhao, G., Deng, Z., Gao, C., Cao, Y., & Gao, D. (2015) Theoretical investigation of a novel microwave antenna aided cryovial for rapid and uniform rewarming of frozen cryoprotective agent solutions. *Applied Thermal Engineering*, 89: 968-977.

Wang, Y., Liu, H., Yu, S., Huang, Y., Zhang, Y., He, X., & Chen, W. (2023) Changes in marker secondary metabolites revealed the medicinal parts, harvest time, and possible synthetic sites of *Rubia cordifolia* L. *Plant Physiology and Biochemistry*, 203: 108-124.

Wang, Y., Liu, H., Yu, S., Zhang, Y., Huang, Y., He, X., & Chen, W. (2024) Effects of geographical, soil and climatic factors on the two marker secondary metabolites contents in the roots of *Rubia cordifolia* L. *Frontiers in Plant Science*, 15: 141-149.

Wang, Z., Li, J., Zhao, J., & Xing, B. (2011) Toxicity and internalization of CuO nanoparticles to prokaryotic alga *Microcystis aeruginosa* as affected by dissolved organic matter. *Environmental Science and Technology*, 45 (14): 6032-6040.

Wawrosch, C., & Zotchev, S. B. (2021) Production of bioactive plant secondary metabolites through *in vitro* technologies—status and outlook. *Applied Microbiology and Biotechnology*, 105 (18): 6649-6668.

Wen, M., Chen, Q., Chen, W., Yang, J., Zhou, X., Zhang, C., . . . Mei, Q. (2022) A comprehensive review of *Rubia cordifolia* L.: Traditional uses, phytochemistry, pharmacological activities, and clinical applications. *Frontiers in Pharmacology*, 13: 965 -970.

Wootton-Beard, P. C., & Ryan, L. (2011) A beetroot juice shot is a significant and convenient source of bio accessible antioxidants. *Journal of Functional Foods*, 3 (4): 329-334.

Wu, H., Guo, J., Chen, S., Liu, X., Zhou, Y., Zhang, X., & Xu, X. (2013) Recent developments in qualitative and quantitative analysis of phytochemical constituents and their metabolites using liquid chromatography–mass spectrometry. *Journal of Pharmaceutical and BiomedicalAnalysis*, 72: 267-291.

Wu, L.-J., Wang, S.-X., Hua, H.-M., Li, X., Zhu, T.-R., Miyase, T., & Ueno, A. (1991) 6-Methoxygeniposidic acid, an iridoid glycoside from *Rubia cordifolia*. *Phytochemistry*, 30(5): 110-1711.

Xavier, J. R., Chauhan, O. P., & Sharma, R. K. (2022) Natural plant products as promising radio protectors. *Bulletin of Environment, Pharmacology and Life Sciences*, 4: 261-276.

Xu, J. F., J, W., Shen, Z. X., L, W. S., Tang, S. H., Y, X. R., ... & Xin, X. Q. (1999). Raman spectra of CuO nanocrystals. *Journal of RamanSspectroscopy*, 30 (5): 413-415.

Yang, Z., Chen, J., Dou, R., Gao, X., Mao, C., & Wang, L. (2015) Assessment of the phytotoxicity of metal oxide nanoparticles on two crop plants, maize (*Zea mays* L.) and rice (*Oryza sativa* L.). *International journal of environmental research and public health*, 12(12): 15100-15109.

Yilmaz, M., Yilmaz, A., Karaman, A., Aysin, F., & Aksakal, O. (2021) Monitoring chemically and green-synthesized silver nanoparticles in maize seedlings via surface-enhanced Raman spectroscopy (SERS) and their phytotoxicity evaluation. *Talanta*, 225: 121952.

Ying, S., Guan, Z., Ofoegbu, P. C., Clubb, P., Rico, C., He, F., & Hong, J. (2022) Green synthesis of nanoparticles: Current developments and limitations. *Environmental Technology and Innovation*, 26: 102-122.

Yu, K. W., Gao, W., Hahn, E. J., & Paek, K. Y. (2002) Jasmonic acid improves ginsenoside accumulation in adventitious root culture of *Panax ginseng* CA Meyer. *Biochemical Engineering Journal*,11 (2-3): 211-215.

Yusuf, M., Khan, M. A., & Mohammad, F. (2016) Investigations of the colourimetric and fastness properties of wool dyed with colorants extracted from Indian madder using reflectance spectroscopy. *Optik*, 127 (15): 6087-6093.

Yusuf, M., Mohammad, F., & Shabbir, M. (2017) Eco-friendly and effective dyeing of wool with anthraquinone colorants extracted from *Rubia cordifolia* roots: Optimization, colorimetric and fastness assay. *Journal of King Saud University-Science*, 29 (2): 137-144.

Yusuf, M., Shahid, M., Khan, S. A., Khan, M. I., Islam, S.-U., Mohammad, F., & Khan, M. A. (2013) Eco-dyeing of wool using aqueous extract of the roots of Indian madder (*Rubia cordifolia*) as natural dye. *Journal of Natural Fibers*, 10 (1): 14-28.

Zakharova, O. V., Gusev, A. A., Muratov, D. S., Shuklinov, A. V., Strekalova, N. S., & Matveev, S. M. (2021) Titanium trisulfide nanoribbons affect the Downy Birch and Poplar× Aspen hybrid in plant tissue culture via the emission of hydrogen sulfide. *Forests*, 12 (6): 713.

Zenk, M., El–Shagi, H., & Schulte, U. (1975) Anthraquinone production by cell suspension cultures of *Morinda citrifolia*. *Planta Medica*, 28 (S01): 79-101.

Zhao, J., Davis, L. C., & Verpoorte, R. (2005) Elicitor signal transduction leading to production of plant secondary metabolites. *Biotechnology Advances*, 23 (4): 283-333.

Zhao, L., Peng, B., Hernandez-Viezcas, J. A., Rico, C., Sun, Y., Peralta-Videa, J. R., . . . Varela-Ramirez, A. (2012) Stress response and tolerance of *Zea mays* to CeO_2 nanoparticles: cross talk among H_2O_2, heat shock protein, and lipid peroxidation. *ACS Nano*, 6 (11): 9615-9622.

Zhishen, J., Mengcheng, T., & Jianming, W. (1999) The determination of flavonoid contents in mulberry and their scavenging effects on superoxide radicals. *Food Chemistry*, 64 (4): 555-559.

Zhong, J. J. (2001) Biochemical engineering of the production of plant-specific secondary metabolites by cell suspension cultures. *Plant Cells*, 8: 1-26.